Extragalactic Cosmic Rays

Pierre Auger Observatory
and Telescope Array

Ralph Engel
Karlsruhe Institute of Technology (KIT)

(photograph by S. Saffi)

Physics of extragalactic cosmic rays

Sources have to produce particles reaching 10^{20} eV

Particle on circular orbit

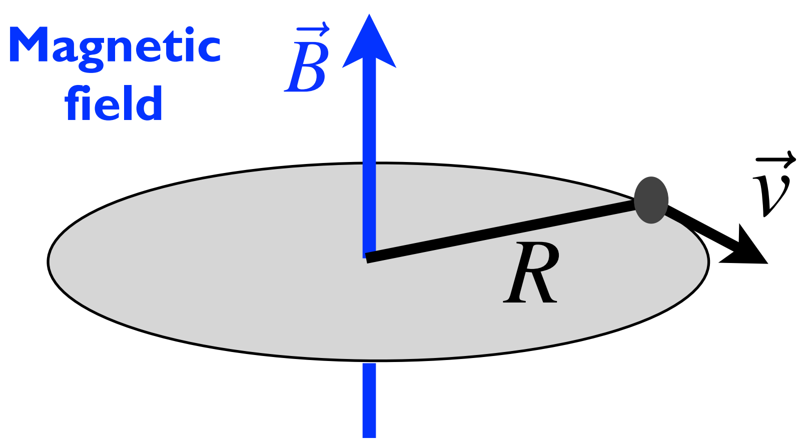

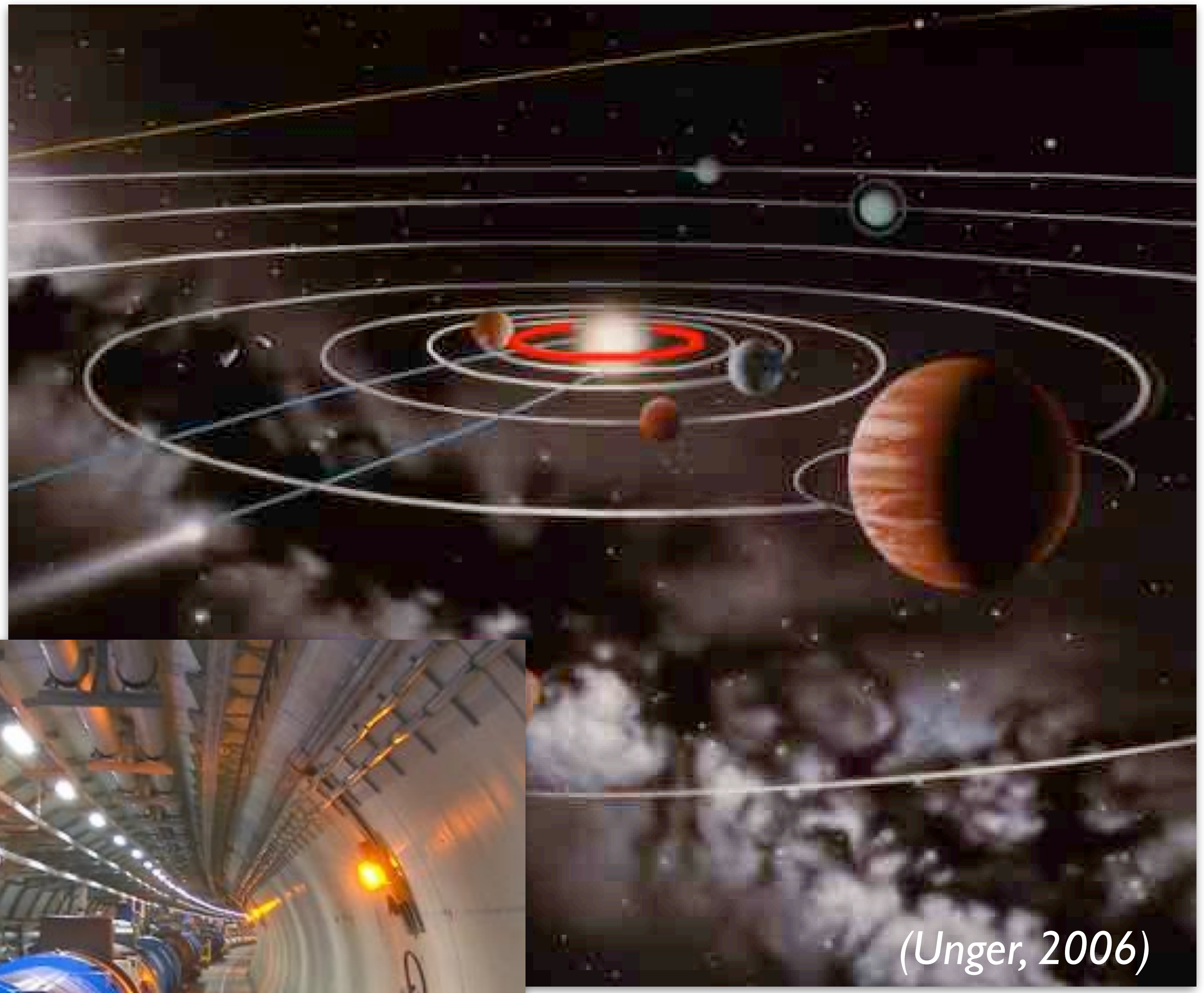

Need accelerator of size of the orbit of the planet Mercury to reach 10^{20} eV with LHC technology

Hillas plot (1984)

(MIAPP review, Front.Astron.Space Sci. 6 (2019) 23)

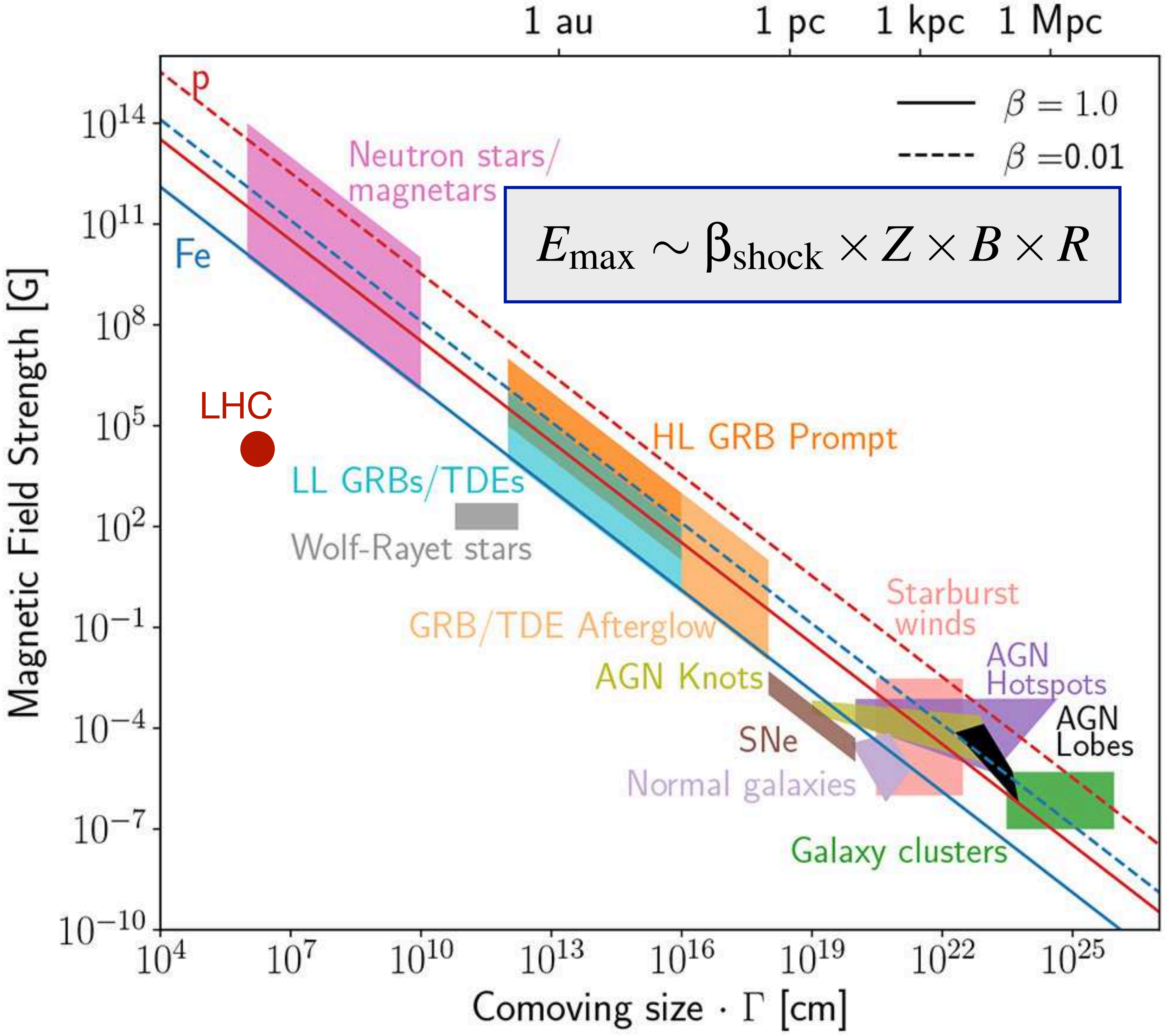

Hardly any source expected to accelerate protons to 10^{20} eV

Galactic vs. extragalactic sources

- Galactic magnetic field: ~ 3 μG   (3.10^{-10} T)
- Gyroradius:

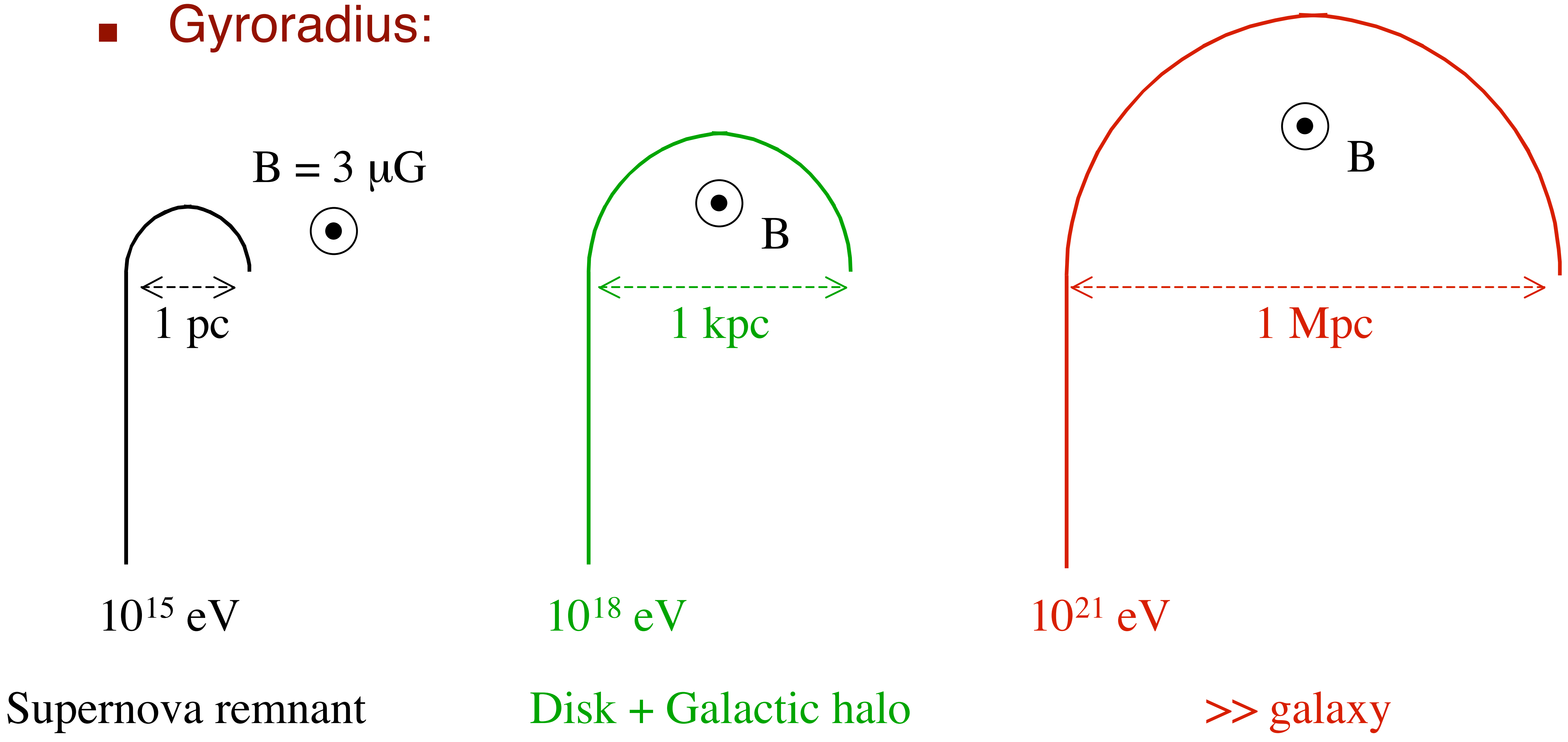

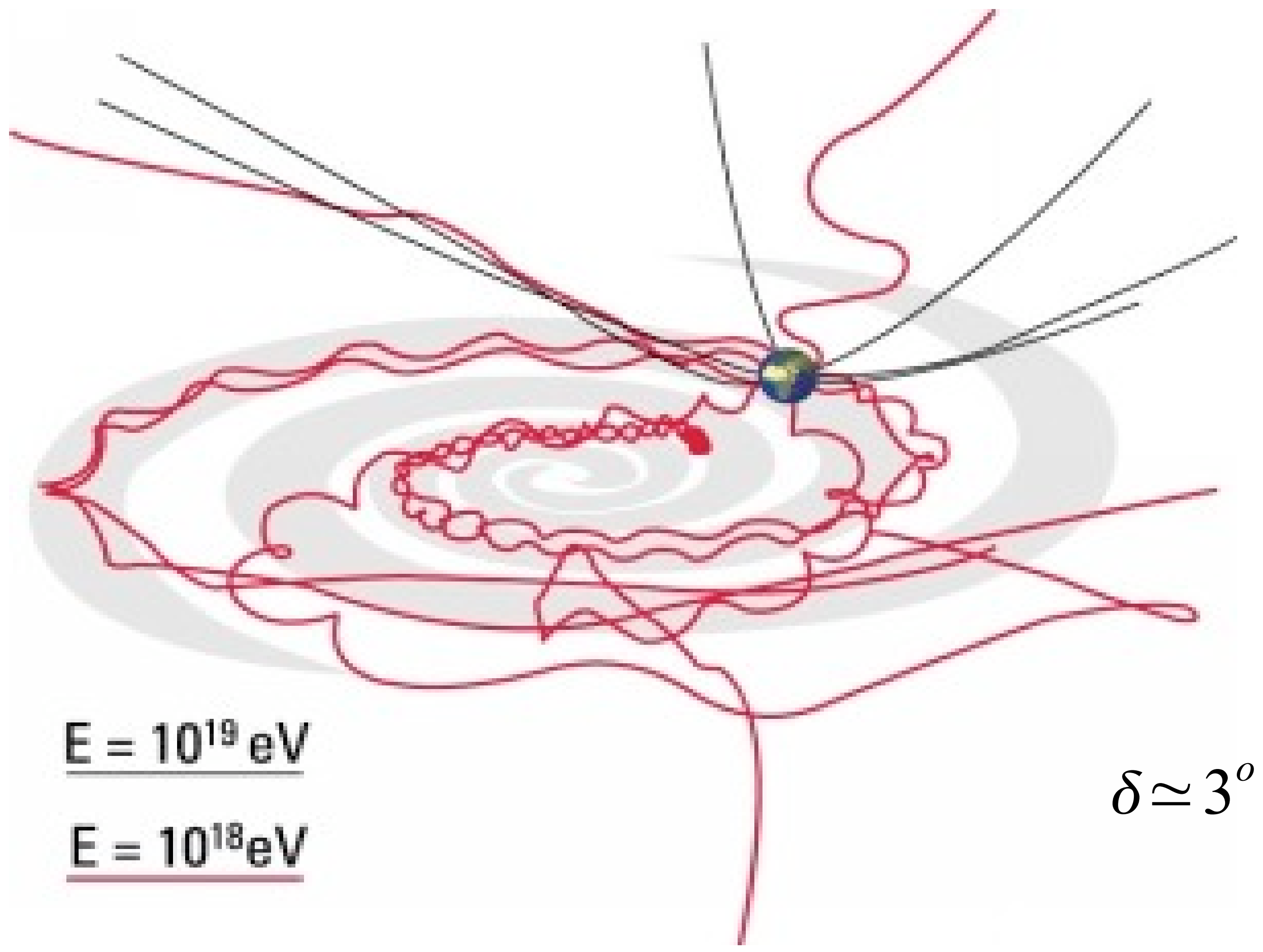

$$\delta \simeq 3^o \frac{B}{3\,\mu G}\,\frac{L}{kpc}\,\frac{6\times 10^{19}\,eV}{E/Z}$$

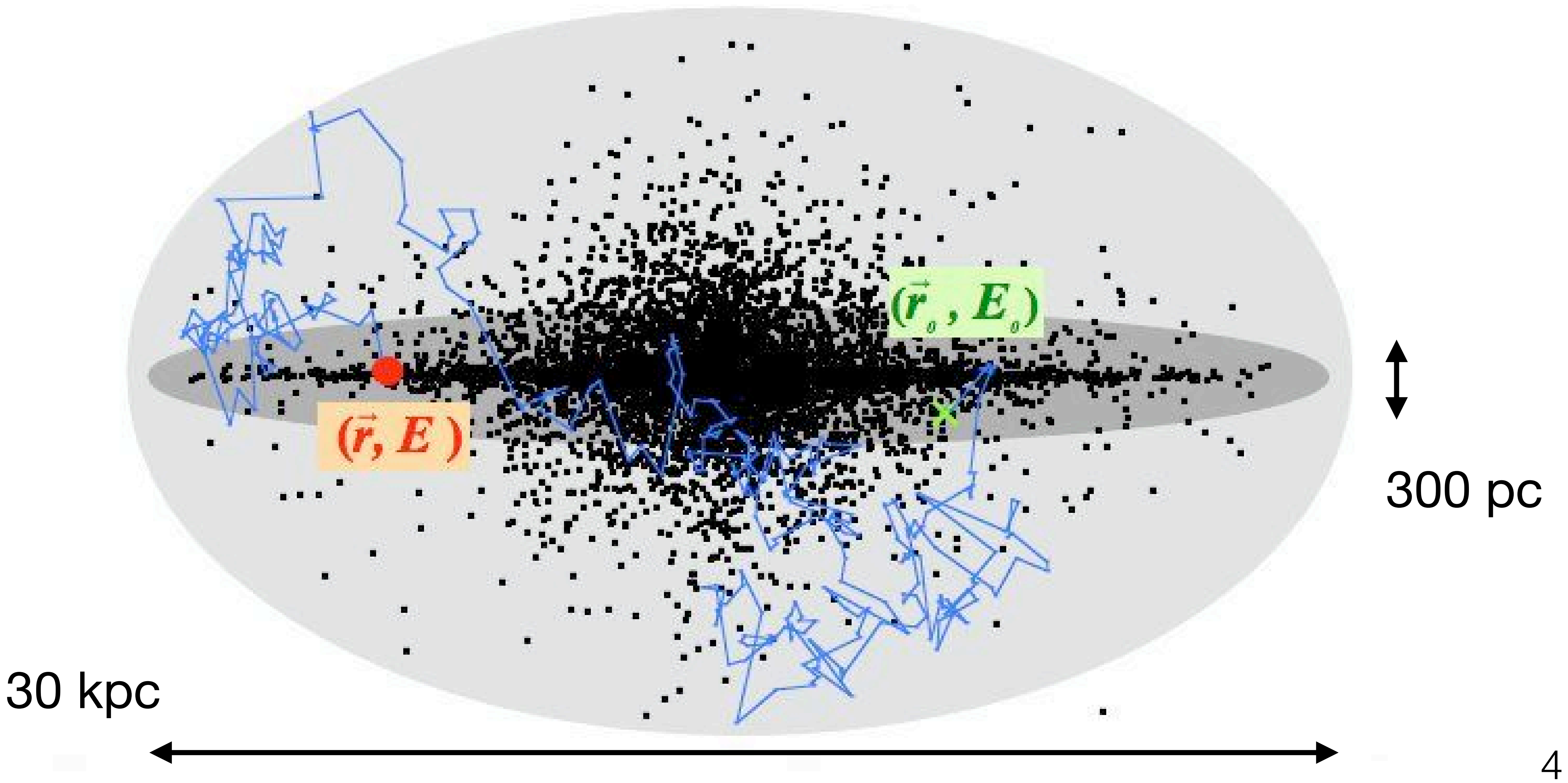

1 pc = 3.26 ly = 3.08 10^{16} m

Acceleration (bottom-up) or exotic (top-down) scenarios?

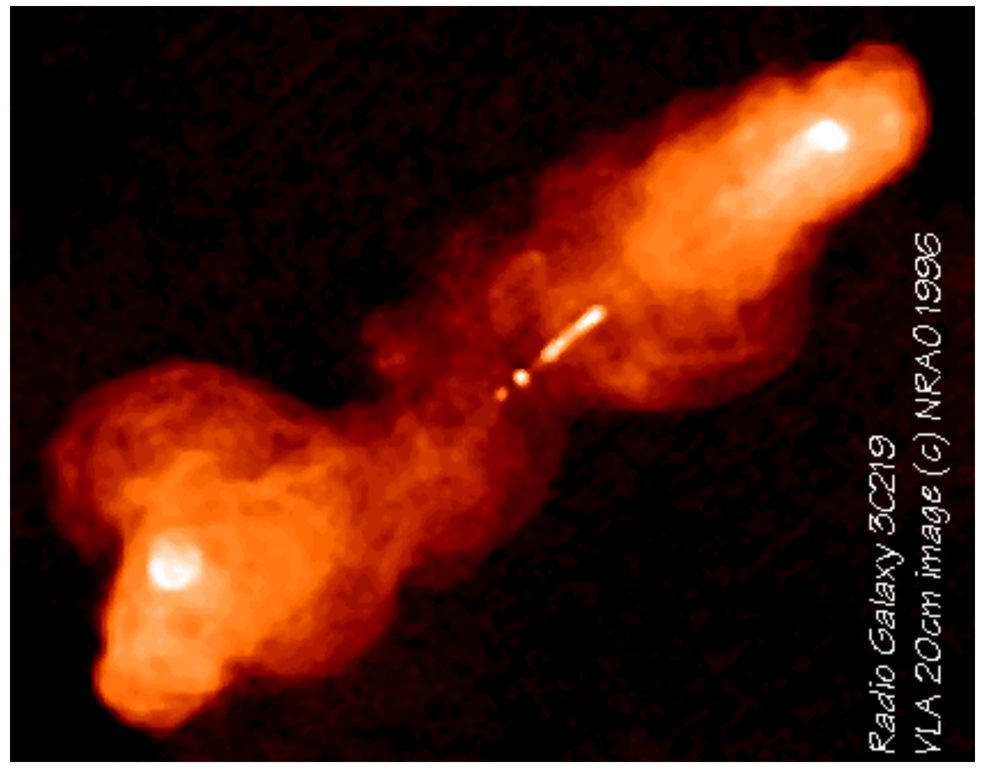

Active Galactic Nuclei (AGN):
Black Hole of ~10^9 solar masses

Magnetars:
magnetic field up to ~10^{15} G

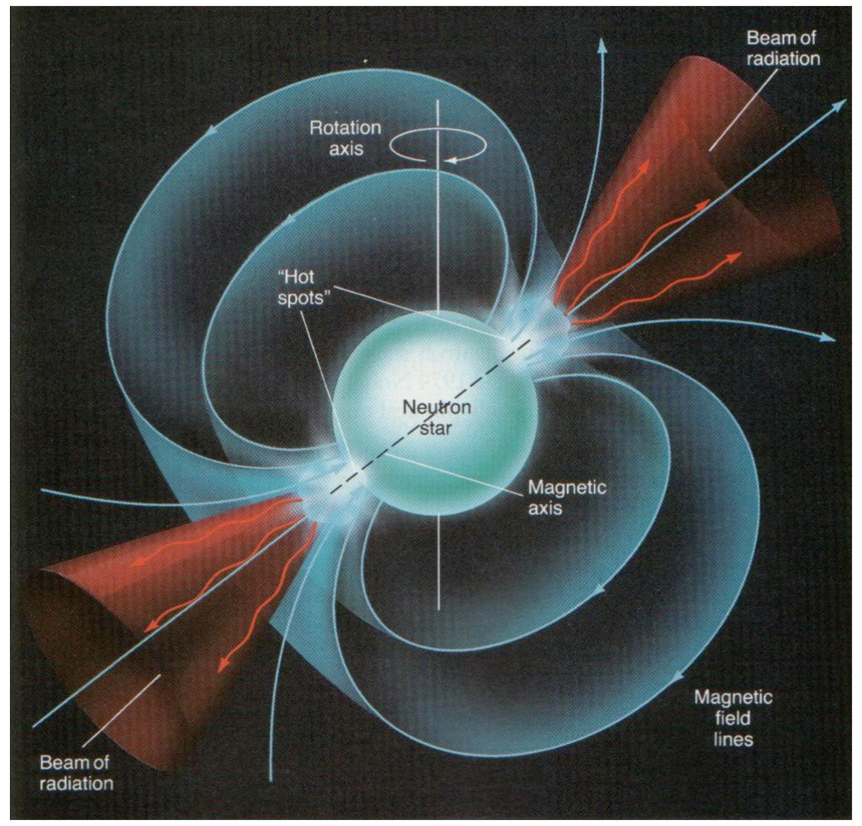

	Process	Distribution	Injection flux
AGNs, GRBs, … (☆)	Diffuse shock acceleration	Cosmological	p … Fe
Young pulsars (☆☆)	EM acceleration	Galaxy & halo	mainly Fe
X particles (☆☆☆)	Decay & particle cascade	(a) Halo (SHDM) (b) Cosmological	ν, γ-rays and p
Z-bursts (☆☆☆☆)	Z^0 decay & particle cascade	Cosmological & clusters	ν, γ-rays and p

X particles from:
- topological defects
- monopoles
- cosmic strings
- cosmic necklaces
- …..

Big Bang:
super-heavy particles,
topological defects:
$M_X \sim 10^{23}$ - 10^{24} eV

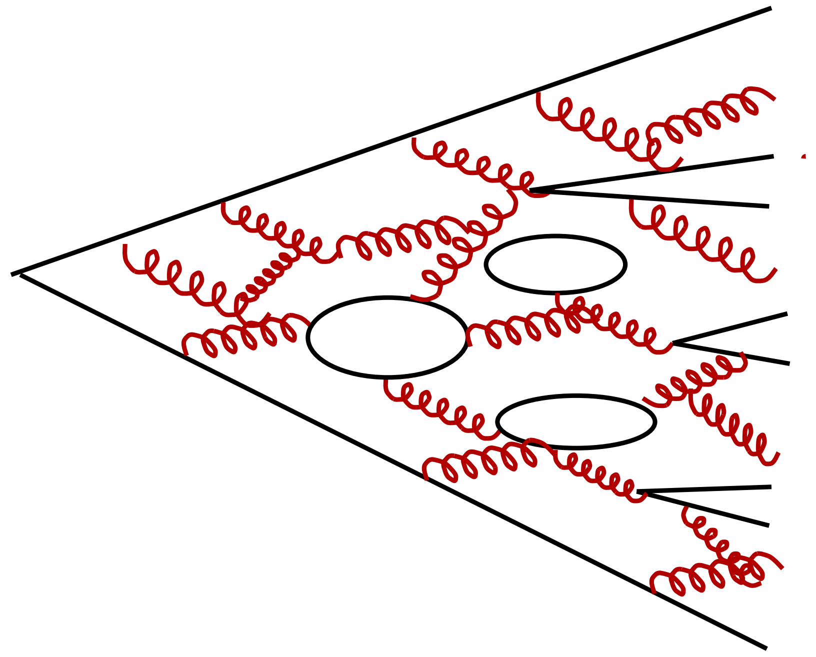

large fluxes of photons and neutrinos

(RE, Nijmegen Summer School, 2006)

Examples of astrophysical source candidates

Diffusive shock acceleration

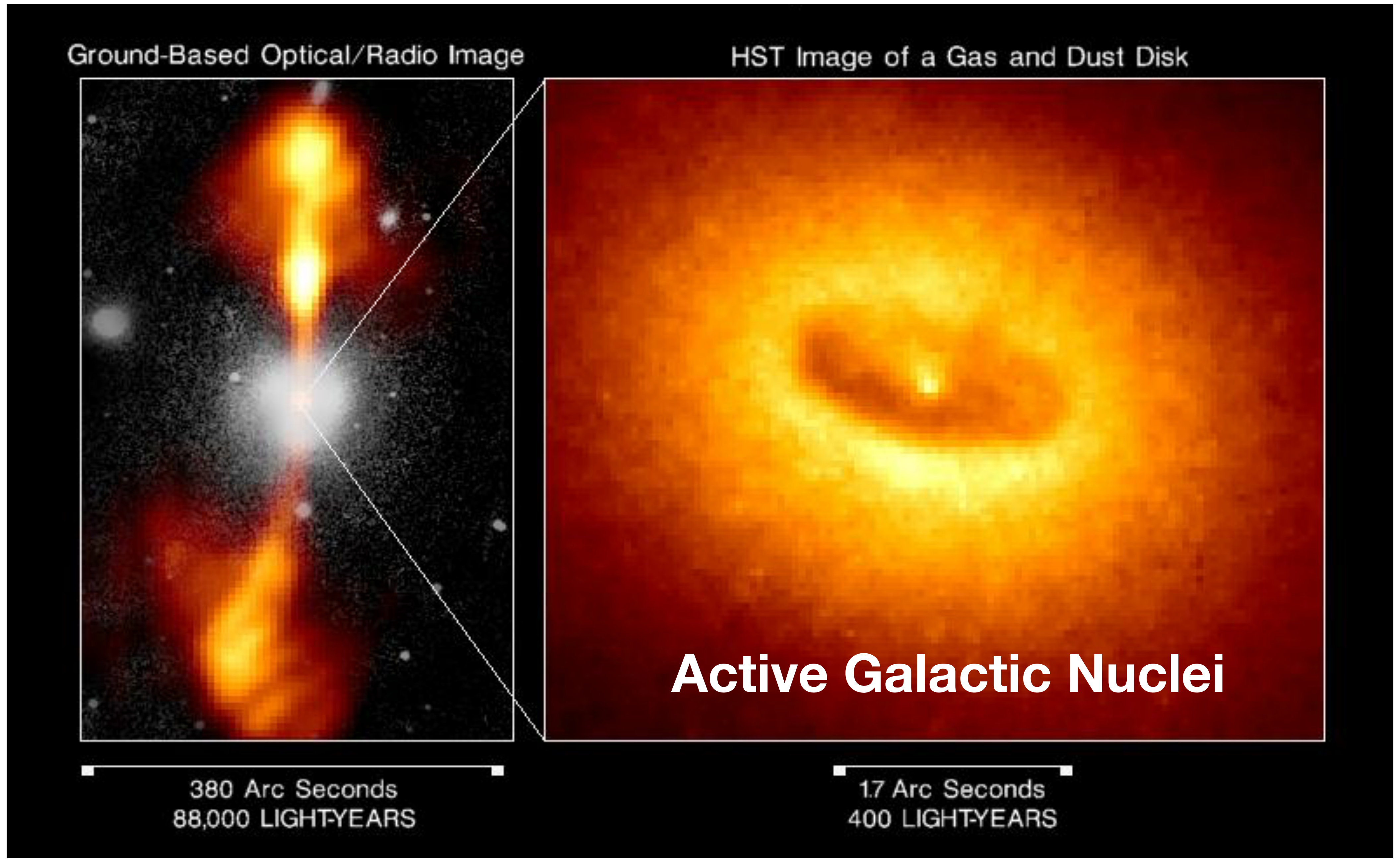

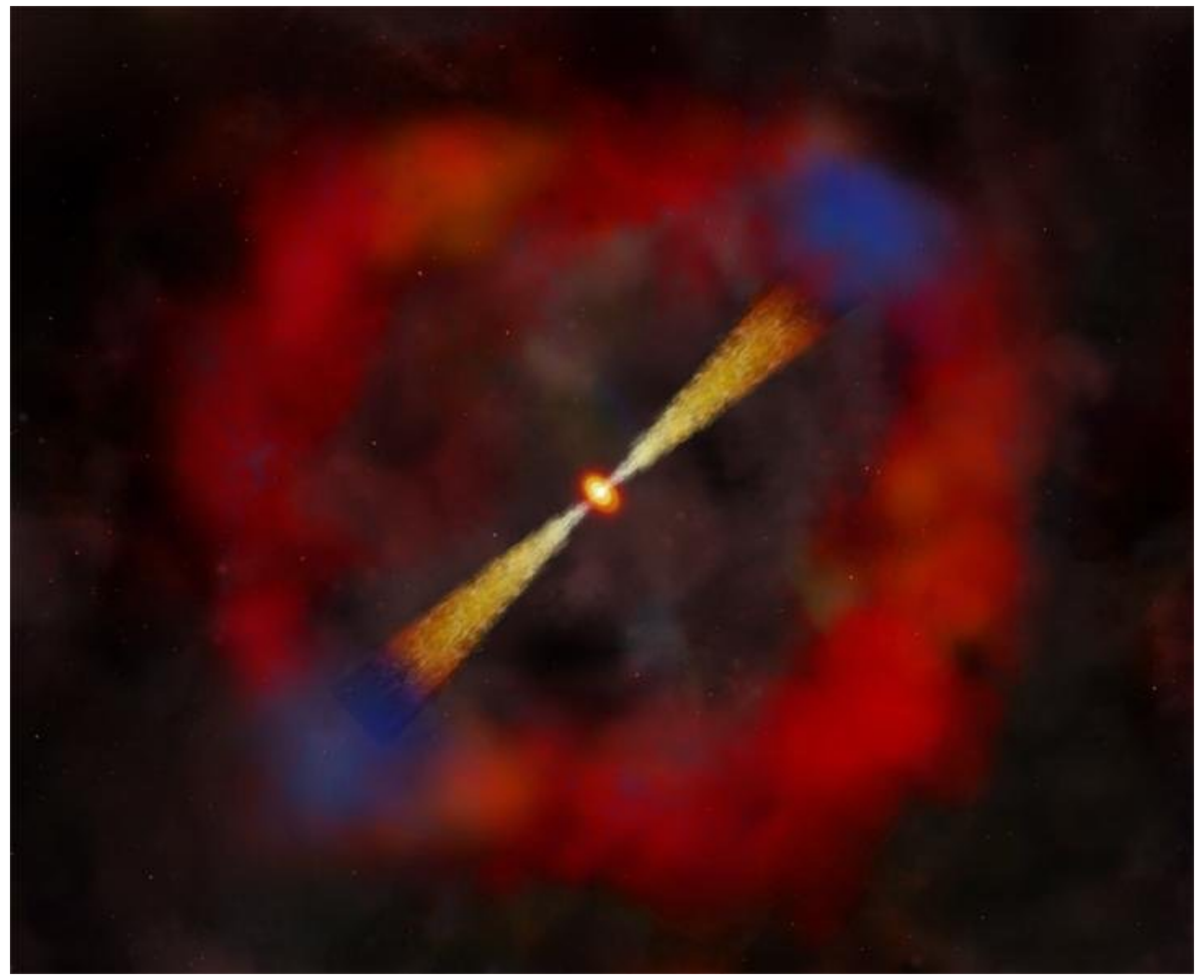

$$\frac{\mathrm{d}N_{\mathrm{inj}}}{\mathrm{d}E} \sim E^{-2}$$

Gamma ray bursts (GRBs)

Inductive acceleration

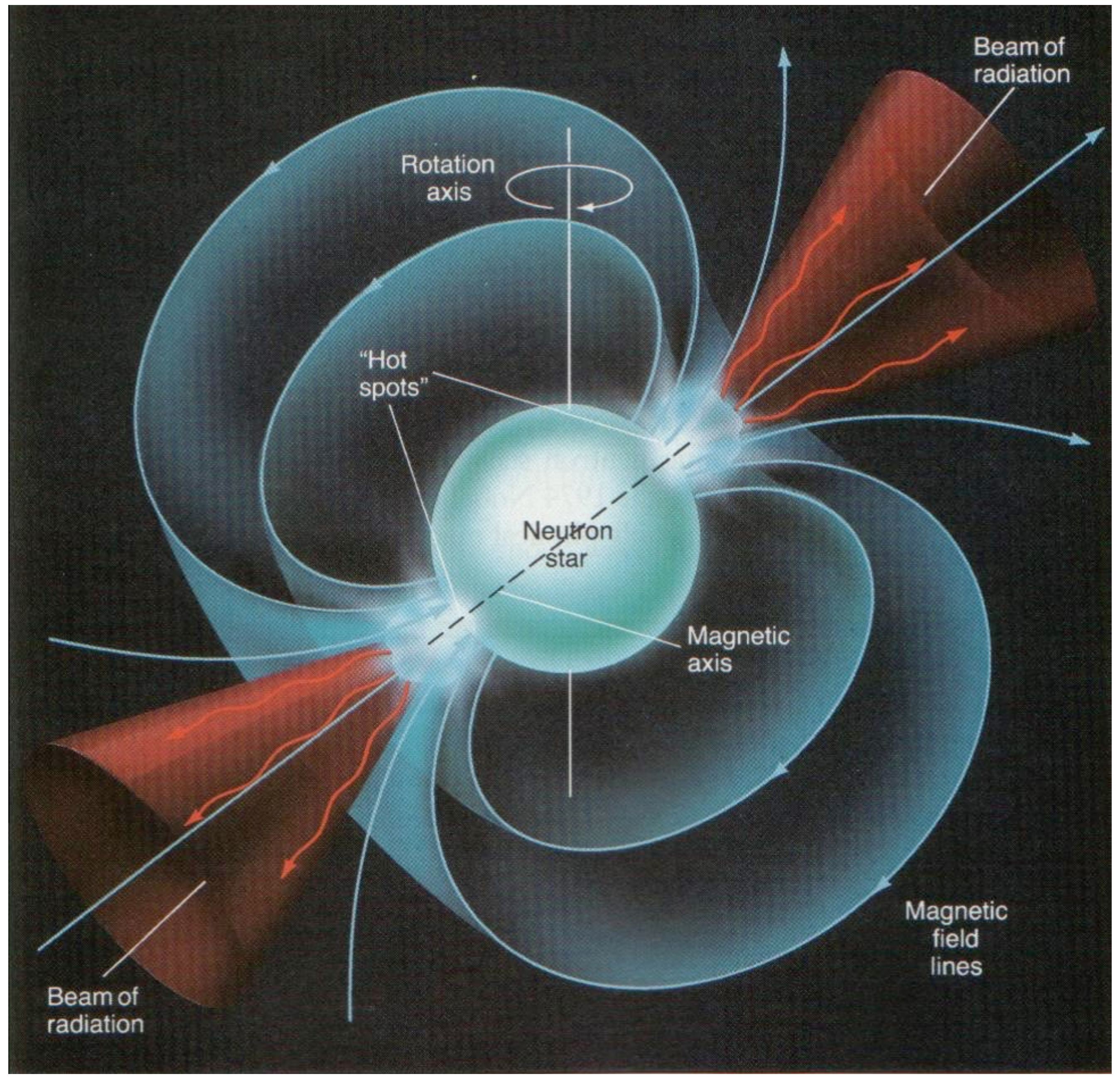

Rapidly spinning neutron stars

$$\frac{\mathrm{d}N_{\mathrm{inj}}}{\mathrm{d}E} \sim E^{-1}\left(1+\frac{E}{E_g}\right)^{-1}$$

Single (relativistic) reflection

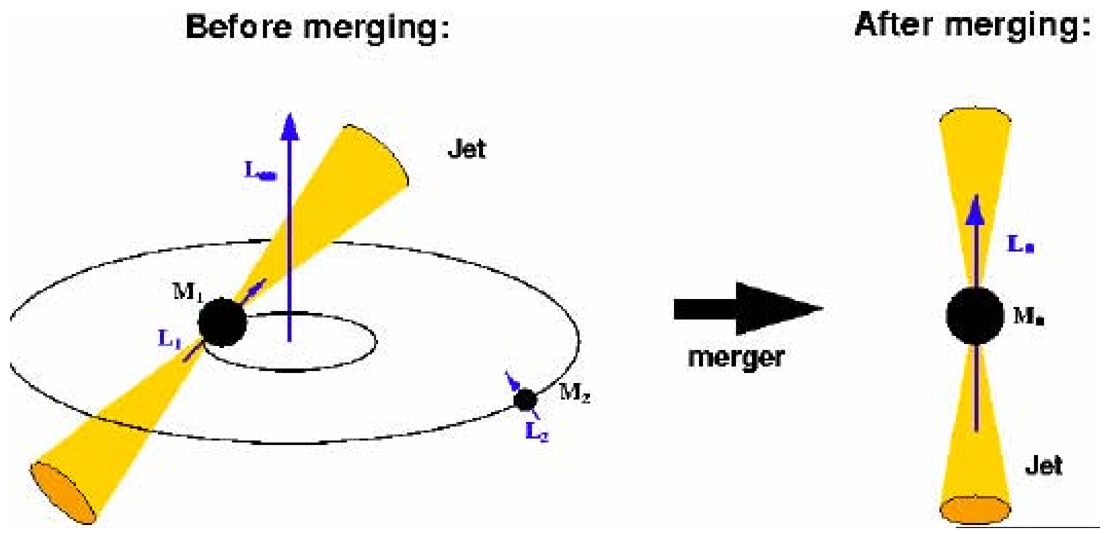

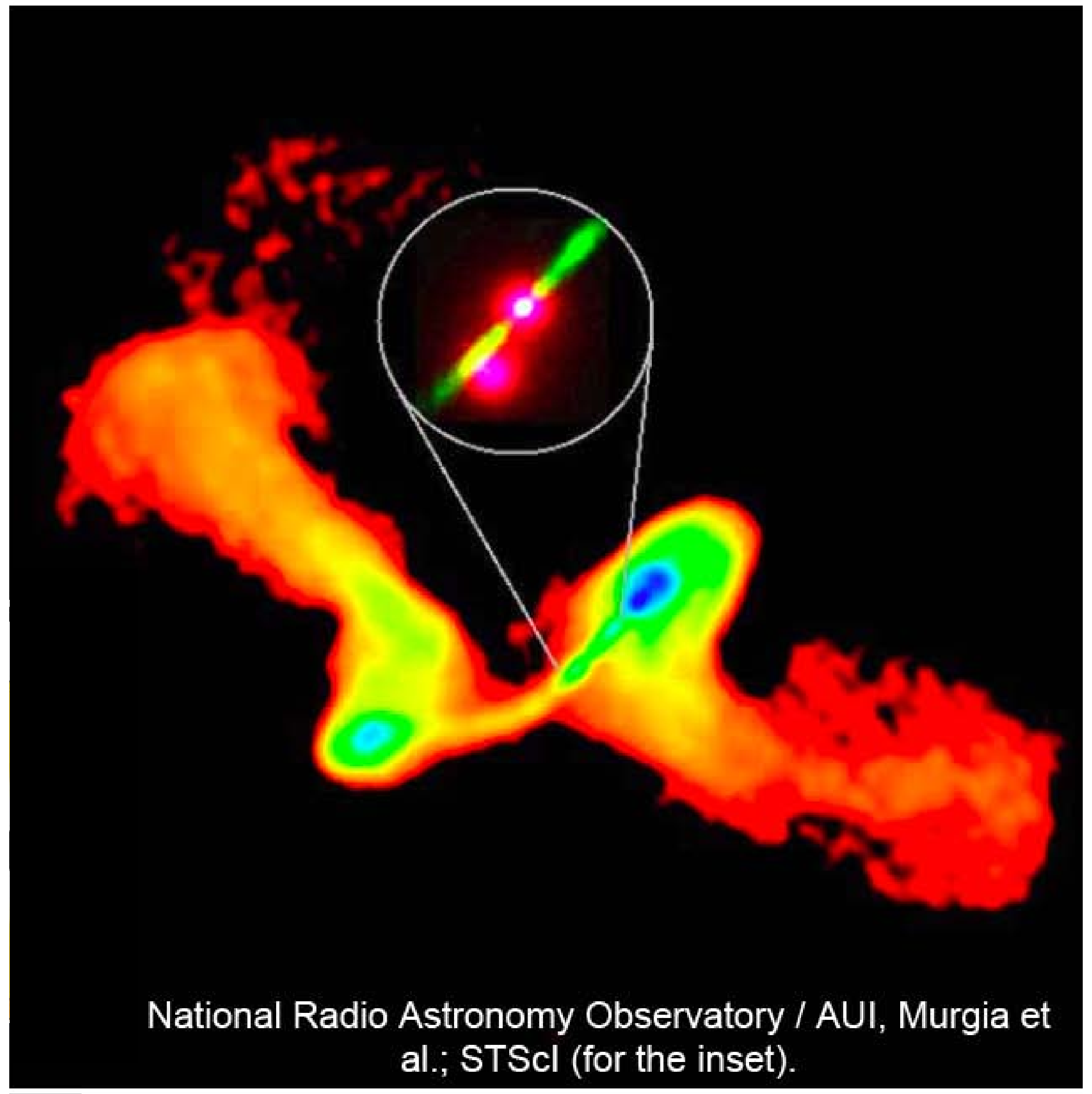

Tidal disruption events (TDEs)

Re-cap: Propagation effects

Magnetic field deflection

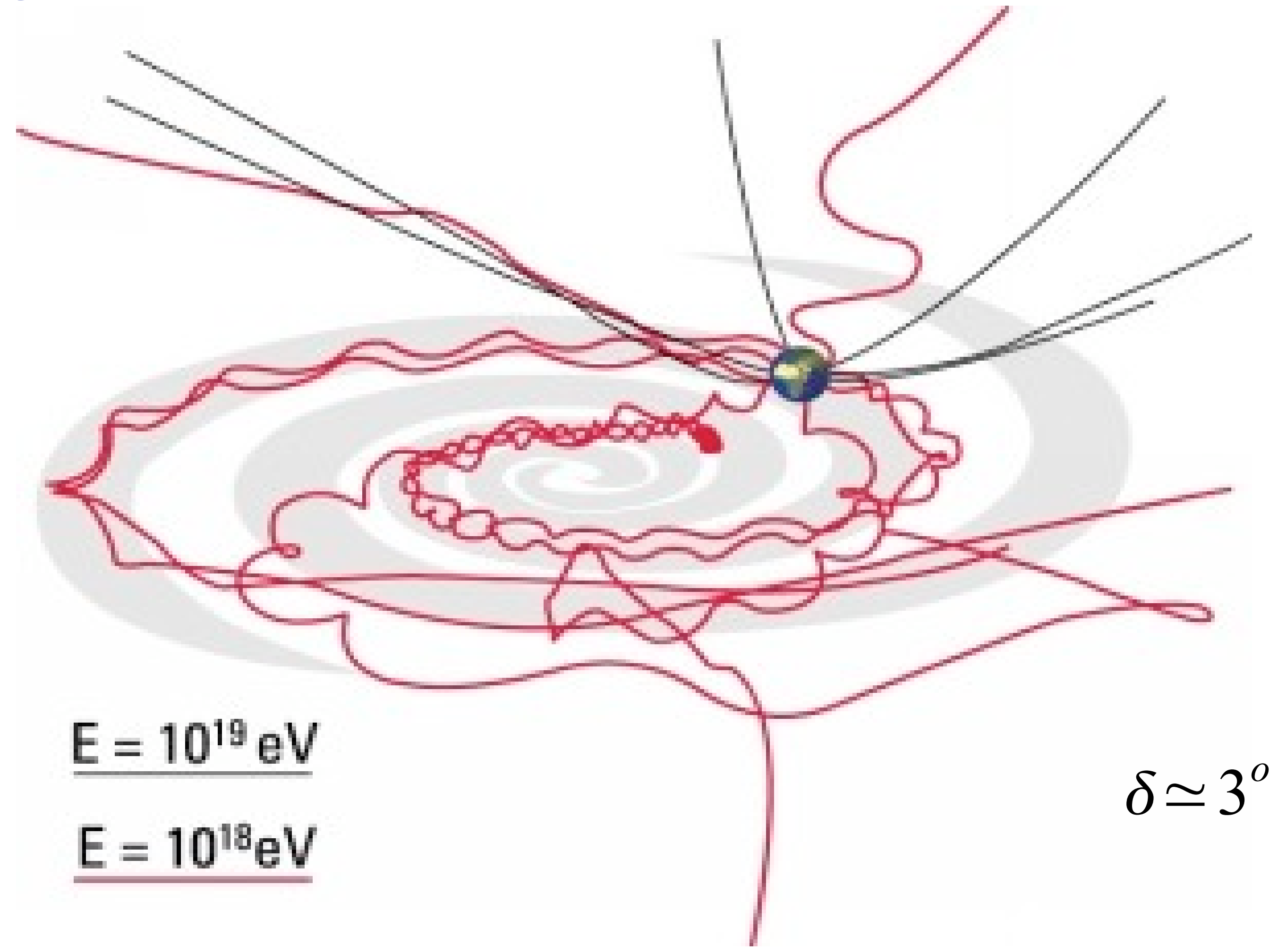

$$\delta \simeq 3^{o} \frac{B}{3\,\mu G} \frac{L}{kpc} \frac{6 \times 10^{19}\, eV}{E/Z}$$

Magnetic horizon effect

$$X_{\rm s} = \frac{d_{\rm s}}{\sqrt{r_H L_{\rm coh}}}$$

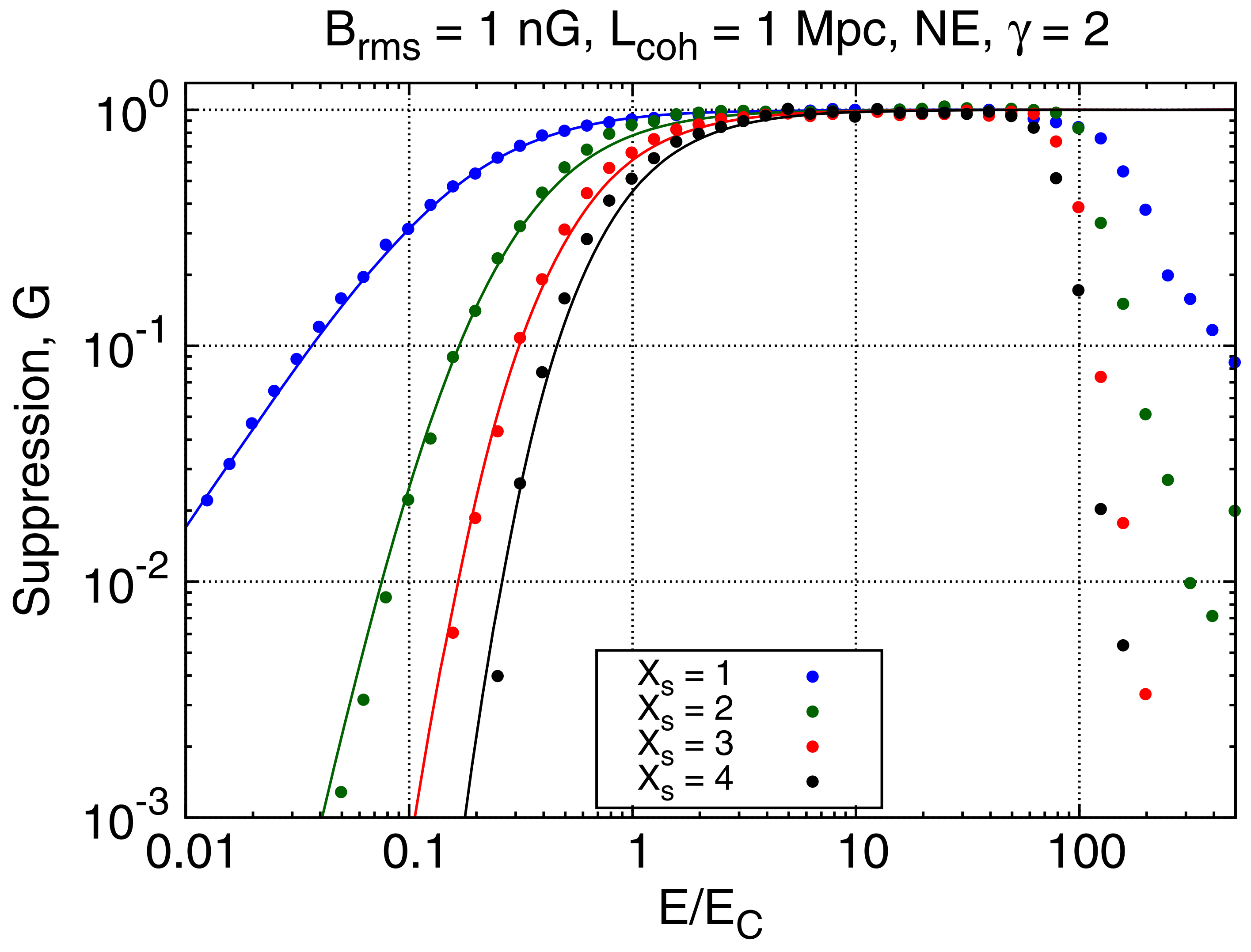

(González et al. PRD104(2021)063005)

Energy loss processes

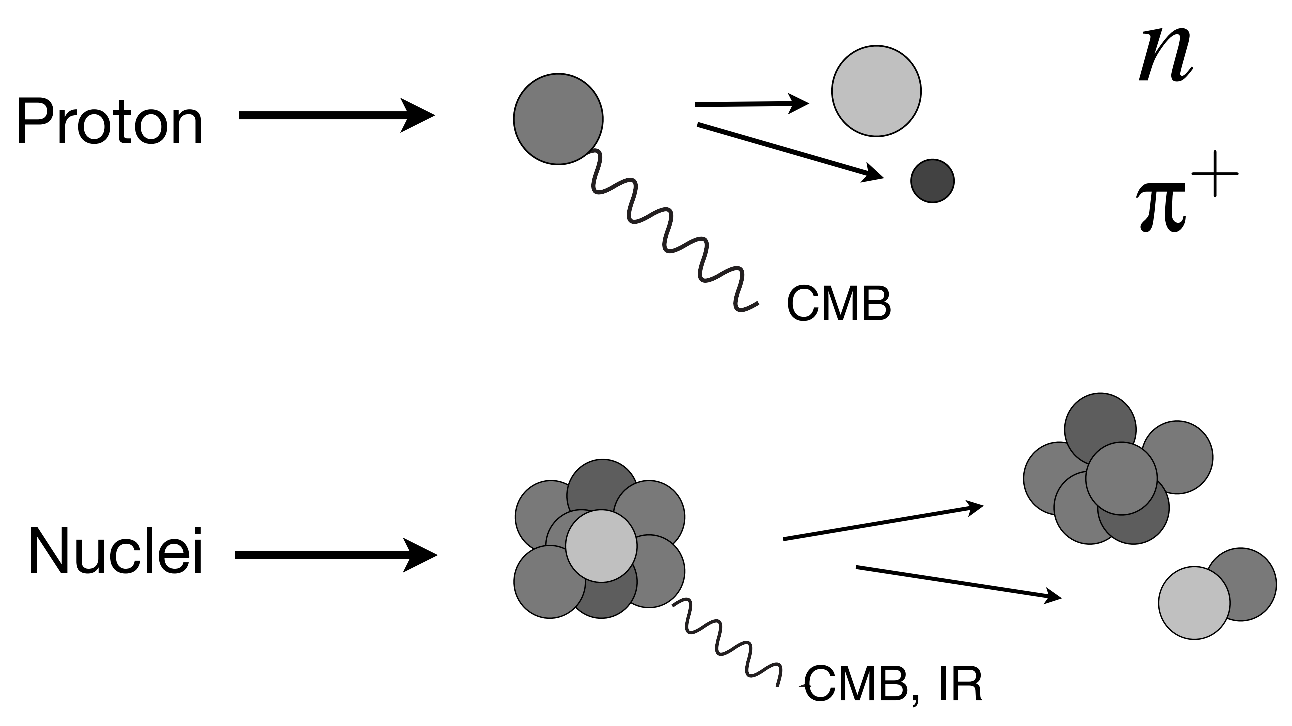

Photo-pion production
(mainly Δ resonance)

Photo-dissociation
(giant dipole resonance)

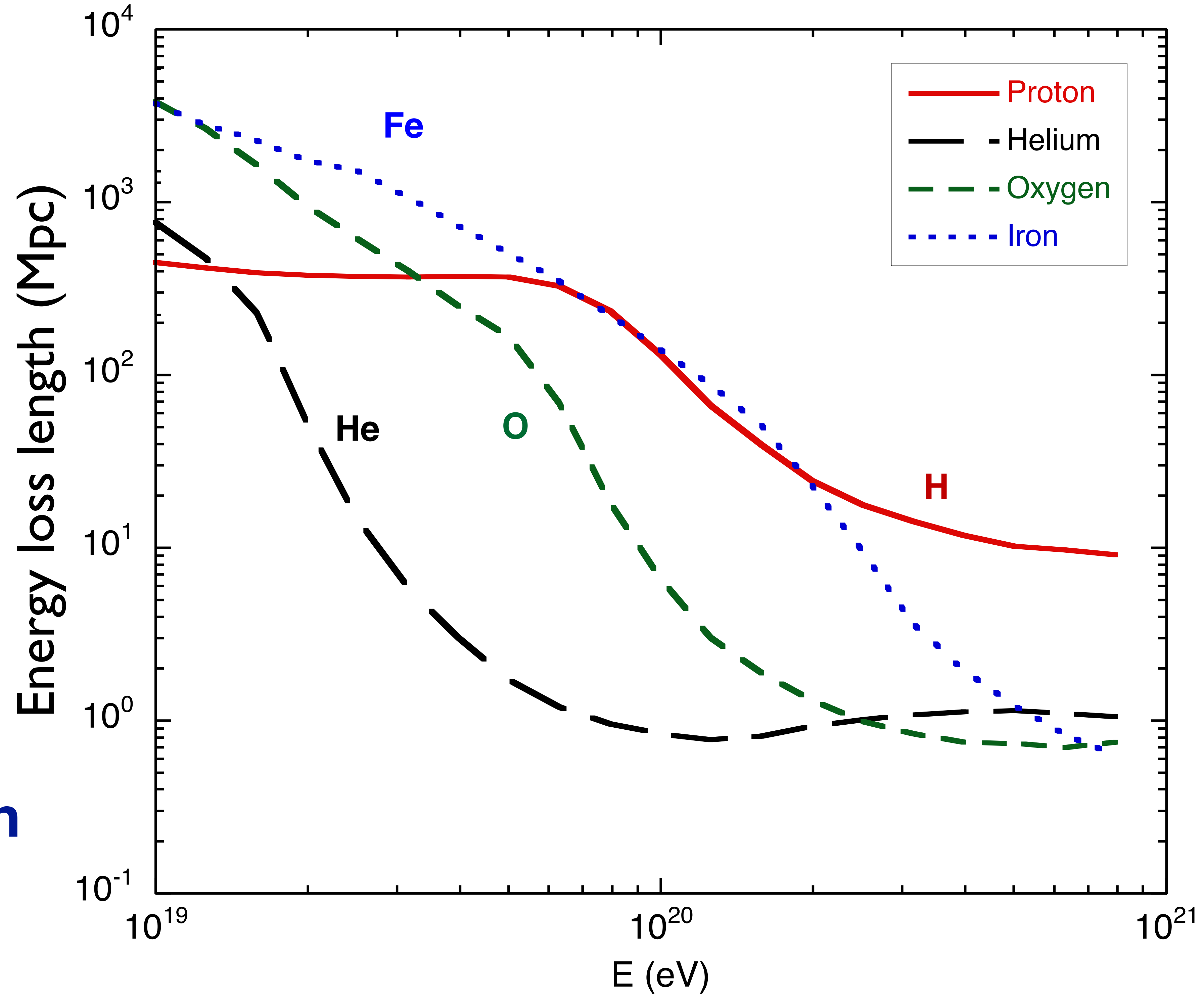

Greisen, Zatsepin & Kuzmin (GZK) effect, 1966

(Allard 2007, Aloisio 2017)

Distance ranges and matter distribution in the Universe

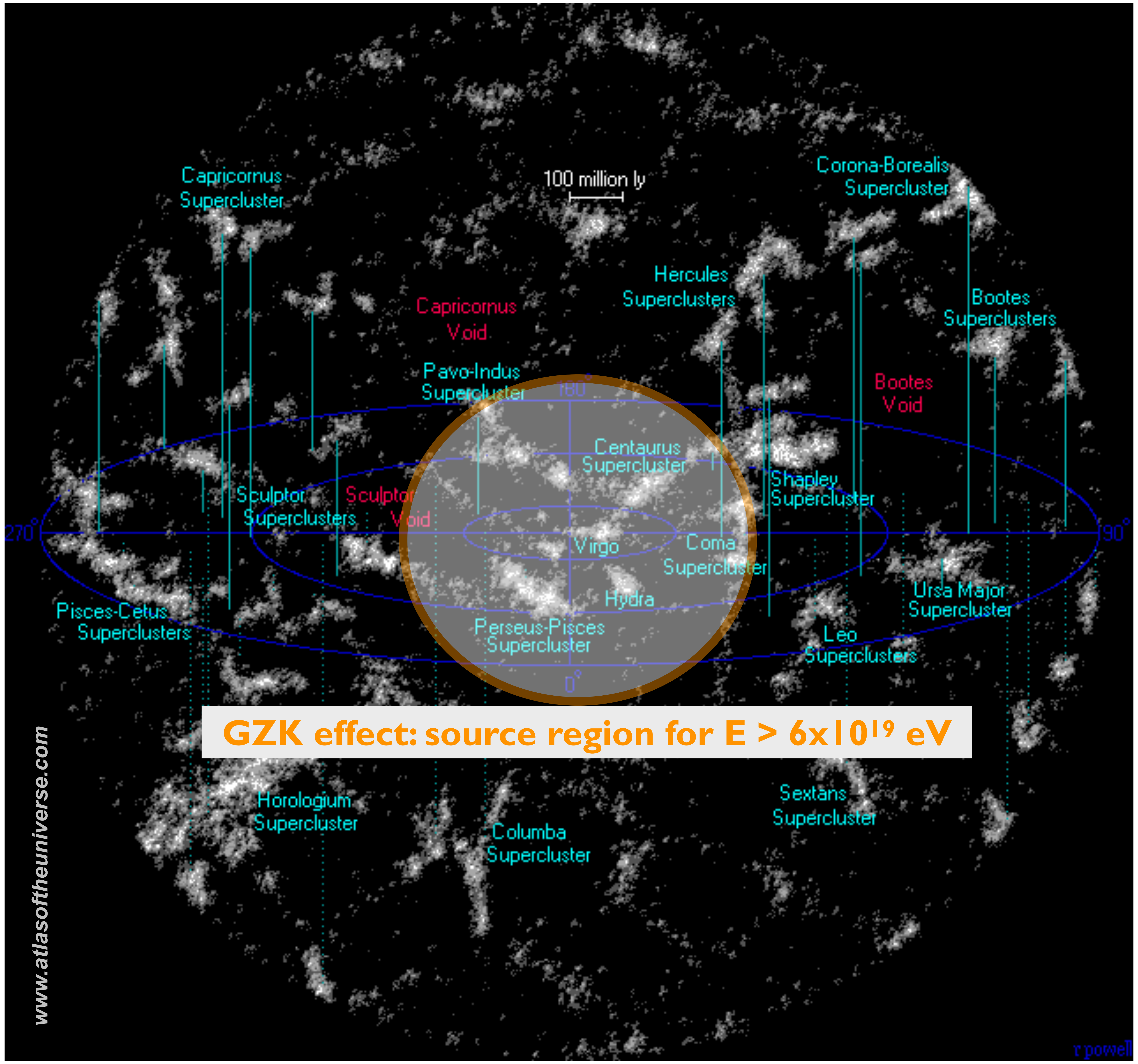

Cosmic rays, gamma-rays

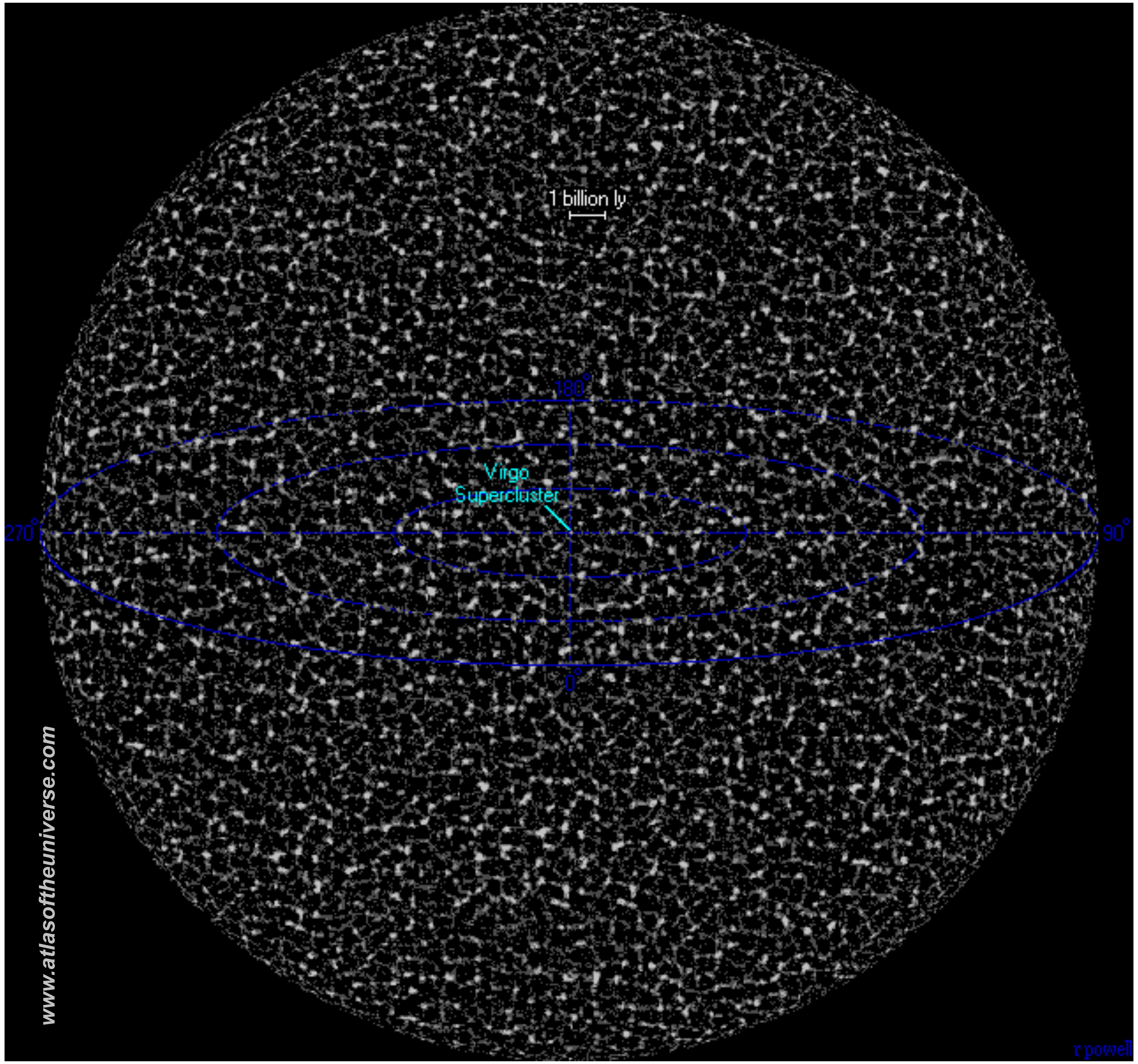

Neutrinos

Source identification by arrival direction distribution

Deflection in Galactic and extragalactic mag. fields

$$\delta \simeq 3^o \frac{B}{3\,\mu G} \frac{L}{kpc} \frac{6\times10^{19} eV}{E/Z}$$

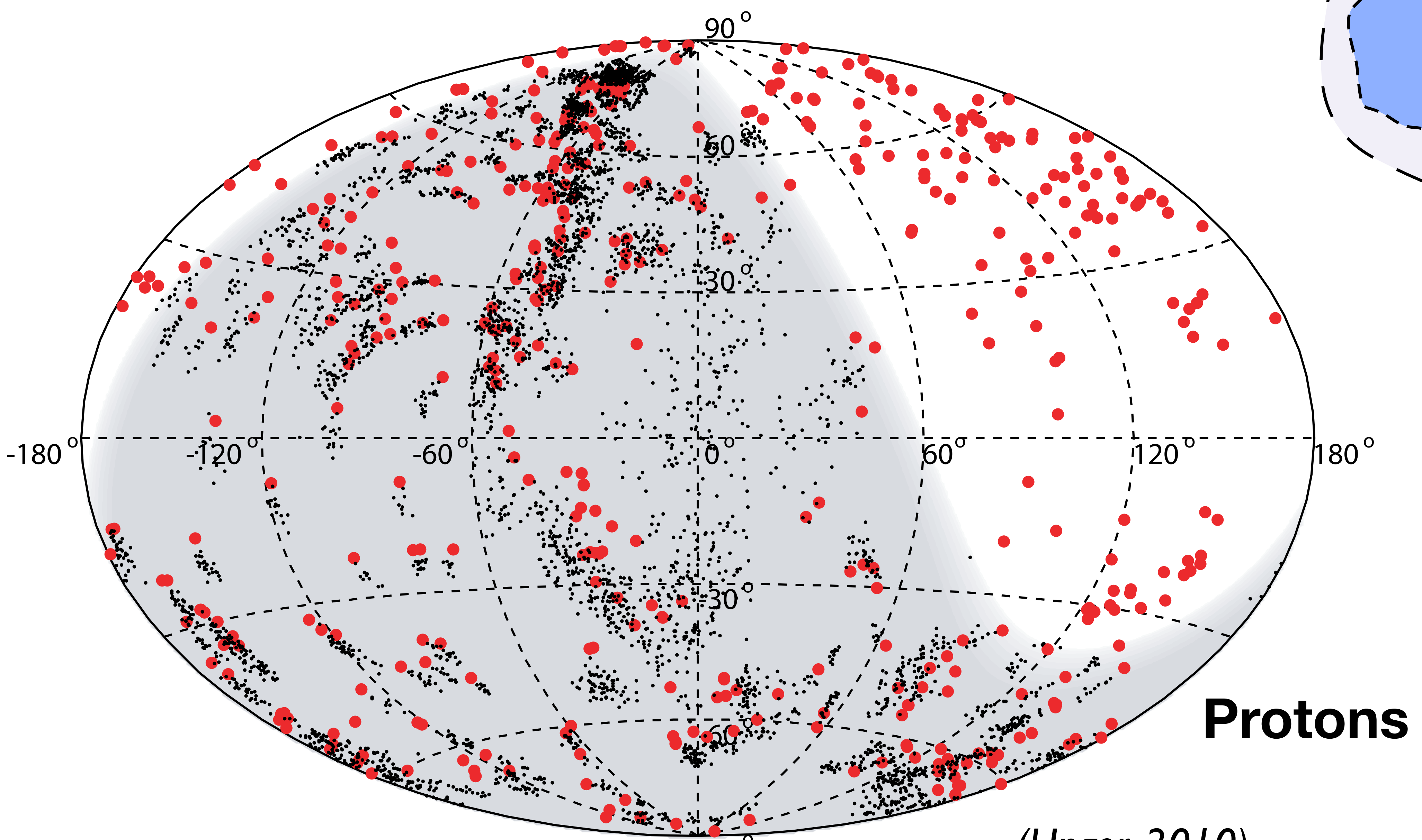

(Unger, 2010)

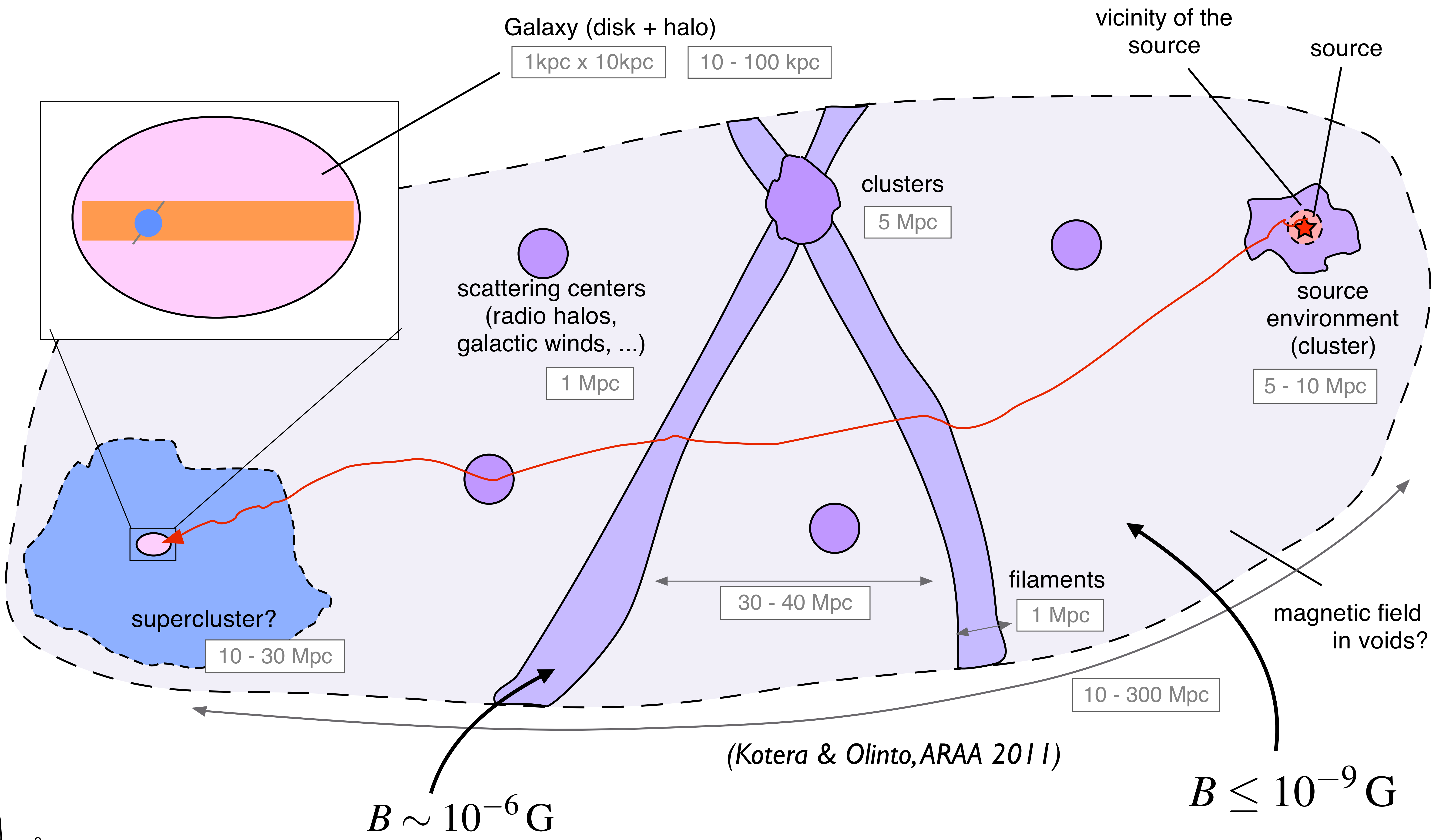

(Kotera & Olinto, ARAA 2011)

Anisotropy in arrival direction distribution on small, intermediate and large scales

Multi-messenger signals (gamma-rays and neutrinos)

Source identification by arrival direction distribution

Deflection in Galactic and extragalactic mag. fields

$$\delta \simeq 3^{o} \frac{B}{3\,\mu G} \frac{L}{kpc} \frac{6\times 10^{19} eV}{E/Z}$$

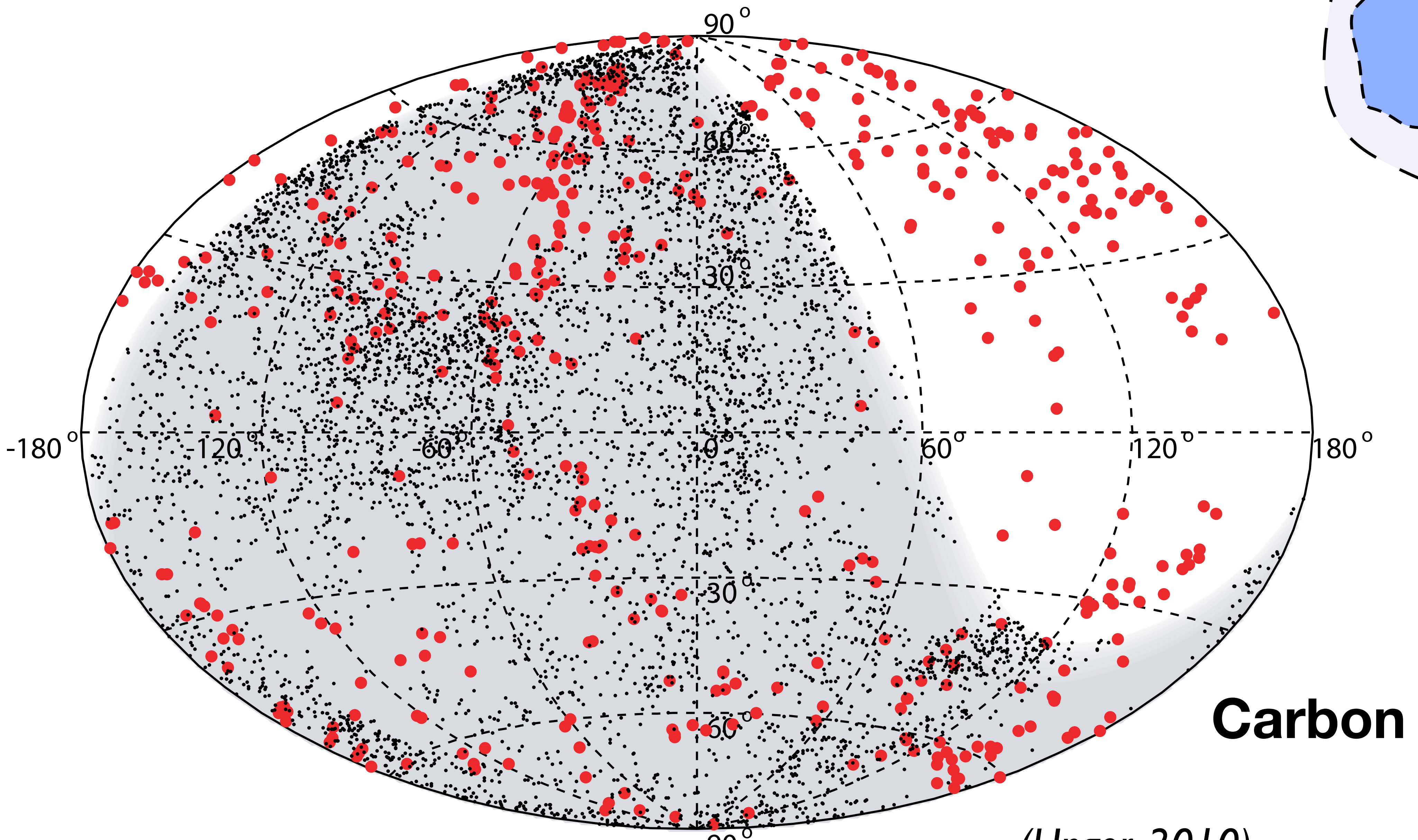

(Unger, 2010)

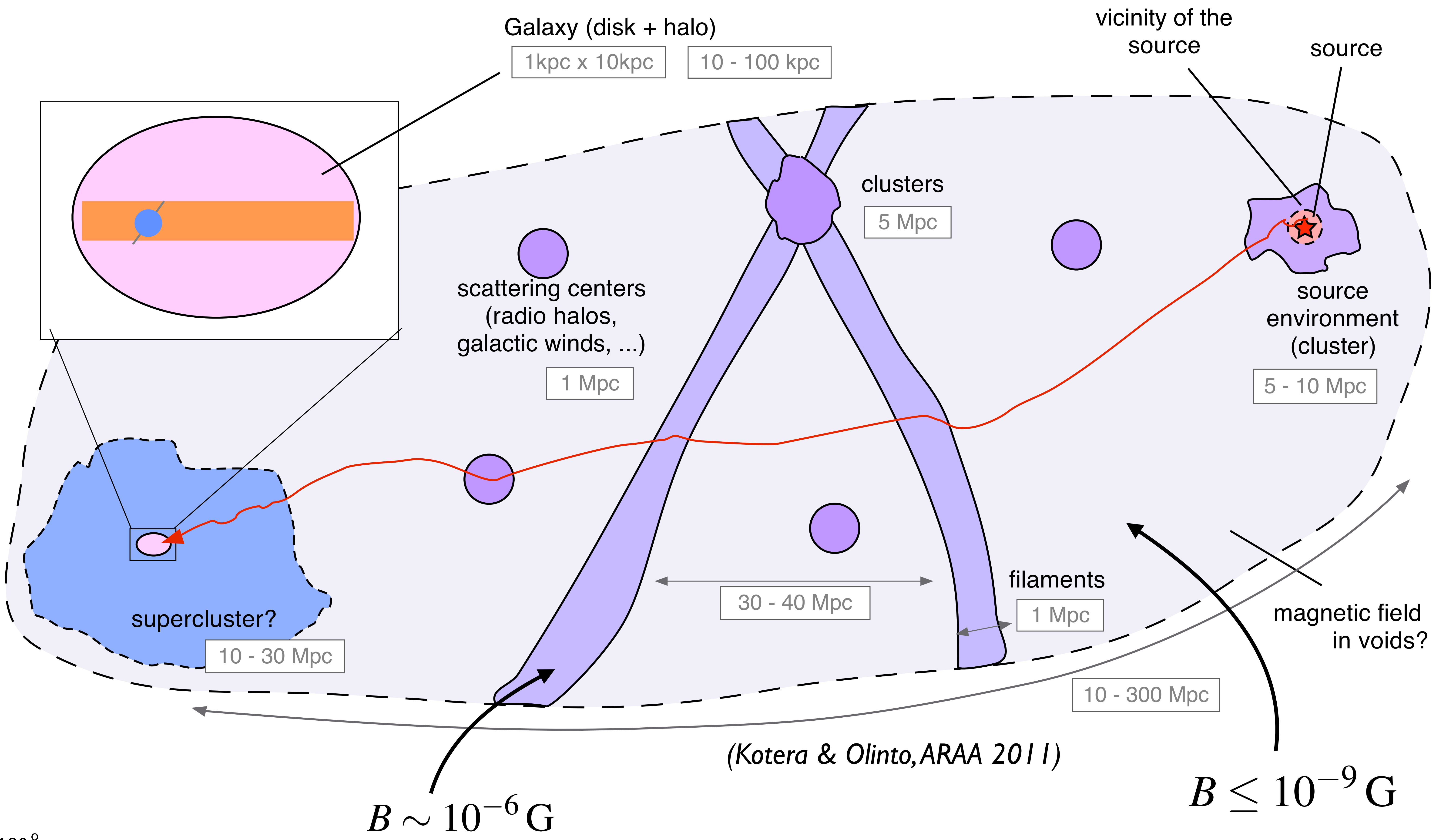

(Kotera & Olinto, ARAA 2011)

Anisotropy in arrival direction distribution on small, intermediate and large scales

Multi-messenger signals (gamma-rays and neutrinos)

Hillas´ model of cosmic ray flux

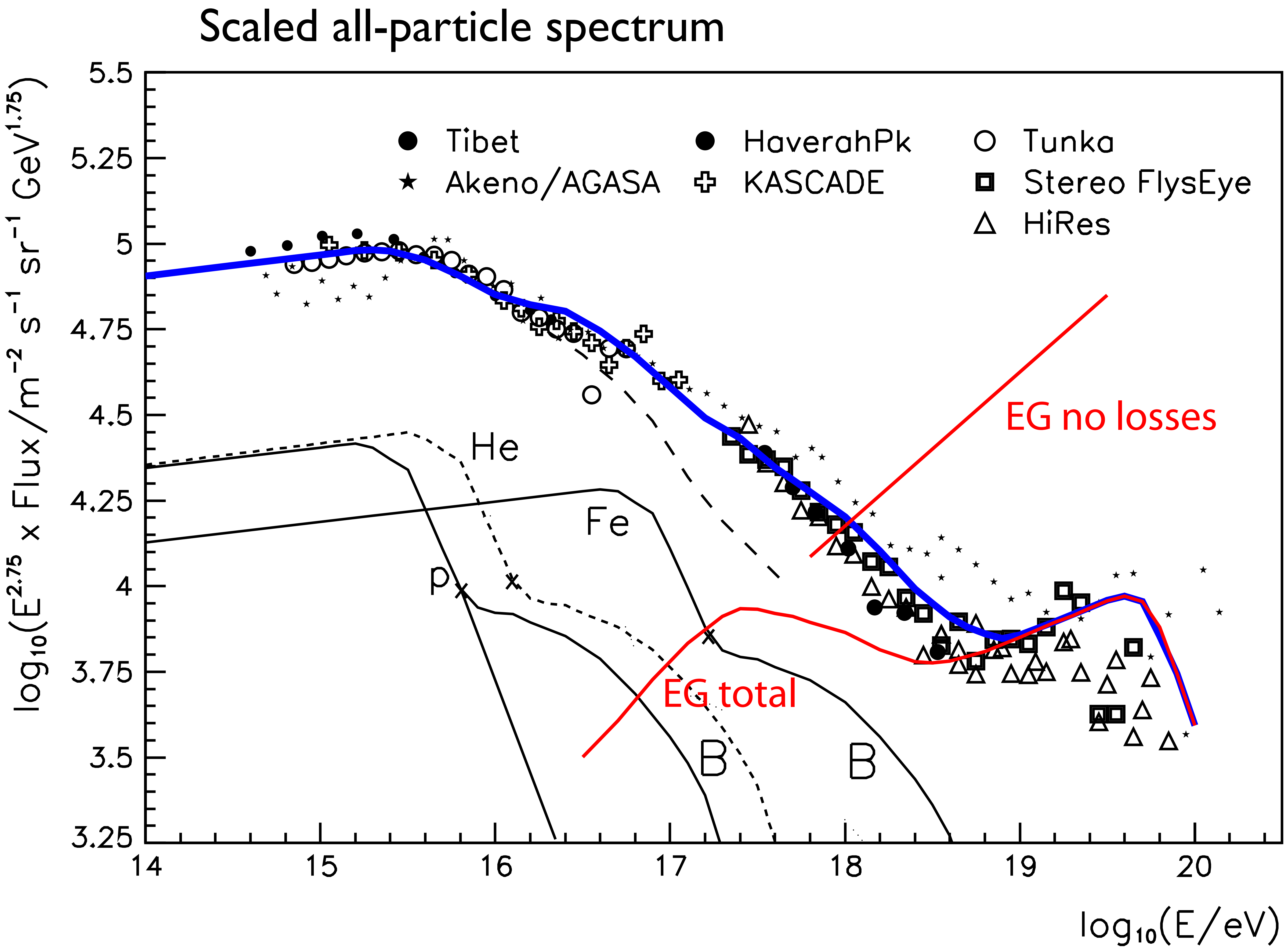

Mainly protons as UHECR

$$\frac{dN_{\mathrm{inj}}}{dE} \sim E^{-2.3}$$

Deformation of injected spectrum fully understood

Need additional "component B"

(Hillas J. Phys. G31, 2005)

Standard models of ultra-high energy cosmic rays (2005)

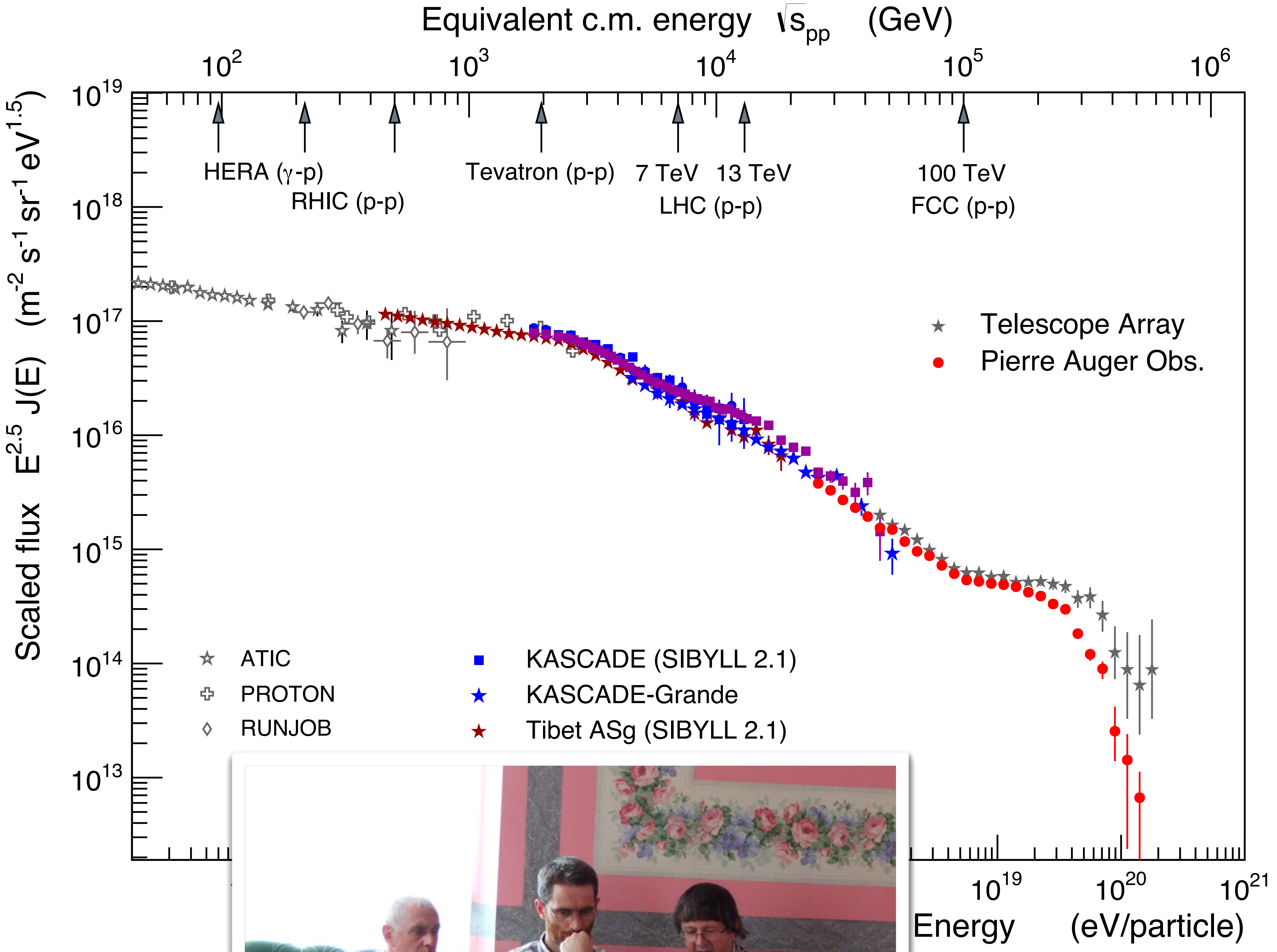

Berezinsky

Hillas

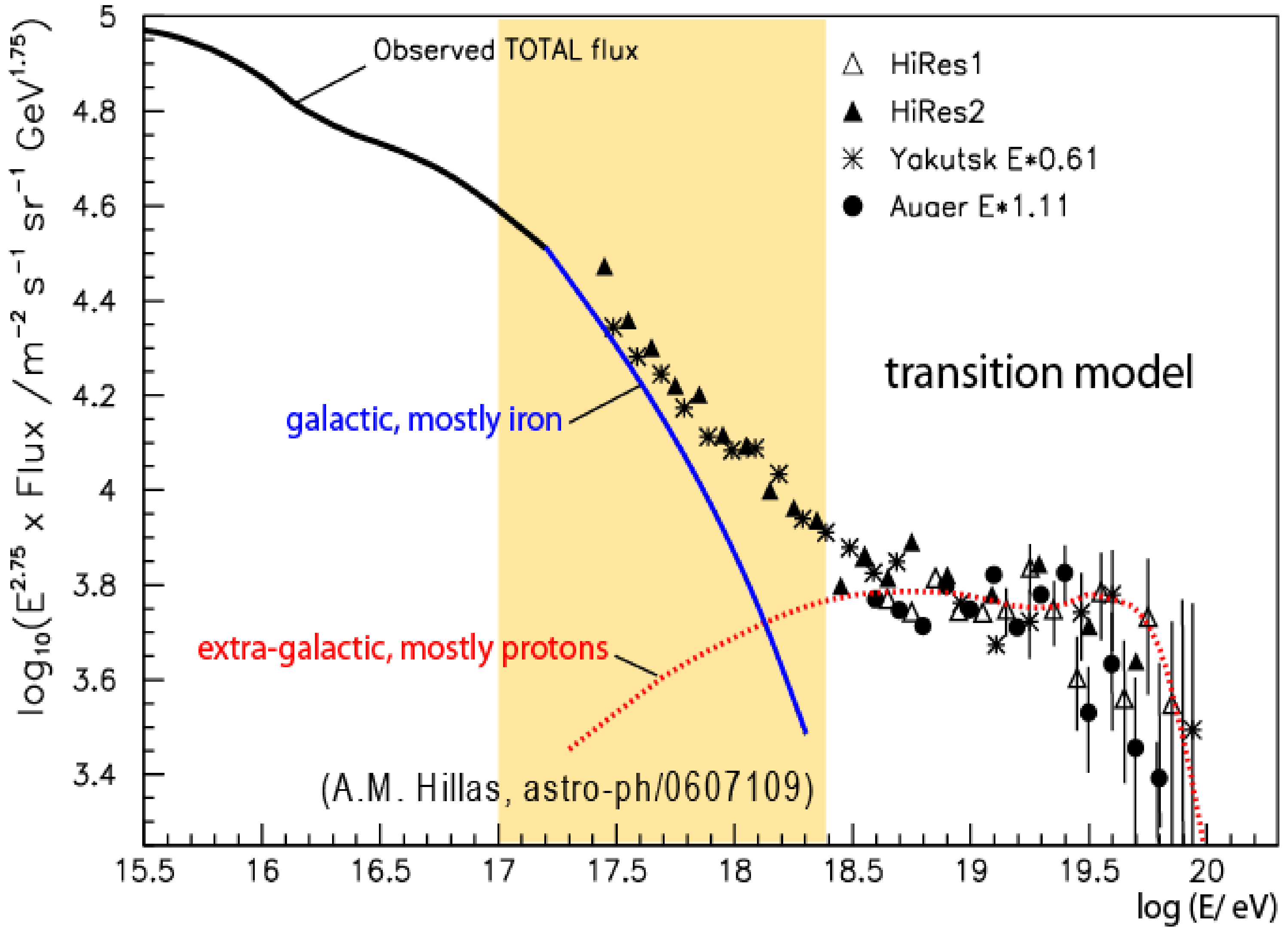

Ankle model: Hillas, Wolfendale et al.

$$\frac{dN_p}{dE} \sim E^{-2.3}$$

(J. Phys. G31 (2005) R95)

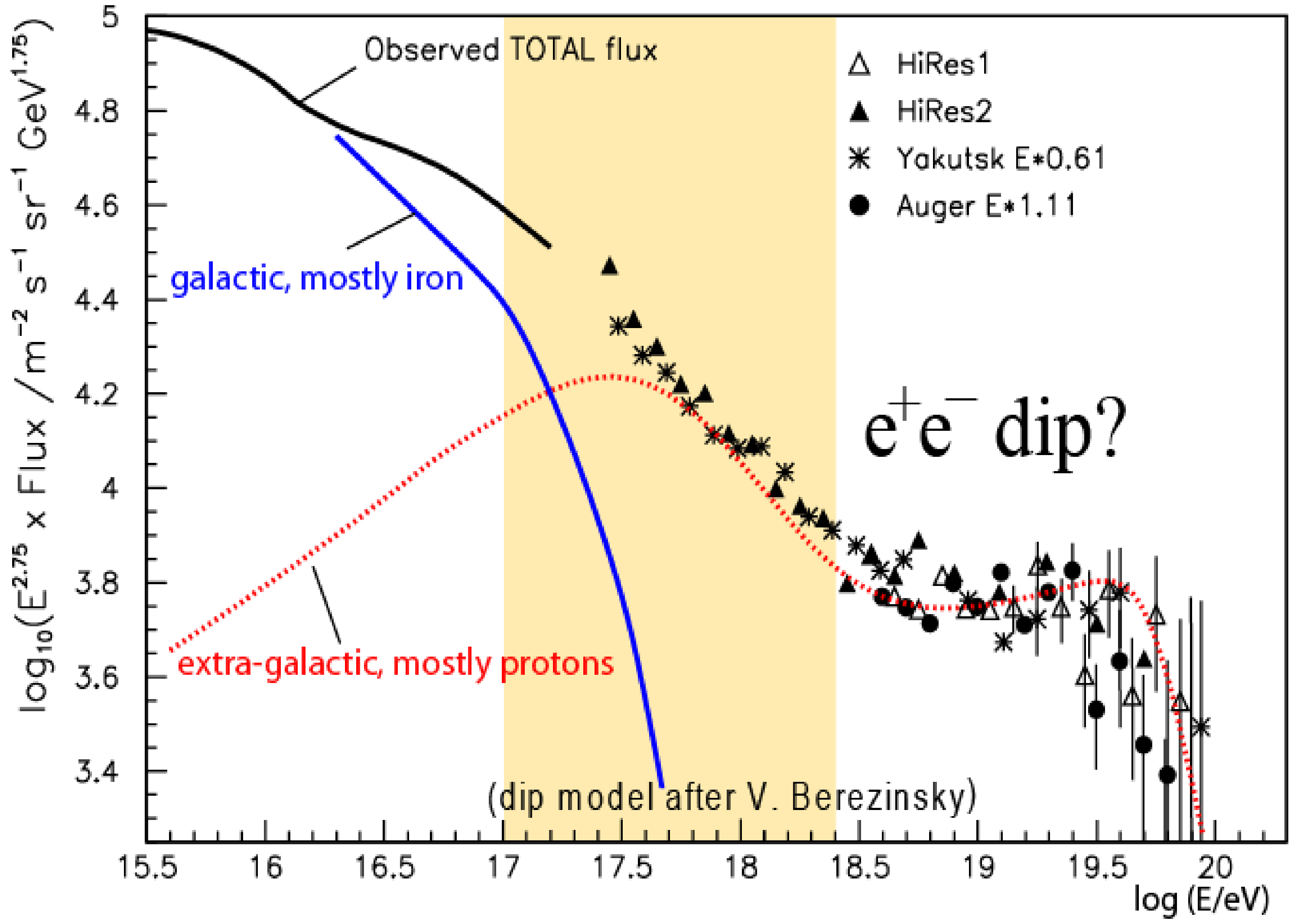

Dip model: Berezinsky et al.

$$p\,\gamma_{\mathrm{CMB}} \rightarrow p\,e^+e^-$$

$$\frac{dN_p}{dE} \sim E^{-2.7}$$

(PRD 74 (2006) 043005)

Observatories for ultra-high energy cosmic rays

T Auger Observatory

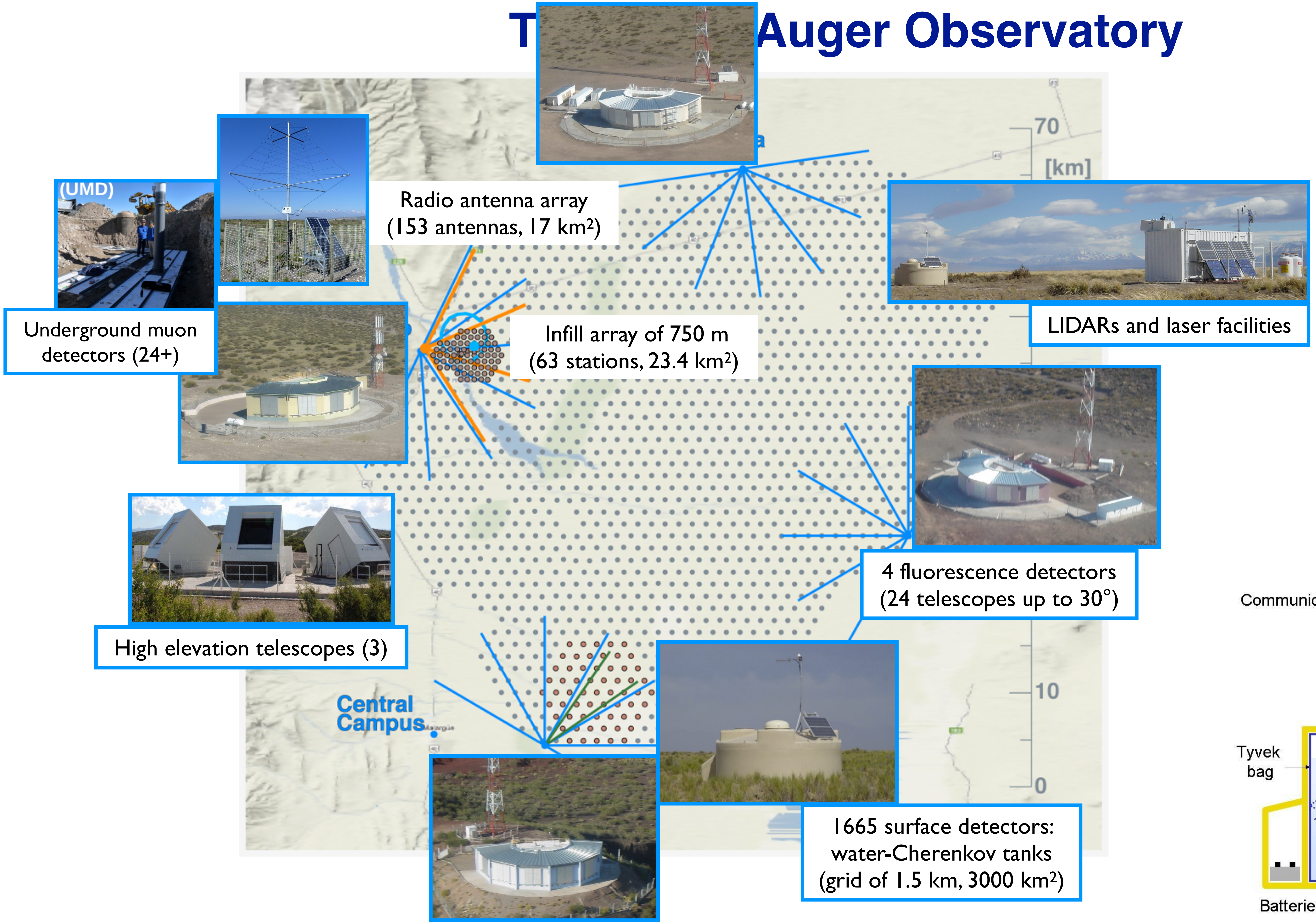

Pierre Auger Observatory
Province Mendoza, Argentina

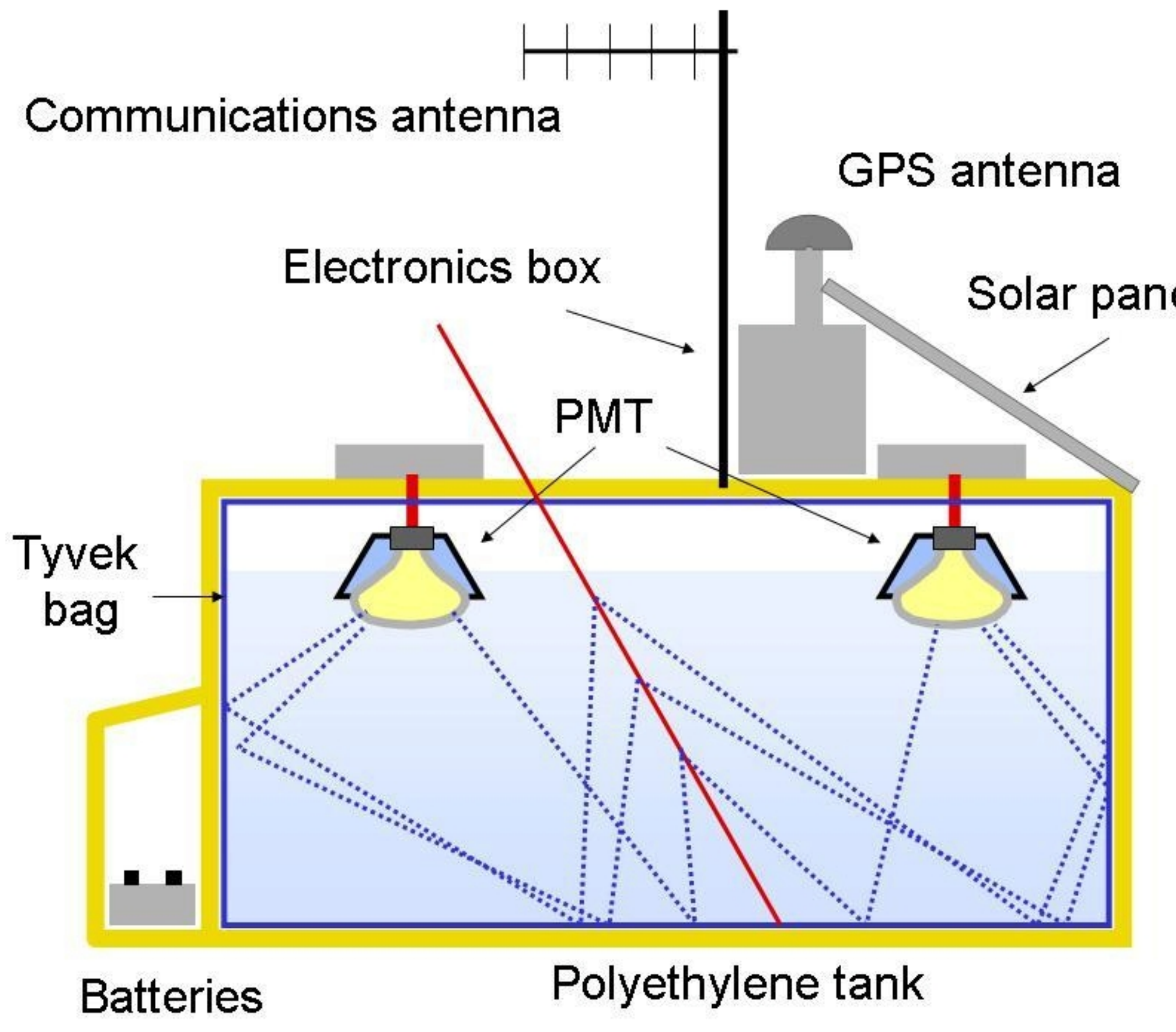

Telescope Array (TA)

Middle Drum: based on HiRes II

TALE (TA low energy extension)

Infill array and high elevation telescopes

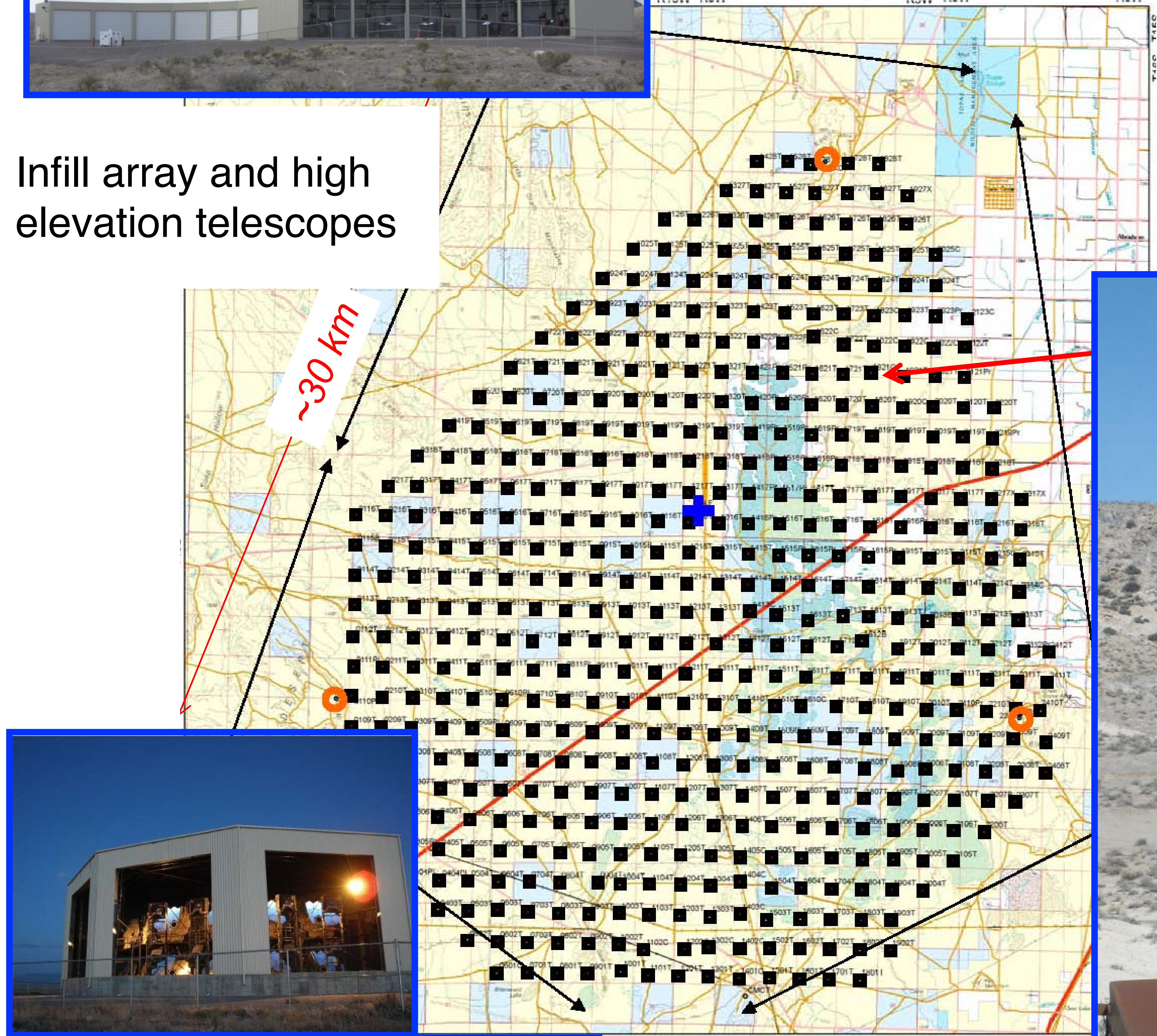

507 surface detectors:
double-layer scintillators
(grid of 1.2 km, 680 km^2)

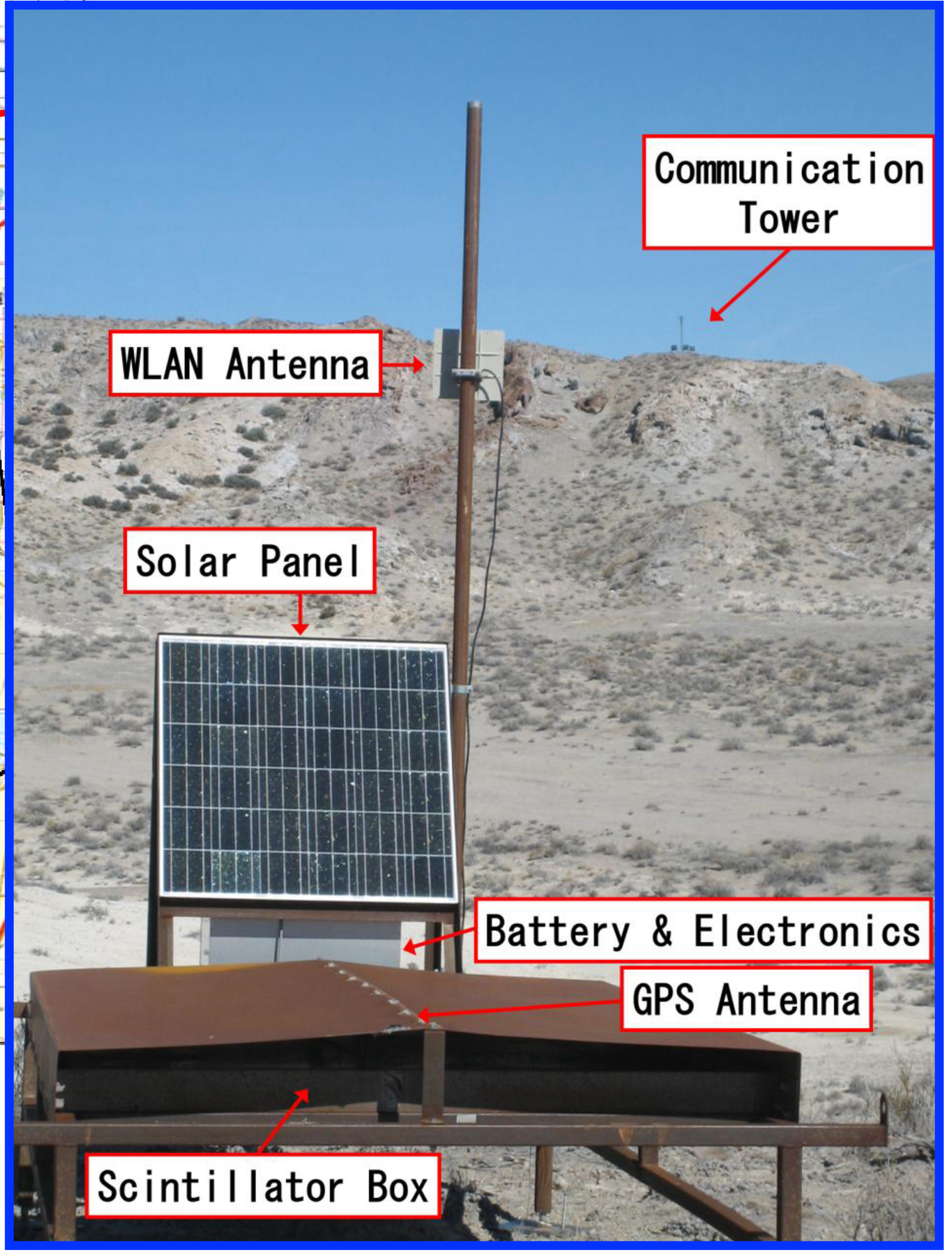

3 fluorescence detectors
(2 new, one station HiRes II)

Northern hemisphere: Delta, Utah, USA

TA
(Delta, Utah)

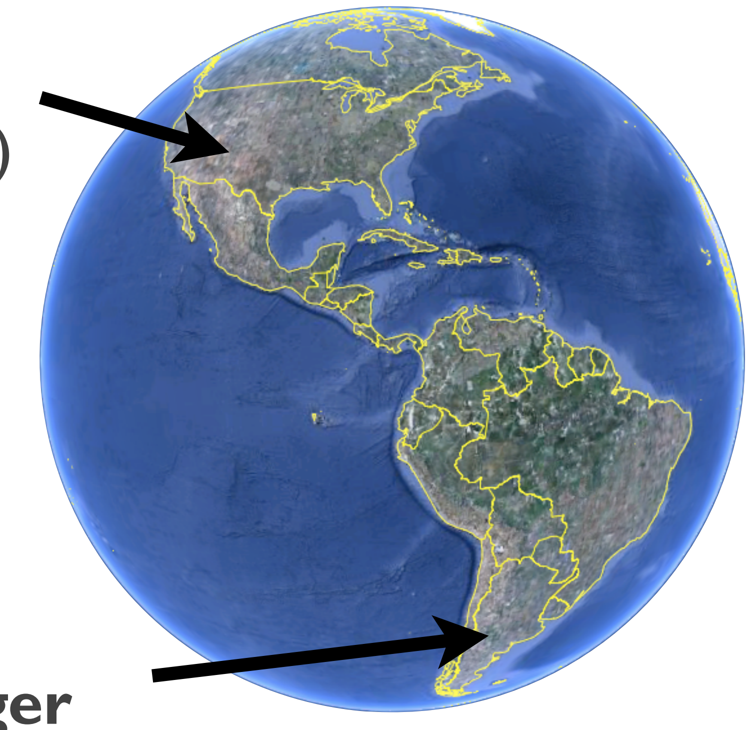

Auger

Exposure of observatories
(Auger 19 years, TA 16 years)

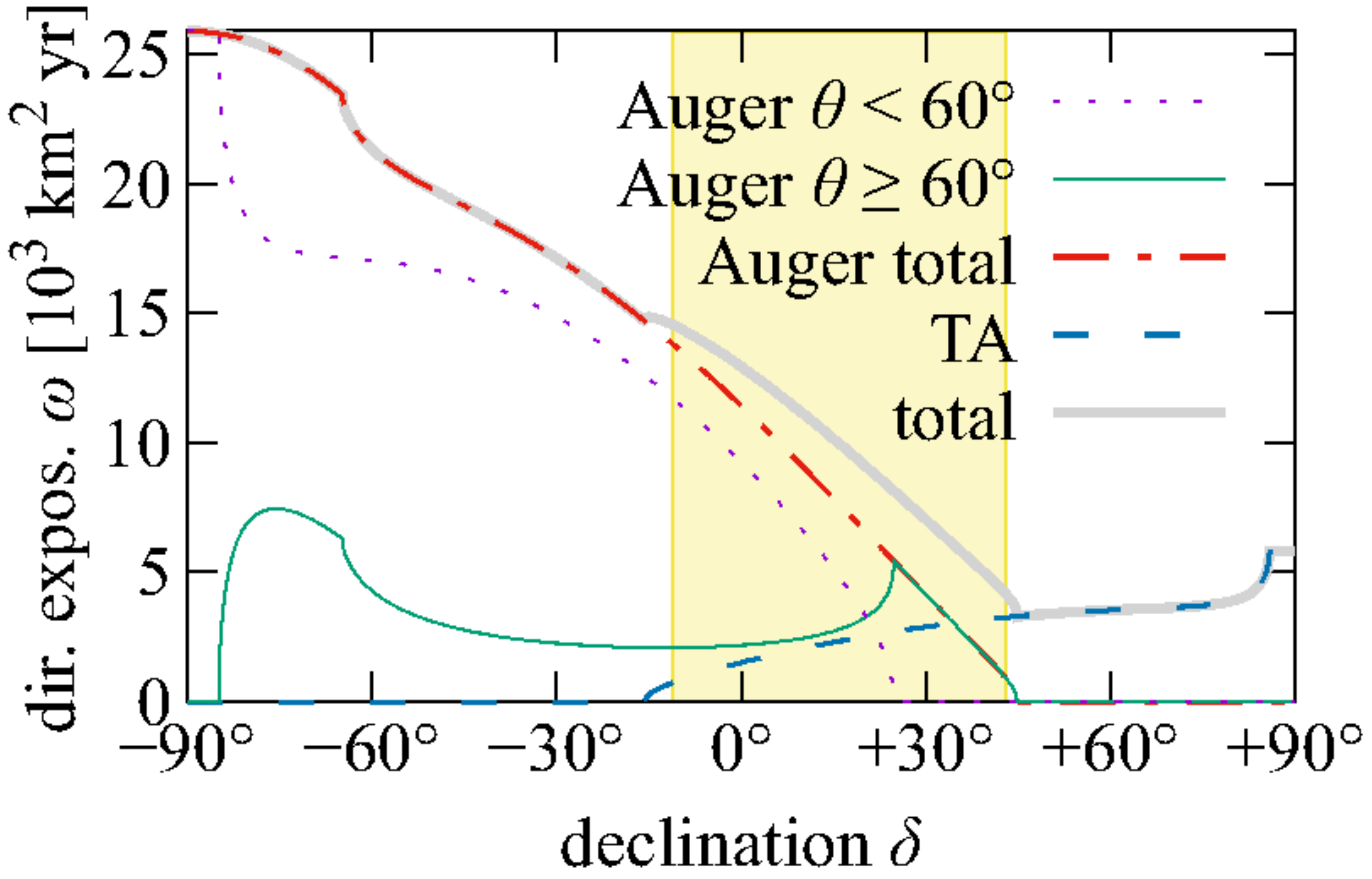

Upgrades AugerPrime and TAx4 – Phase II

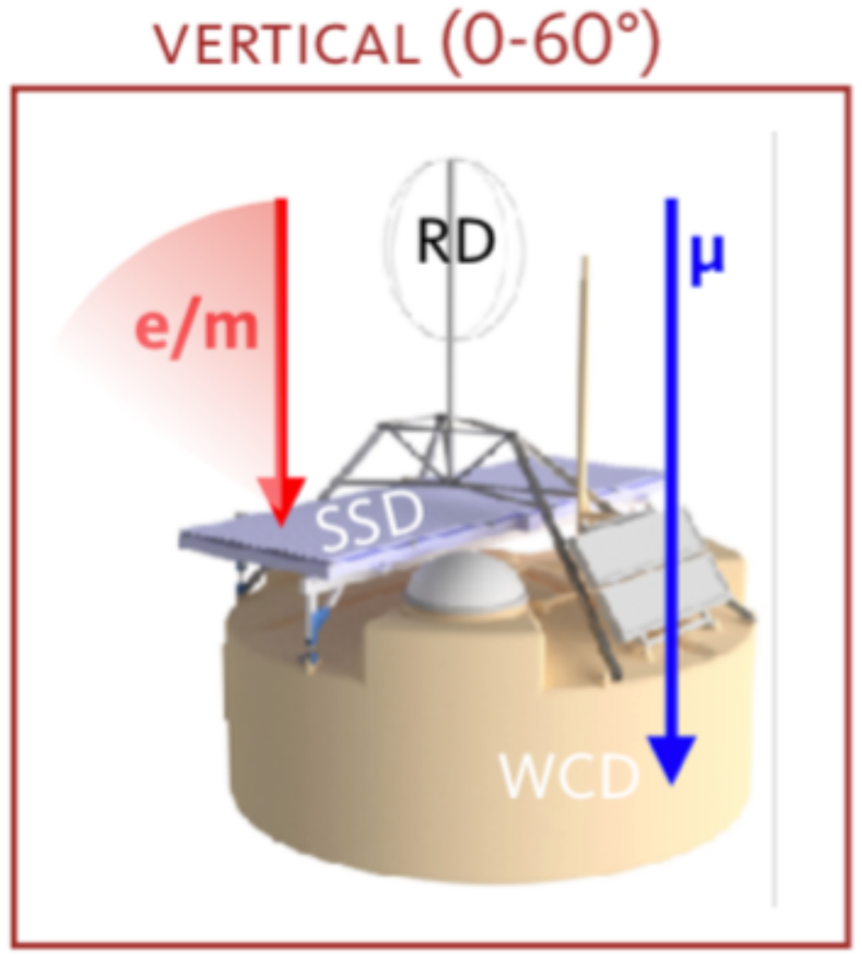

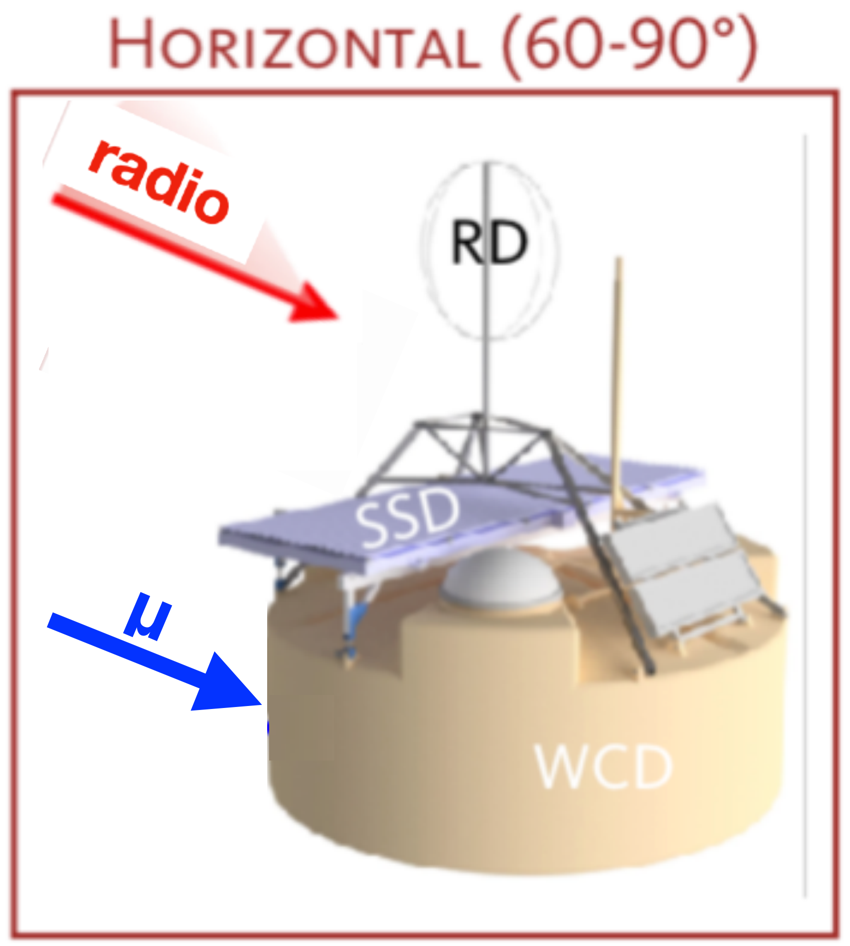

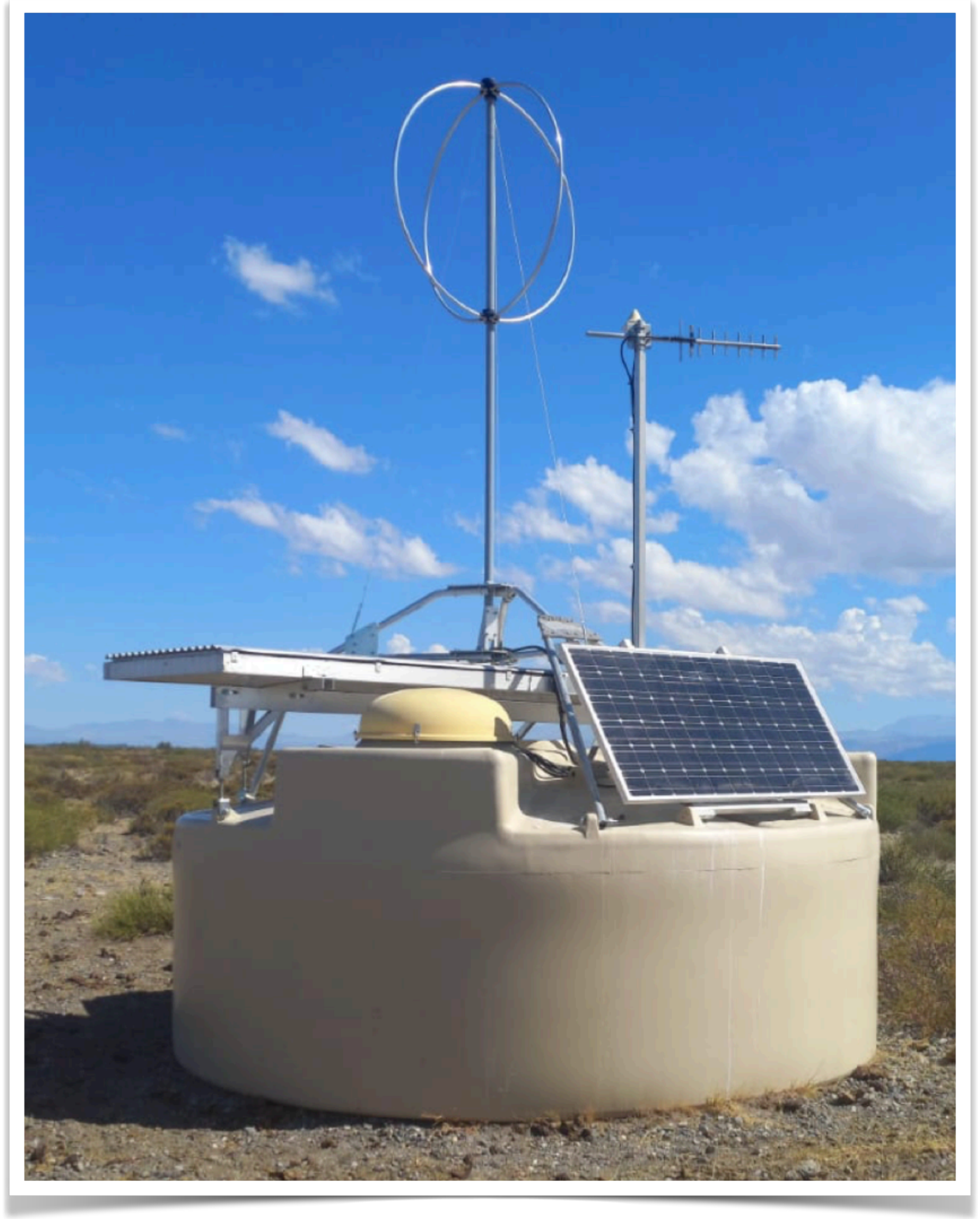

Auger and TAx4

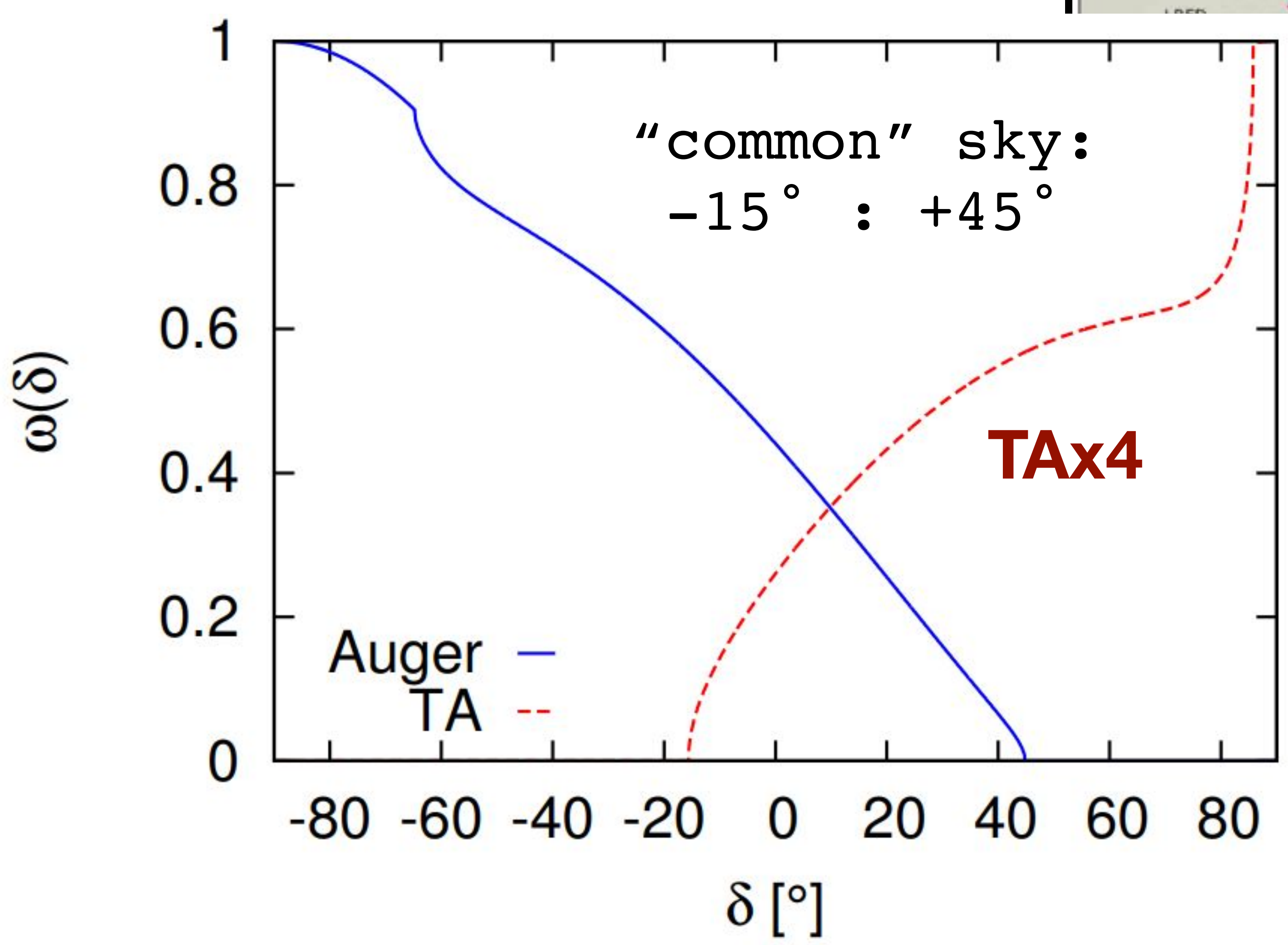

Detector spacing 1.2 km and 2.08 km, 257 out of 500 detectors installed

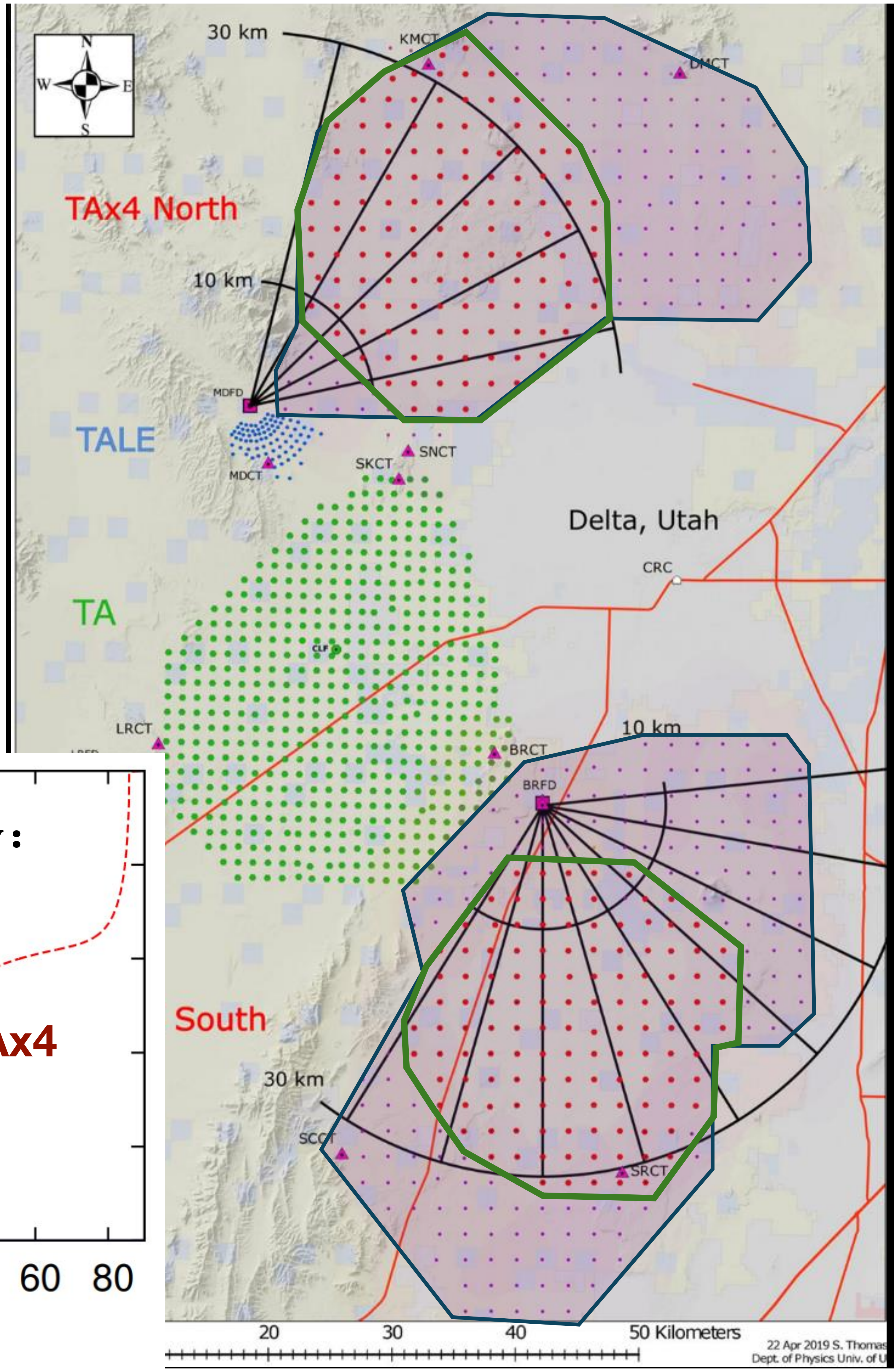

Measurement principles (hybrid observation)

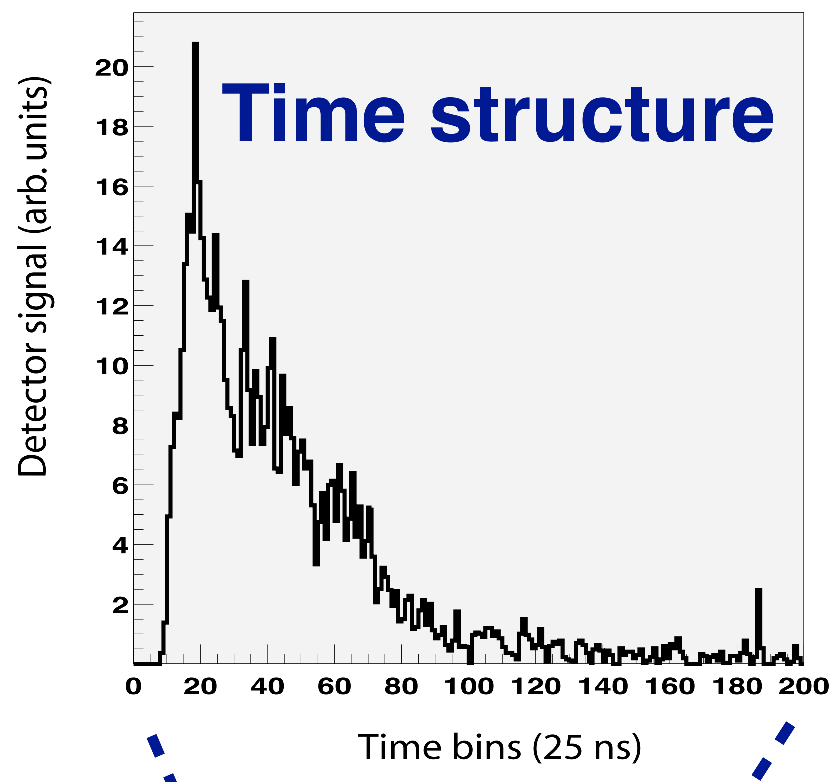

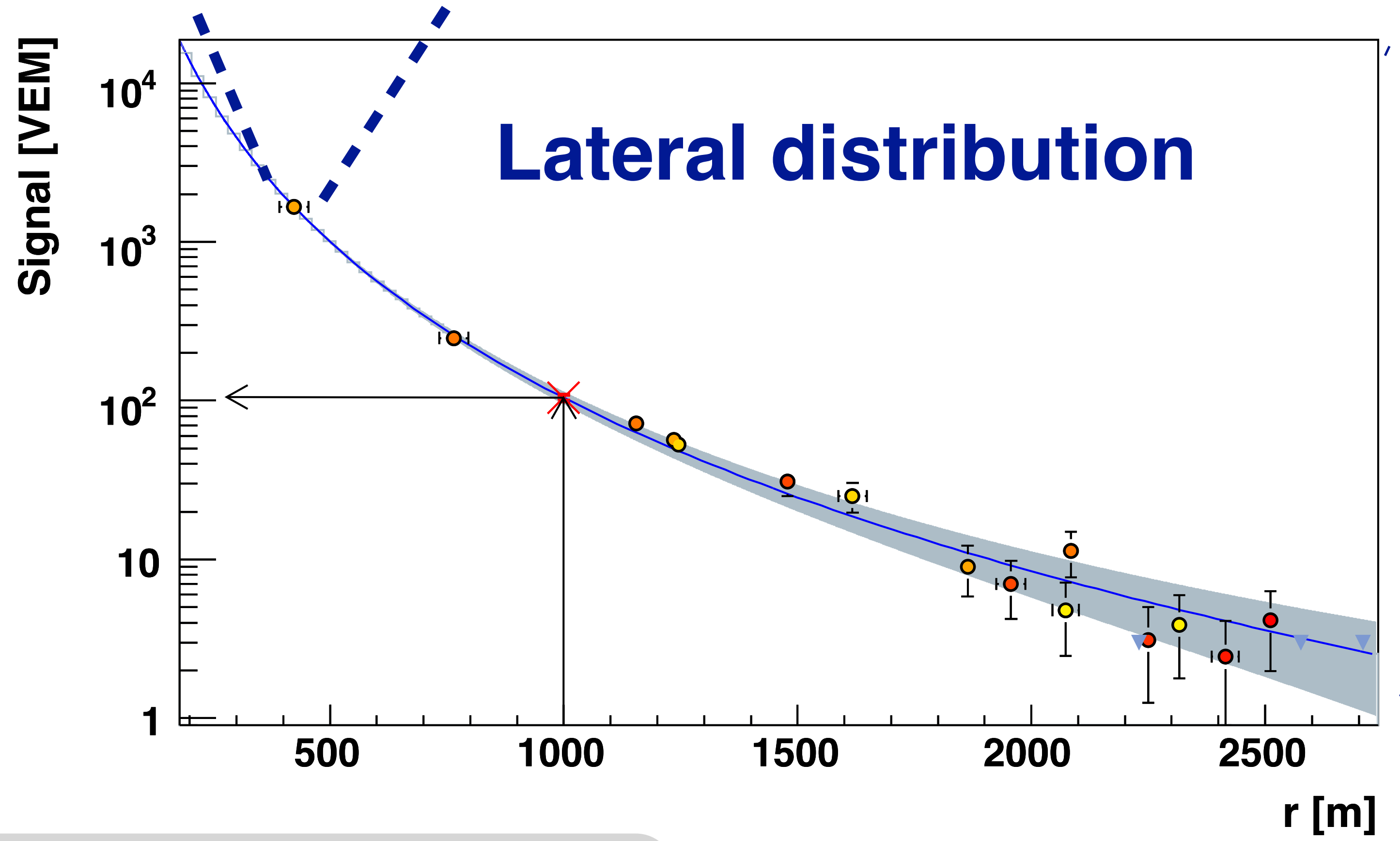

$$E_{\text{rec}} = f(S_{1000}, \theta)$$

Surface Detector (SD)
100% duty cycle

Fluorescence Detector (FD):
15% duty cycle

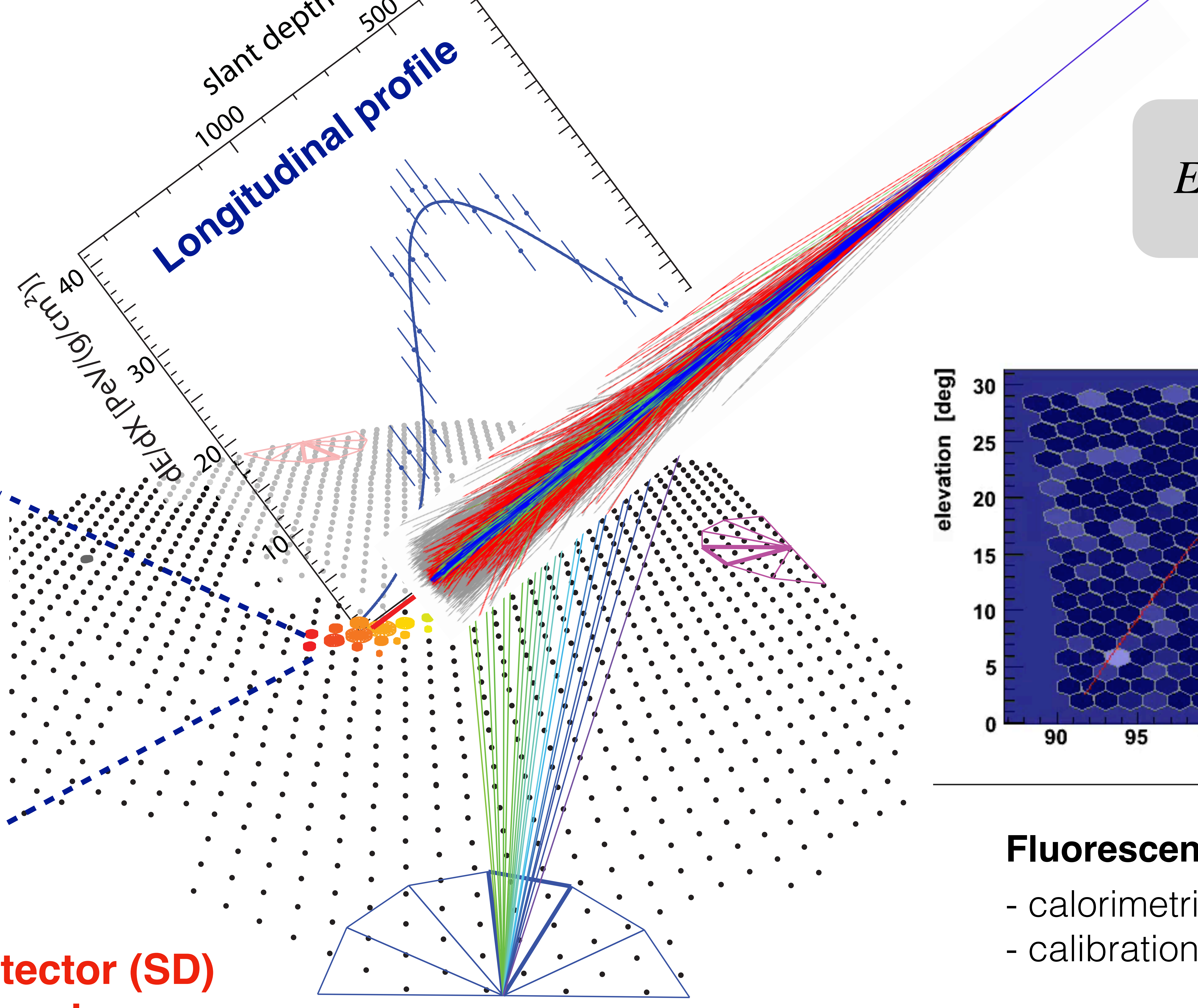

$$E_{\text{cal}} = \int_0^\infty \left(\frac{dE}{dX}\right)_{\text{obs}} dX$$

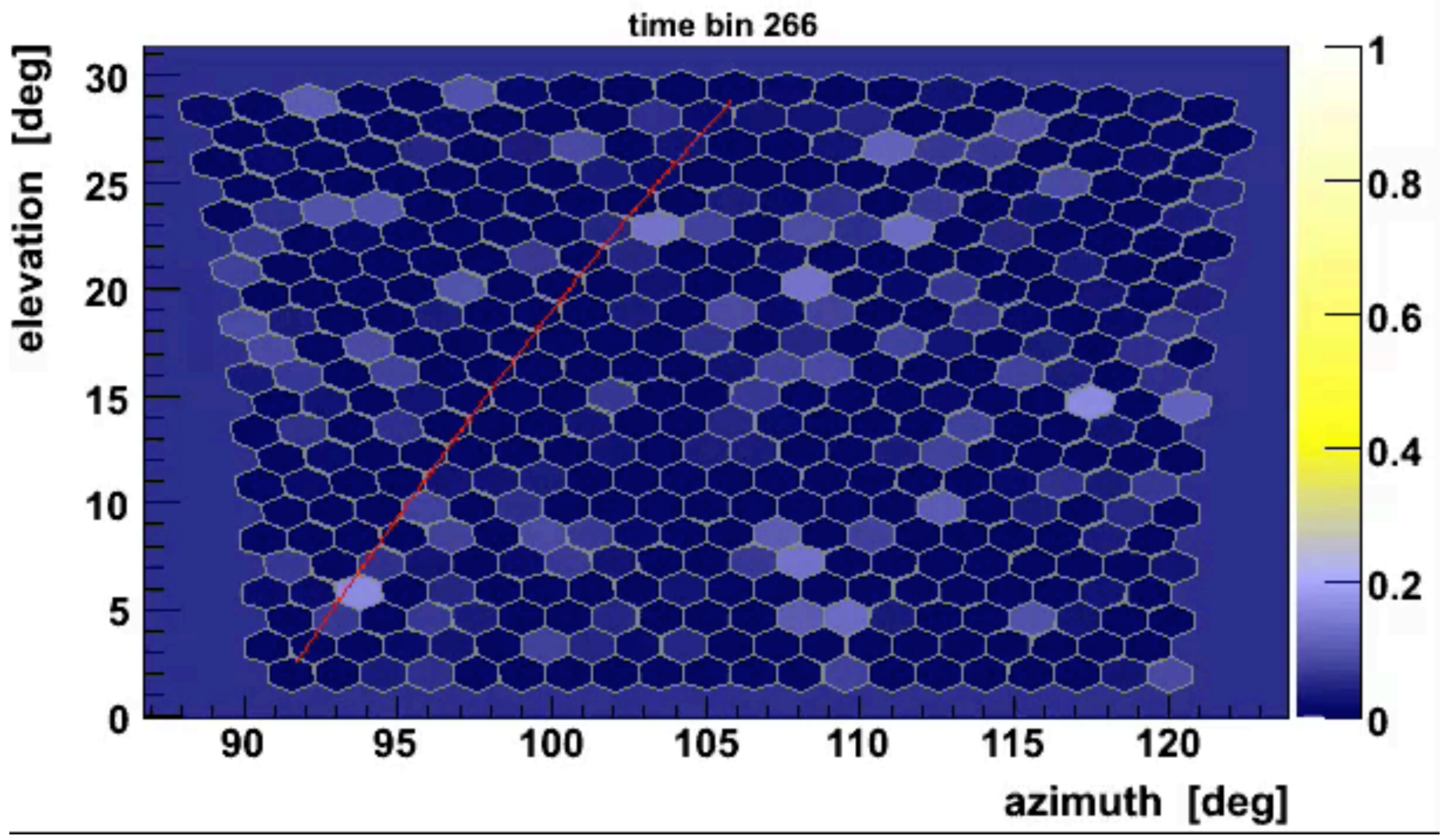

Fluorescence signal:

- calorimetric in shower energy
- calibration of surface detector array

Measurement principles (hybrid observation)

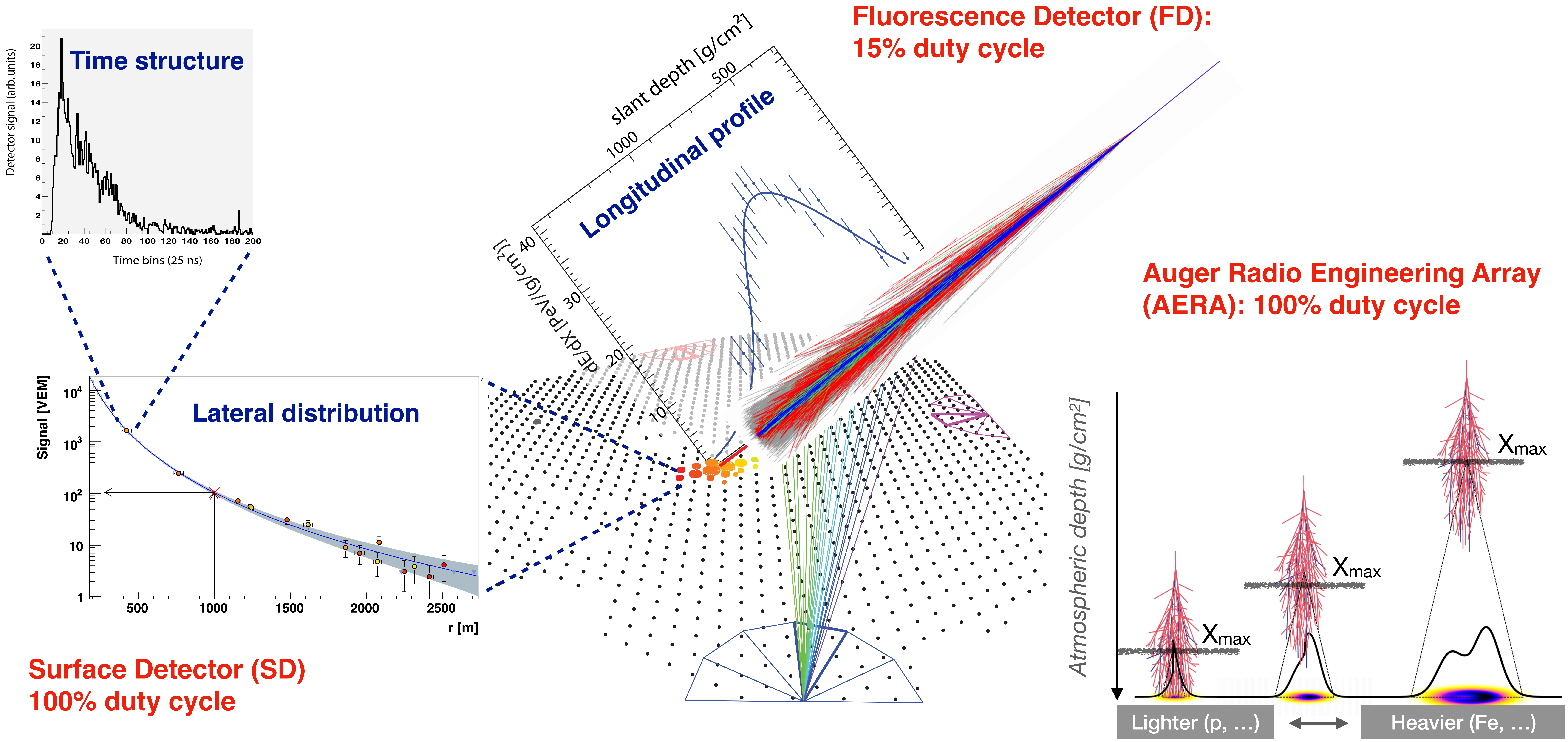

Examples of observed events

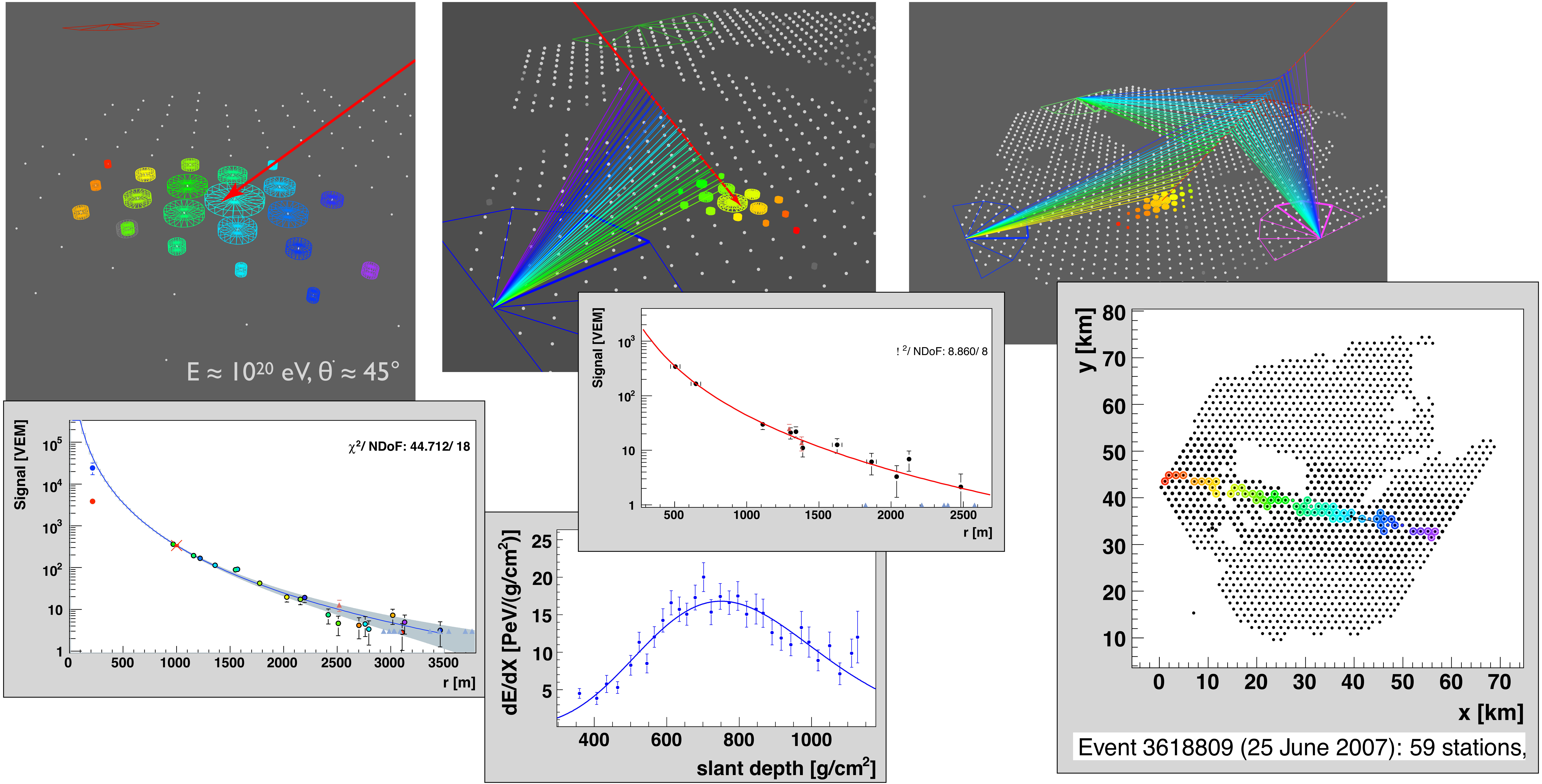

Exposure Phase I and calibration of Auger data sets

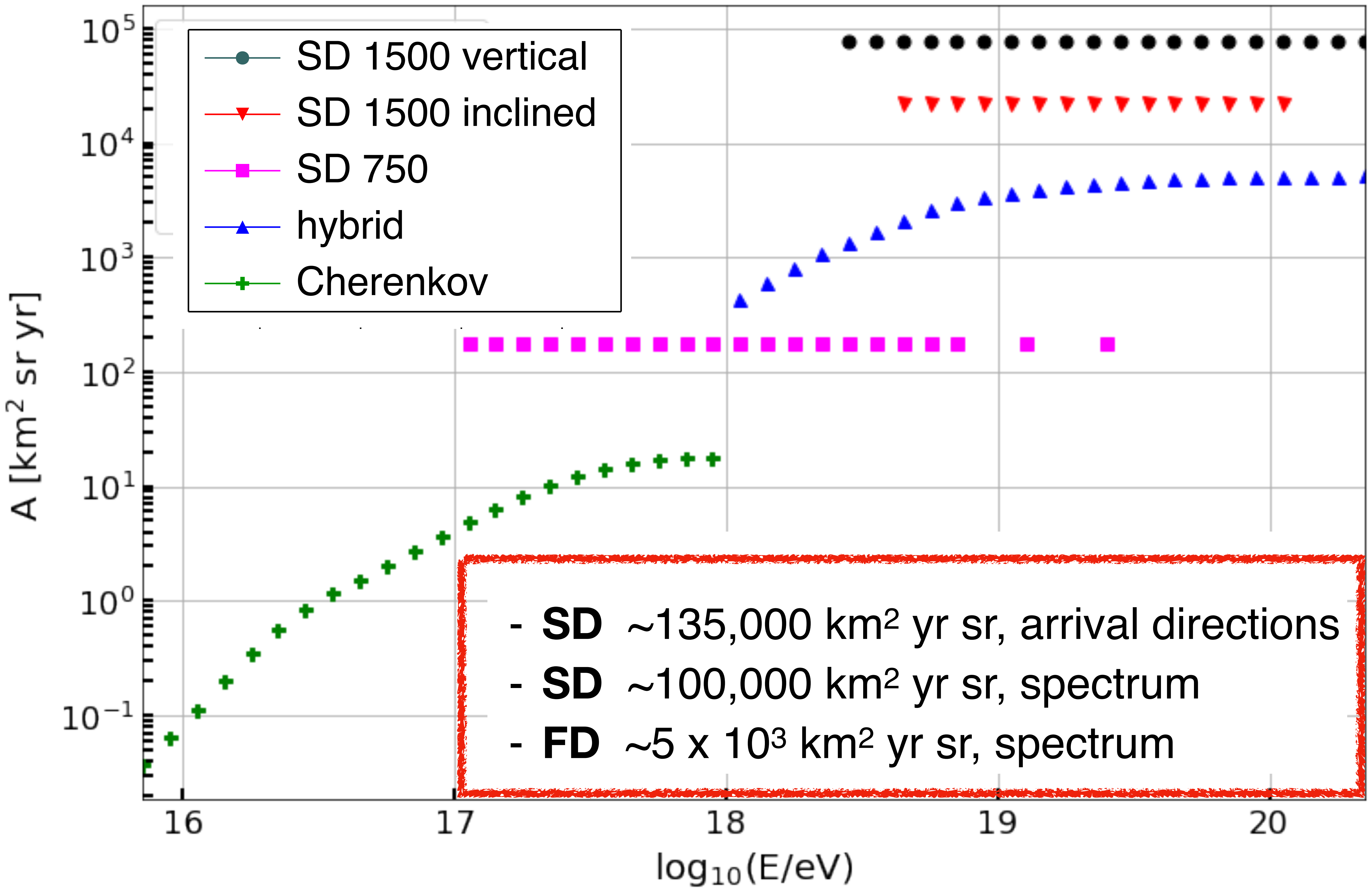

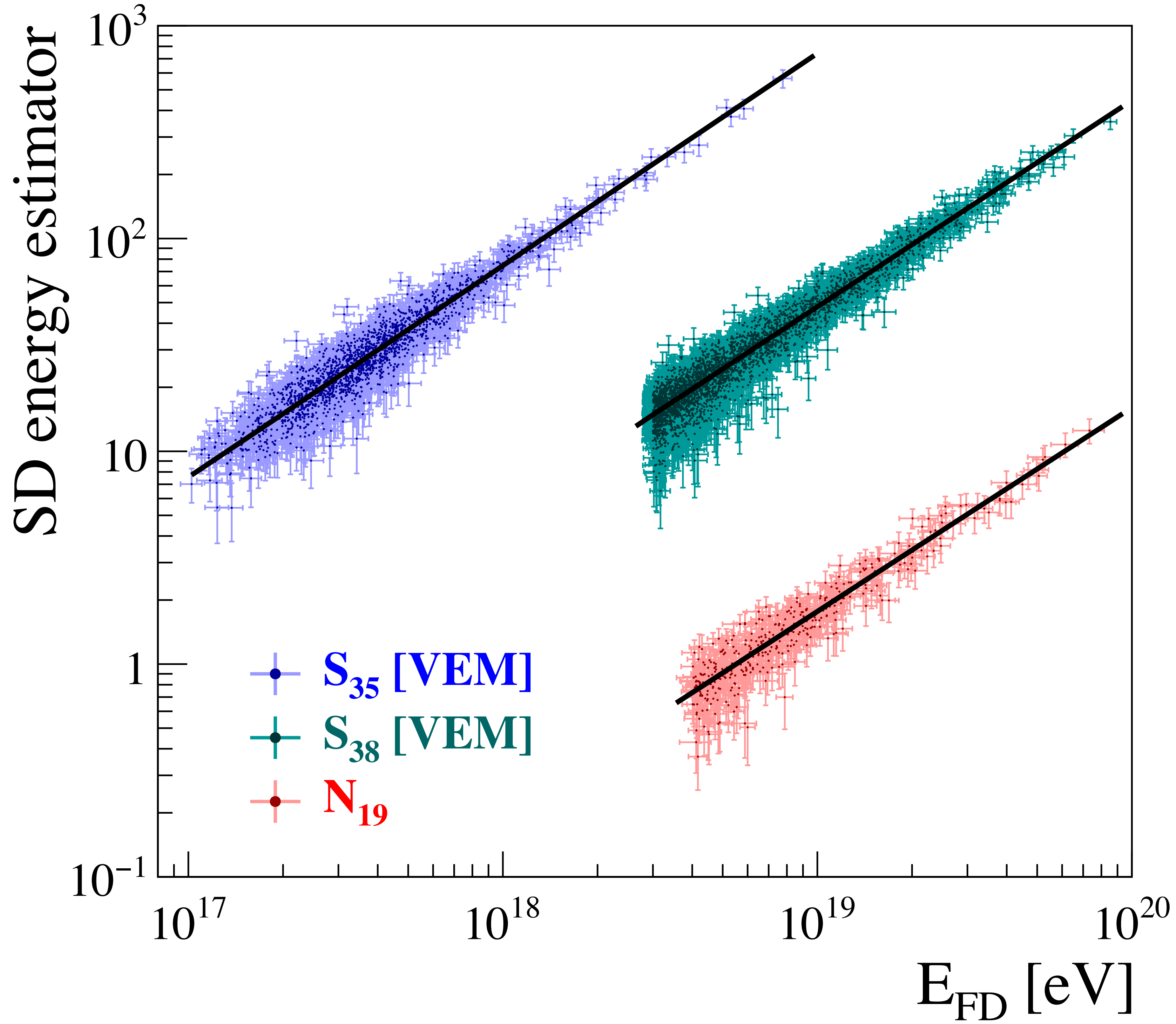

$$E_{\rm FD} = A S_{35}^{B}$$

E > 10^{17} eV
σ(E) : 25% - 10%

$$E_{\rm FD} = A S_{38}^{B}$$

E > $10^{18.4}$ eV
σ(E) : 22% - 7%

$$E_{\rm FD} = A N_{19}^{B}$$

E > $10^{18.6}$ eV
σ(E) ~ 19%

SD 1500 m vertical – S_{38}
- S(1000)+CIC
- threshold 2.5 EeV

SD 750 m – S_{35}
- S(450)+CIC
- threshold 0.1 EeV

SD 1500 m inclined – N_{19}
- scaling parameter
- threshold 4 EeV

Energy calibration with fluorescence telescopes

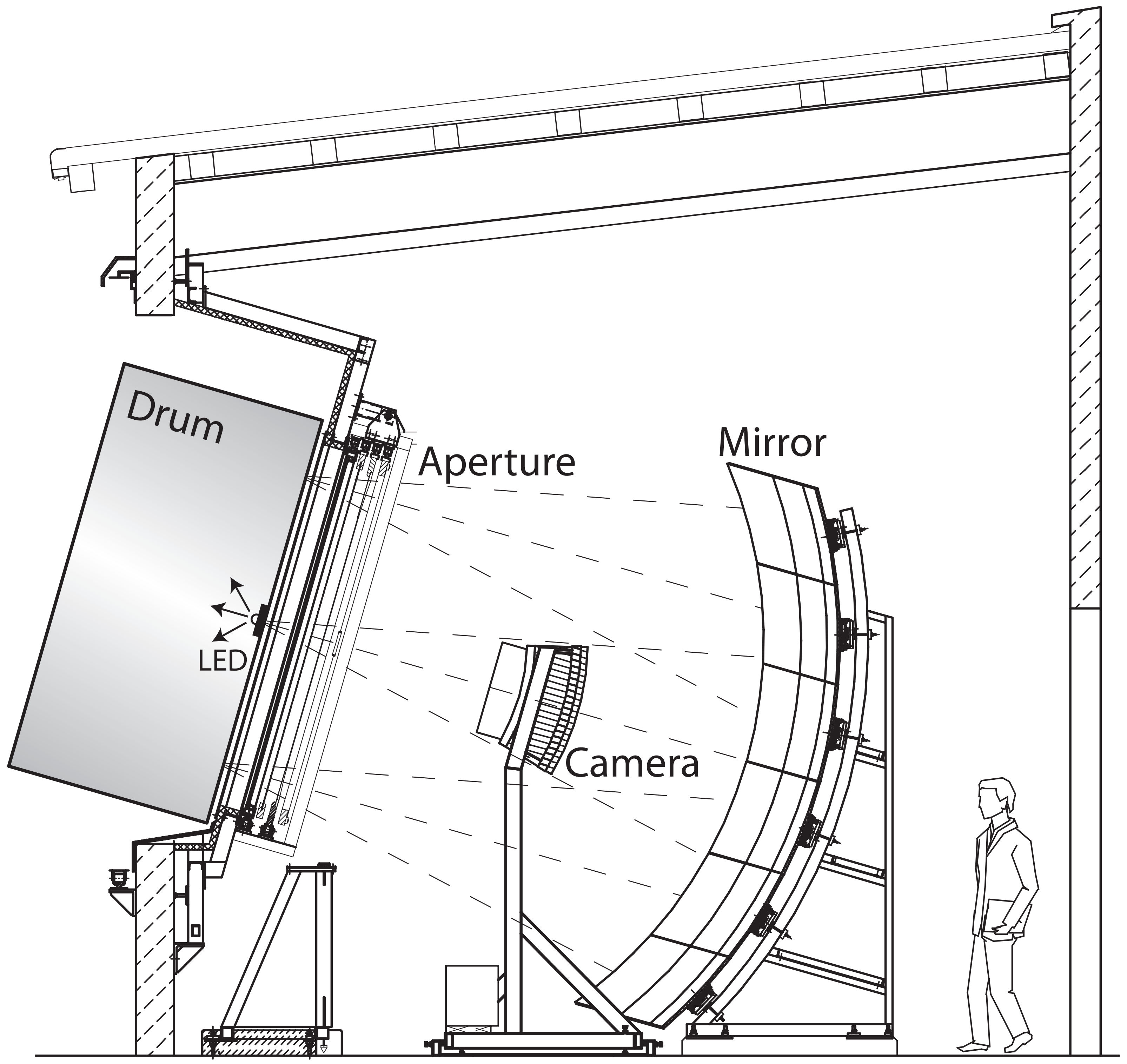

SD 750 m – S_{35}
- S(450)+CIC
- threshold 0.1 EeV

SD 1500 m vertical – S_{38}
- S(1000)+CIC
- threshold 2.5 EeV

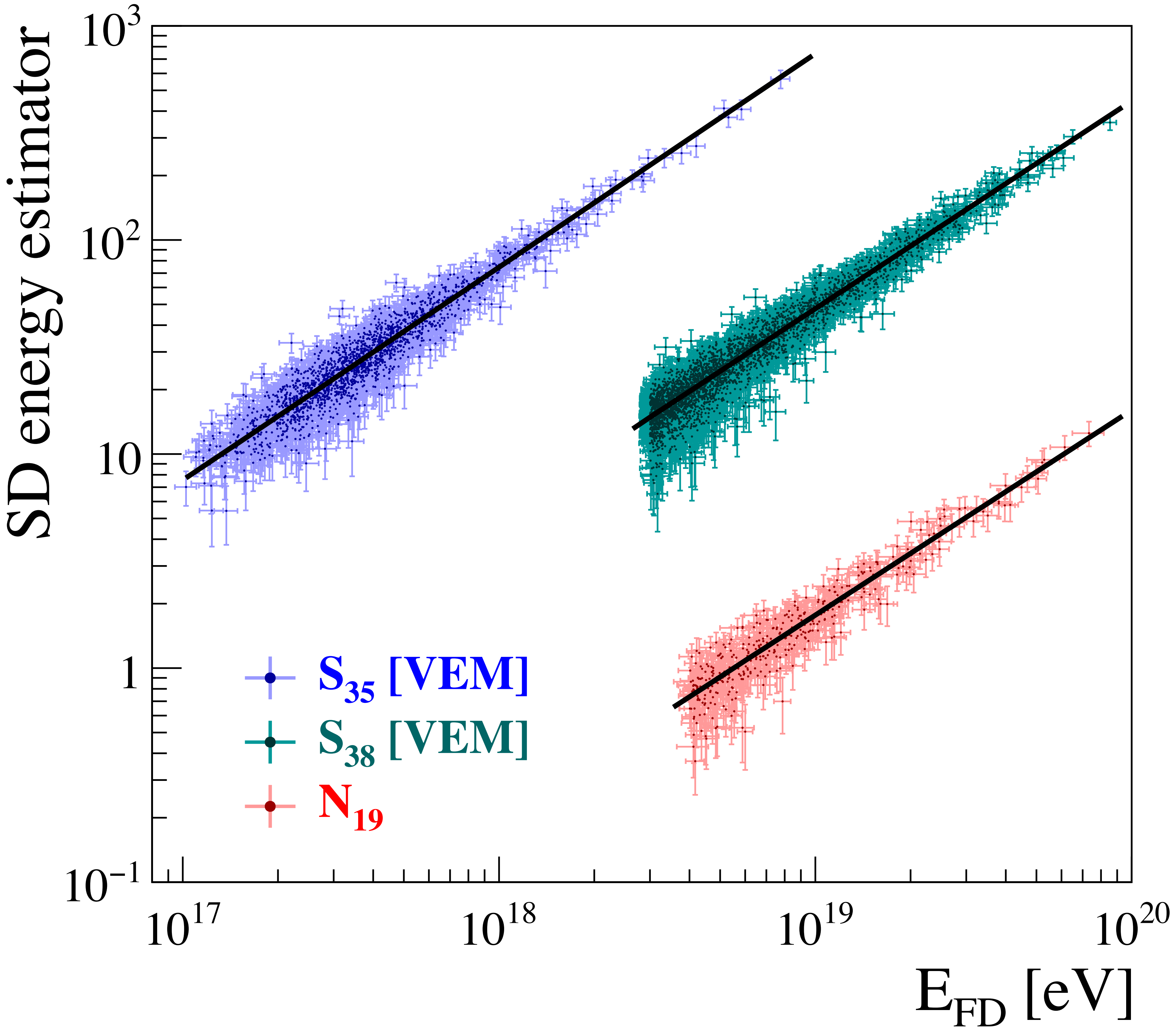

SD 1500 m inclined – N_{19}
- scaling parameter
- threshold 4 EeV

Drum: very precise end-to-end calibration
Cal-A: hourly relative calibration of camera only

Observations – selected highlights

All-particle flux

Energy spectrum 2013 and GZK expectation

Source spectrum

$$\frac{dN_{inj}}{dE} \sim E^{-\gamma} \exp\left(-\frac{E}{E_{cut}}\right)$$

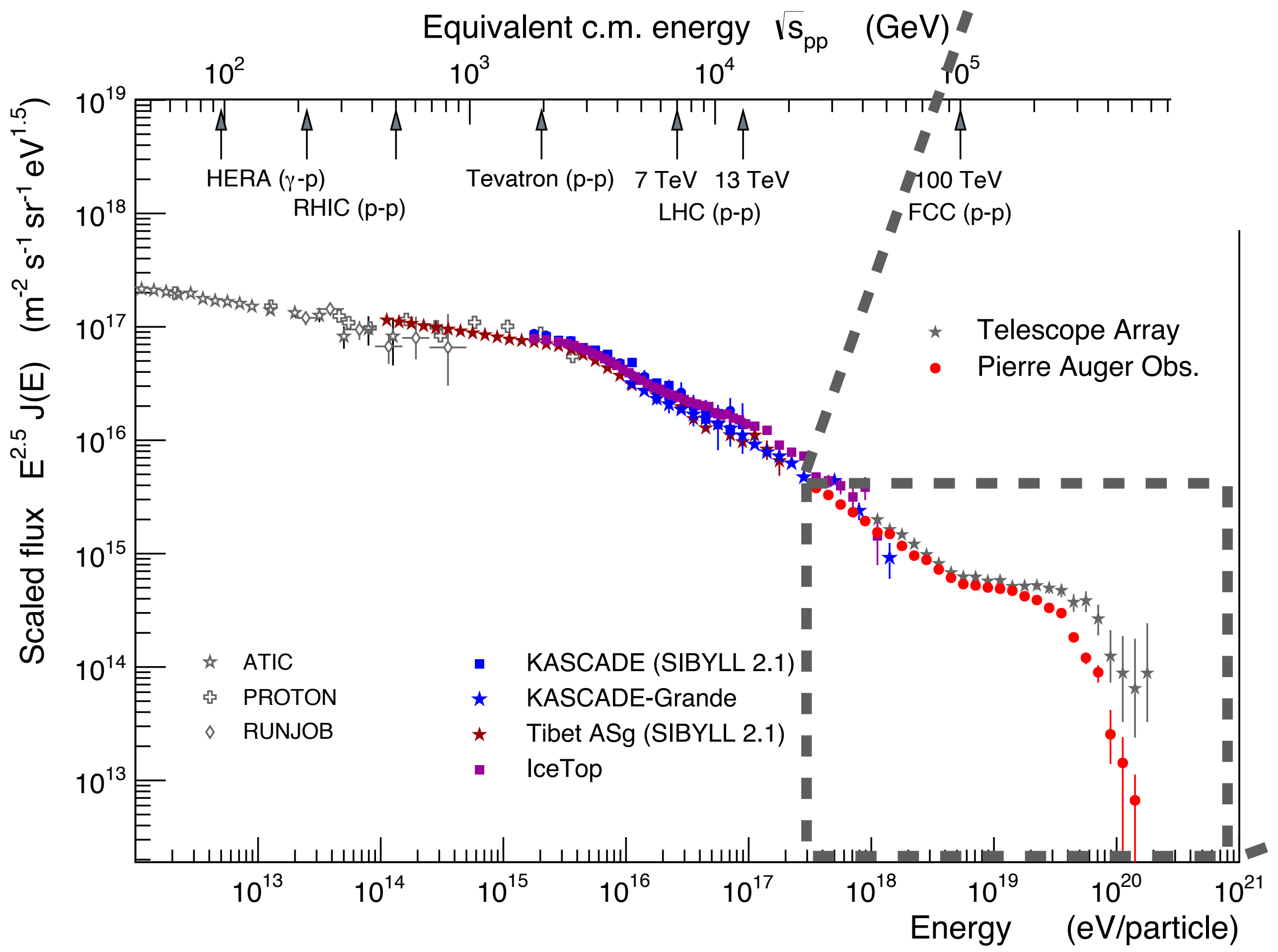

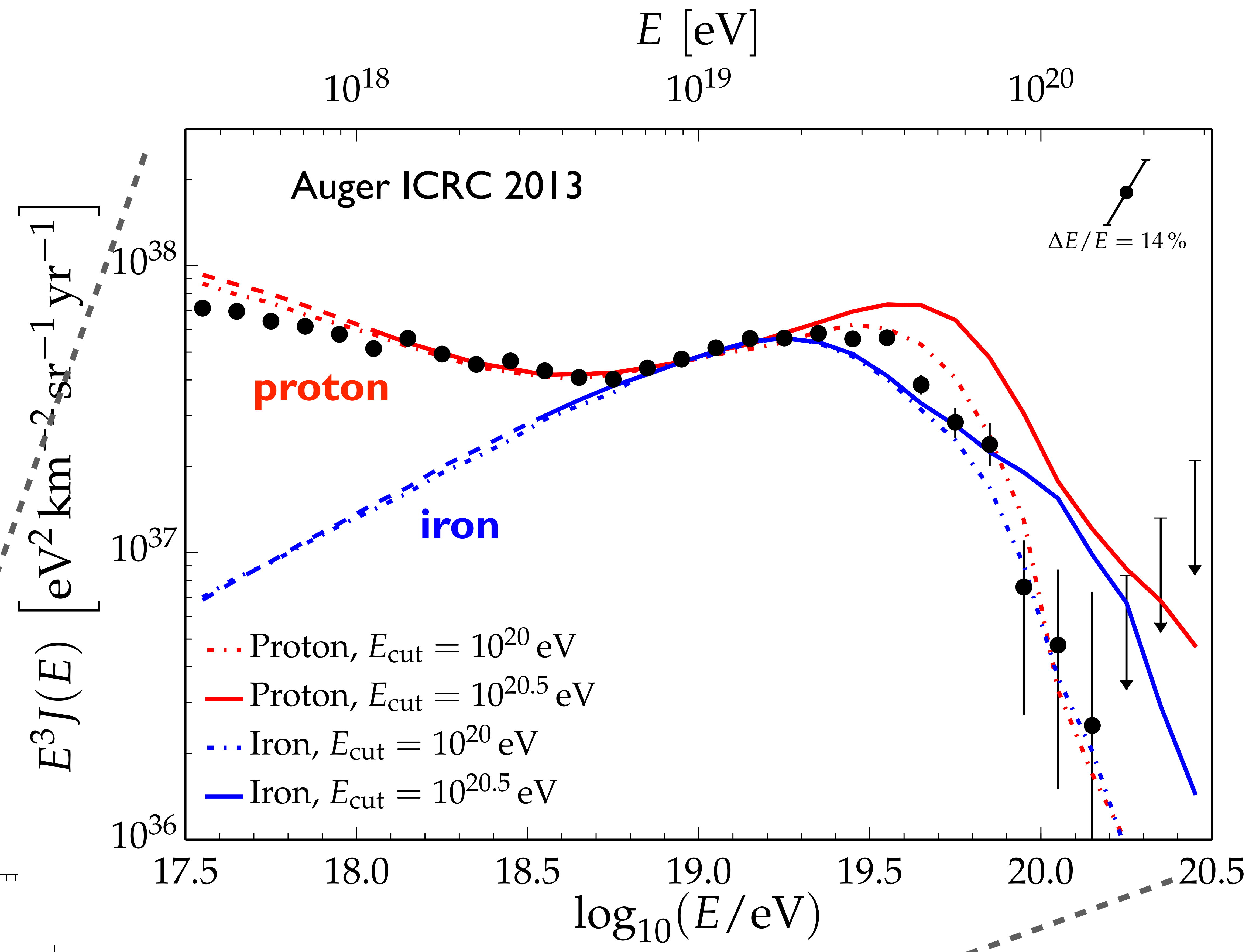

Greisen-Zatsepin-Kuzmin (GZK) effect

Photo-pion production (mainly Δ resonance) and e^+e^- pair production

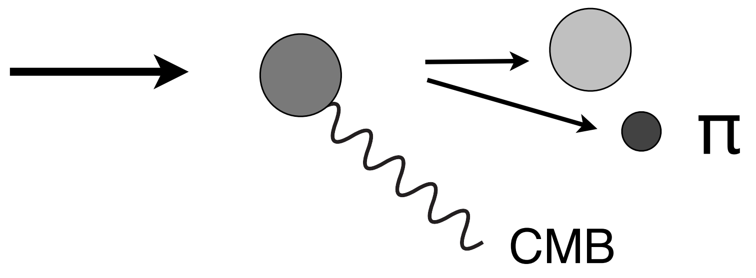

Photo-dissociation (giant dipole resonance)

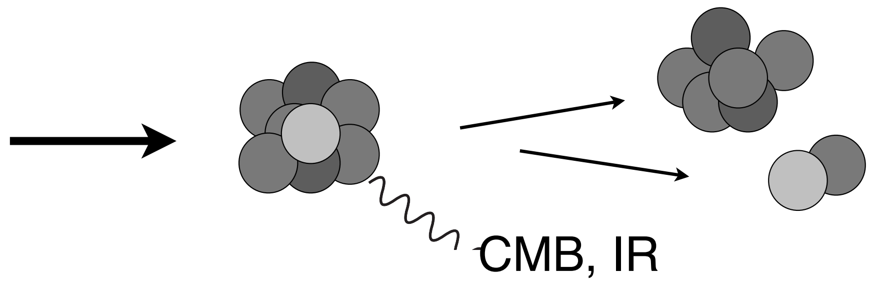

Iron dominated flux

Suppression: giant dipole resonance

Ankle: transition to galactic sources

Combined energy spectrum of Auger Observatory

Phys. Rev. Lett. 125 (2020) 121106
Phys. Rev. D102 (2020) 062005
Eur. Phys. J. C81 (2021) 966

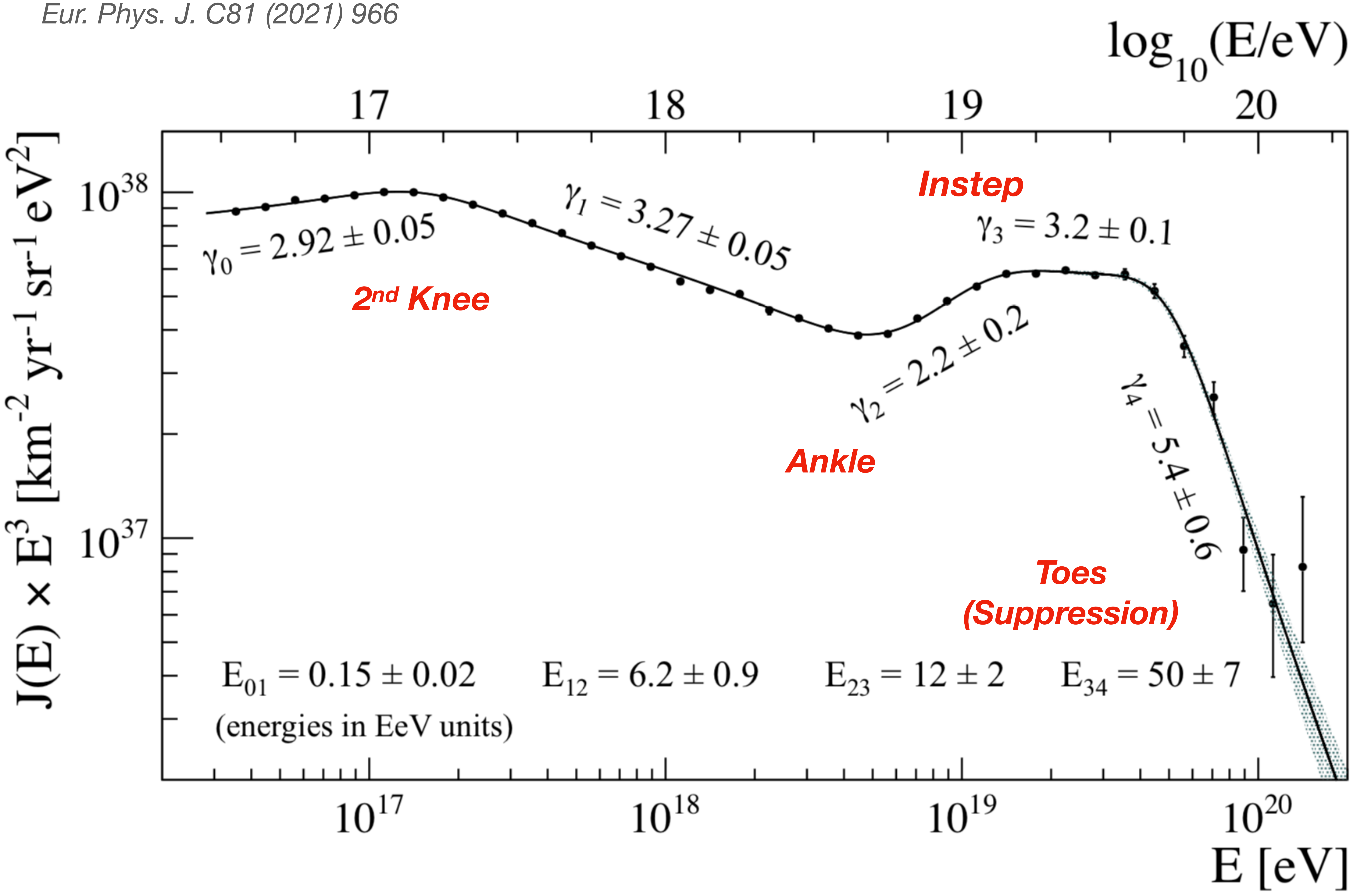

(UHECR 2024)

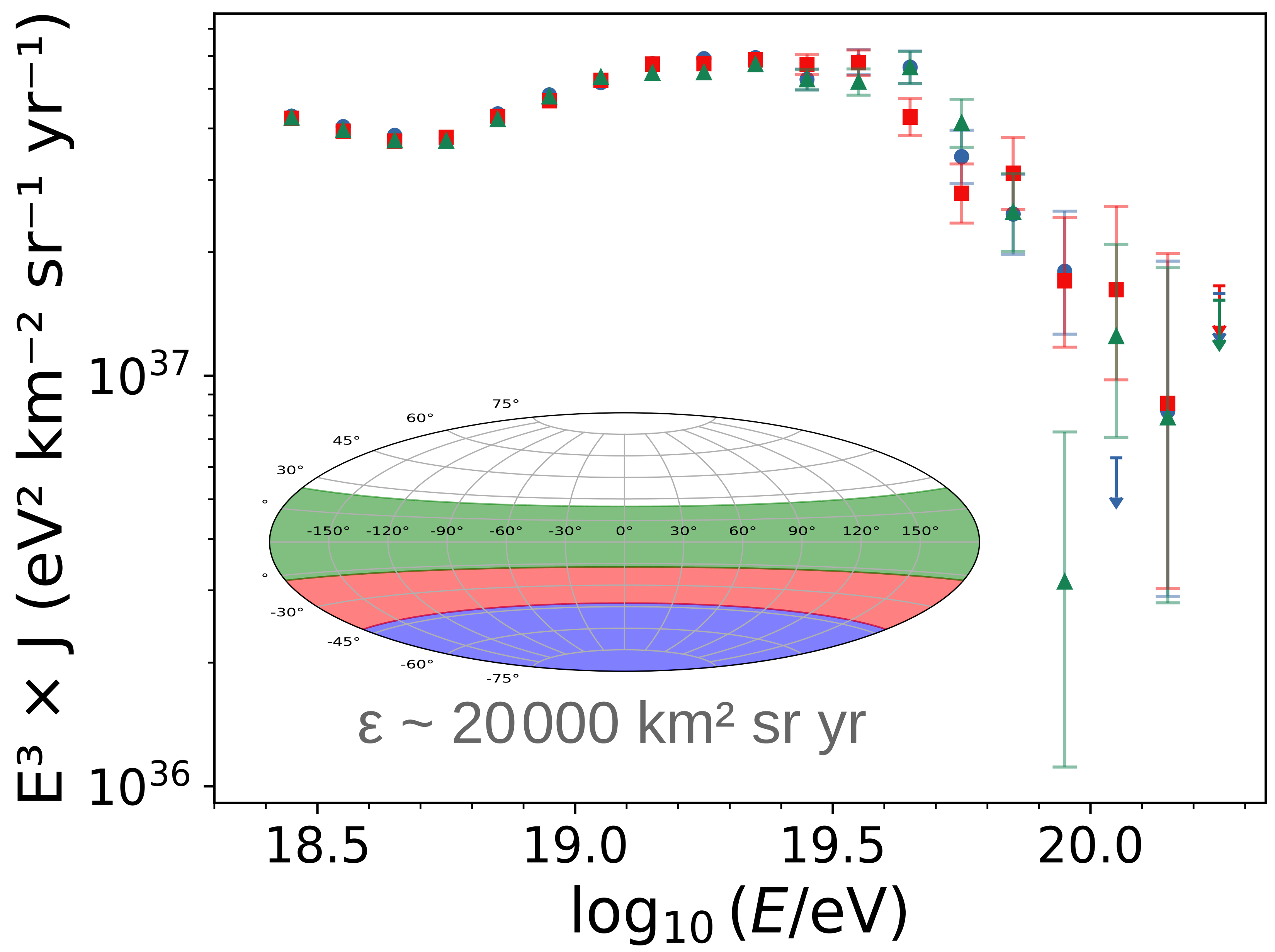

No declination dependence found beyond the expectation from dipole (shown later)

Energy spectrum of TA

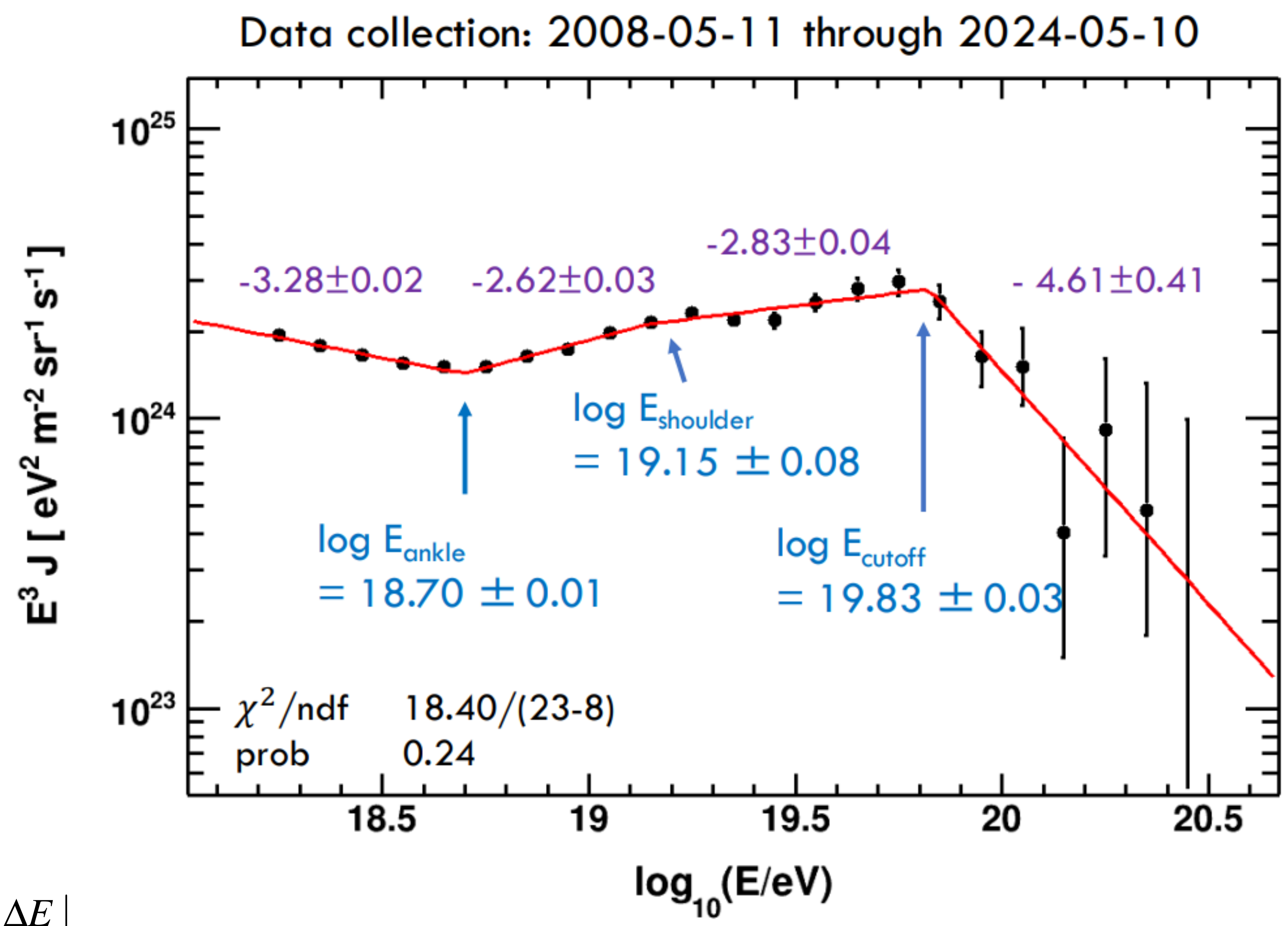

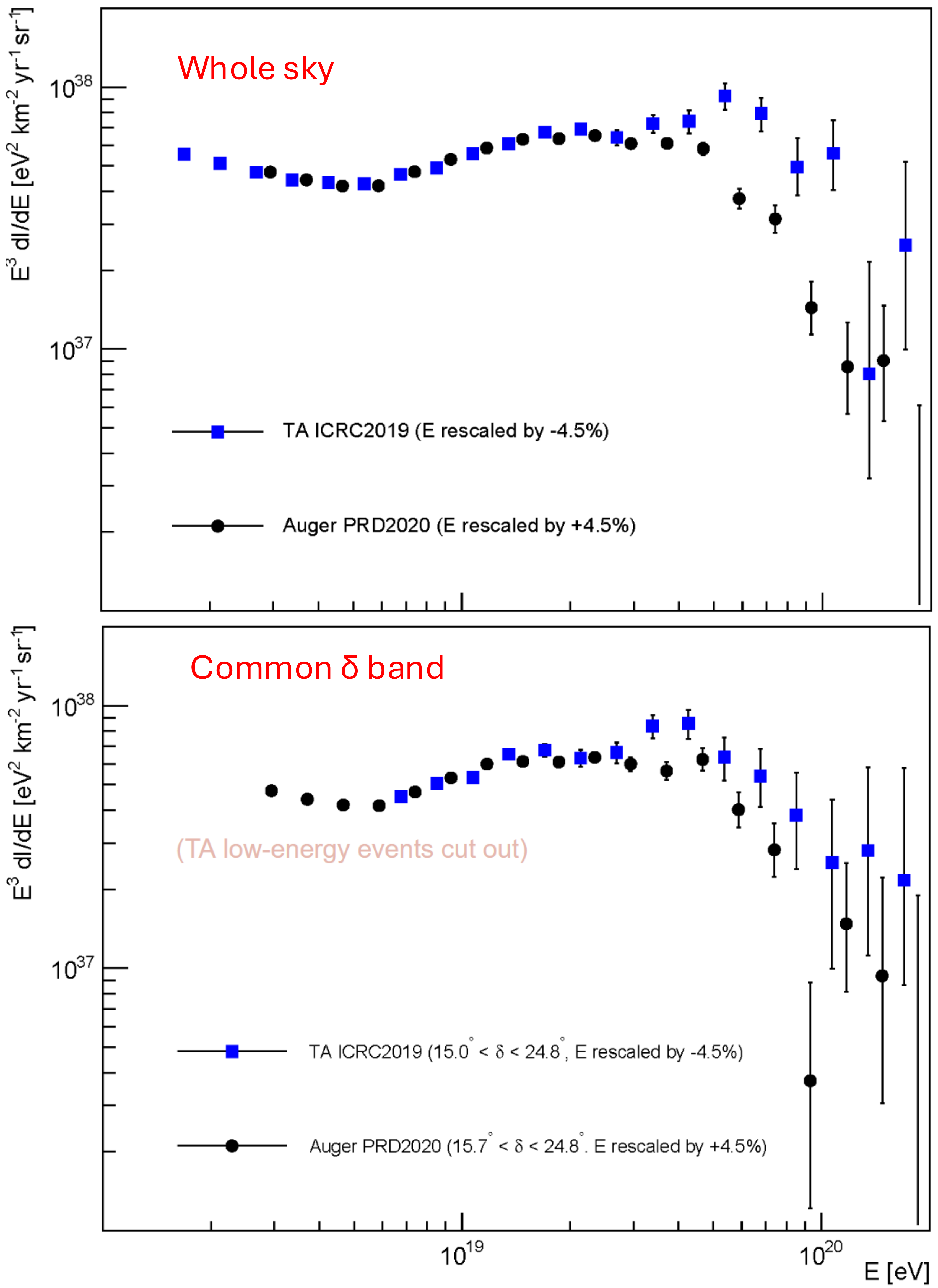

$$\left.\frac{\Delta E}{E}\right|_{\text{Auger}} = 14\,\%$$

$$\left.\frac{\Delta E}{E}\right|_{\text{TA}} = 21\,\%$$

Difference physics or measurement effect?

(Joint working group, UHECR 2024)

Comparison in common declination band

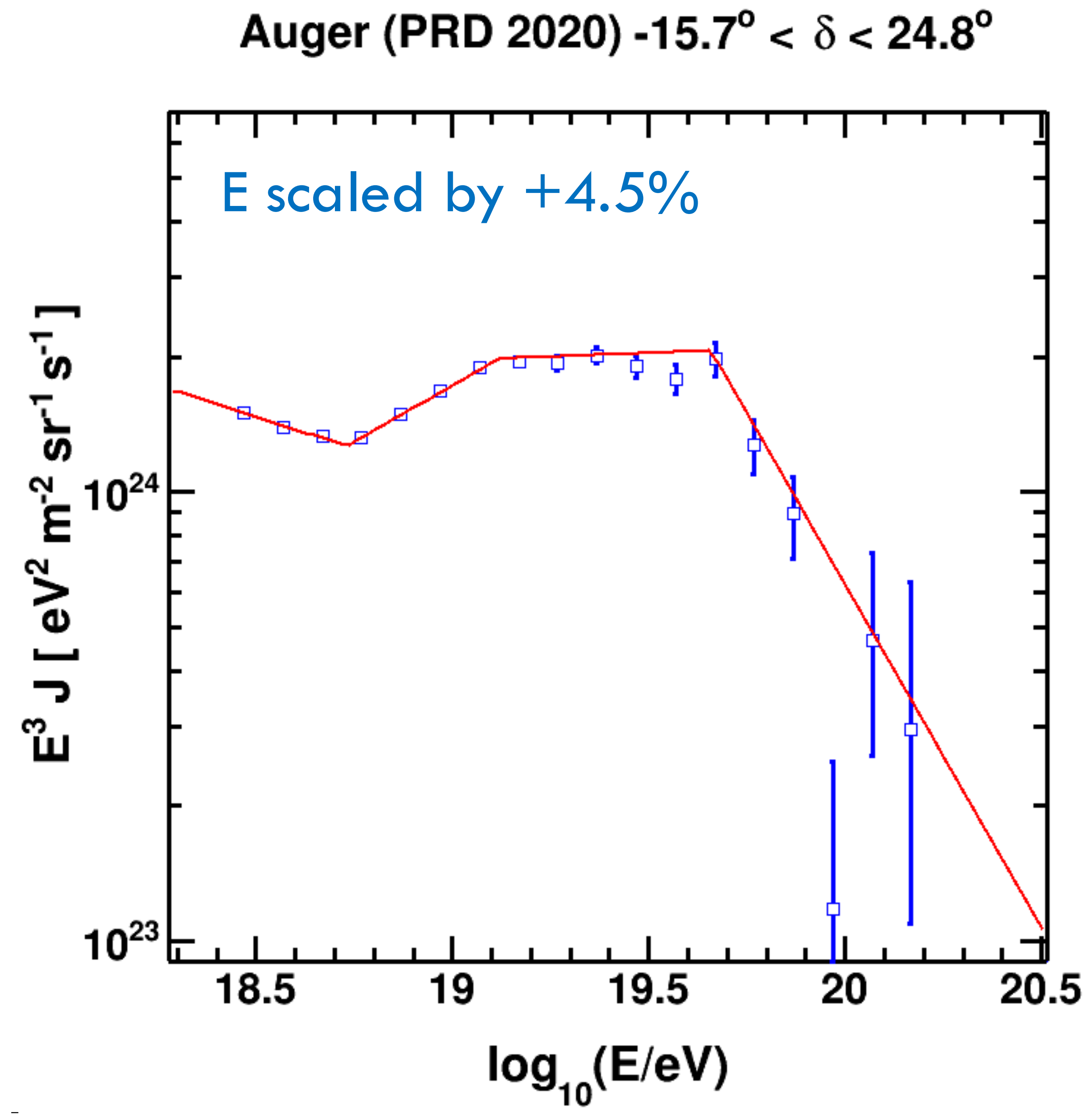

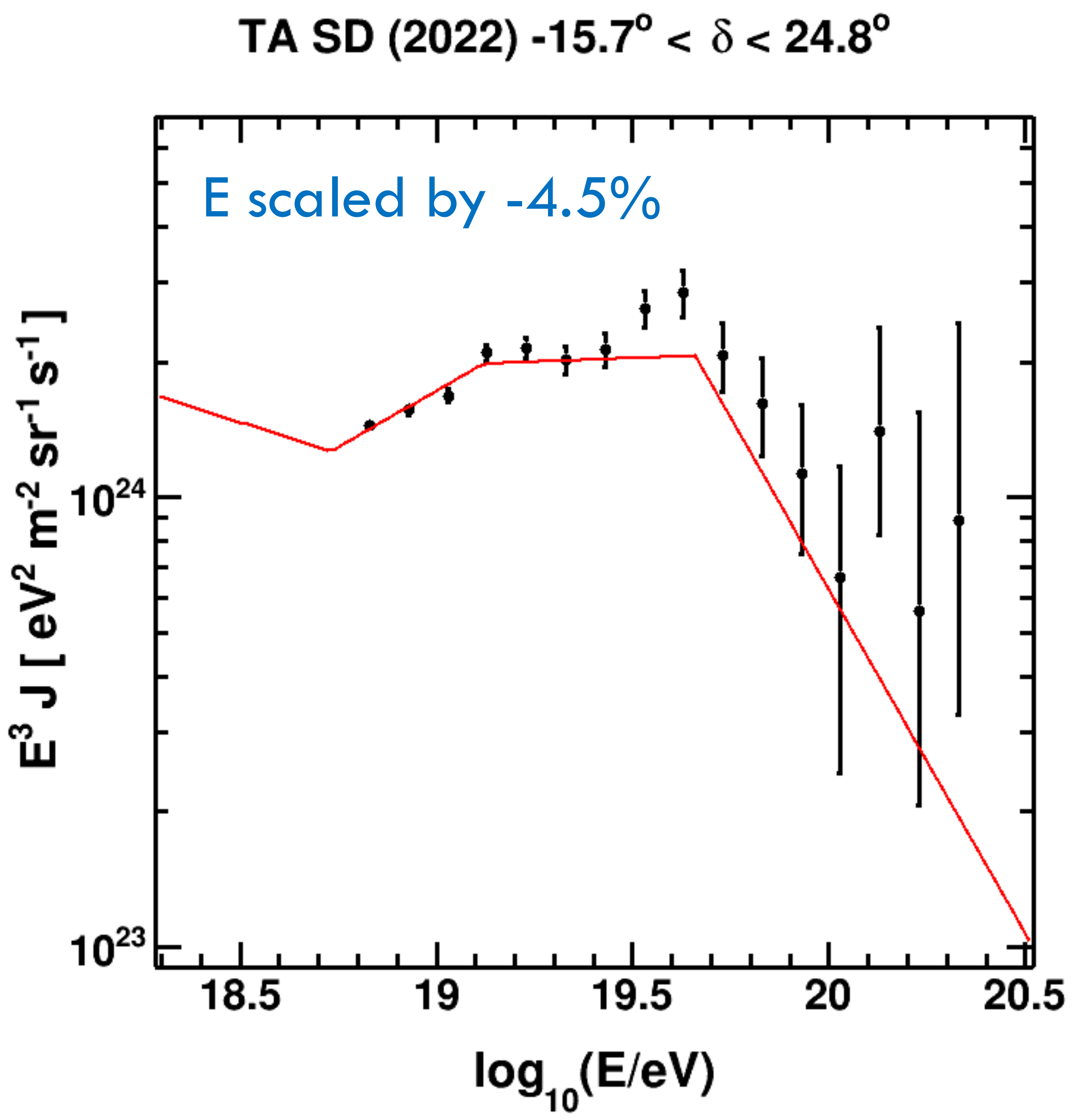

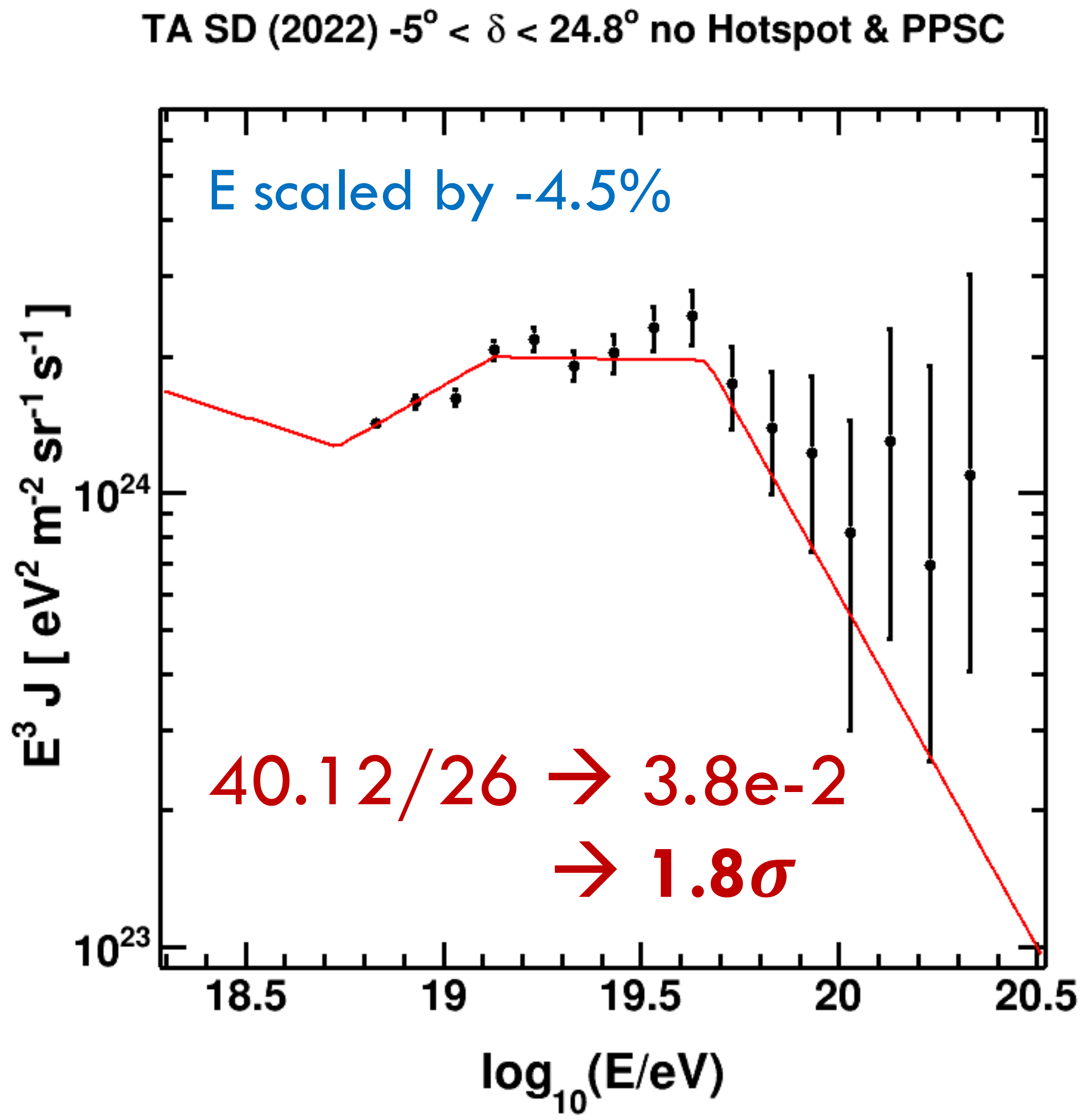

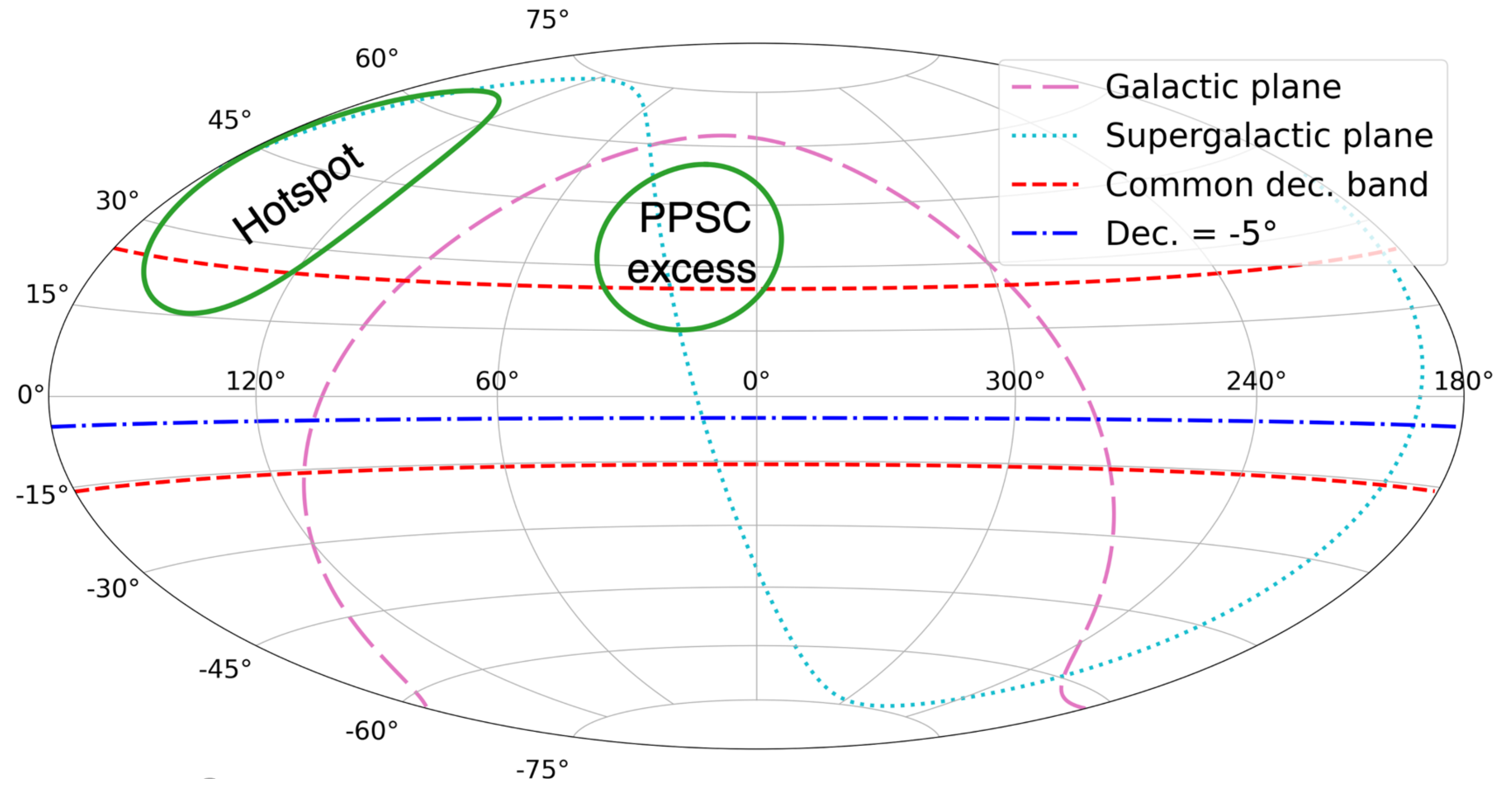

How much a difference in norther/southern hemisphere?

(TA 2406.08612, UHECR 2024)

Masse composition, photons, neutrons

Mass composition results of Auger Observatory

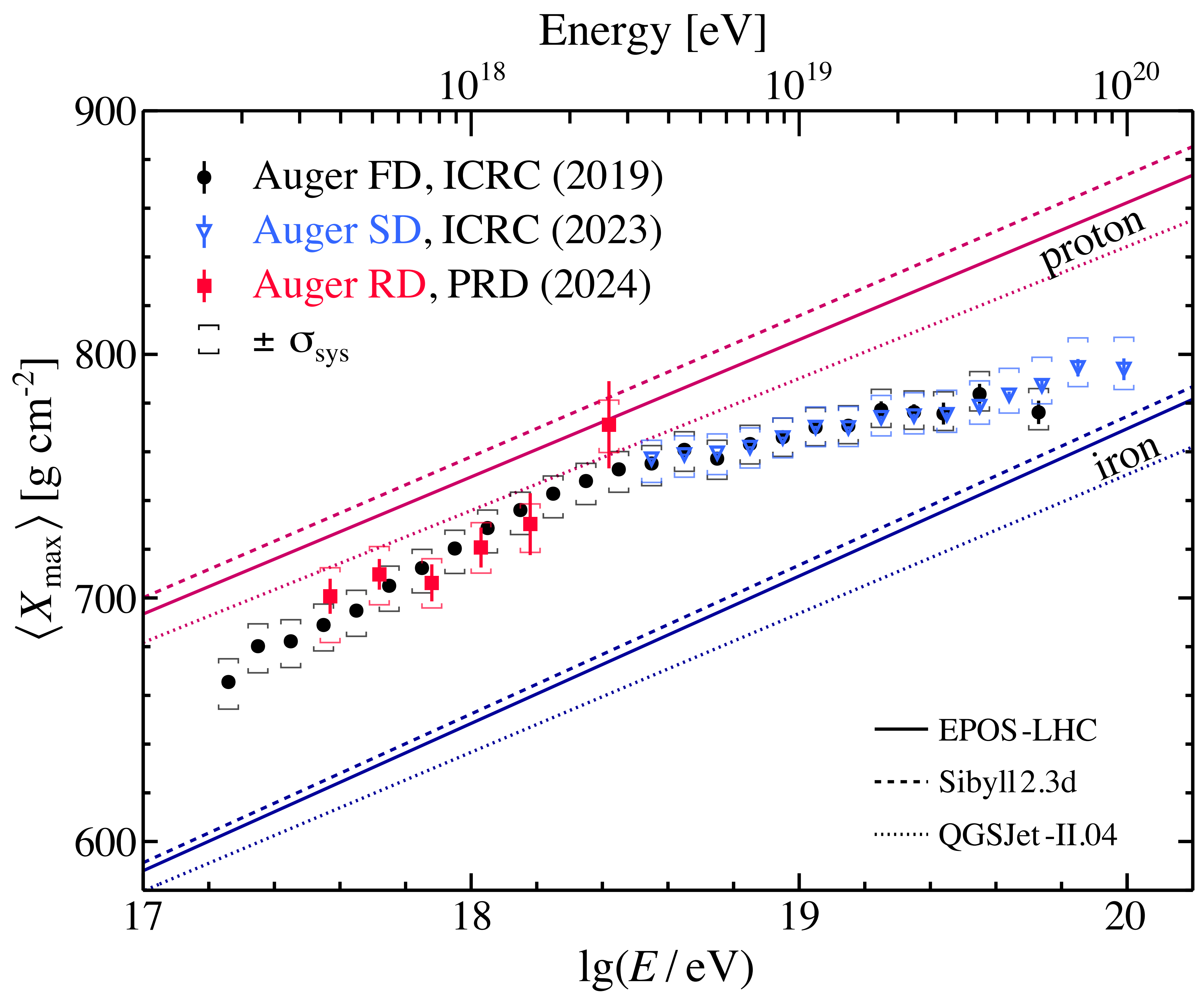

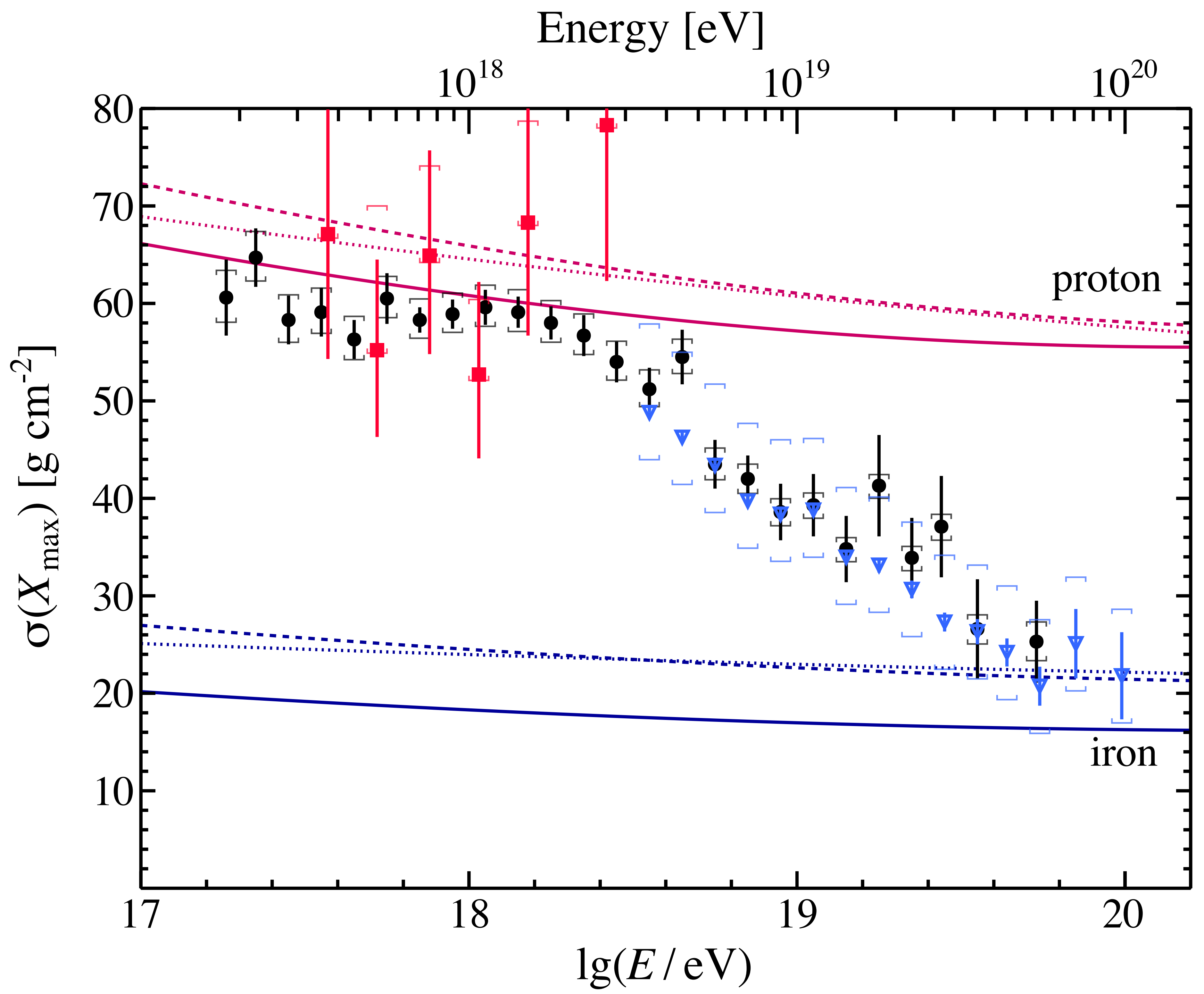

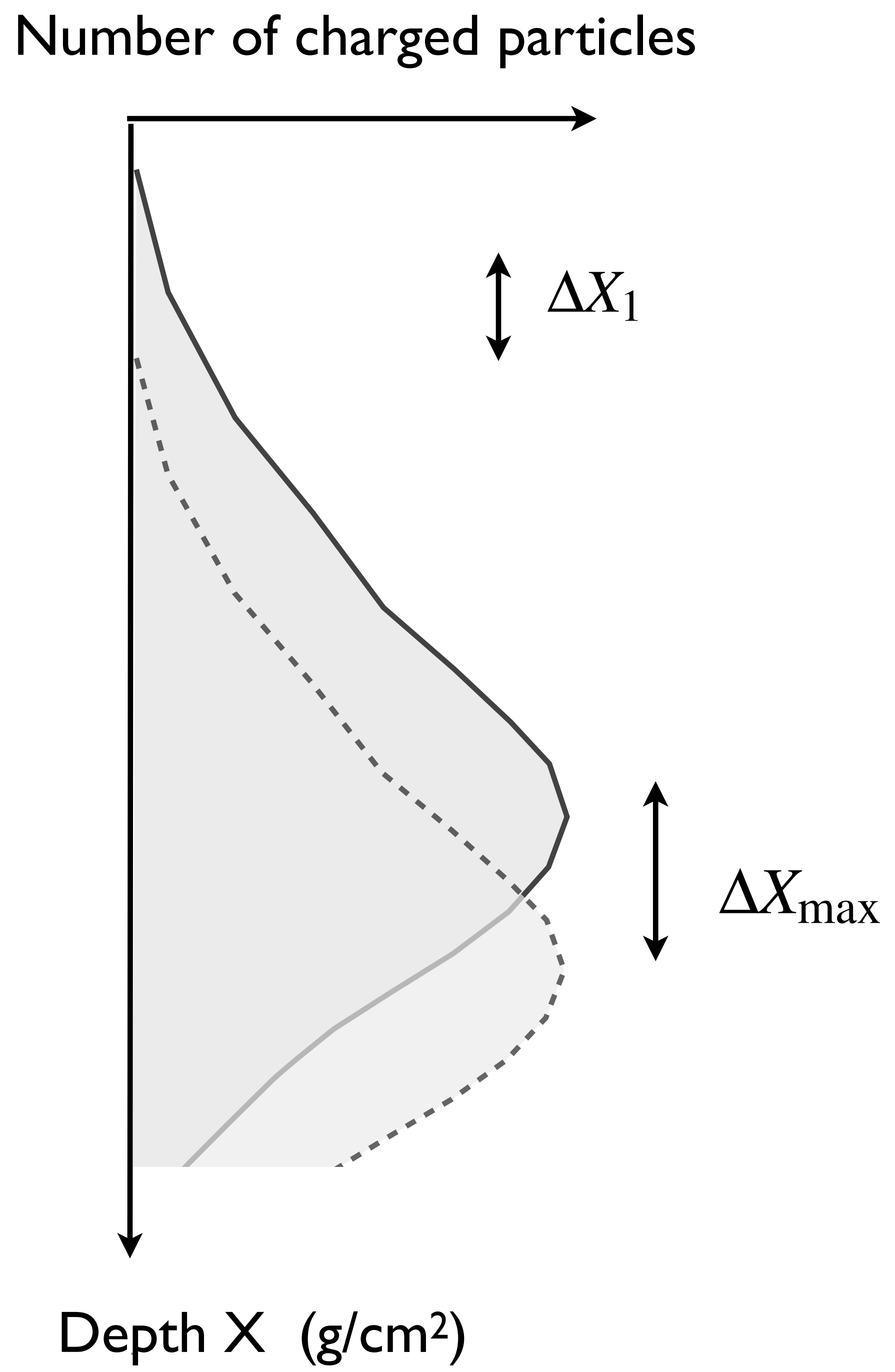

$$\frac{dP}{dX_1} = \frac{1}{\lambda_{int}} e^{-X_1/\lambda_{int}}$$

Important: LHC-tuned interaction models used for interpretation

$$\sigma_{X_1,p} \sim 45 - 55\,\mathrm{g/cm^2}$$
$$\sigma_{X_1,Fe} \sim 10\,\mathrm{g/cm^2}$$

$(E \sim 10^{18}\,\mathrm{eV})$

(FD telescopes: PRD 90 (2014), 122005 & 122005, updated ICRC 2023)

(SD risetime: Phys. Rev. D96 (2017), 122003)

(AERA/radio: PRL & PRD 2023)

(SD DNN: PRL & PRD 2025)

Auger-TA comparison of X_{max} distributions (2022)

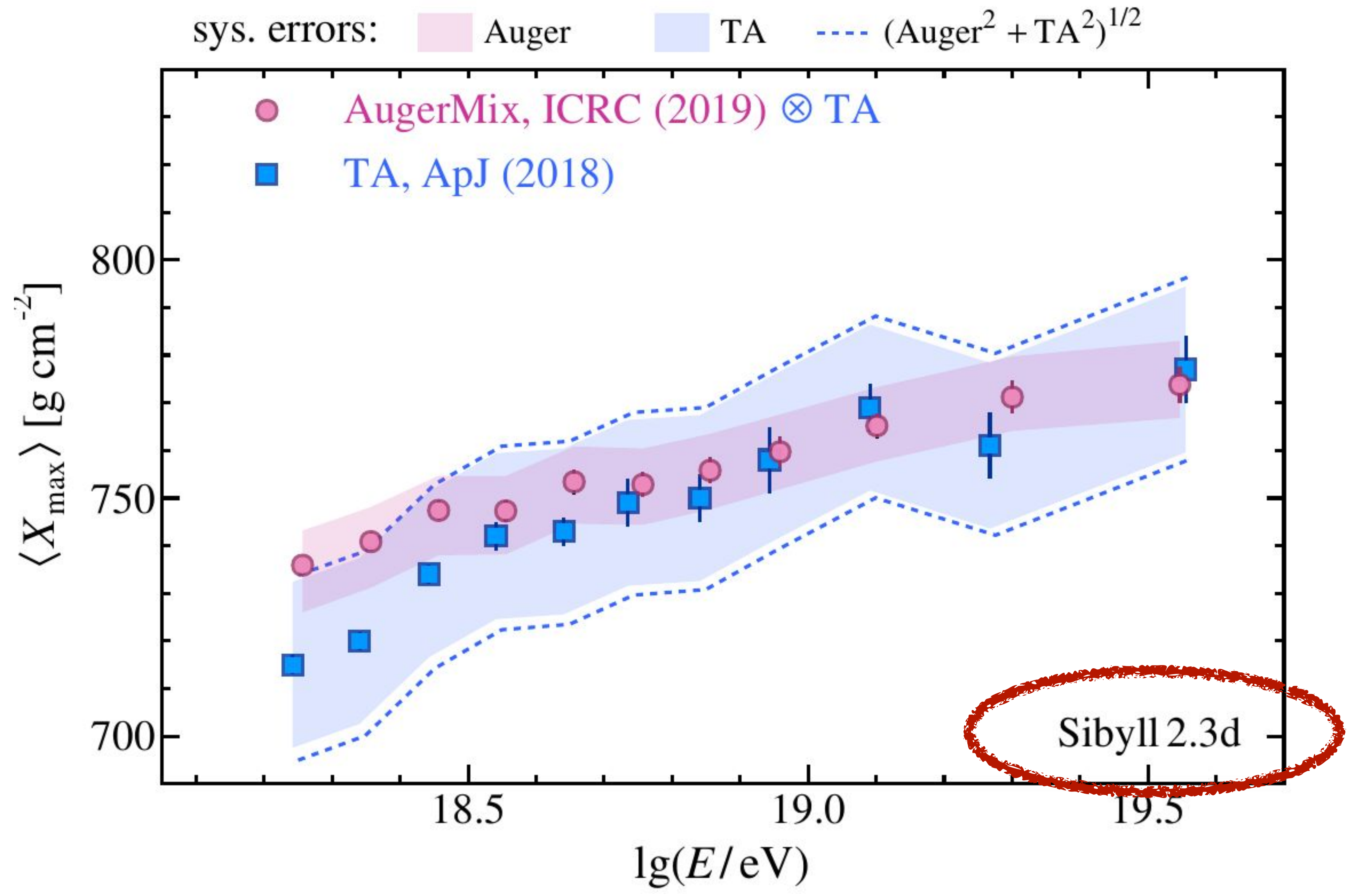

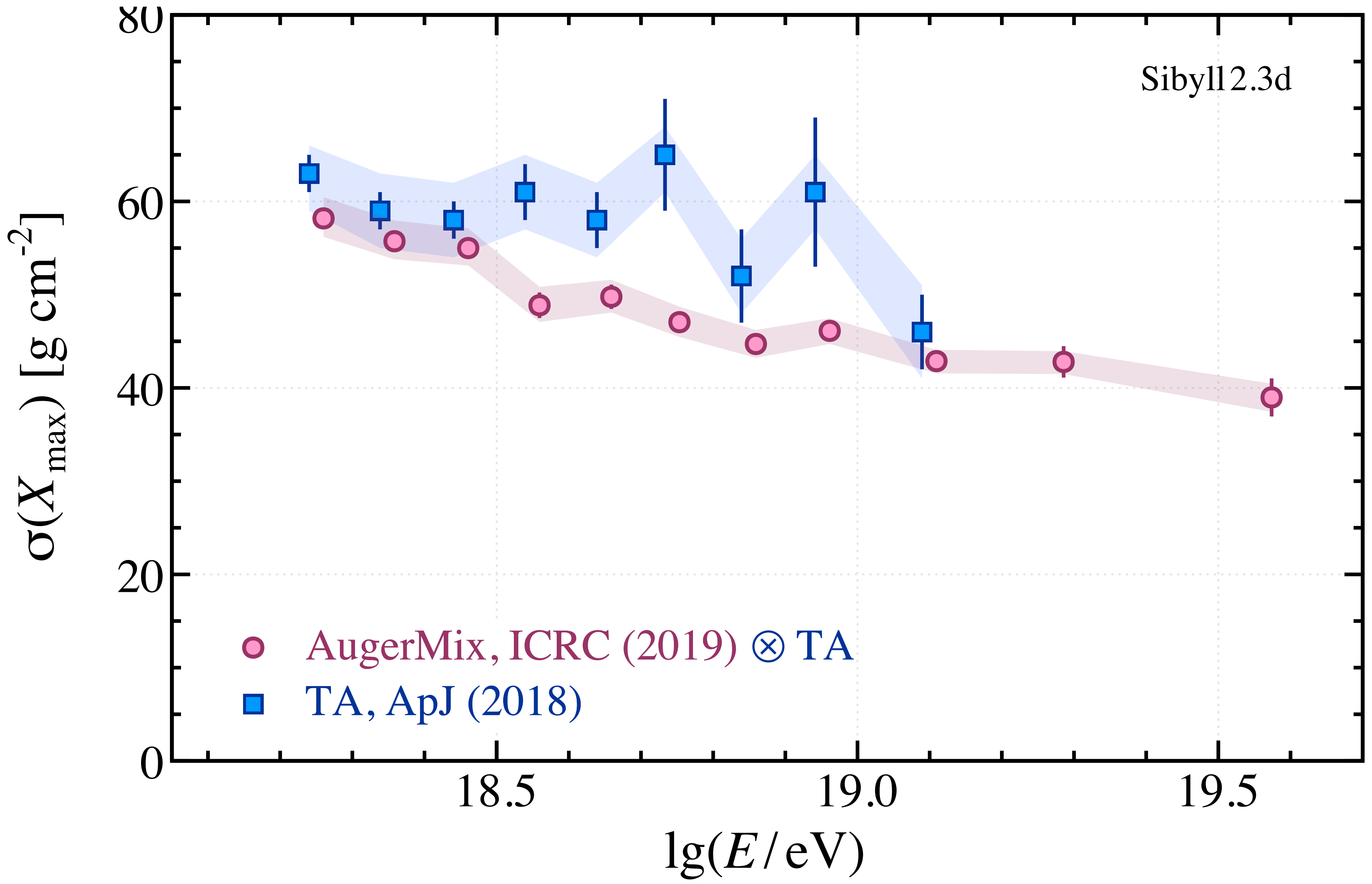

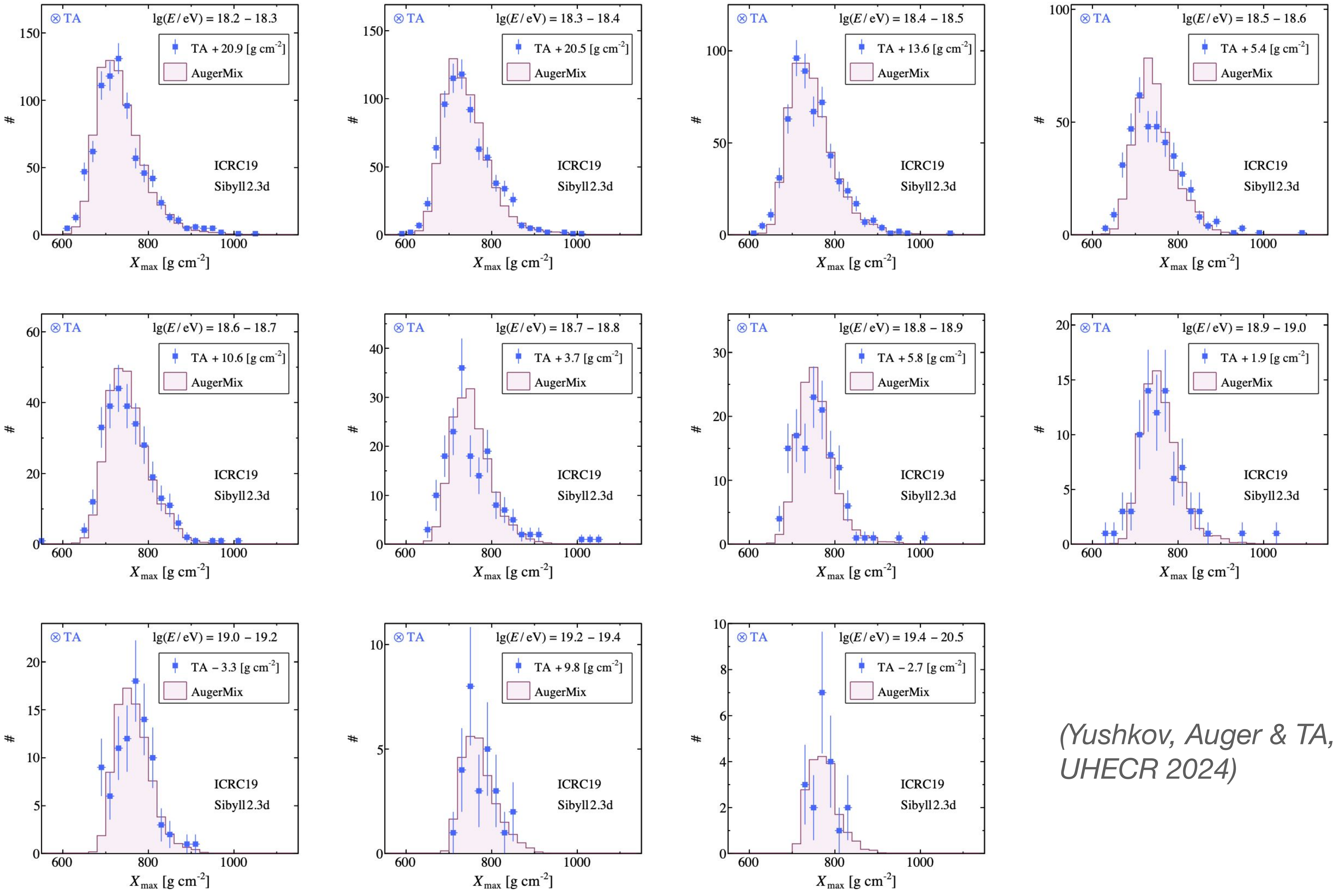

(Yushkov, Auger & TA, UHECR 2024)

Joint working group: no significant difference found

Mass composition from surface detector data

Simulated signal of one surface station

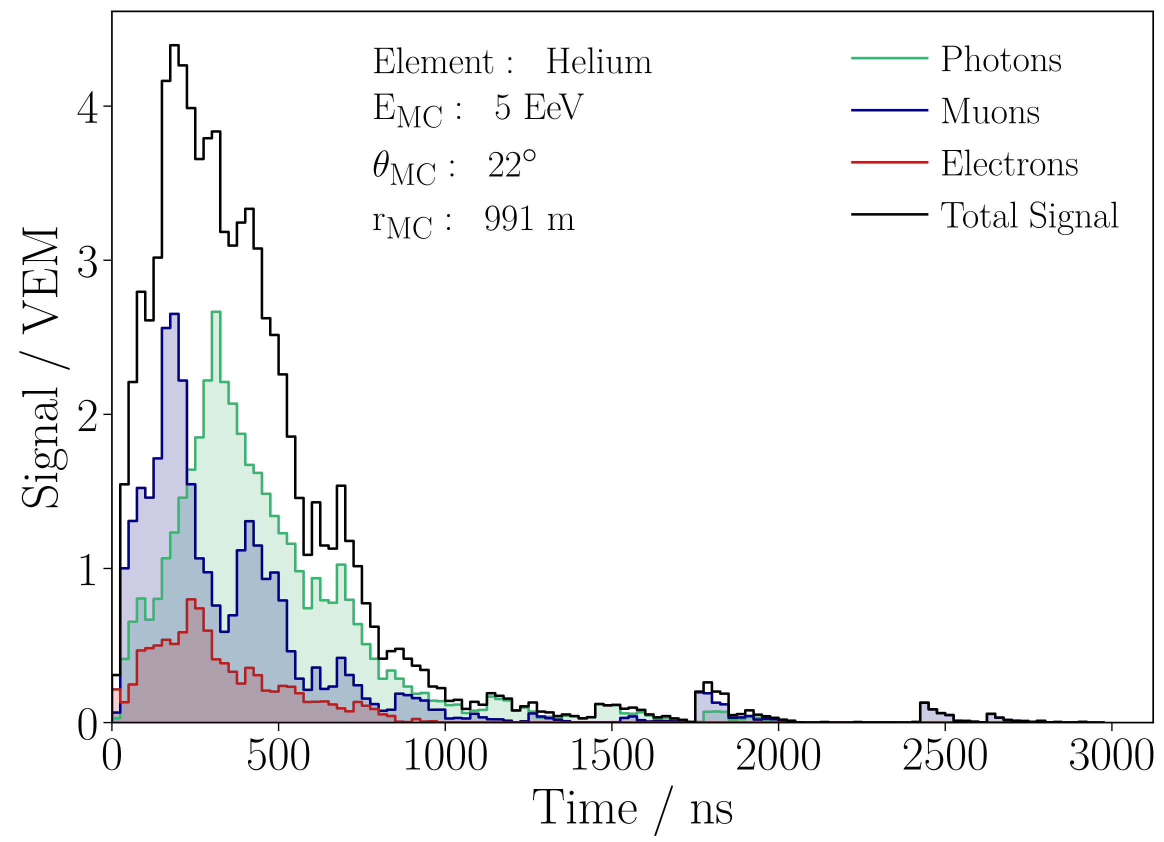

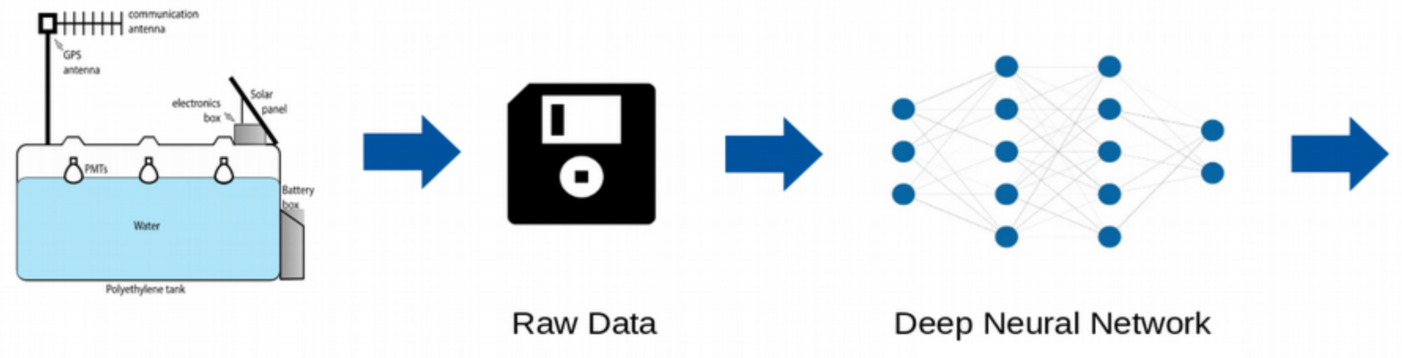

Reconstructing Xmax with DNNs: ultimate check with hybrid data

(Auger, JINST 16 (2021) P07019)

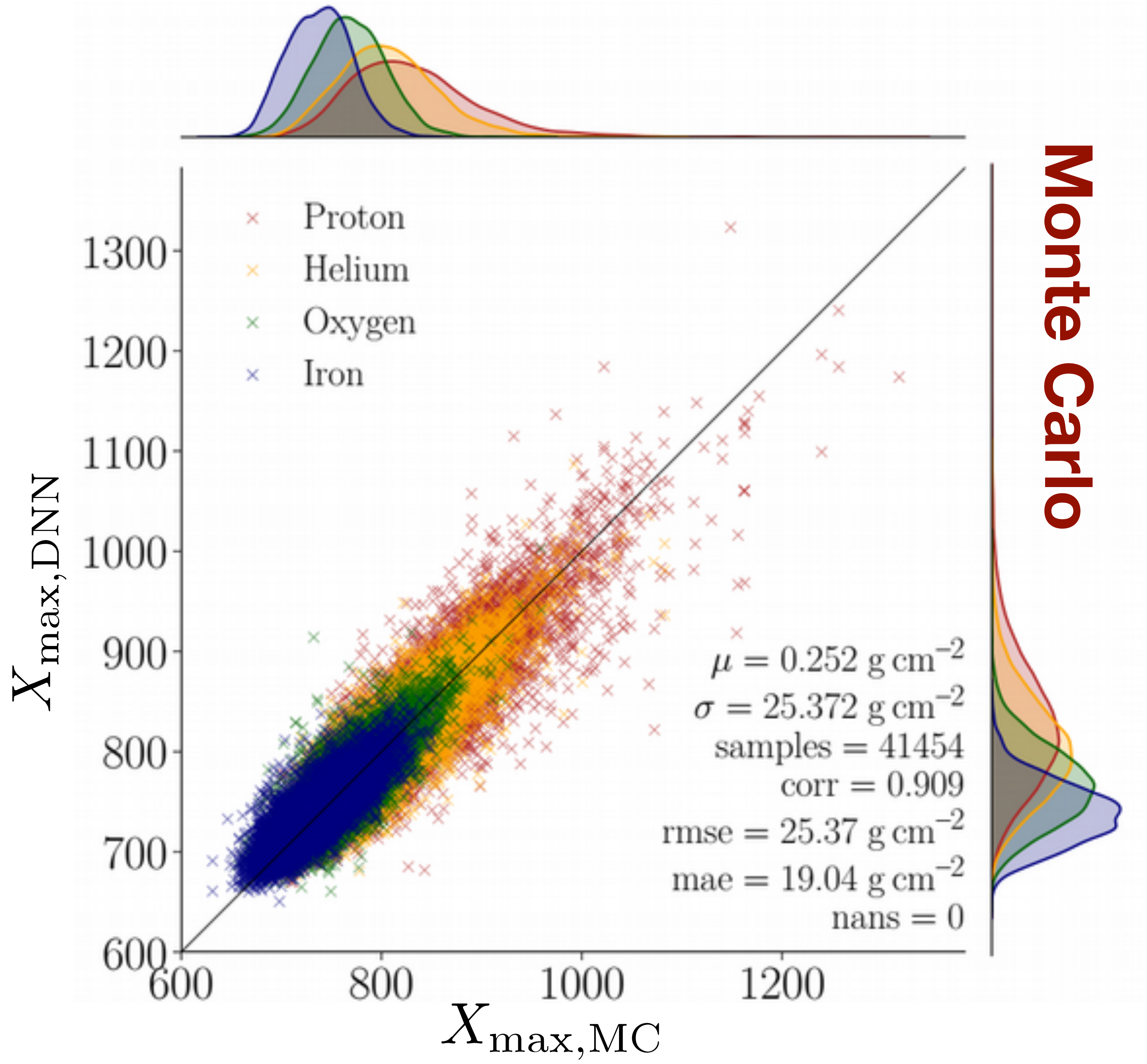

Monte Carlo

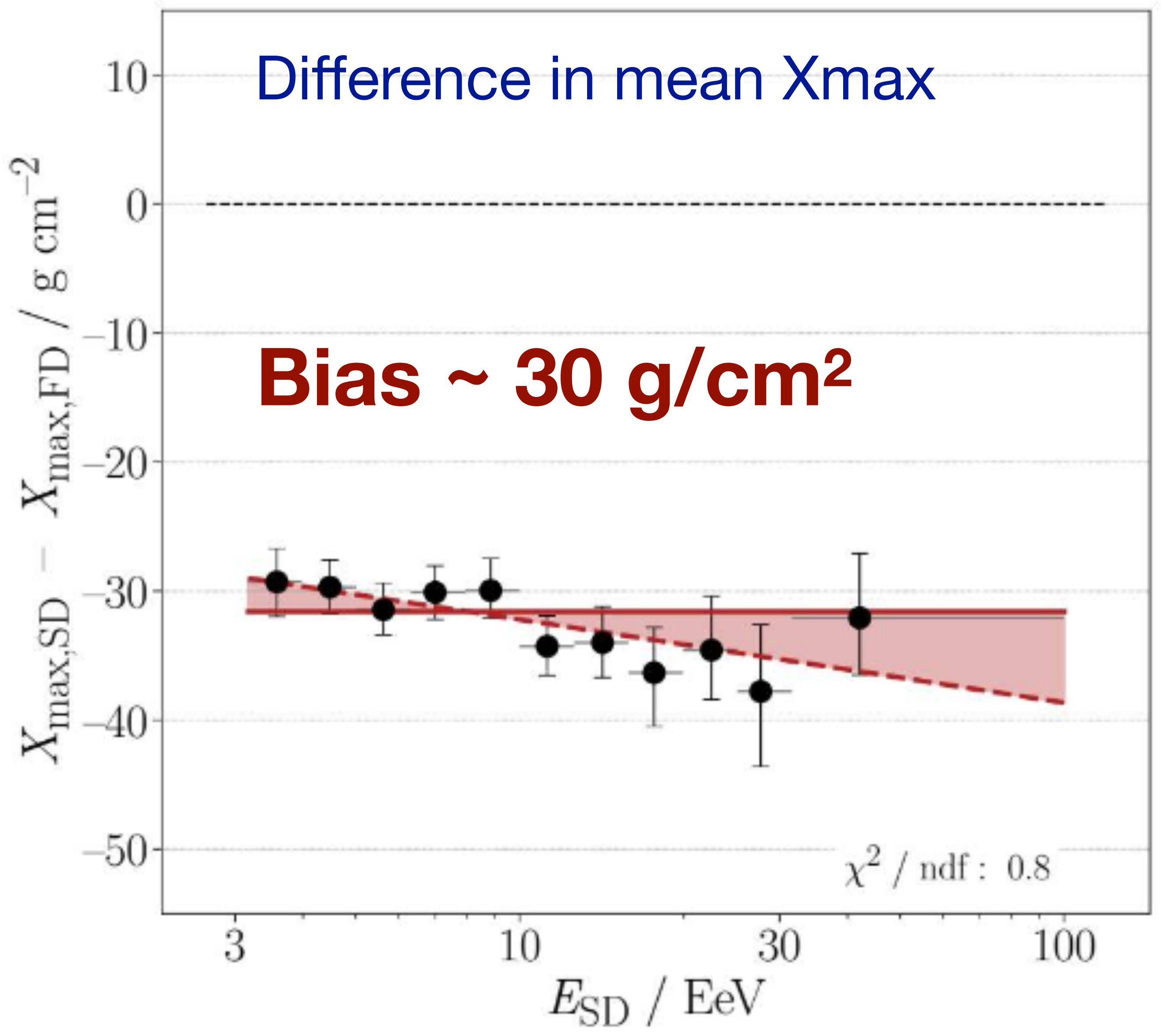

Shower-by shower Xmax resolution

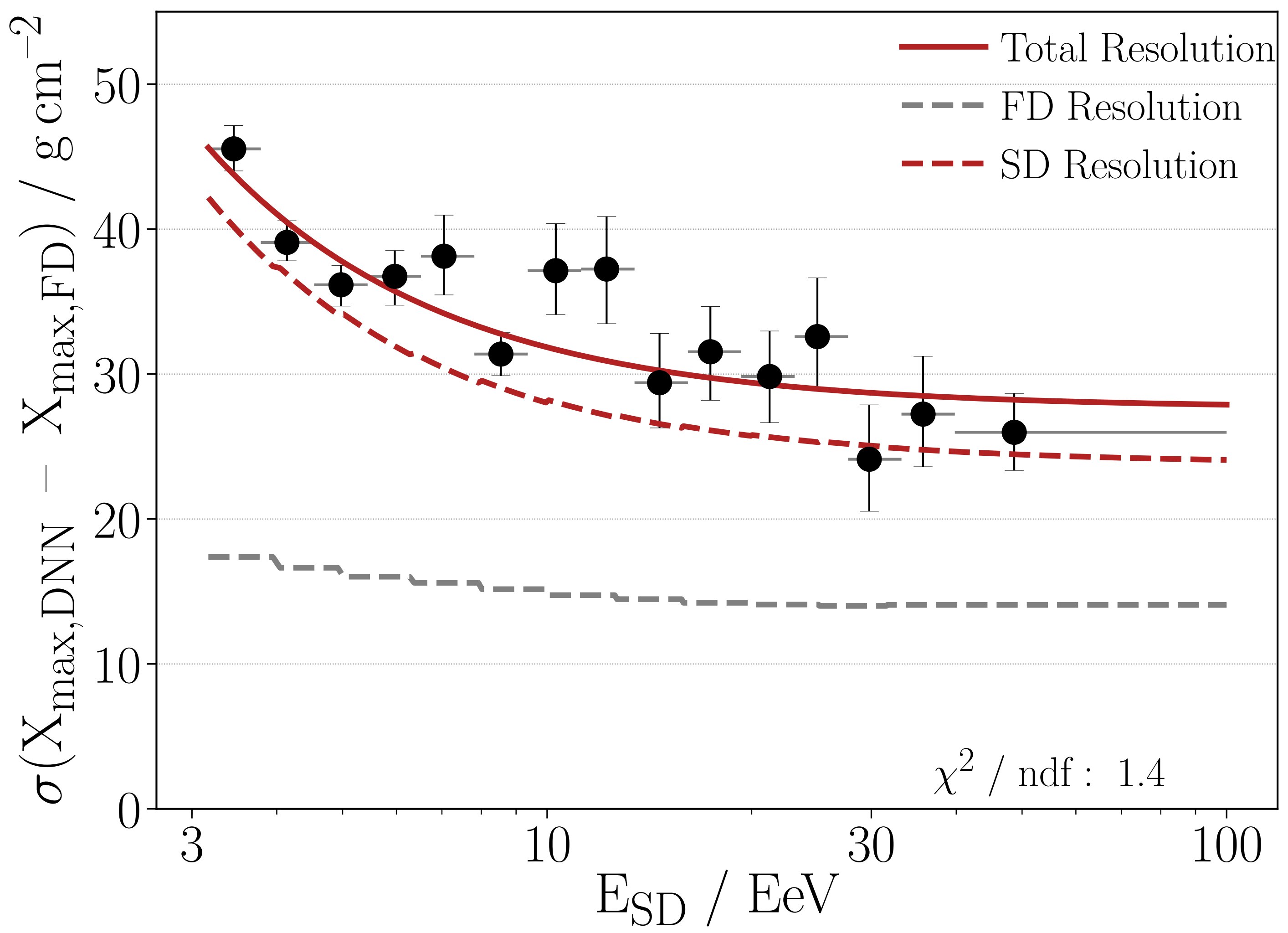

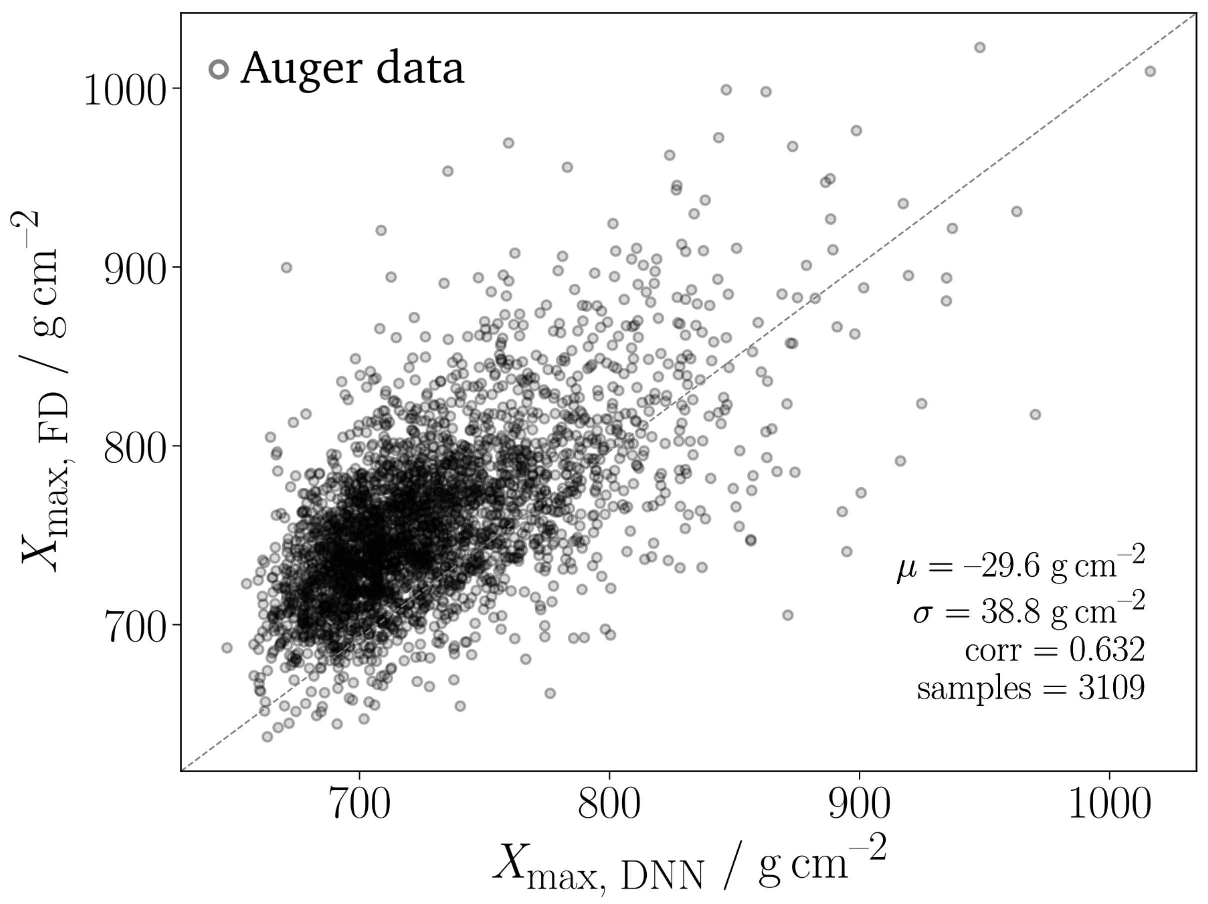

Hybrid data

Model-independent observation in DNN data set

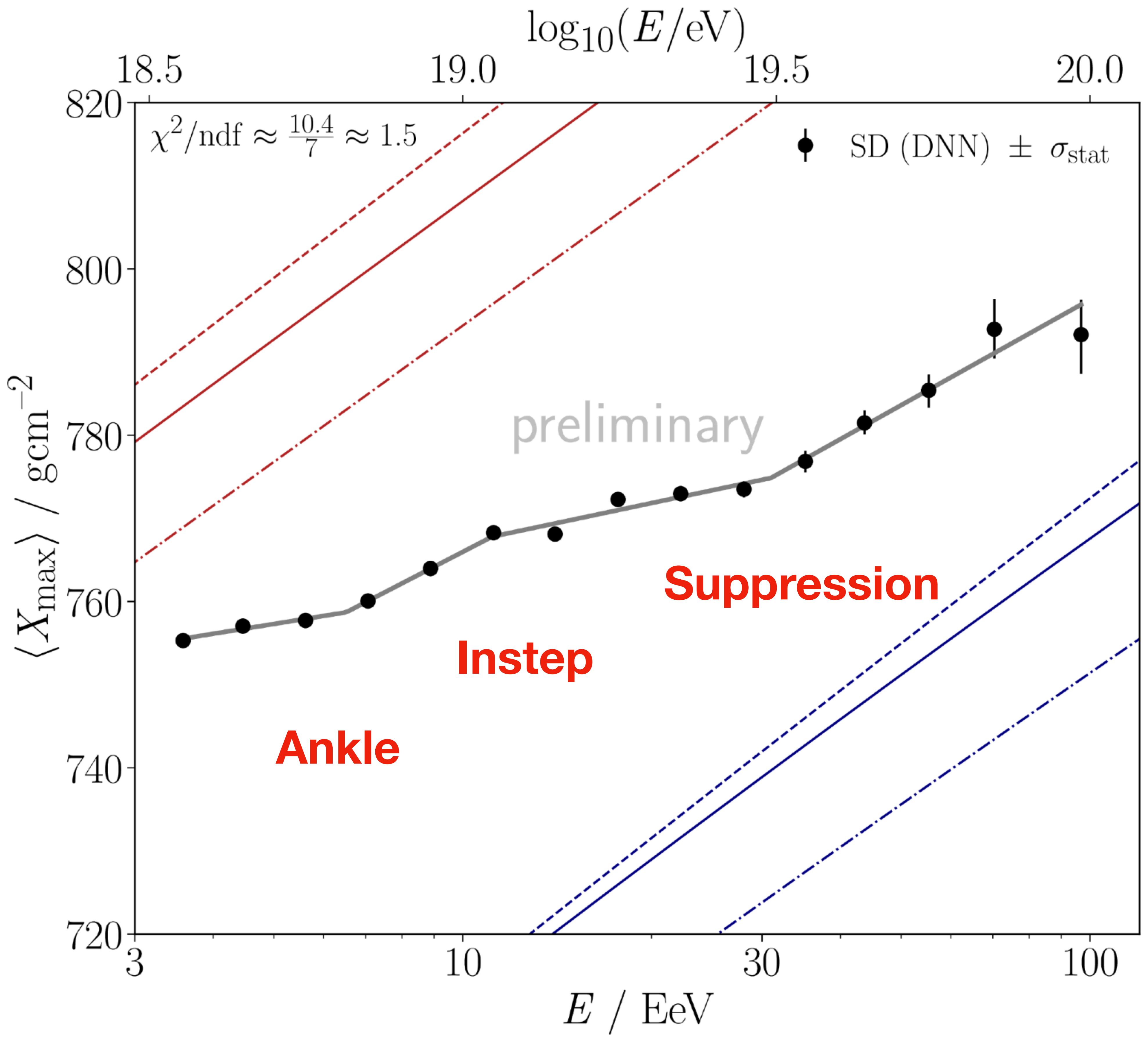

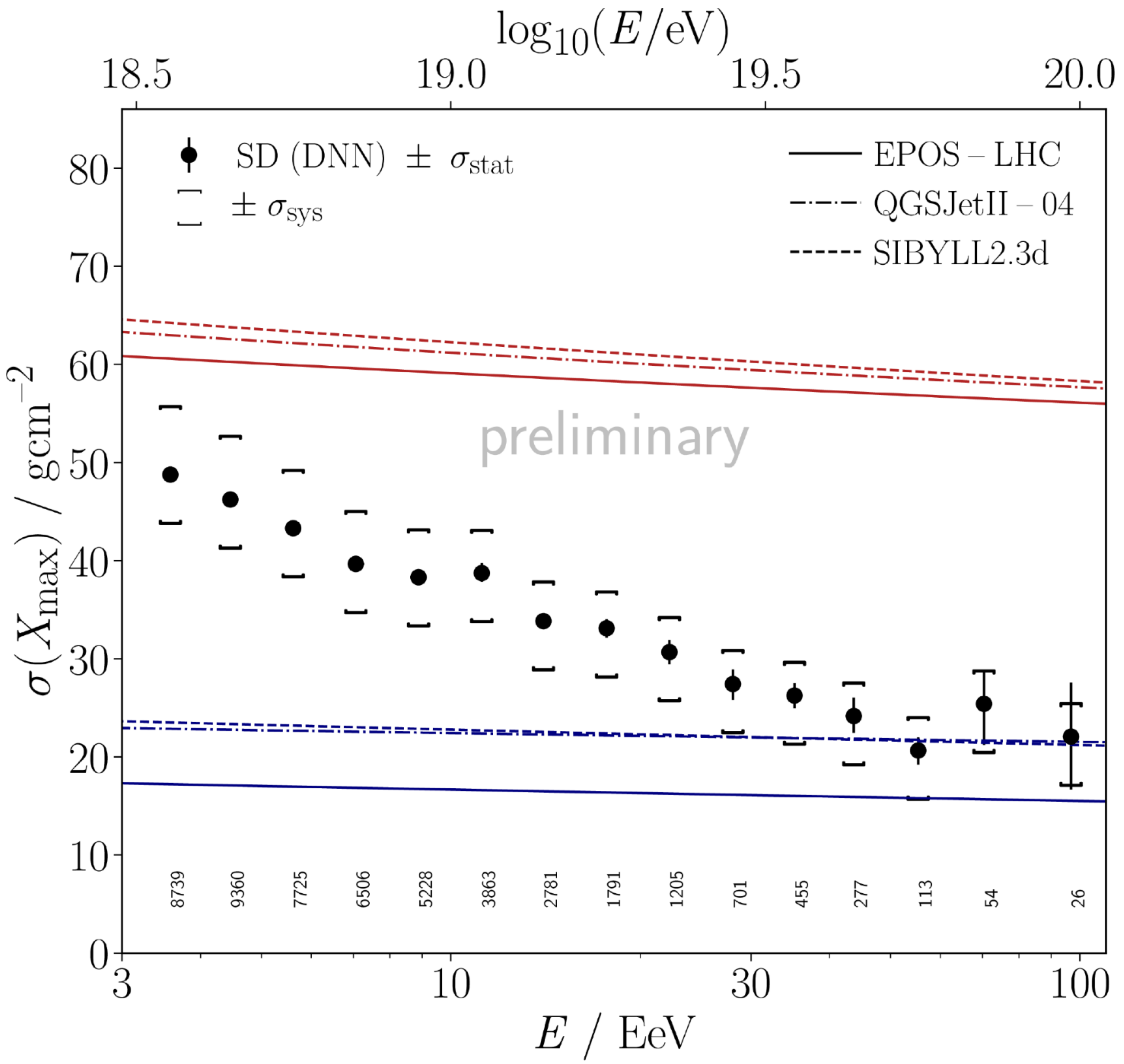

Energy-independent elongation rate excluded at 4.4 sigma

Breaks of elongation rate correlated with breaks in energy spectrum

(Auger to appear in PRL & PRD 2406.06315, 2406.06319)

Multi-messenger searches: photons

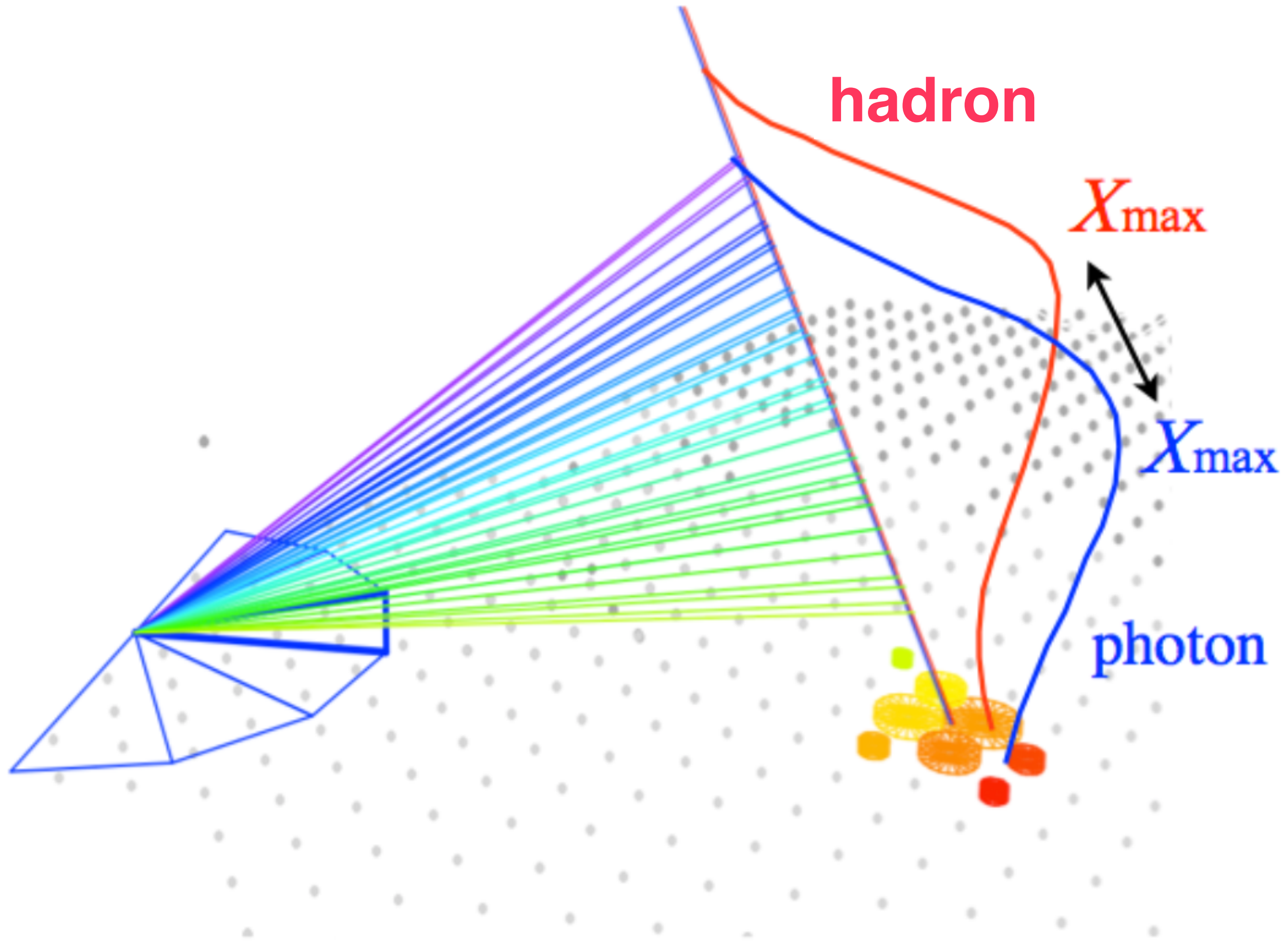

Photons interact deeper (larger X_{max}), fewer muons (rise time, lateral slope)

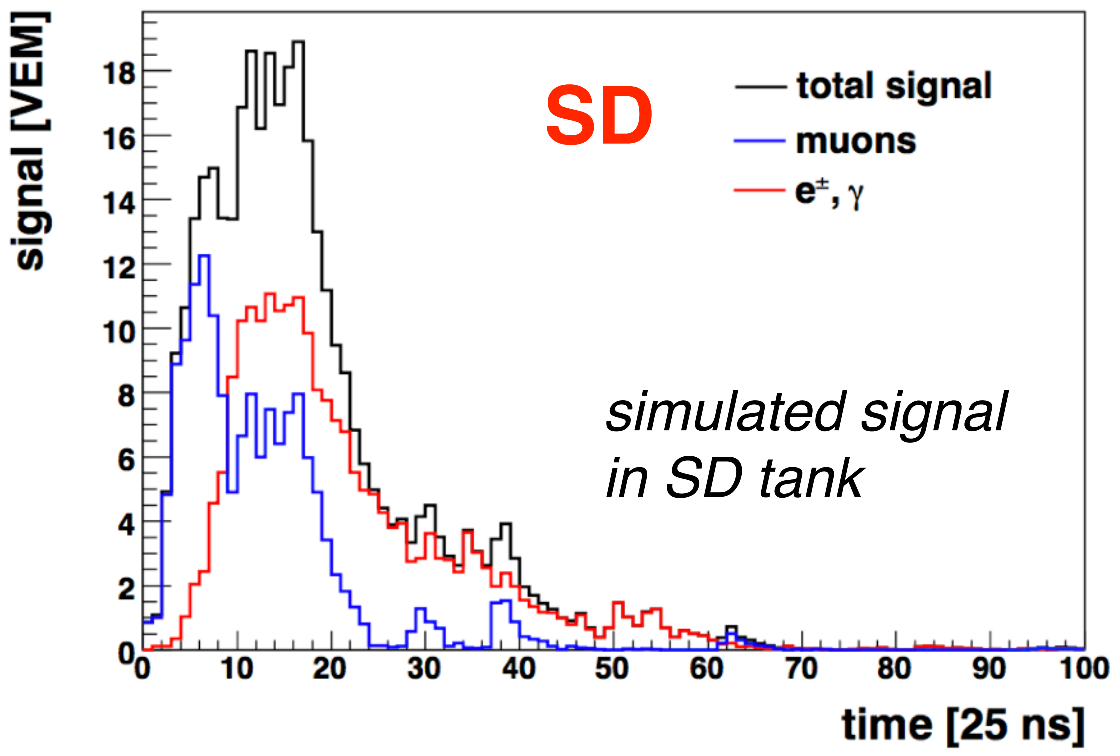

(Auger, 2006 – 2011)

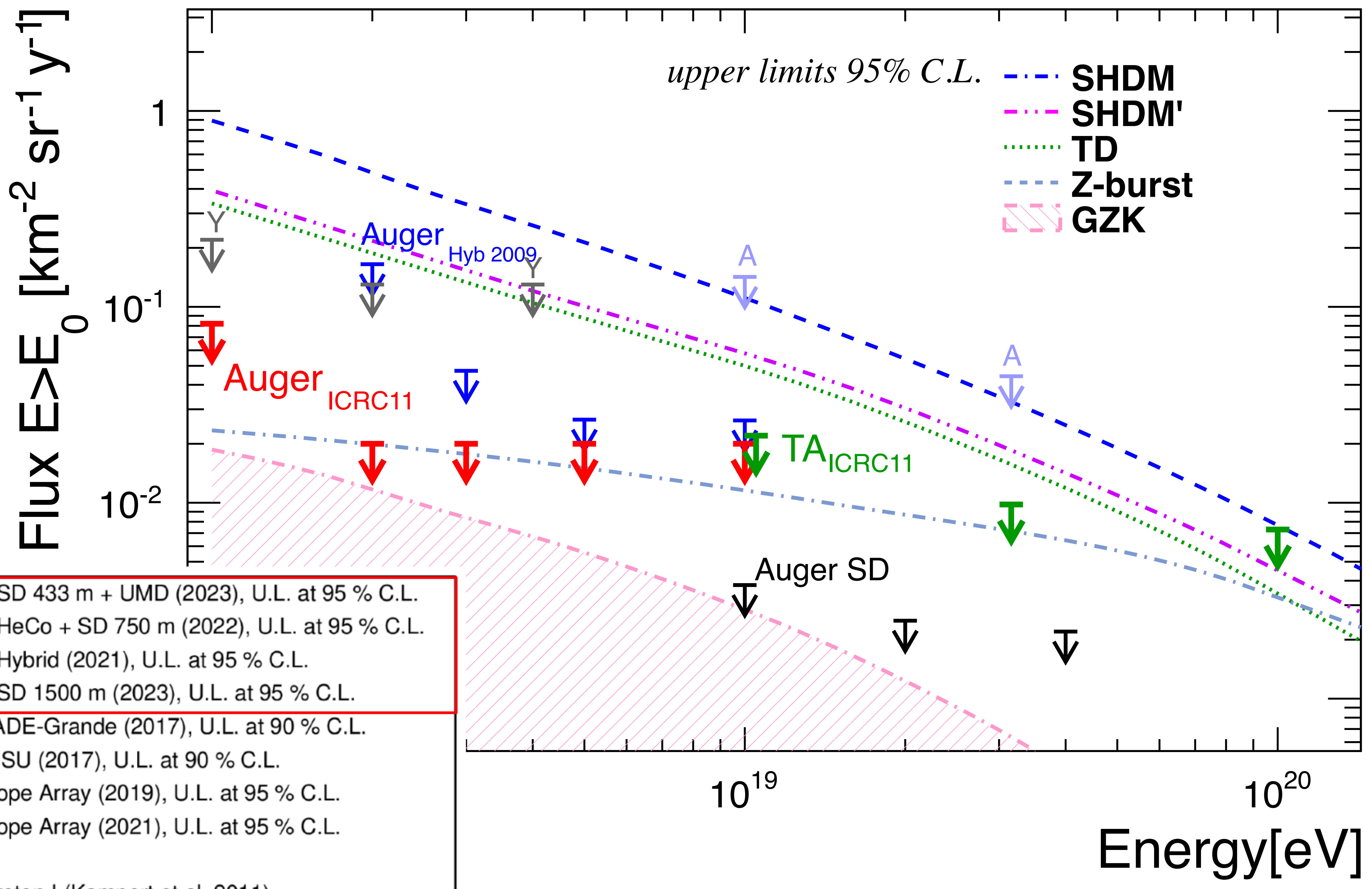

(Auger, ICRC 2023)

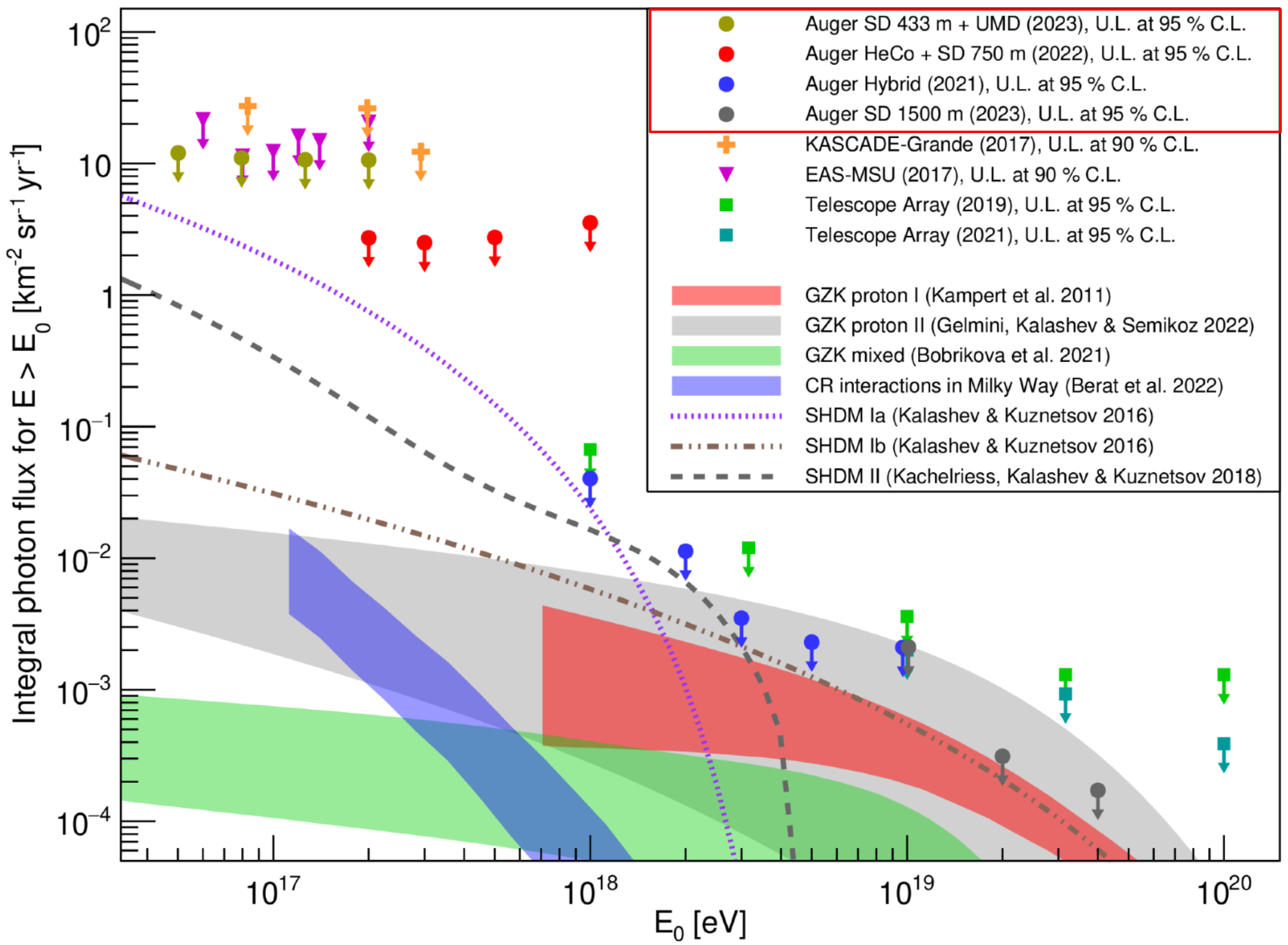

Exotic processes as dominant sources excluded

Sensitivity reaches GZK predictions

Multi-messenger searches: neutrinos

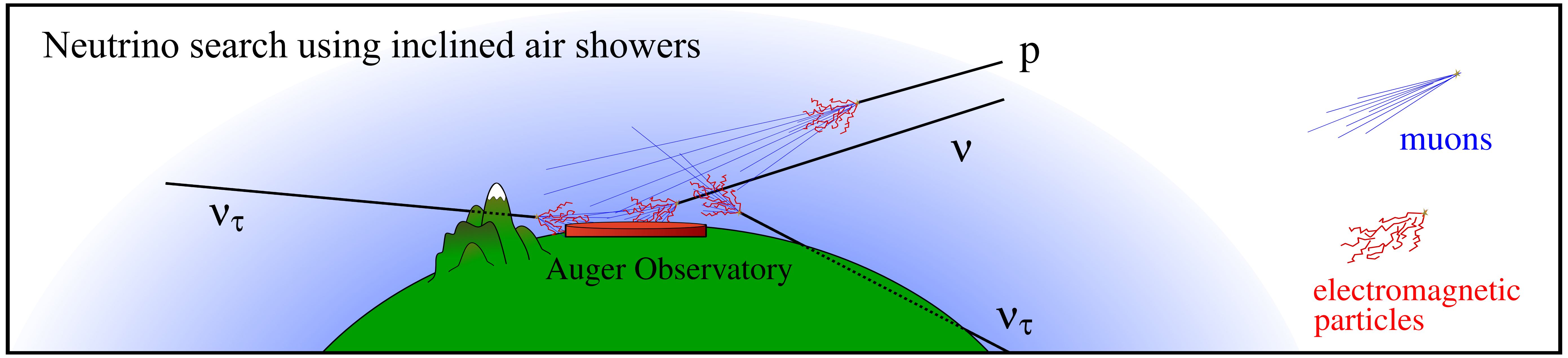

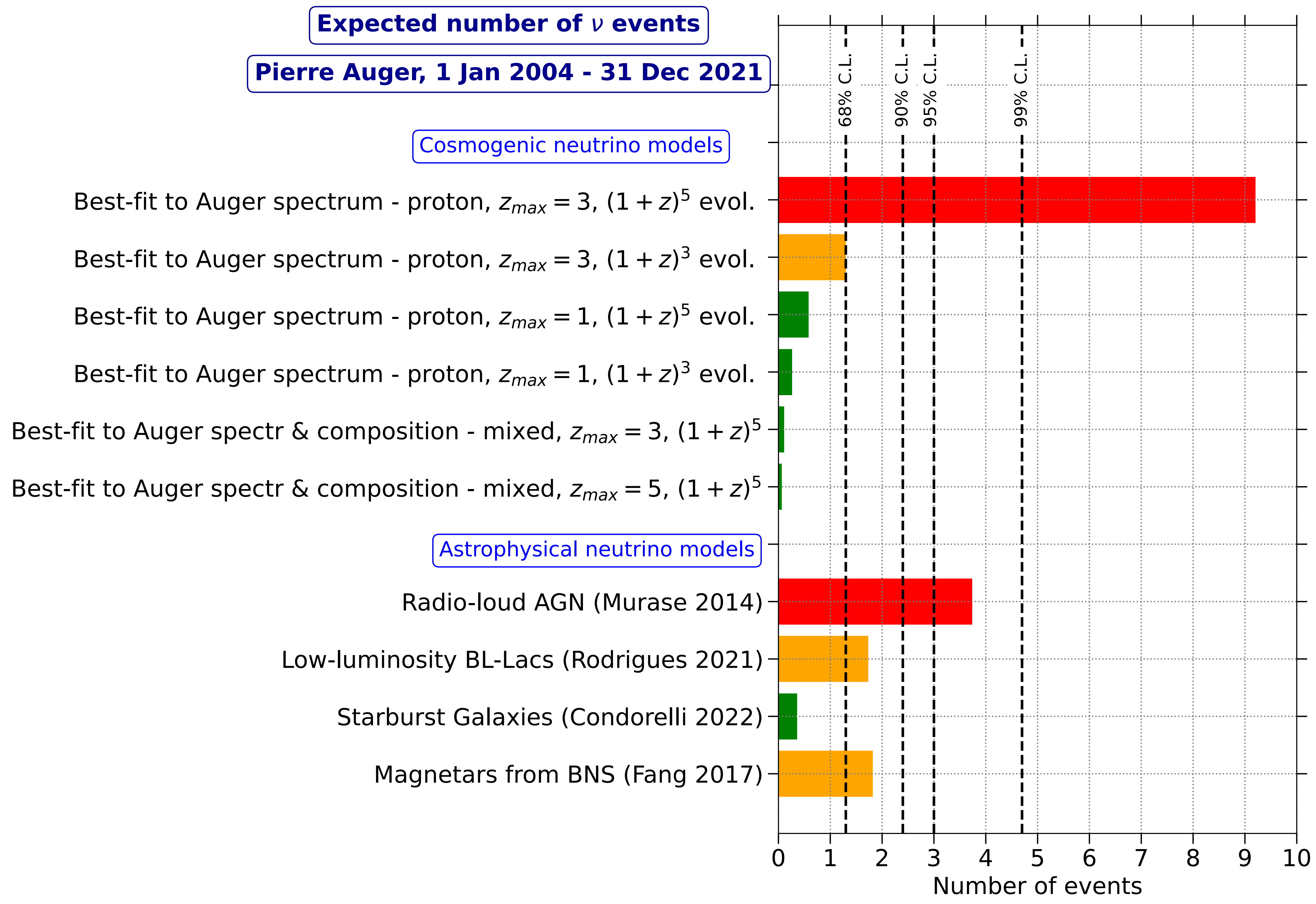

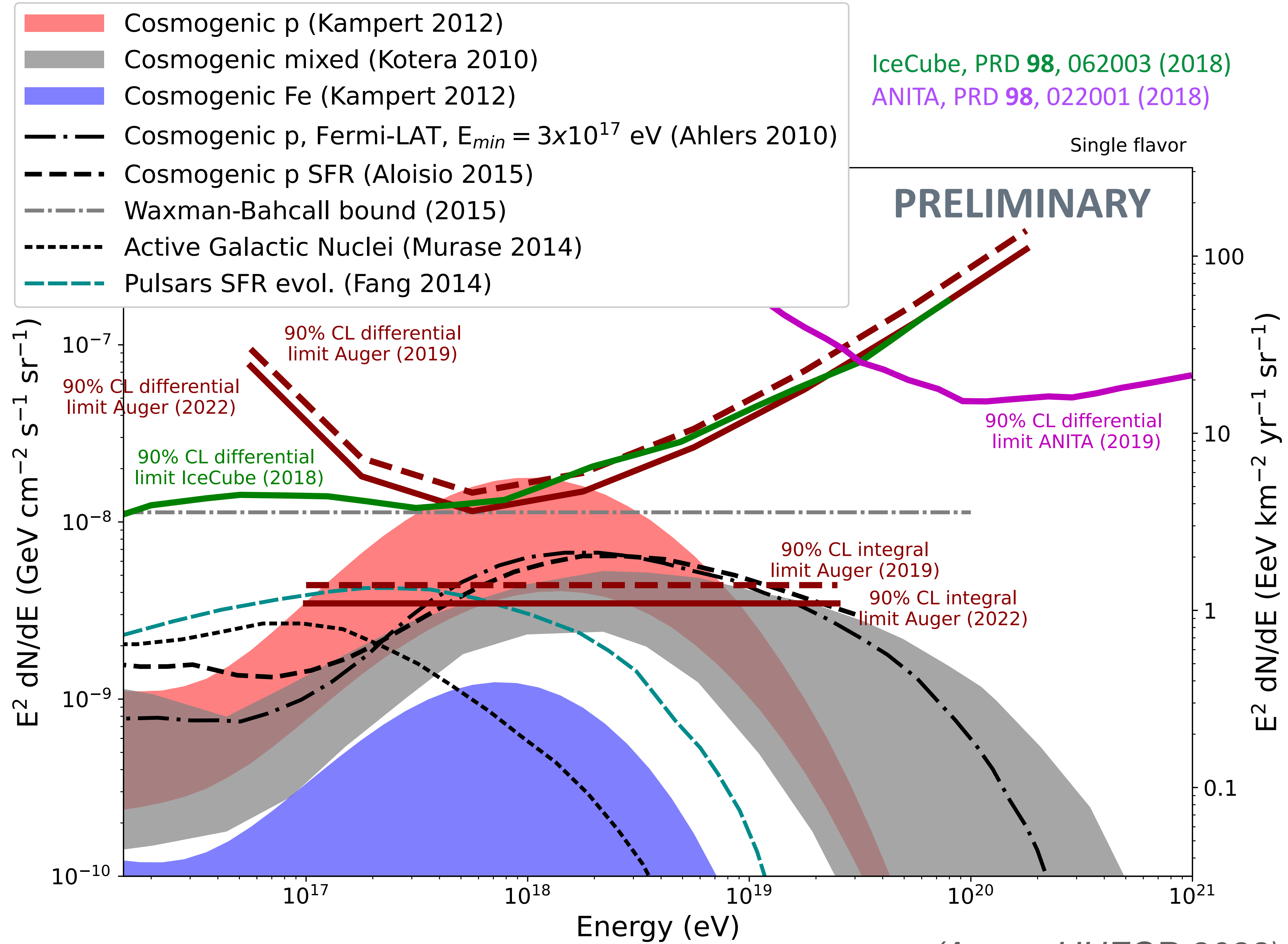

(Auger, UHECR 2022)

Neutrino sensitivity better than Waxman-Bahcall bound
Limits constrain GZK & astrophysical neutrino models

Arrival direction distribution

Arrival direction distribution surprisingly isotropic

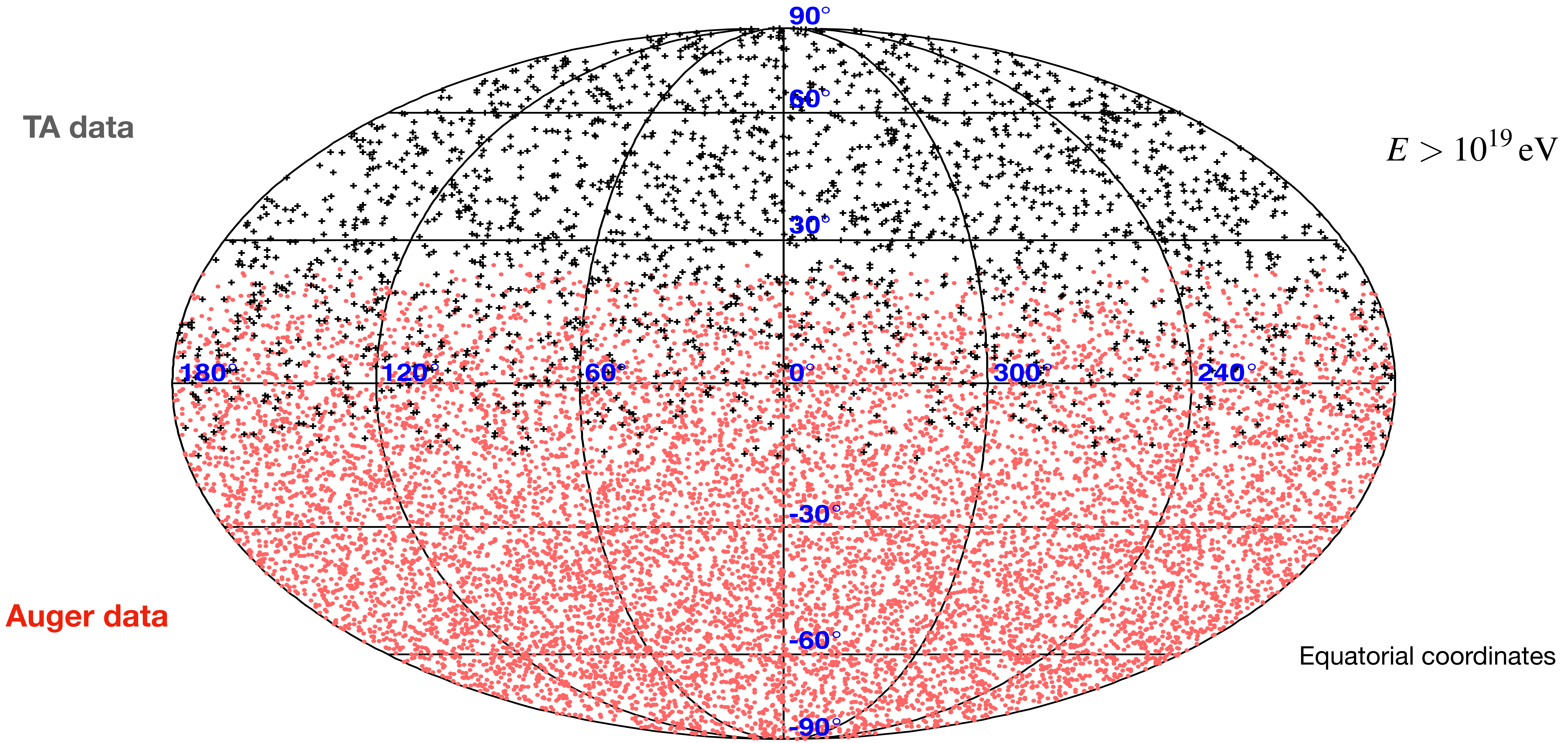

Pierre Auger and TA Collaborations, ApJ **794** (2014) 2, 172

Auger data – large angular scales (dipole)

physicsworld TOP 10 BREAKTHROUGH 2017

Science 357 (2017) 1266)

E [EeV]	N	$d_\perp$ [%]	d_z [%]	d [%]	α_d [°]	δ_d [°]	$P(\geq r_1^\alpha)$
4-8	118,722	$1.0^{+0.6}_{-0.4}$	-1.3 ± 0.8	$1.7^{+0.8}_{-0.5}$	92 ± 28	-52^{+21}_{-19}	0.14
≥ 8	49,678	$5.8^{+0.9}_{-0.8}$	-4.5 ± 1.2	$7.4^{+1.0}_{-0.8}$	97 ± 8	-38^{+9}_{-9}	8.7×10^{-12}
8-16	36,658	$5.7^{+1.0}_{-0.9}$	-3.1 ± 1.4	$6.5^{+1.2}_{-0.9}$	93 ± 9	-29^{+11}_{-12}	1.4×10^{-8}
16-32	10,282	$5.9^{+2.0}_{-1.8}$	-7 ± 3	$9.4^{+2.6}_{-1.9}$	93 ± 16	-51^{+13}_{-13}	4.3×10^{-3}
≥ 32	2,738	11^{+4}_{-3}	-13 ± 5	17^{+5}_{-4}	144 ± 18	-51^{+14}_{-14}	9.8×10^{-3}

6.8σ

5.7σ

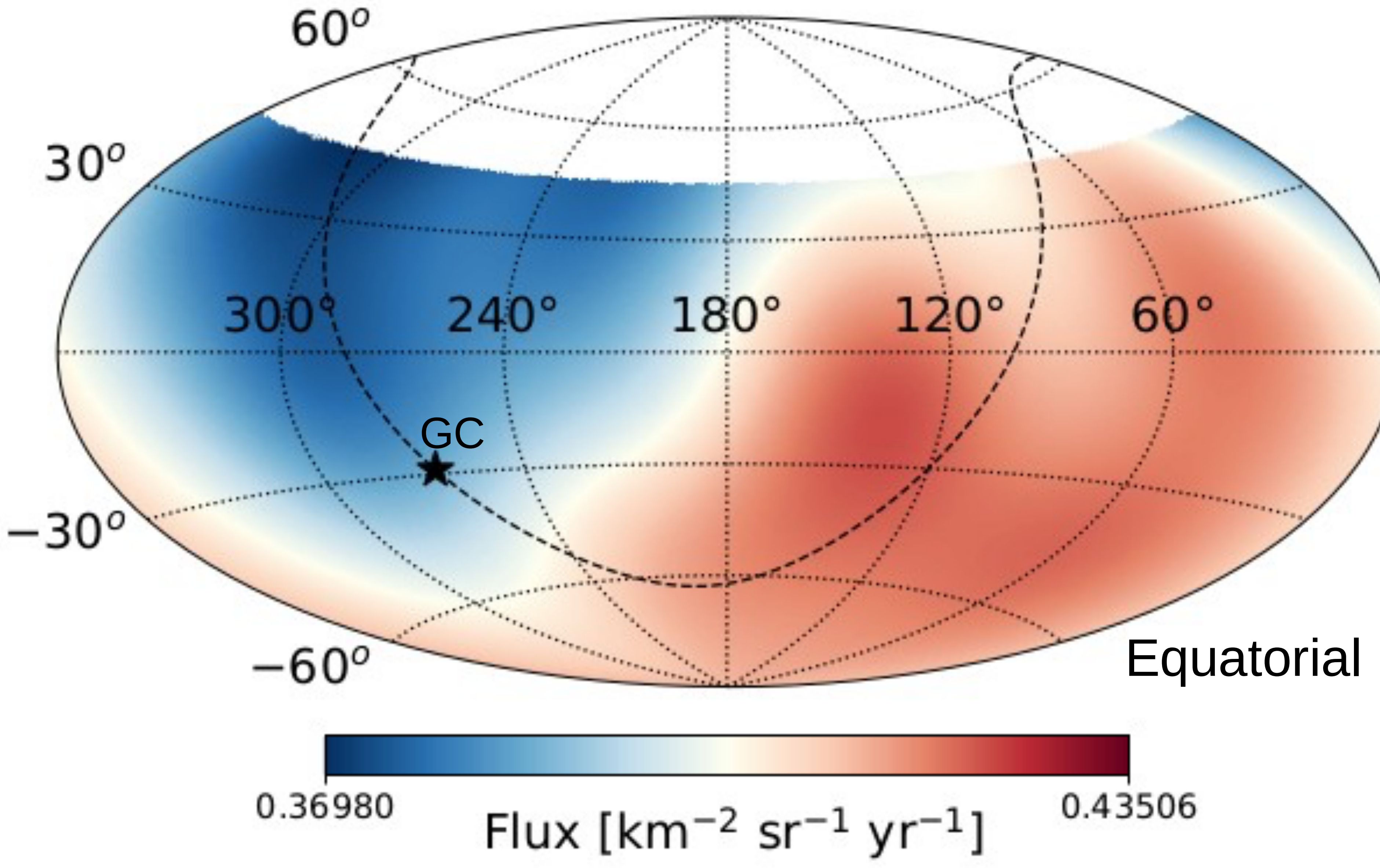

E>8 EeV

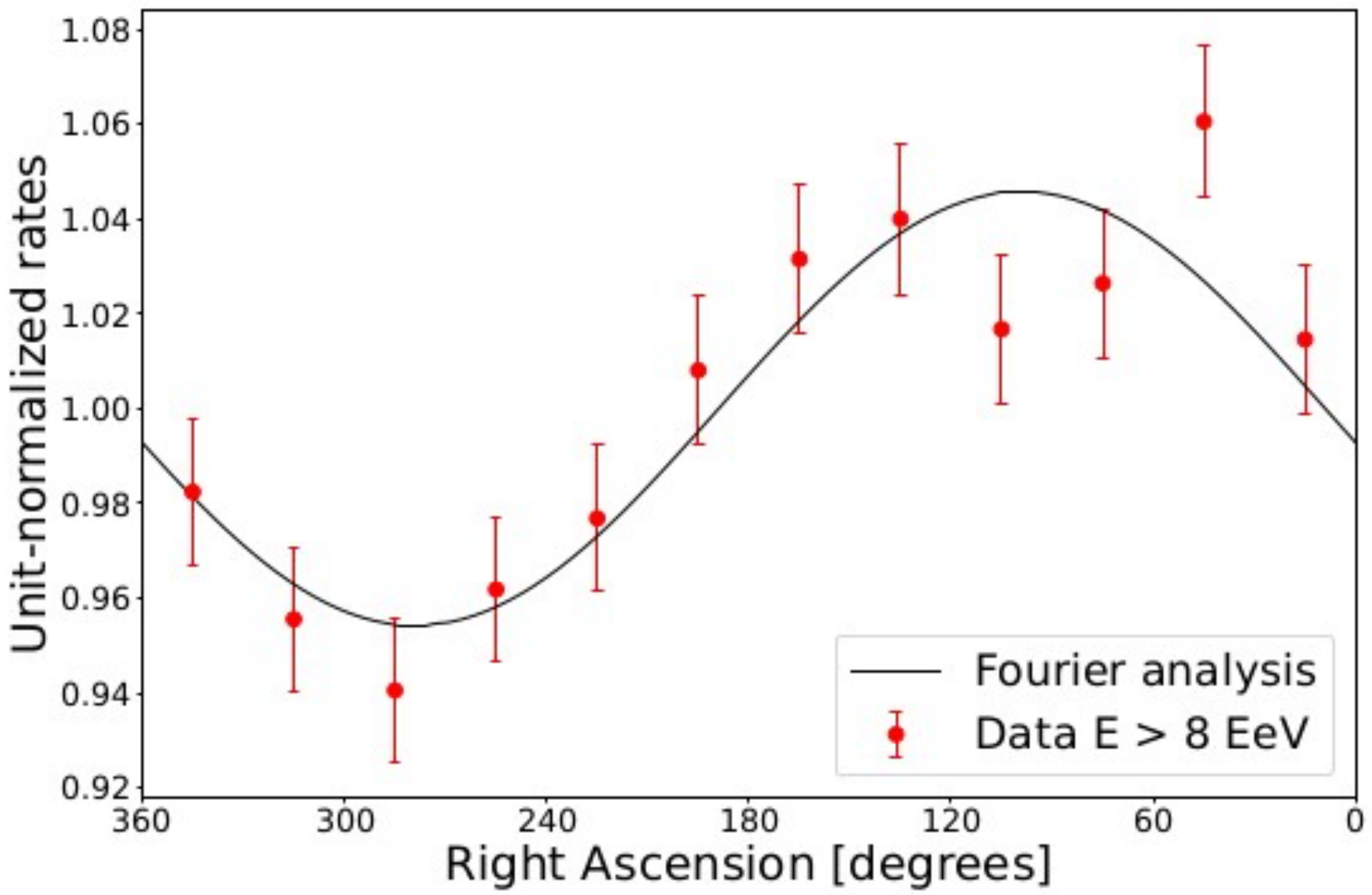

Arrival direction distribution at highest energies

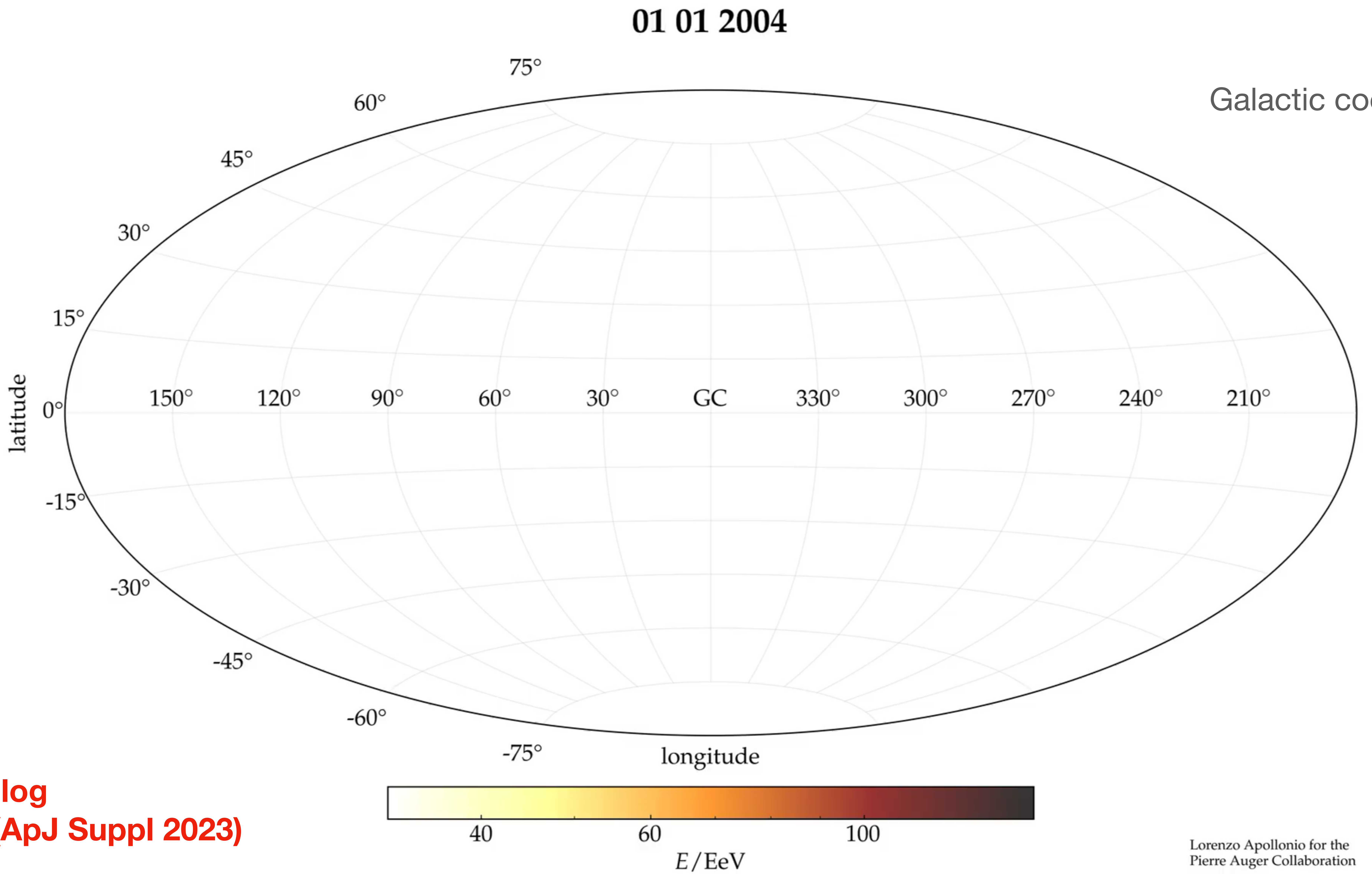

Galactic coordinates

Published catalog of Auger data (ApJ Suppl 2023)

Lorenzo Apollonio for the Pierre Auger Collaboration

Intermediate-scale anisotropy at highest energies

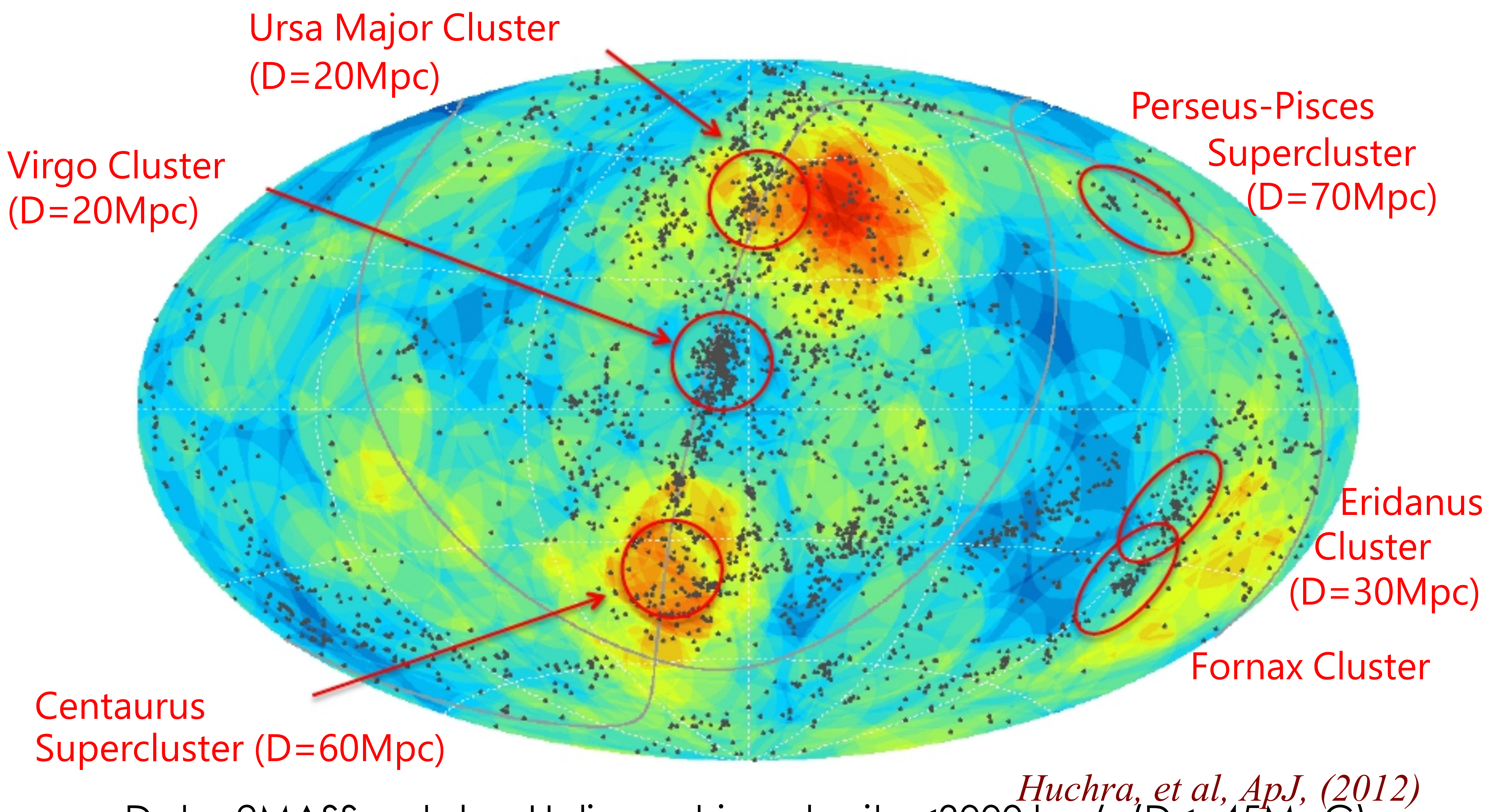

Dots : 2MASS catalog Heliocentric velocity <3000 km/s (D<~45MpC)

(Ogio et al. ISVHECRI 2018, world data set of UHECR)

TA data – high-energy anisotropy searches

Hot Spot

Li-Ma Significance Map with E ≥ 57 EeV

25° angular distance oversampling

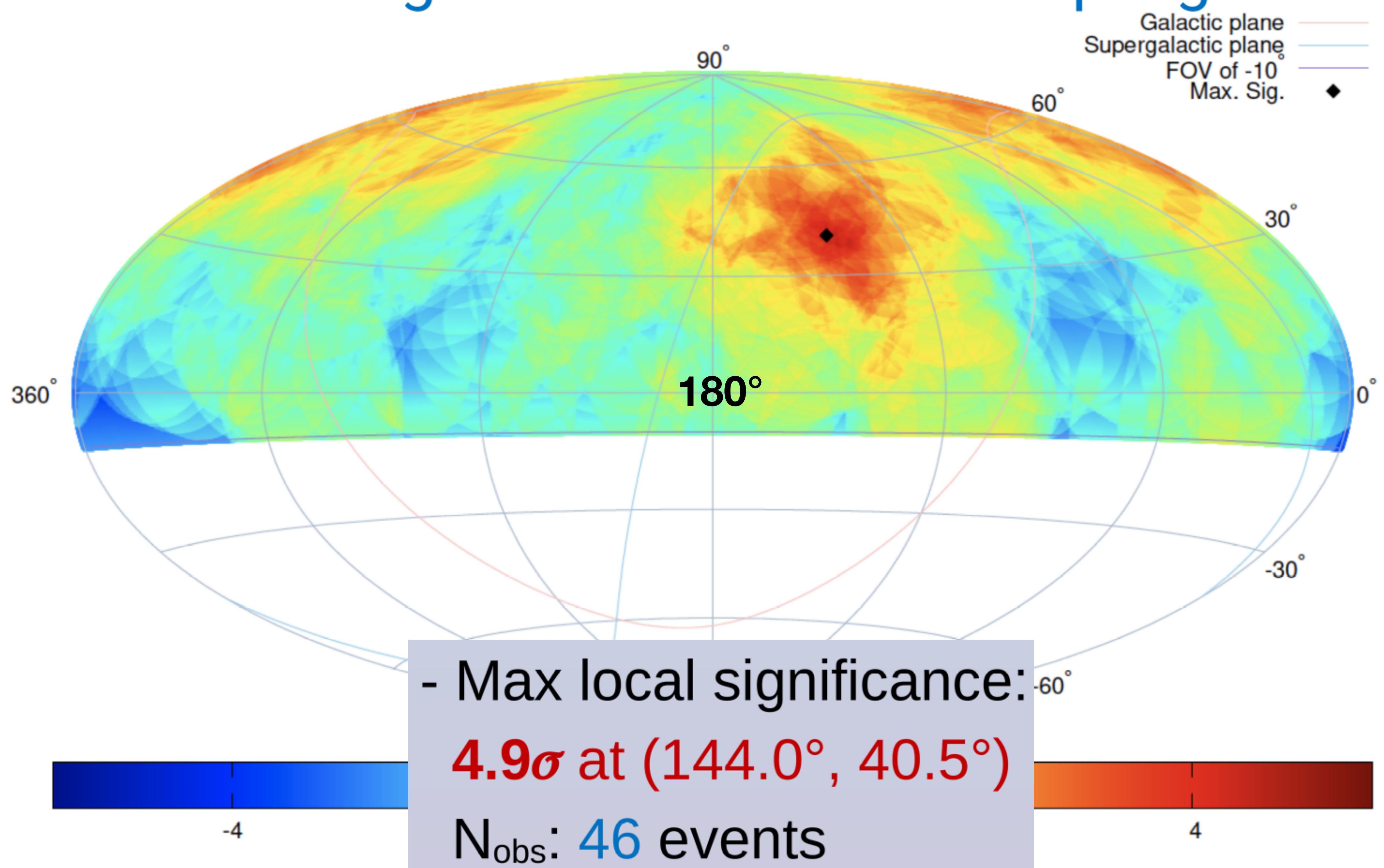

- Max local significance: **4.9σ** at (144.0°, 40.5°)
  N_{obs}: 46 events
  N_{bg} : 19.1 events
- Post-trial probability: **2.9σ**

Perseus-Pisces supercluster

Li-Ma Significance Map with E ≥ $10^{19.4}$ eV

20° angular distance oversampling

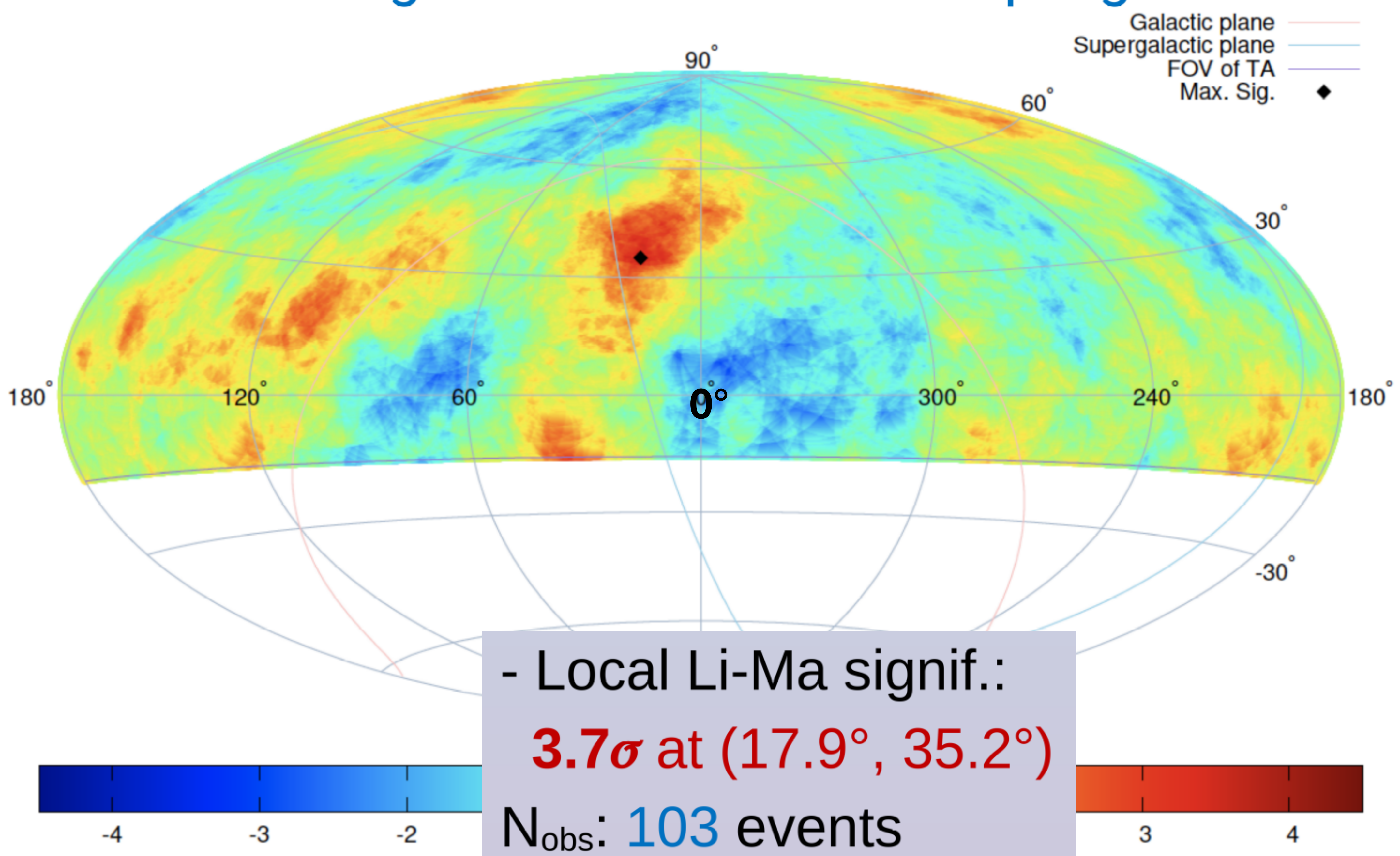

- Local Li-Ma signif.: **3.7σ** at (17.9°, 35.2°)
  N_{obs}: 103 events
  N_{bg} : 68.5 events
  Signif. of correlation with PPSC: **3.1σ**

(TA, UHECR 2024)

Auger data – high-energy anisotropy searches

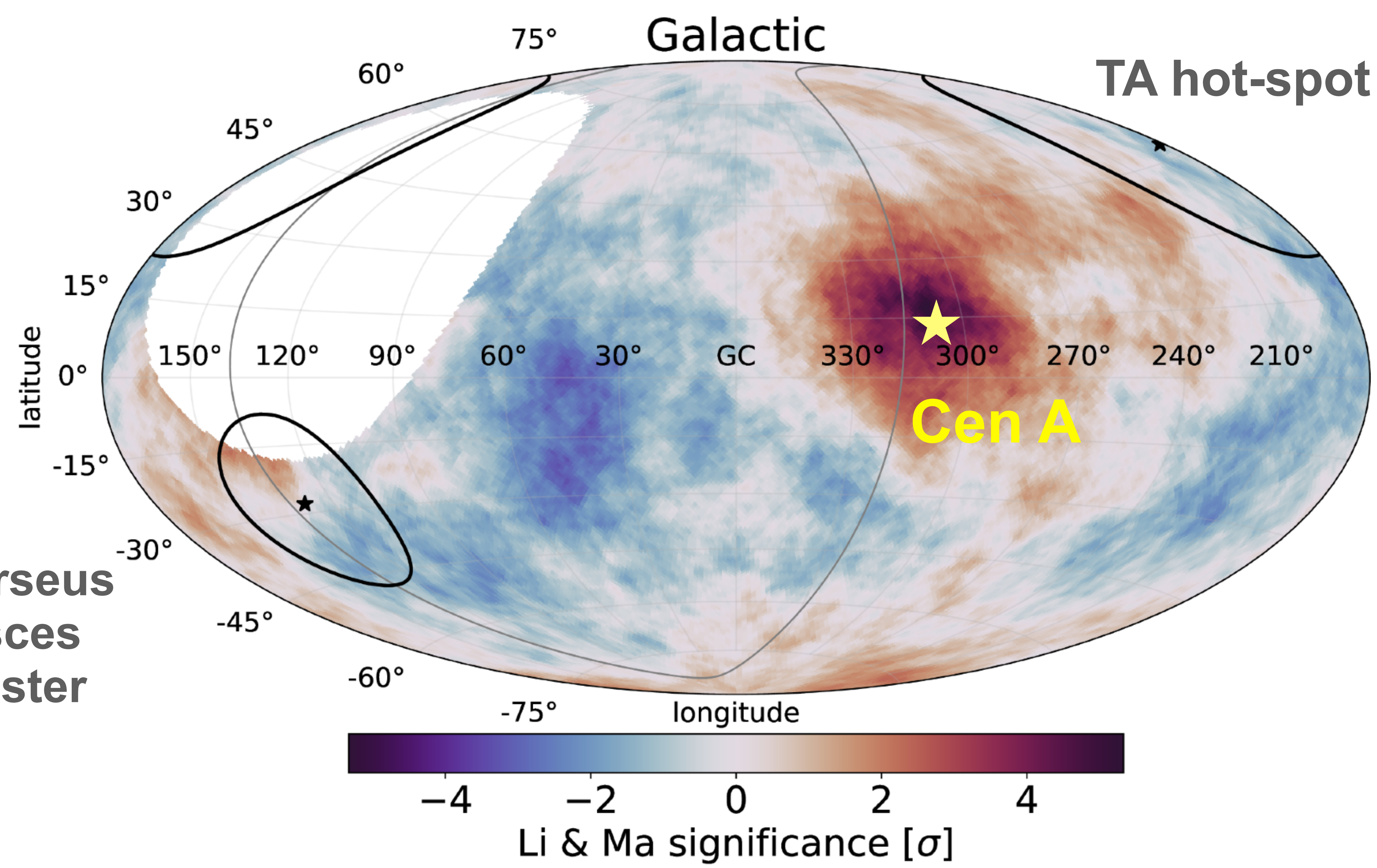

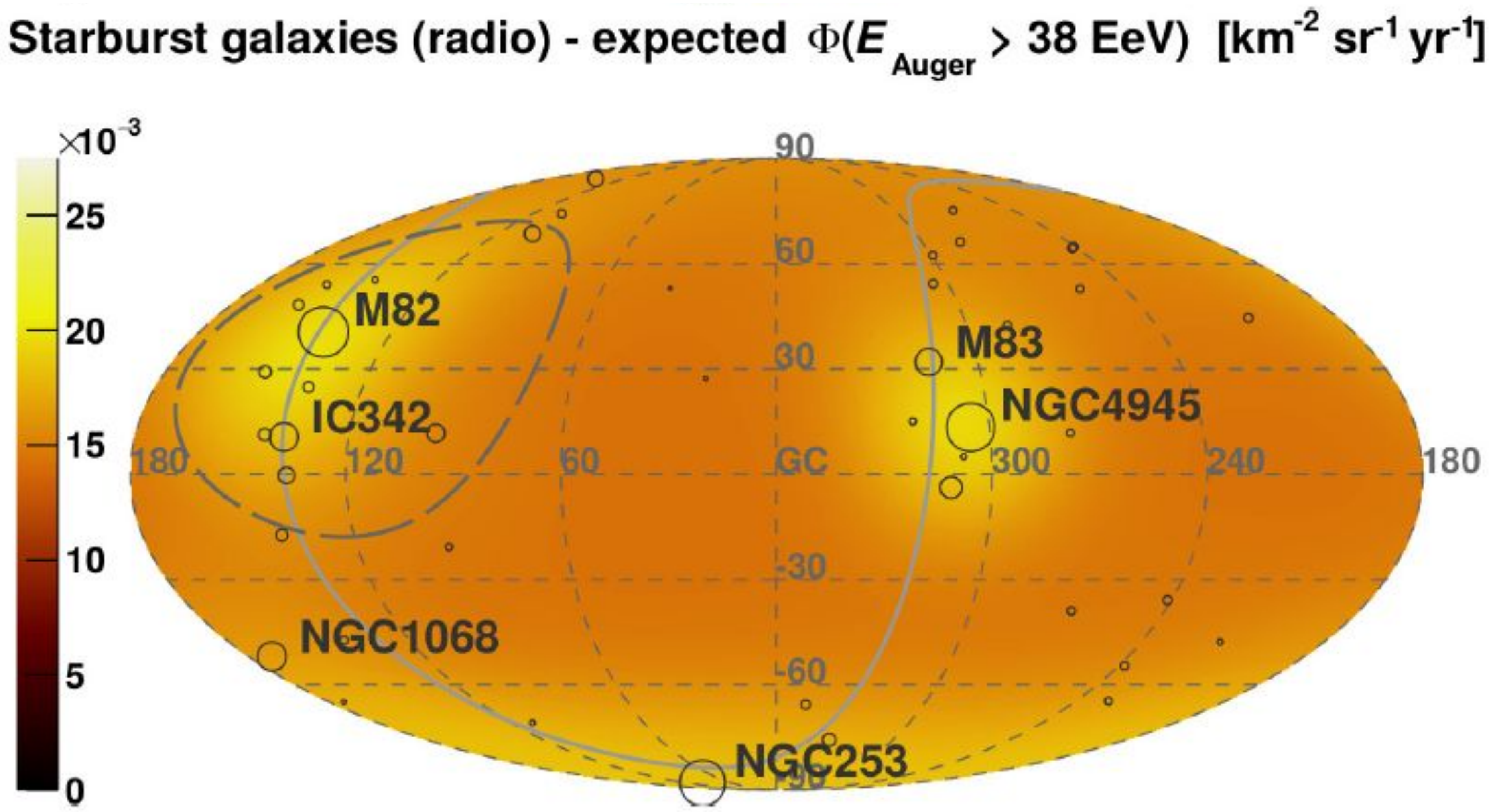

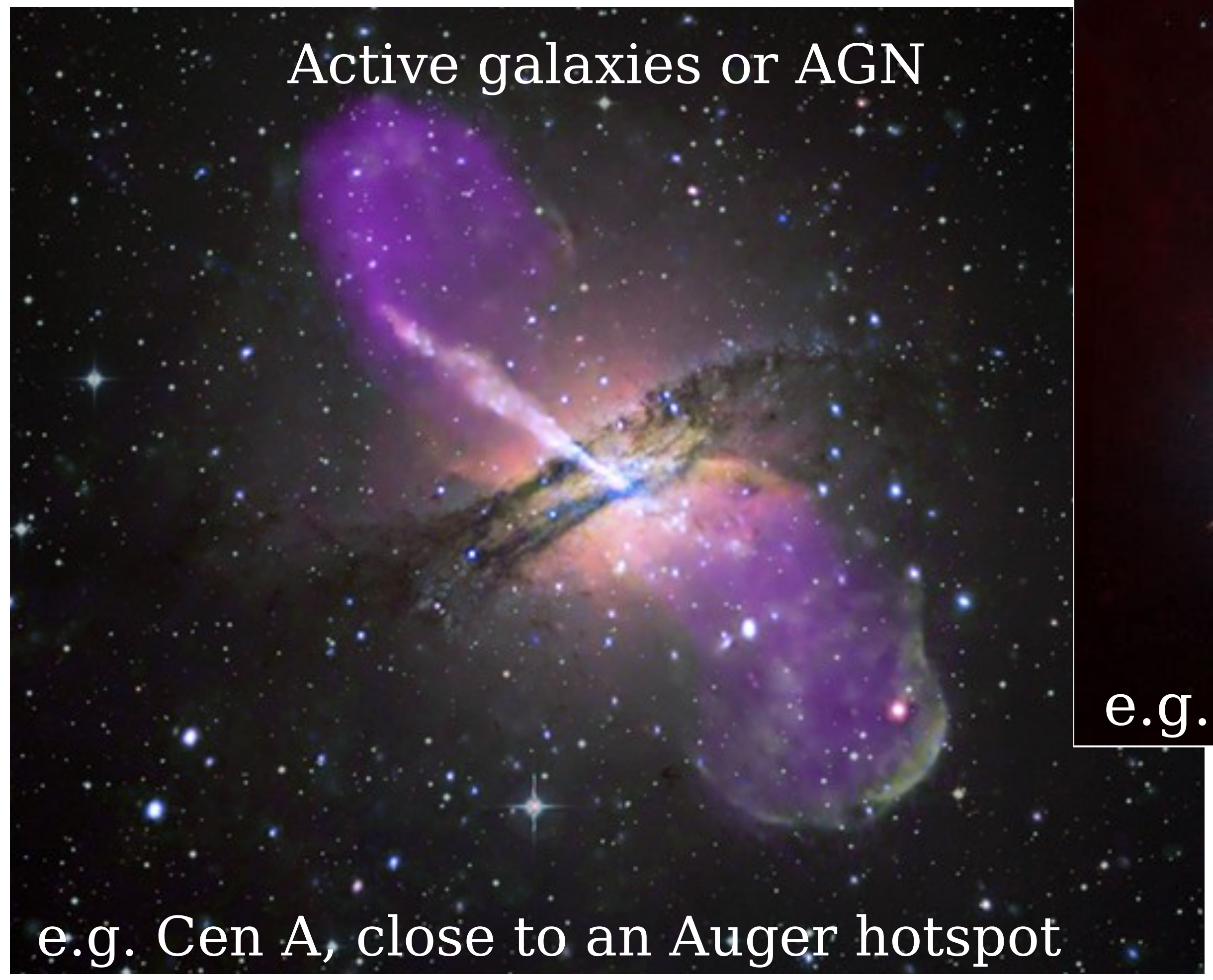

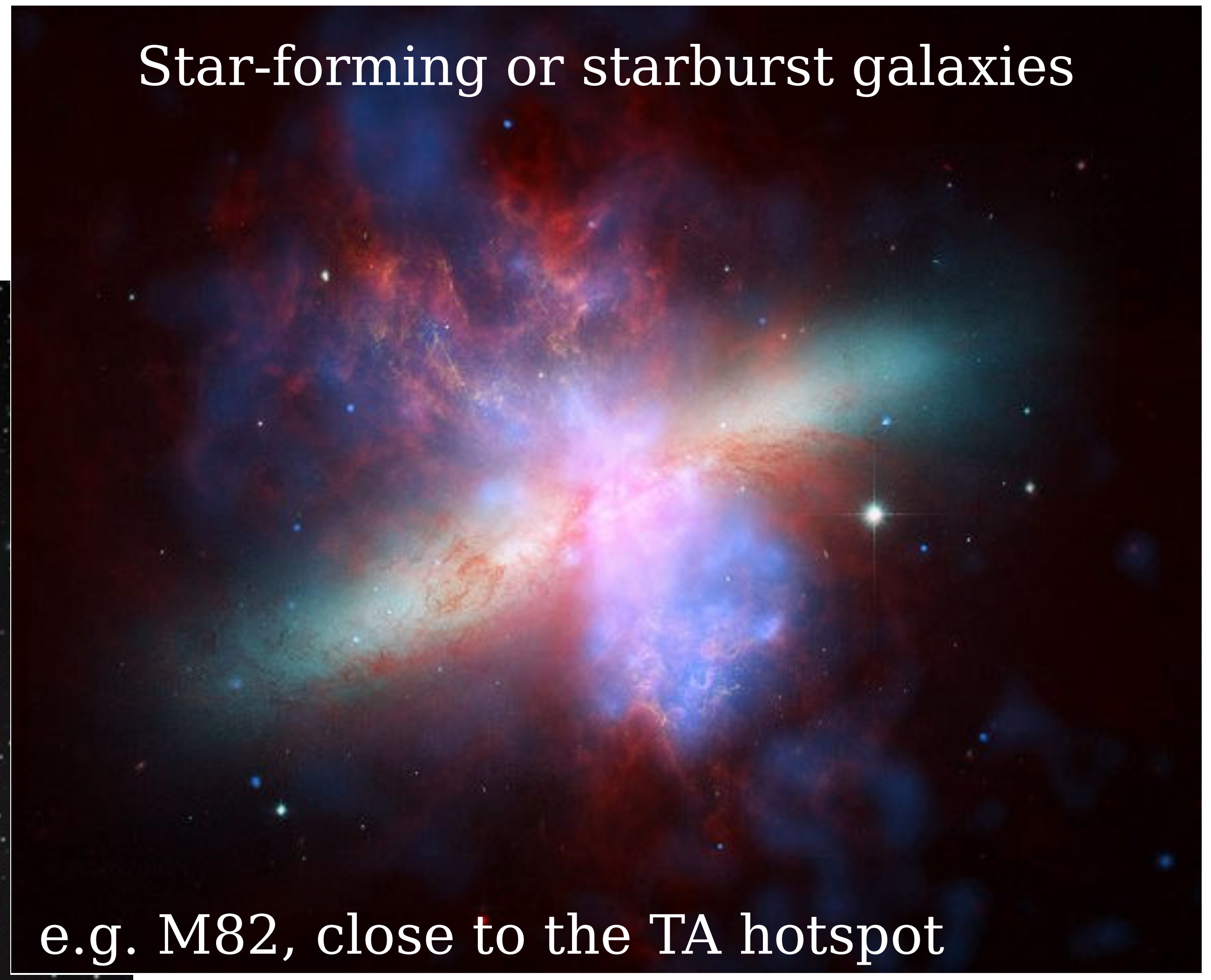

Centaurus A: E > 3.8 10^{19} eV, ~27° radius, 4.0 σ (post trial)

Starburst galaxies: E > 3.8 10^{19} eV, ~25° radius, 3.8 σ (post trial)

Discovery level of 5σ expected only after 2025

First probe of TA over-densities thanks to inclined showers

(Astrophysical Journal, 935:170, 2022, update ICRC 2023)

Arrival directions – Auger-TA overlap region

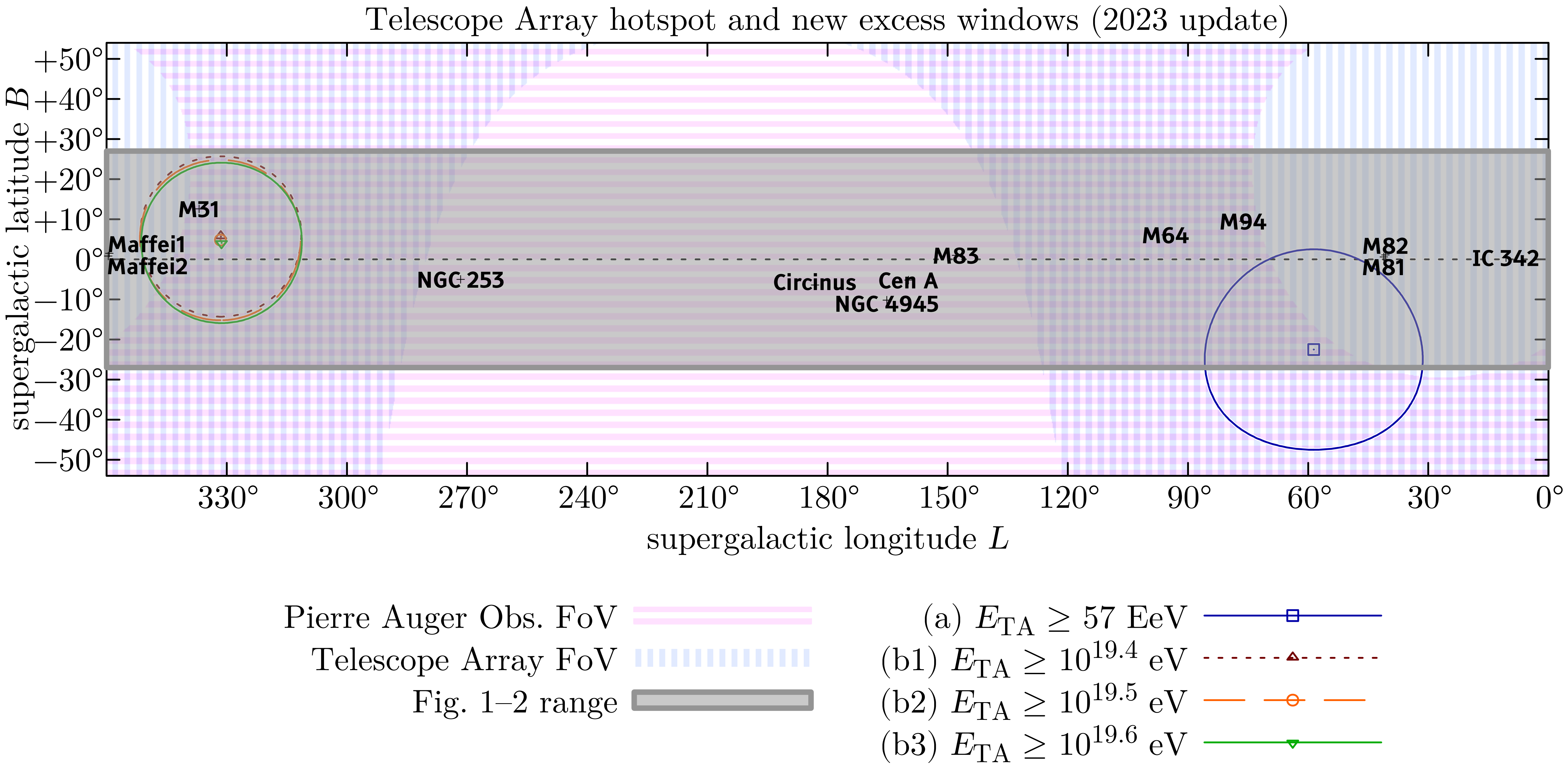

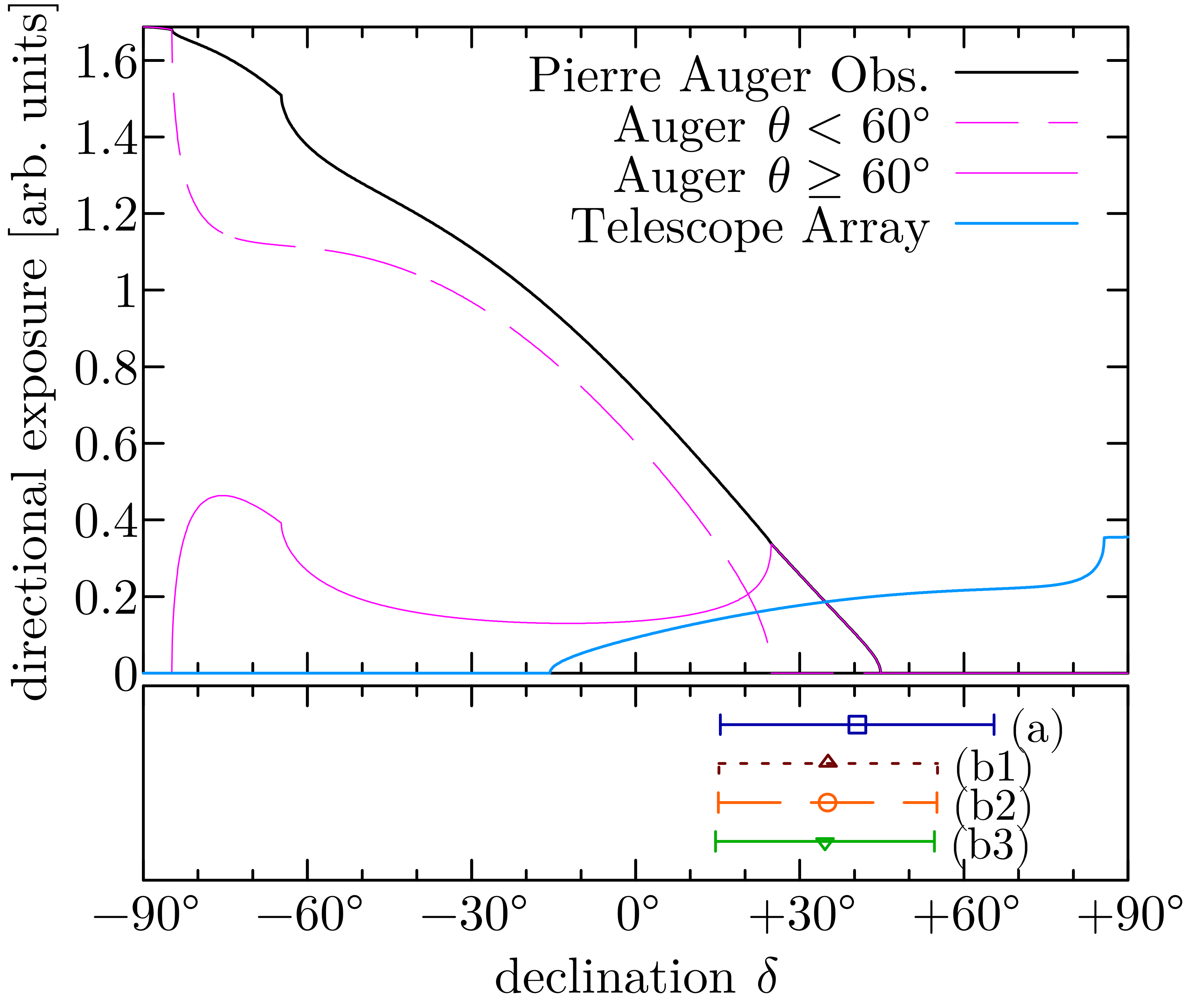

	Telescope Array									Pierre Auger Observatory							
	$E_{\min}$	N_{tot}	$\frac{\mathcal{E}_{\text{in}}}{\mathcal{E}_{\text{tot}}}$	N_{bg}	N_{in}	$\frac{\Phi_{\text{in}}}{\Phi_{\text{out}}}$	Z_{LM}	99% L.L.	post-trial	$E_{\min}$	N_{tot}	$\frac{\mathcal{E}_{\text{in}}}{\mathcal{E}_{\text{tot}}}$	N_{bg}	N_{in}	$\frac{\Phi_{\text{in}}}{\Phi_{\text{out}}}$	Z_{LM}	99% U.L.
(a)	57 EeV	216	9.47%	18.0	44	$2.44^{+0.44}_{-0.39}$	$+4.8\sigma$	1.60	2.8σ	44.6 EeV	1074	1.00%	10.7	9	$0.84^{+0.31}_{-0.25}$	-0.5σ	1.76
(b1)	$10^{19.4}$ eV	1125	5.88%	64.0	101	$1.58^{+0.17}_{-0.16}$	$+4.1\sigma$	1.22	3.3σ	20.5 EeV	8374	0.84%	70.1	65	$0.93^{+0.12}_{-0.11}$	-0.6σ	1.23
(b2)	$10^{19.5}$ eV	728	5.87%	41.1	70	$1.70^{+0.22}_{-0.20}$	$+4.0\sigma$	1.25	3.2σ	25.5 EeV	5156	0.84%	43.5	39	$0.90^{+0.15}_{-0.14}$	-0.7σ	1.29
(b3)	$10^{19.6}$ eV	441	5.84%	24.6	45	$1.83^{+0.31}_{-0.27}$	$+3.6\sigma$	1.23	3.0σ	31.7 EeV	2990	0.87%	26.0	27	$1.04^{+0.21}_{-0.19}$	$+0.2\sigma$	1.61

(Auger, ICRC 2023 UHECR 2024)

Interpretation of data

Model calculations for mass composition and flux

(Auger, JCAP 05 (2023) 024 & JCAP 01 (2024) 022 & JCAP 07 (2024) 094)

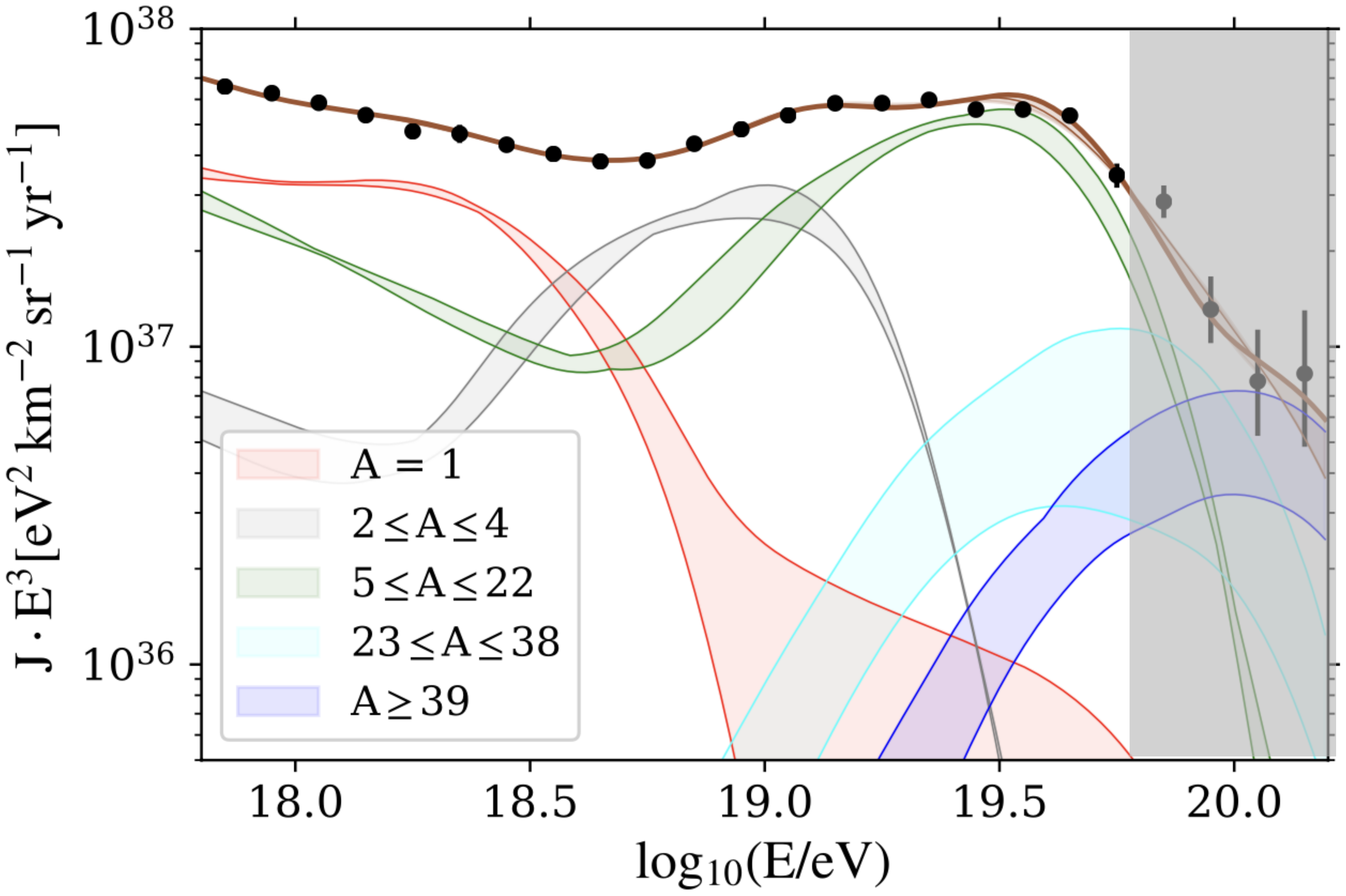

Flux suppression due mainly to limit of injection energy of sources

New problem of limited source variance *(Ehlert et al. PRD 2023)*

Assumption: source injection spectra universal in rigidity $R = E/Z$ (acceleration, scaling with charge Z)

$$E_{\mathrm{p,cut}} = 1.4 \ldots 1.6 \times 10^{18}\,\mathrm{eV}$$

Exceptionally hard injection spectrum (except for very strong mag. horizon)

$$\frac{dN}{dE} \sim E^{1.5\ldots2}$$

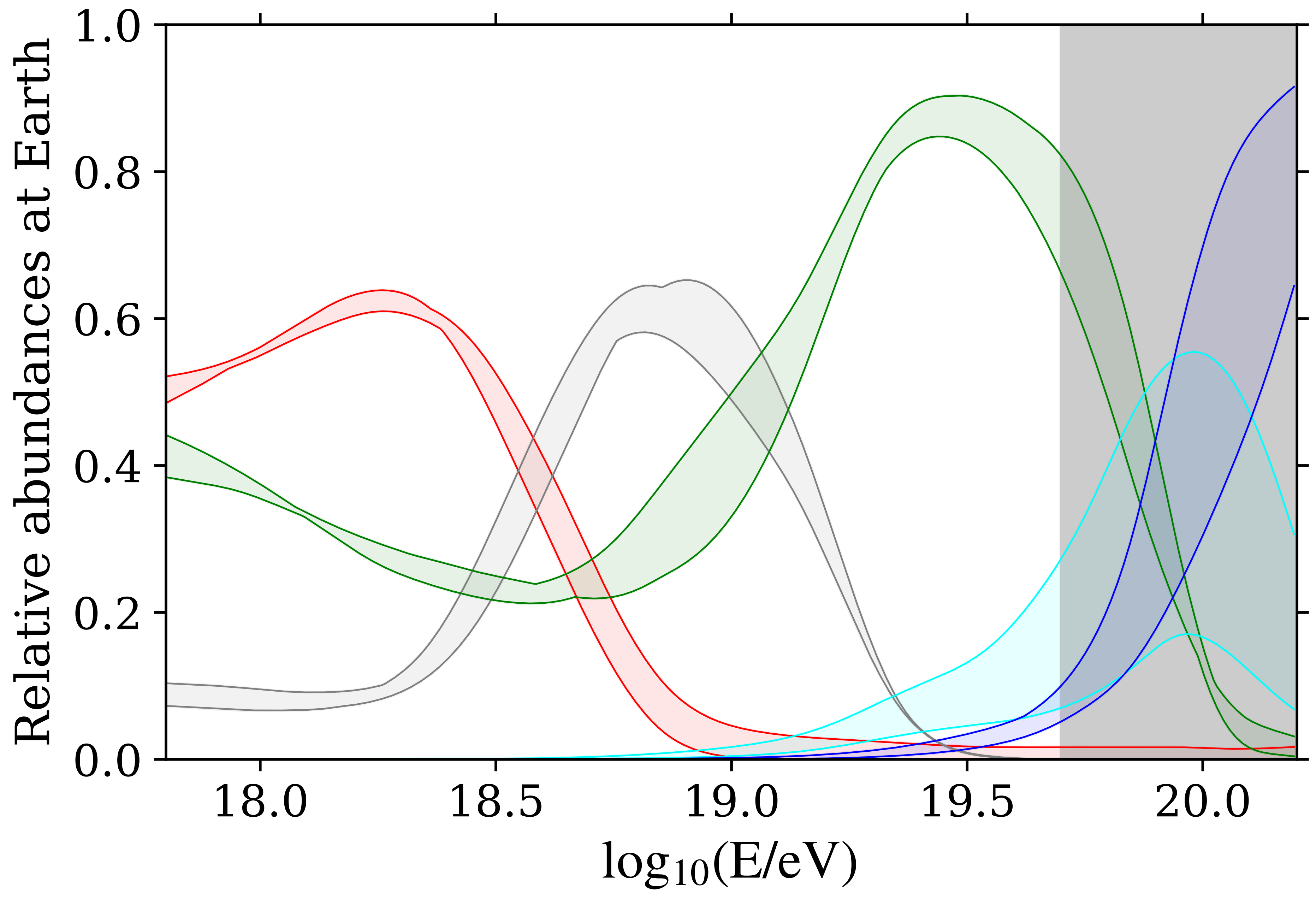

No direct composition data

Index depends on suppression function

(Comisso et al. ApJL 977 (2025) 18)

Arrival directions – large angular scales (dipole)

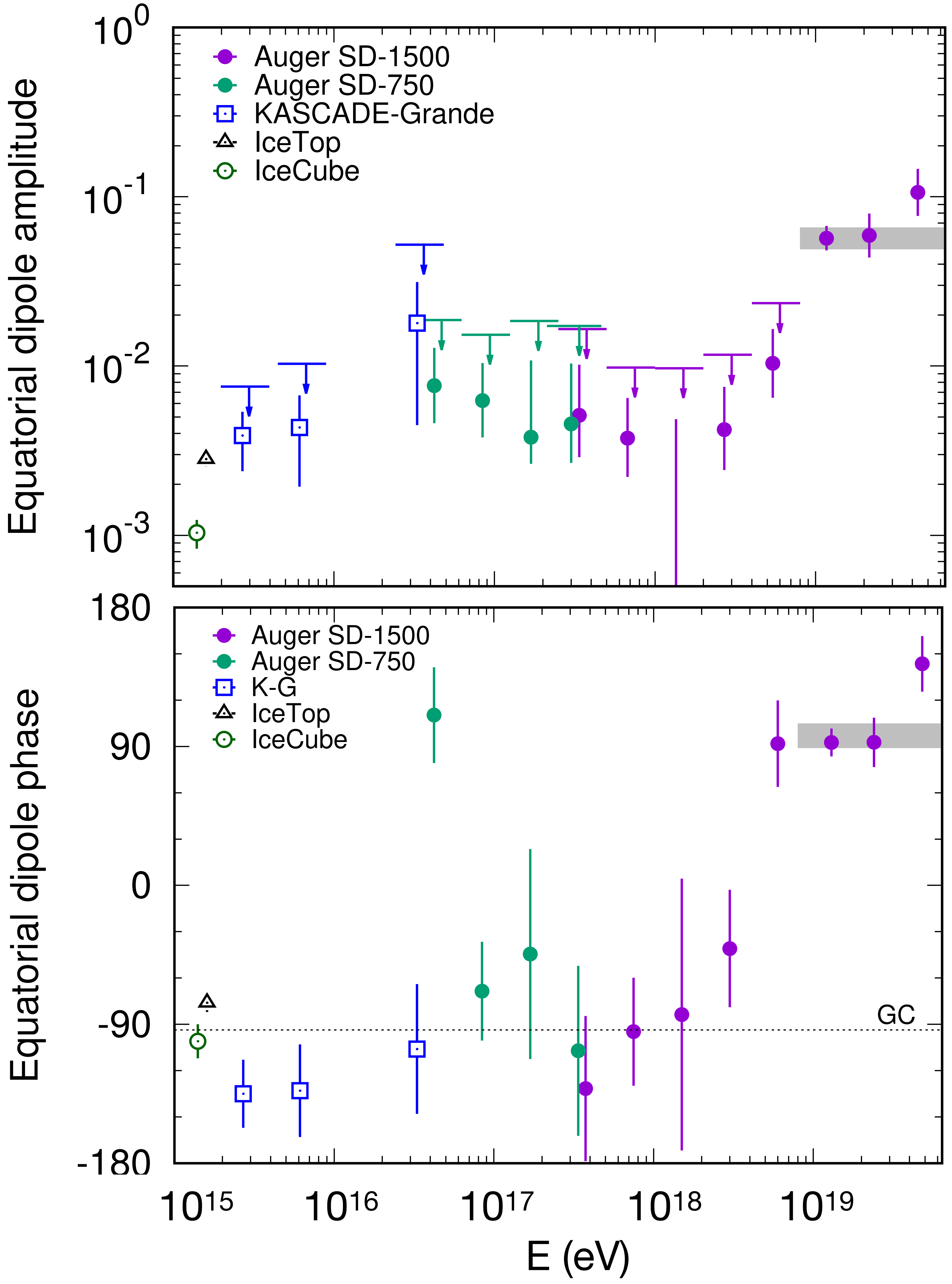

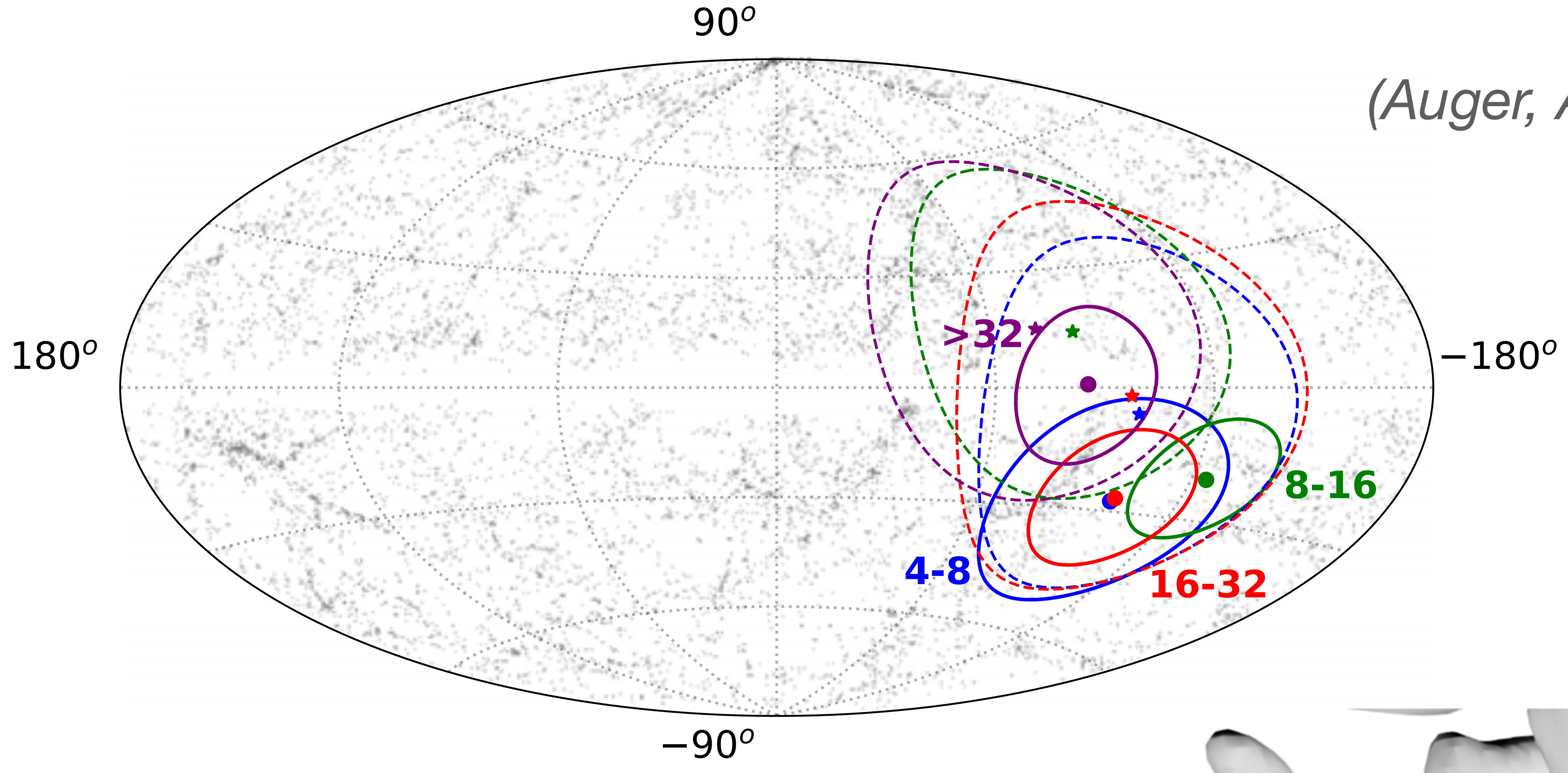

(Auger, ApJ 976 (2024) 48)

2MASS IR catalog:

dashed: prediction

solid: observation

(Ding, Globus & Farrar ApJ 913 (2021) L13)

Bister, Farrar, Unger, ApJL 975 L21 (2024) ApJ 966 71 (2024)

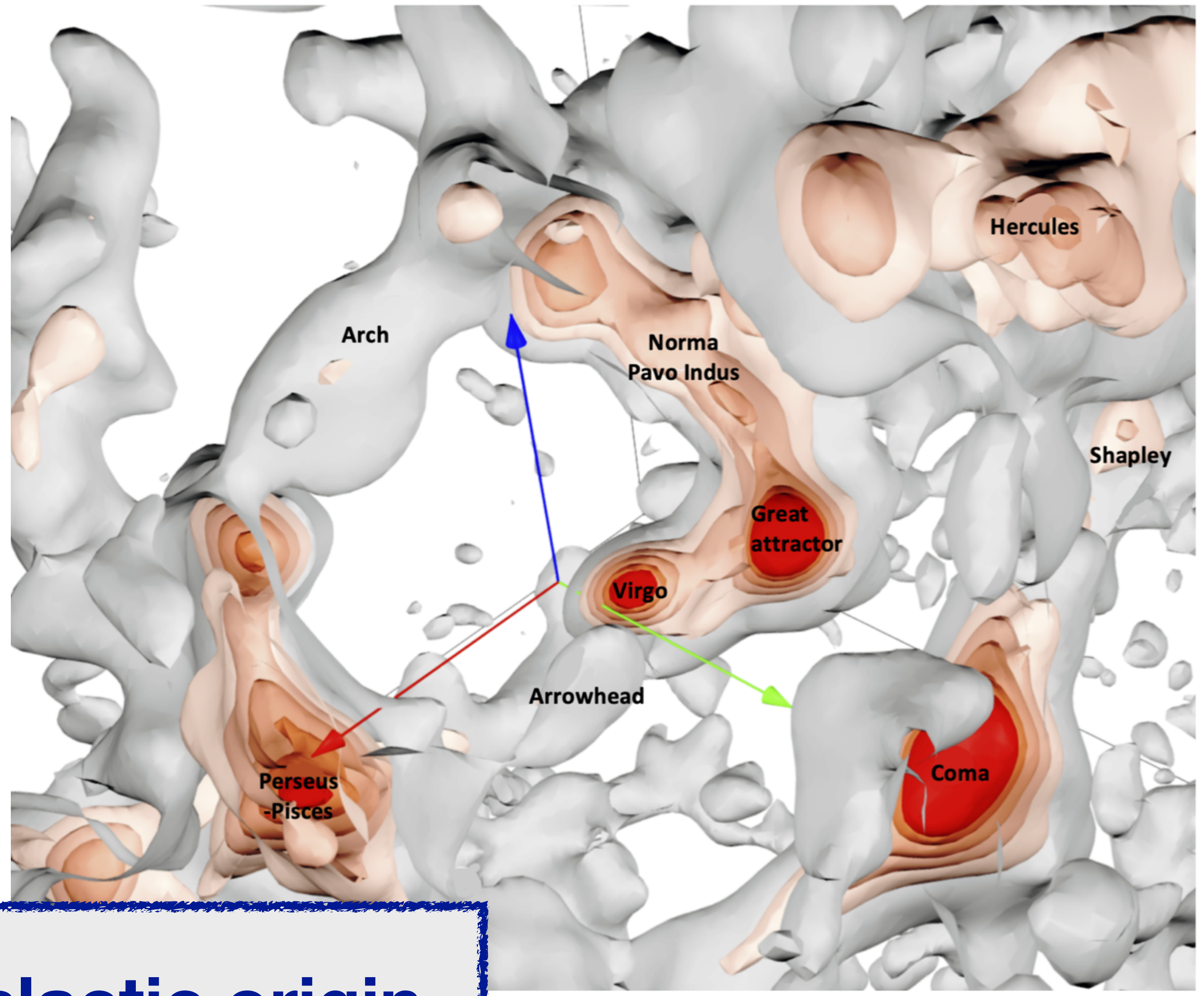

Source density of ~ 10^{-4} Mpc^{-3} needed

Dipole compatible with extragalactic origin

Arrival directions – large angular scales (dipole)

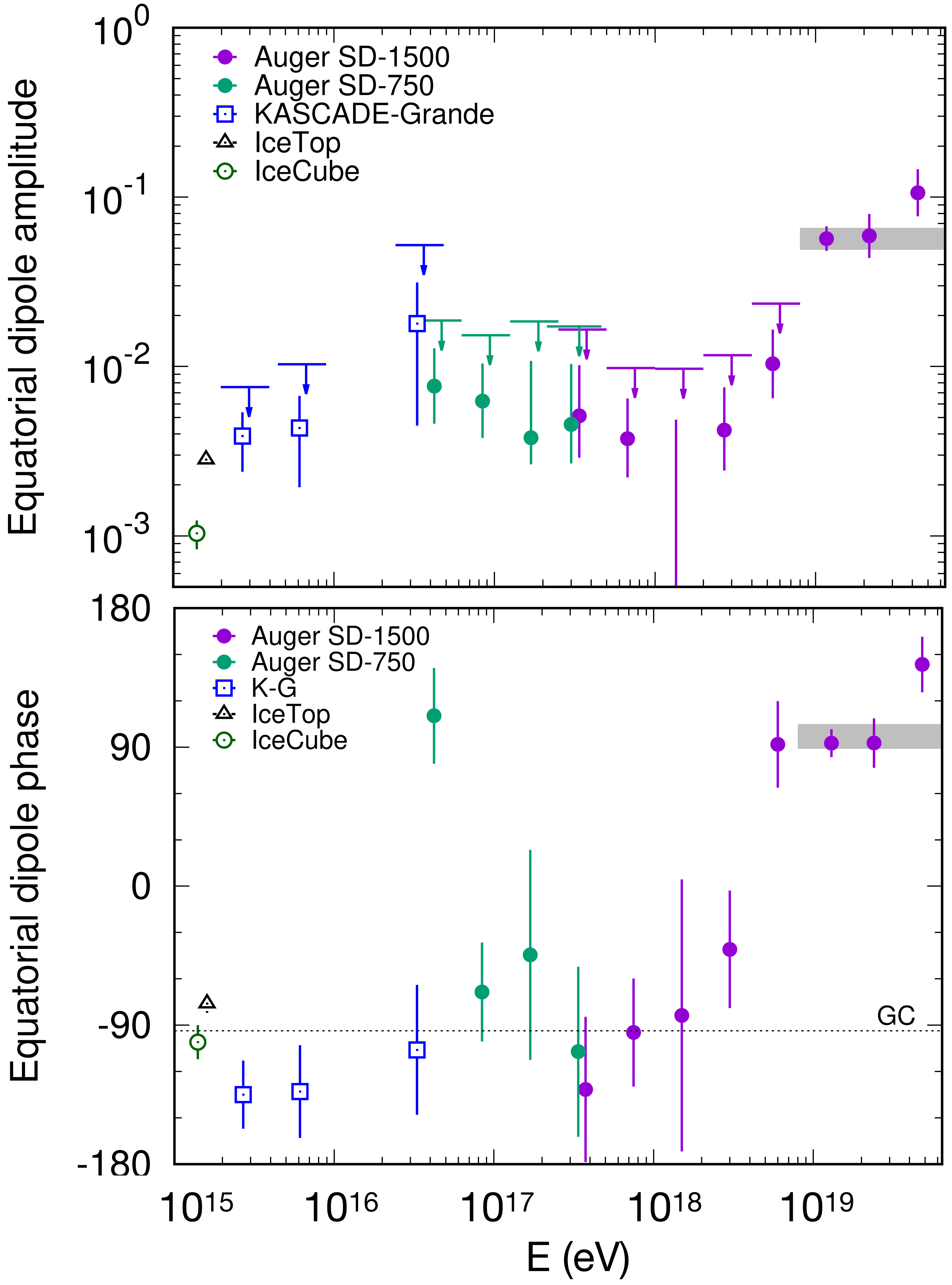

Expected anisotropy from escape from Galaxy

Simulation: Sources in galactic plane

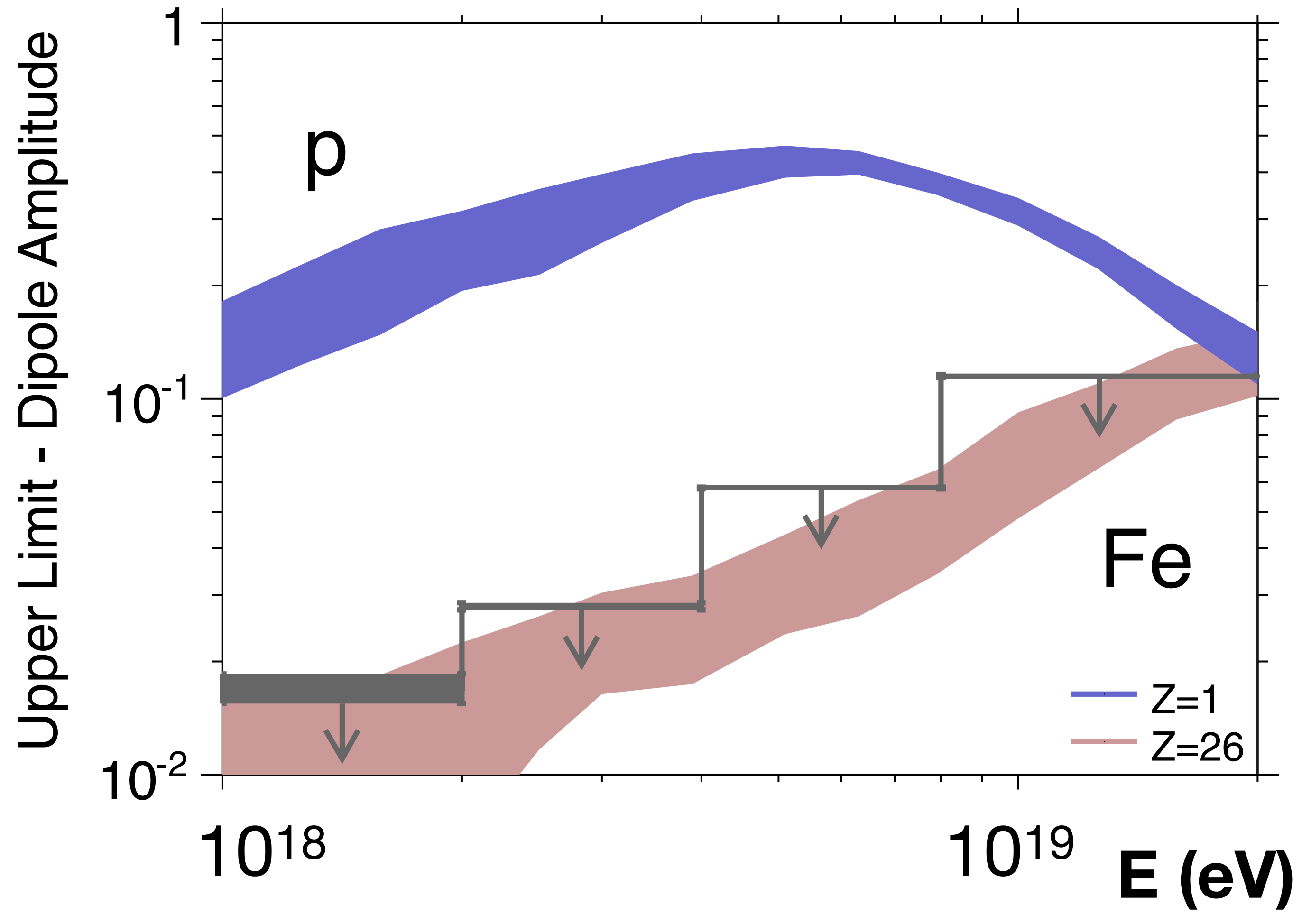

(Auger, ApJ 203, 2012, Giacinti et al. JCAP 2012, 2015)

Large proton fraction just below $10^{18.5}$ eV and lack of anisotropy:

Transition from galactic to extragalactic sources below 10^{18} eV

Combined fit spectrum, mass composition & anisotropy

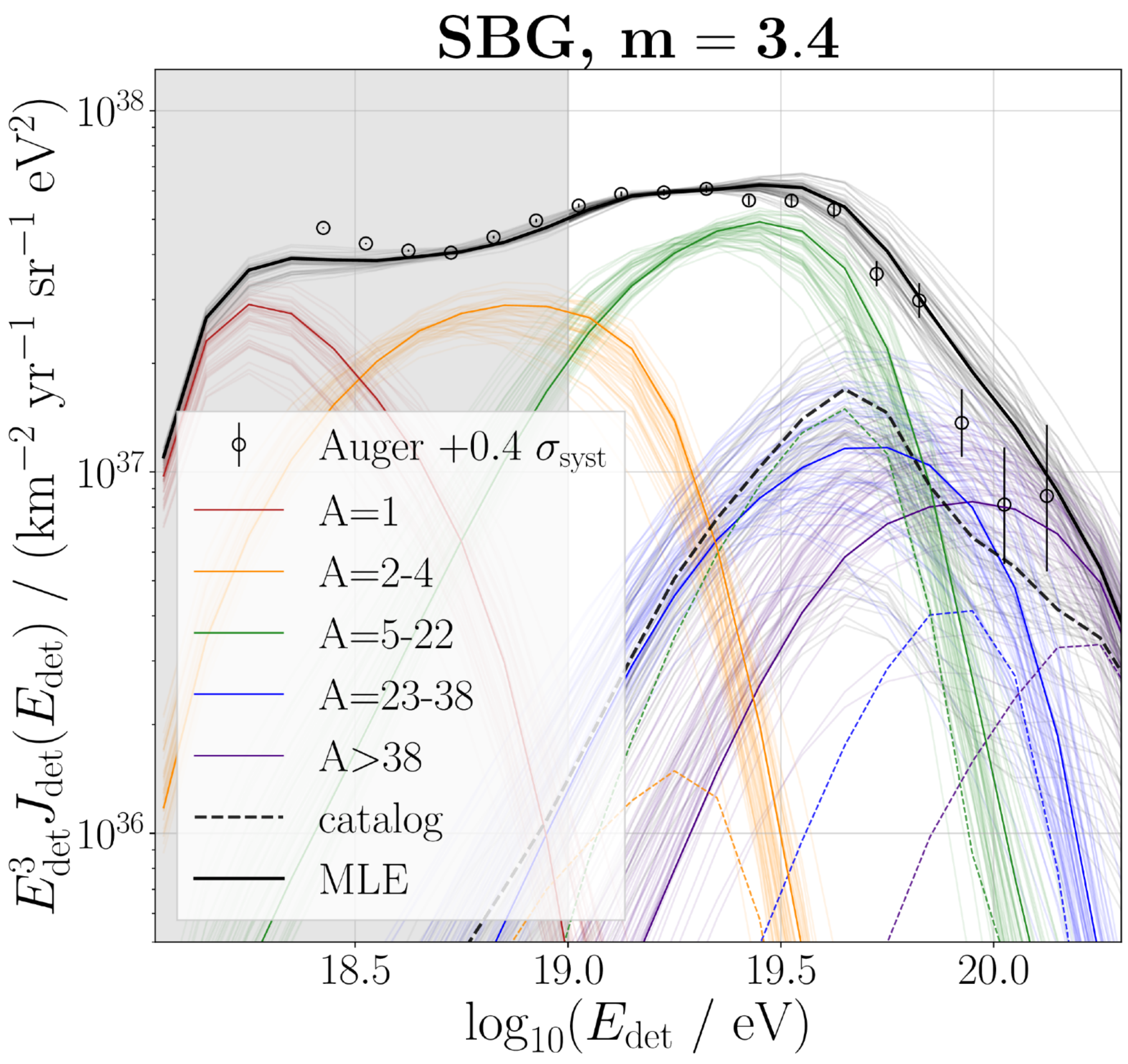

(Auger, JCAP 01 (2024) 022)

Fit with additional model parameters:
magnetic field blurring, catalog contribution fraction

- signal fraction of 20% for SBG catalog;
- main contribution from Centaurus region,
- results compatible with standard combined fit
- significance of TS is ~4.5 σ
- but no coherent deflection

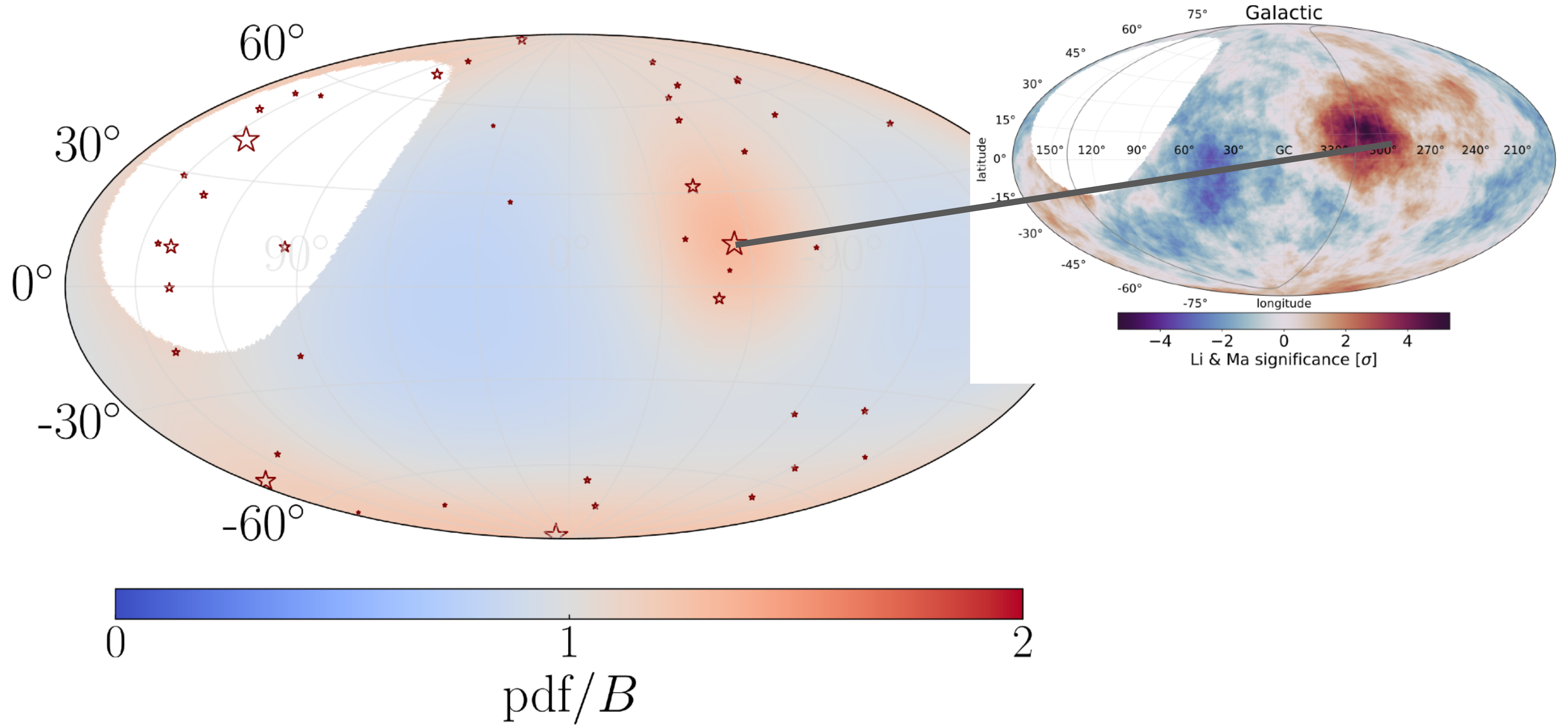

Mass composition and deflection at highest energy

Correlation of highest energy events of TA with large-scale structure

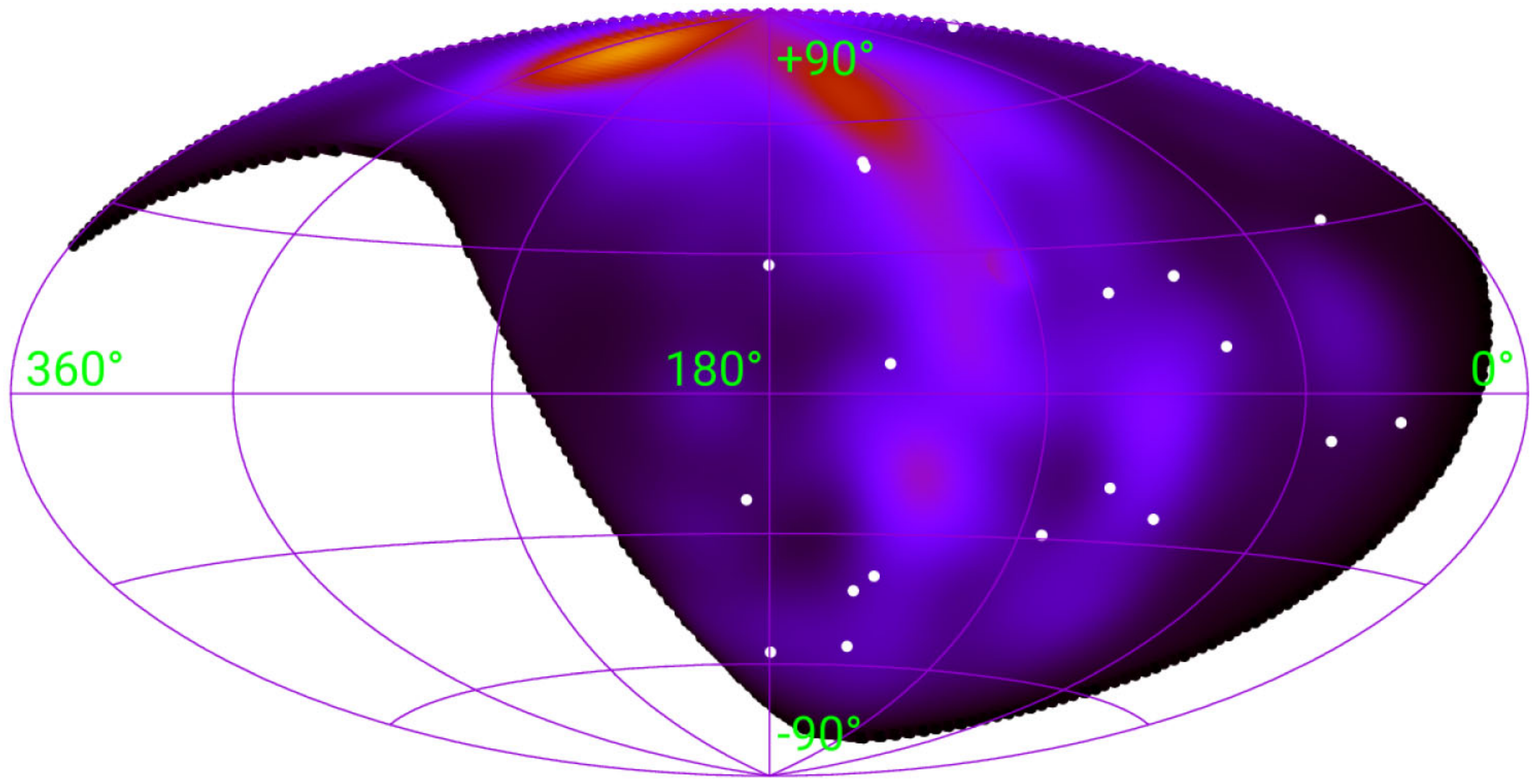

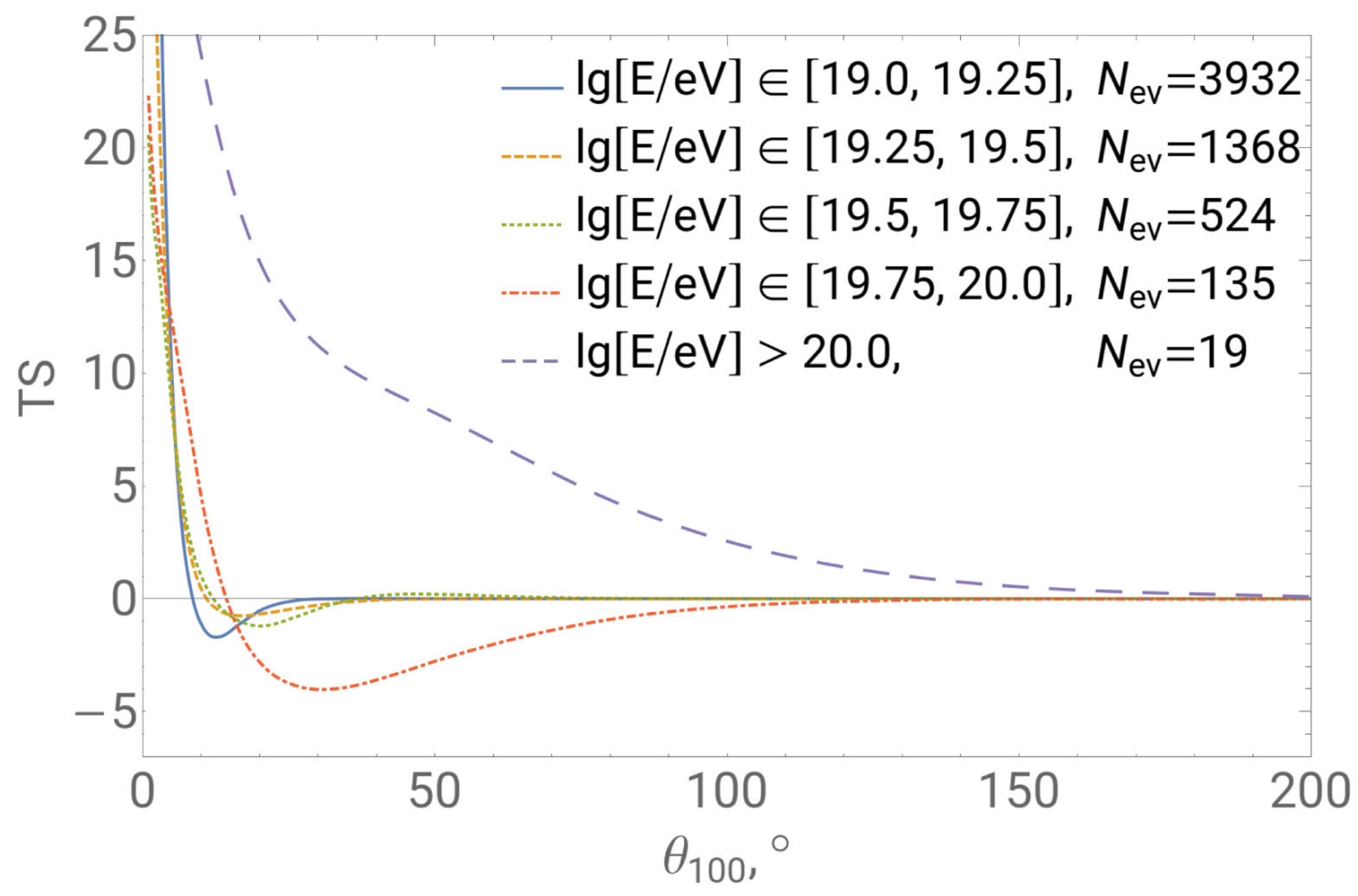

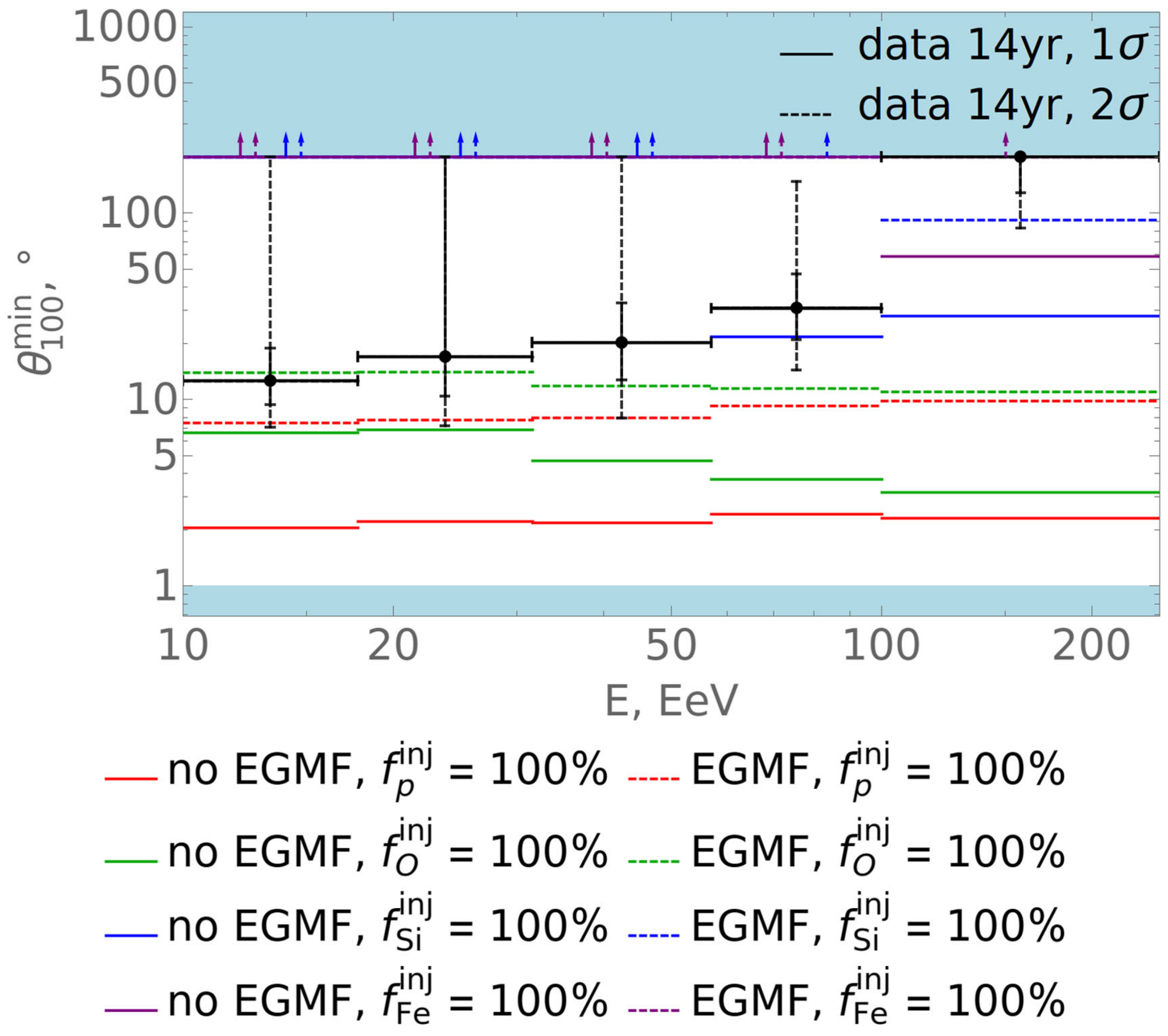

Interpretation depends on EGMF assumptions
Large deflection at highest energies: heavy mass

(TA, Phys. Rev. Lett. 133 (2024) 041001, Phys. Rev. D110 (2024) 022006)

Searching for sources at the highest energies

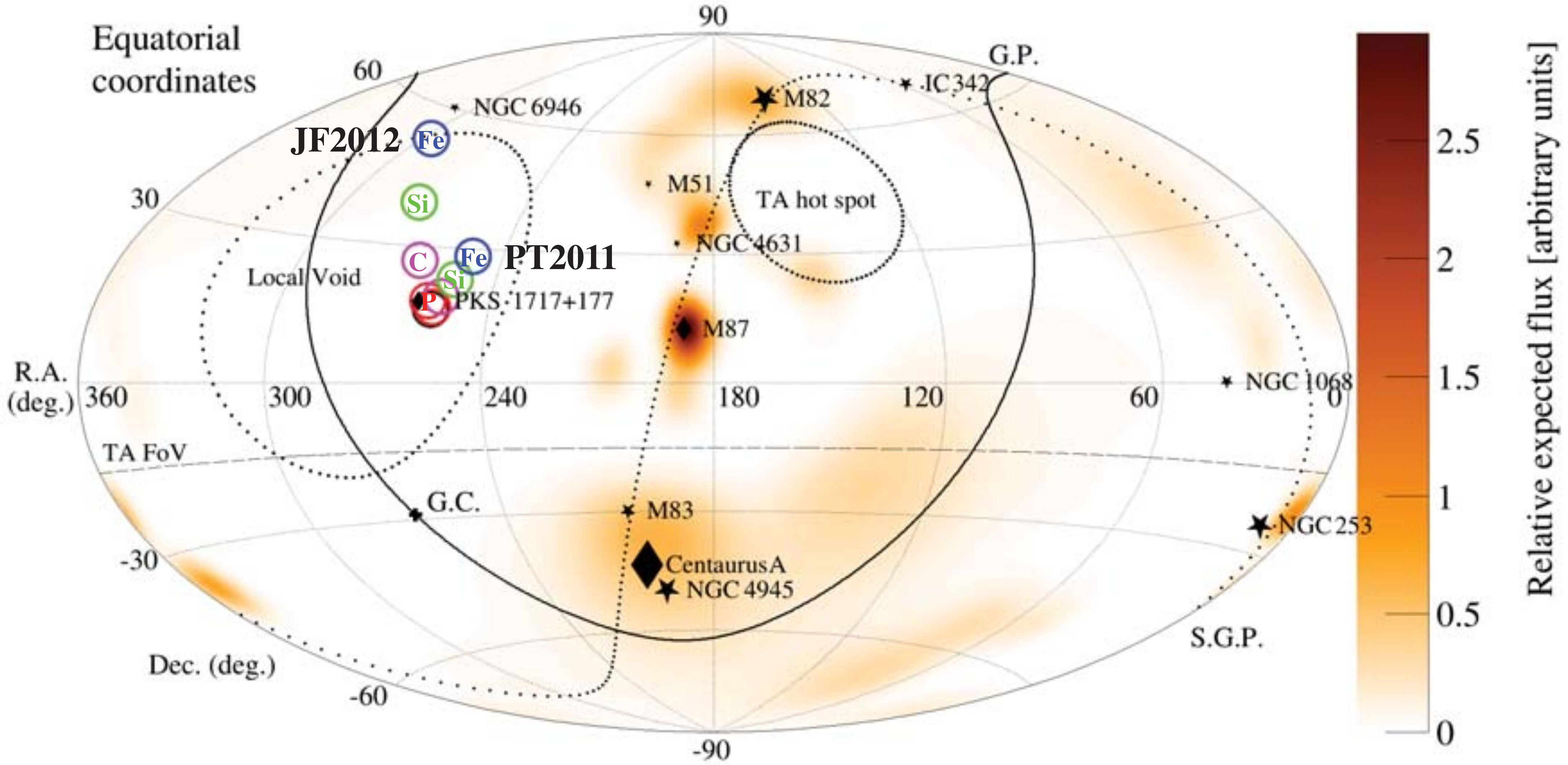

Amaterasu event (~2.4x10^{20} eV) *(TA, Science 382 (2023) 903)*

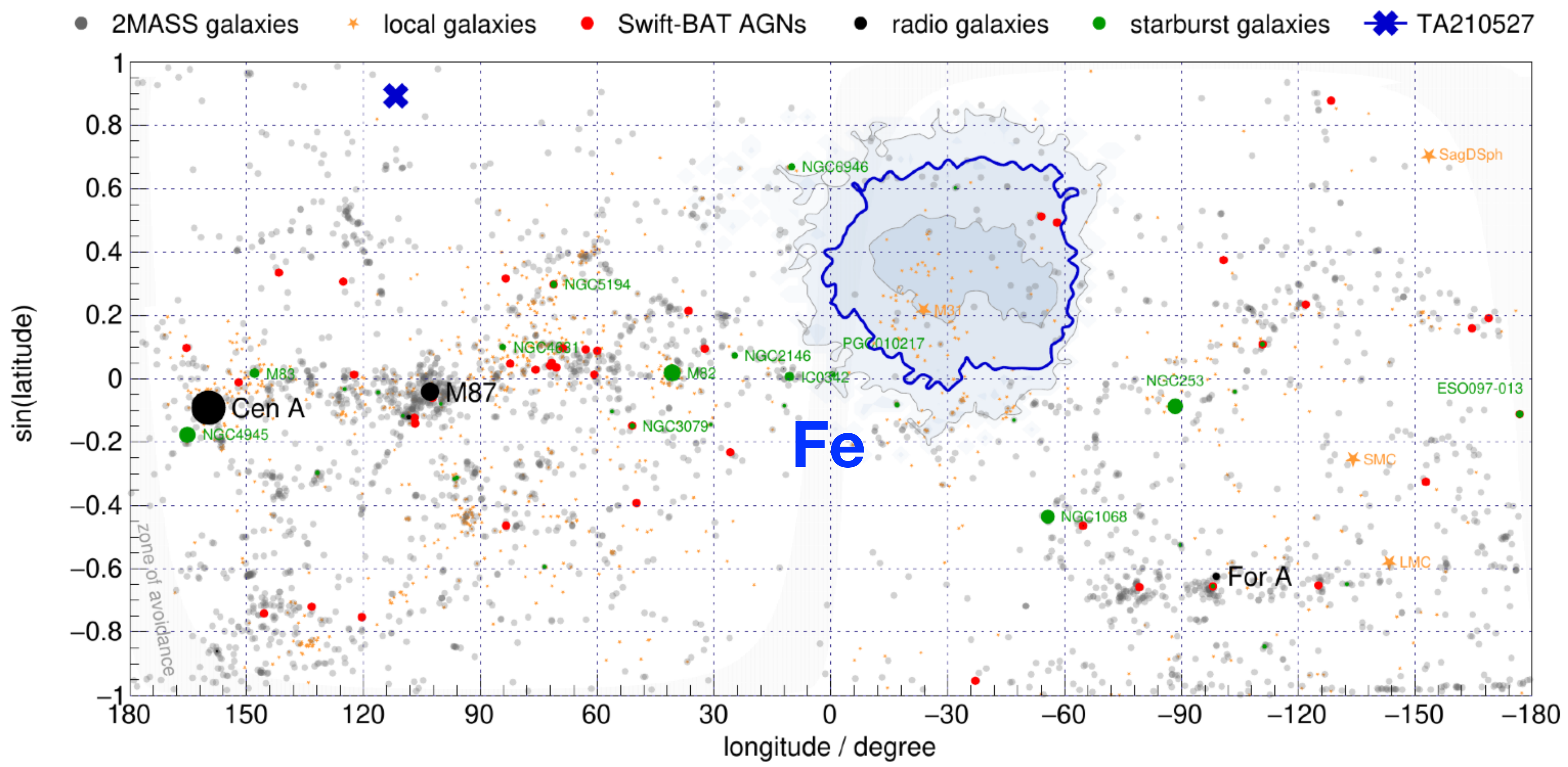

Amaterasu event (~1.7x10^{20} eV) *(Unger & Farrar, ApJ 962 (2024) L5)*

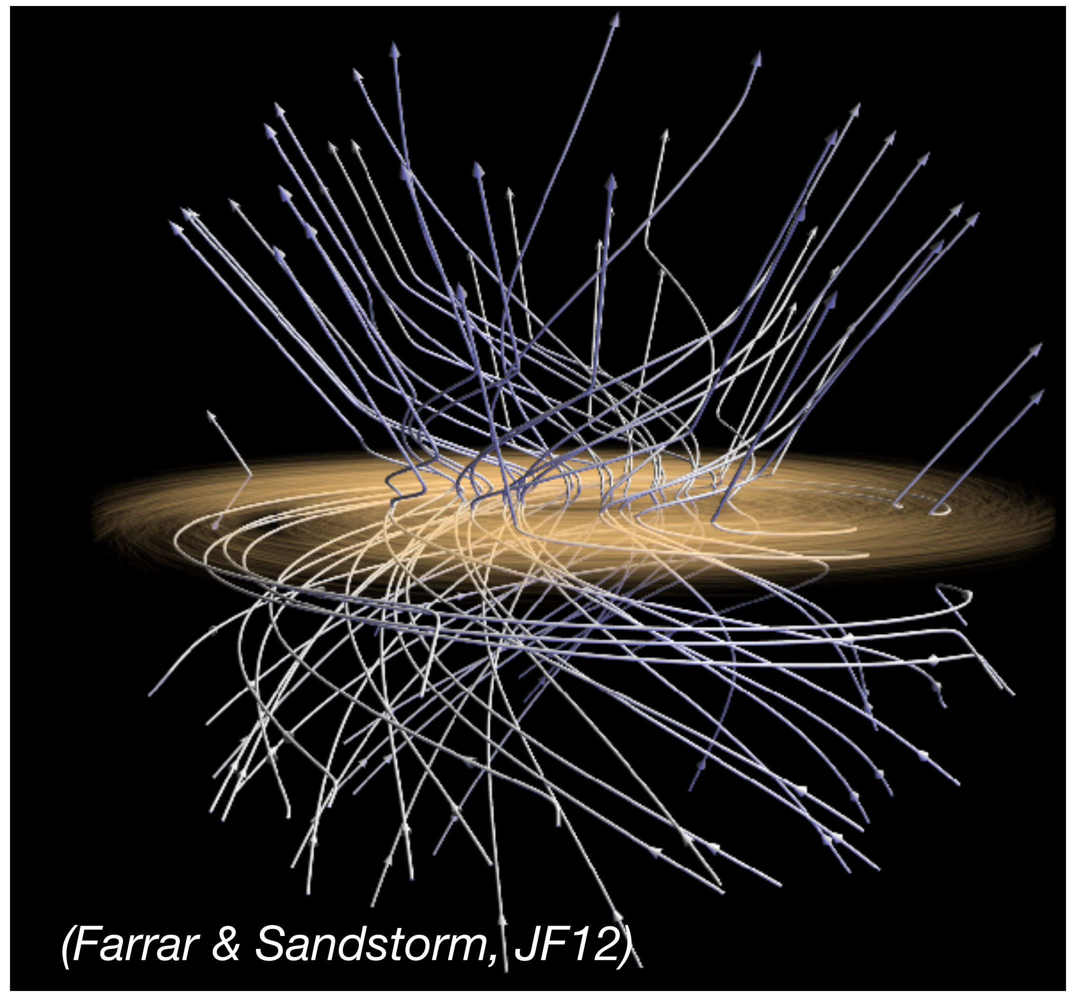

Transient sources?

Backtracking of particles through Galactic mag. field

New mag. field model UF24

(Unger & Farrar, ApJ 970 (2024) 95)

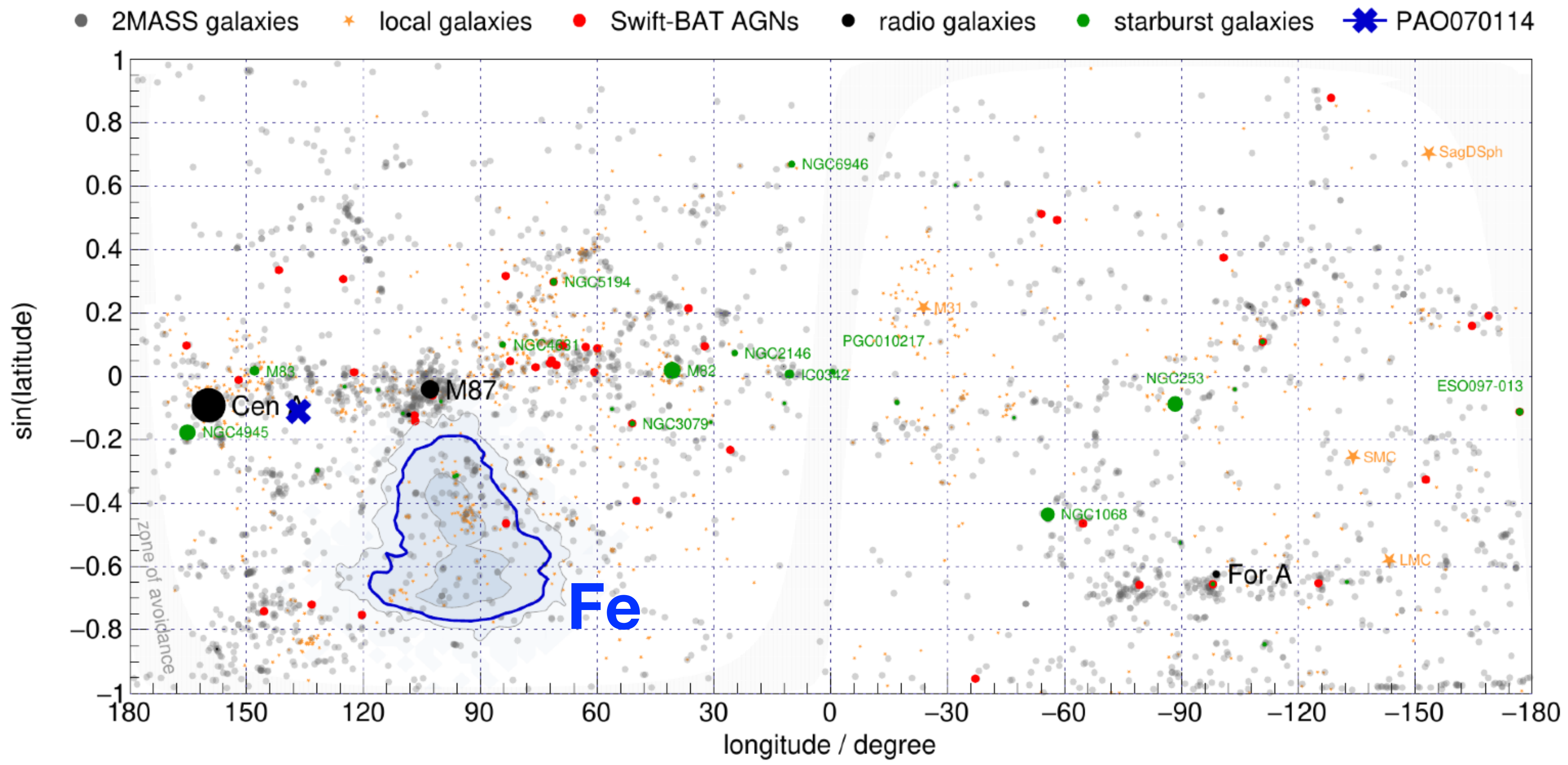

(Unger UHECR 2024)

Auger highest energy event (~1.6x10^{20} eV)

Closest Active Galactic Nucleus: Centaurus A

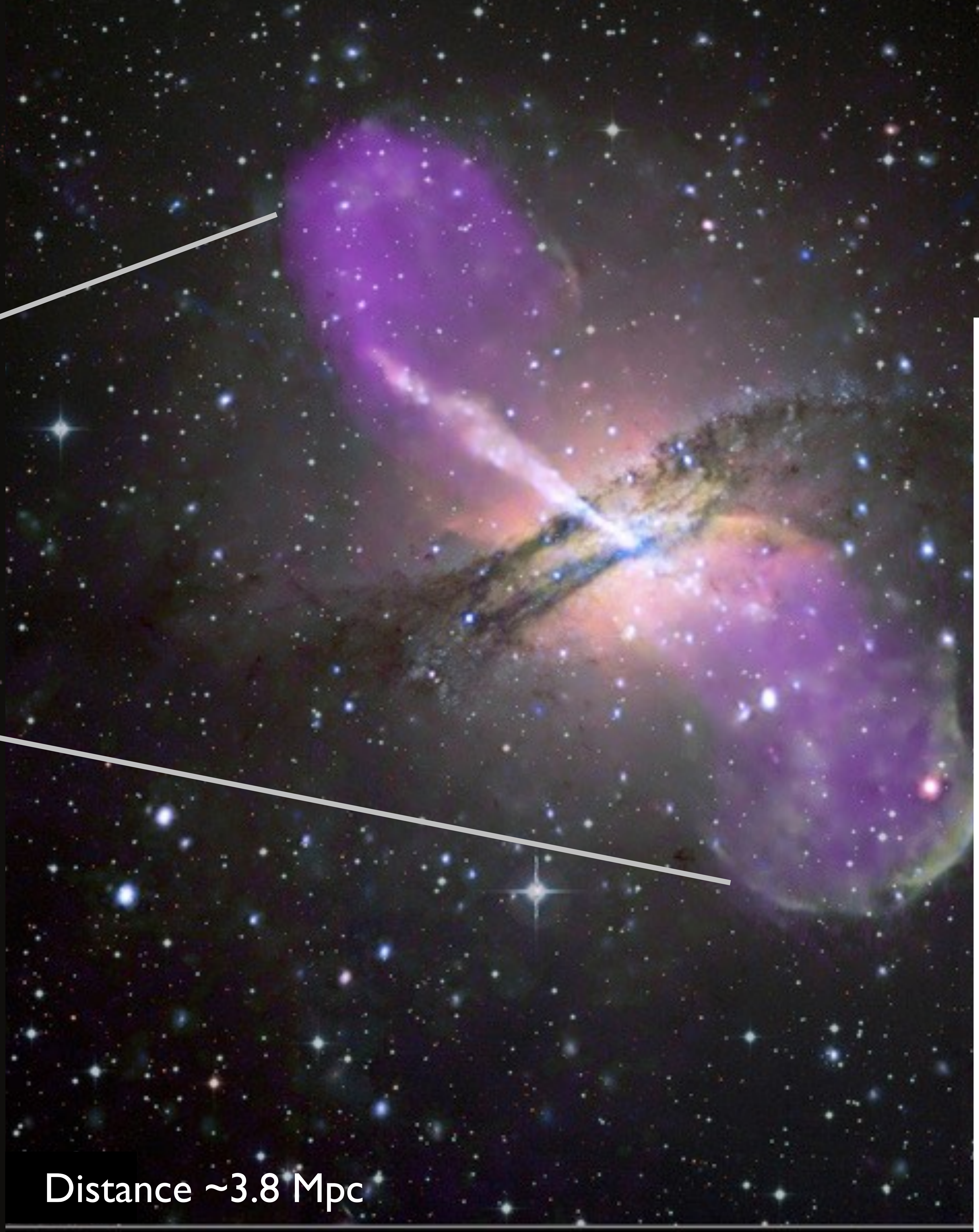

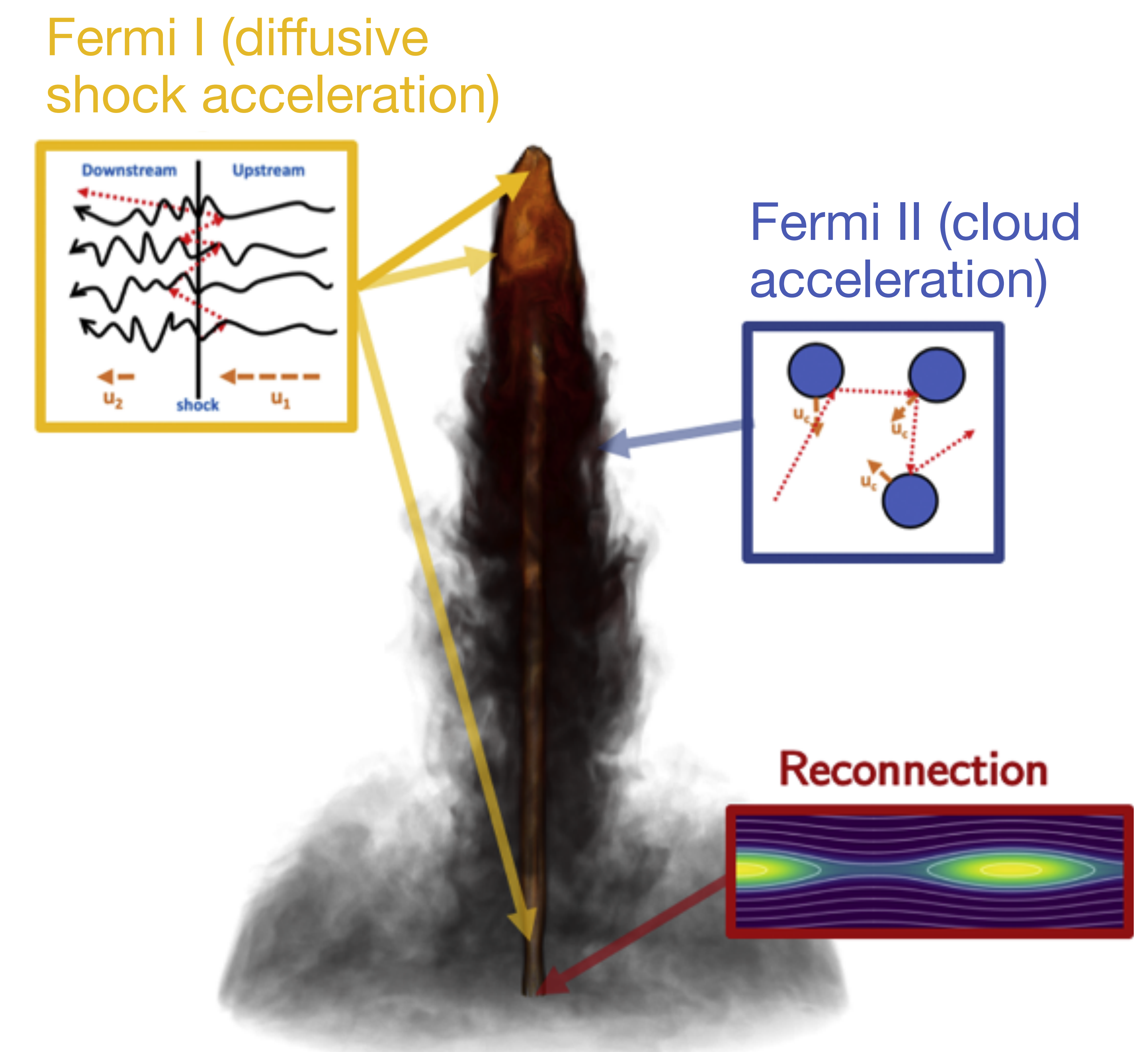

(Matthews, Bell, Blundel New Ast. Rev. 89 (2020) 101543)

Importance of source regions

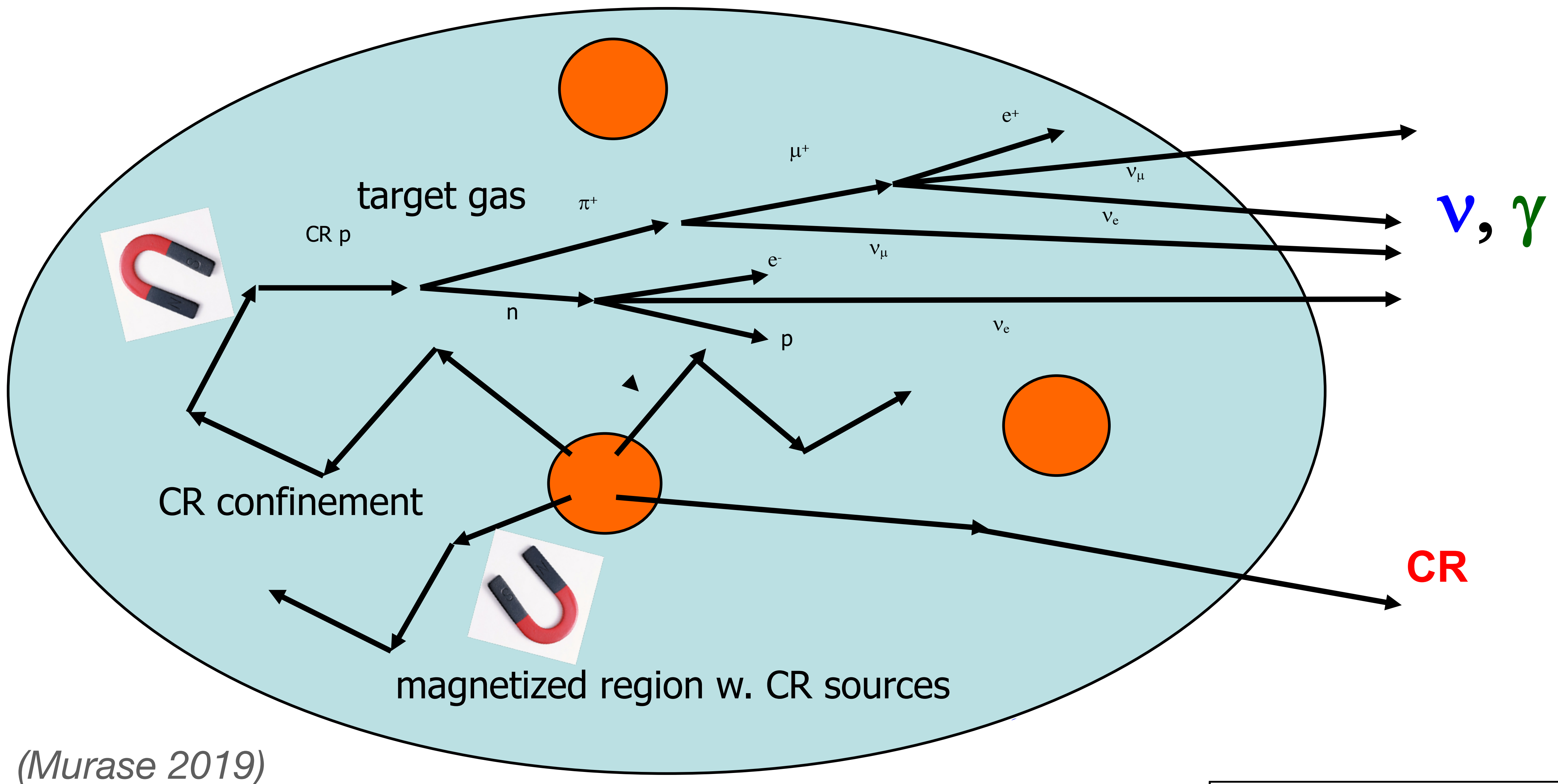

(Murase 2019)

Interplay between
- **Energy-dependent escape from source region**
- **Interaction with high photon densities**
- **Energy loss and secondary particle production**

(Unger, Farrar, Anchordoqui, PRD 92, 2015)

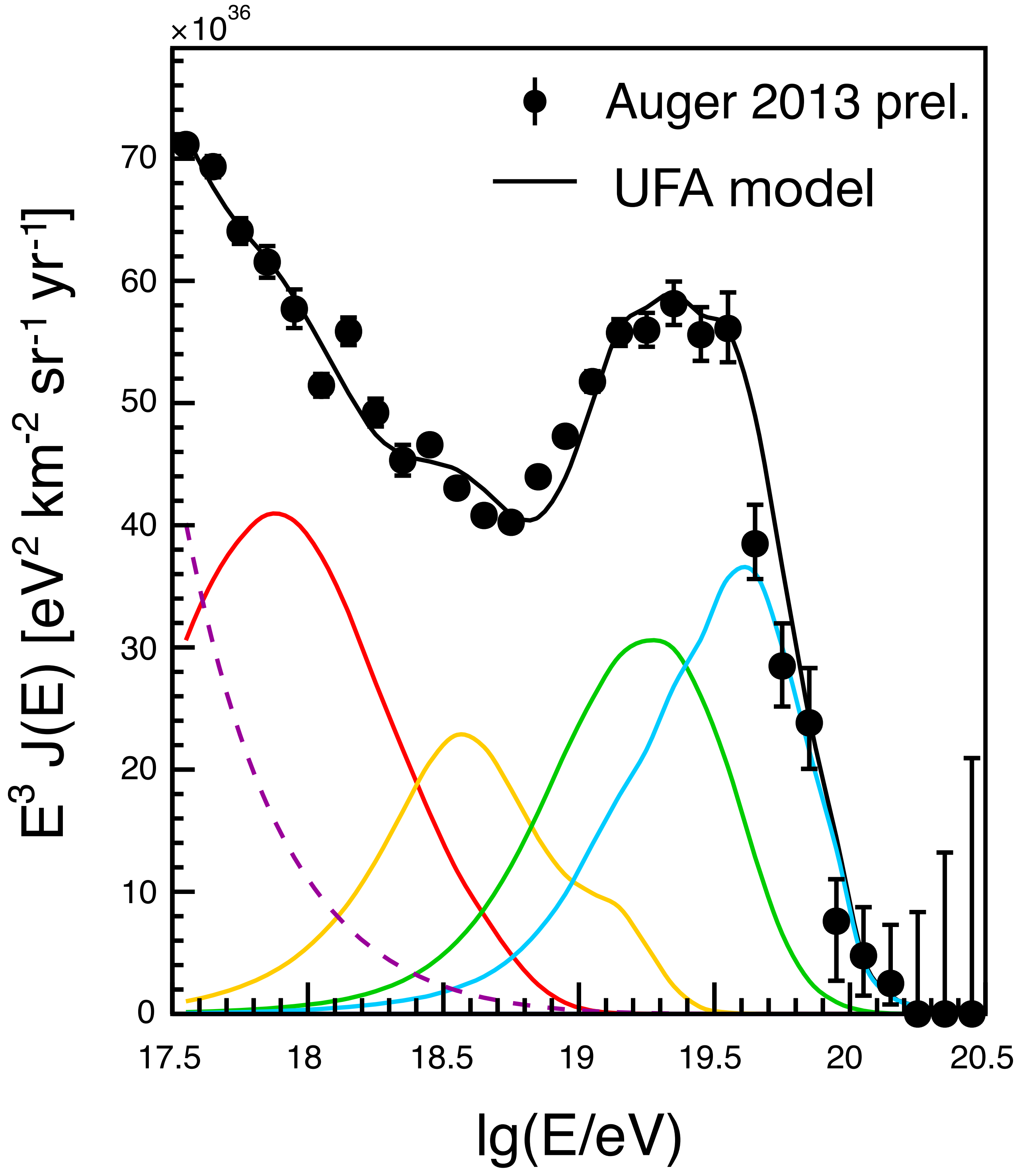

$$\frac{\mathrm{d}N_{\rm ini}}{\mathrm{d}E} \sim E^{-1}$$

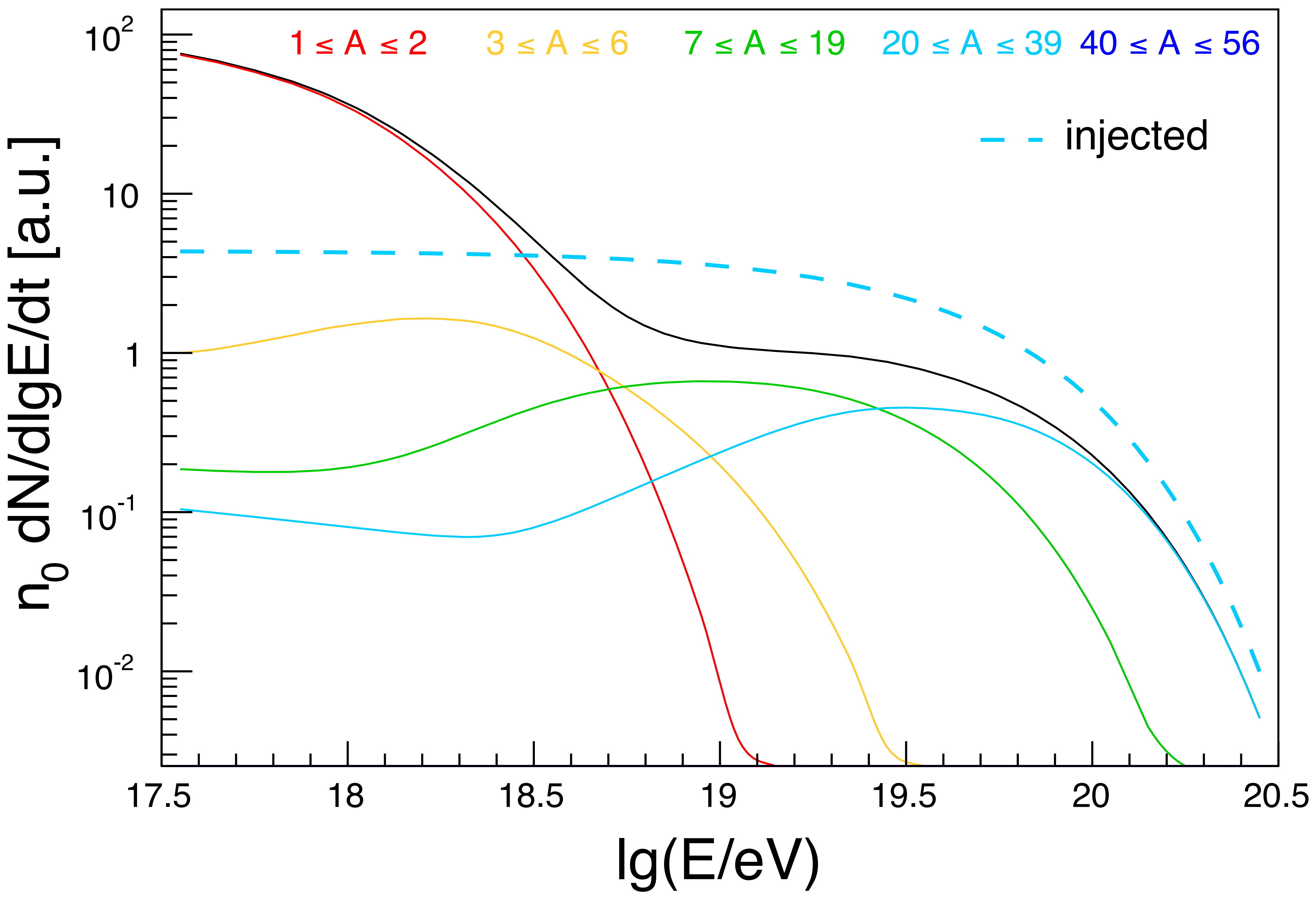

Nuclear disintegration in source region (scaling with mass *A*)

(Globus et al. 2015, Unger et al. 2015, Fang & Murase 2017)

New generation of complex model scenarios

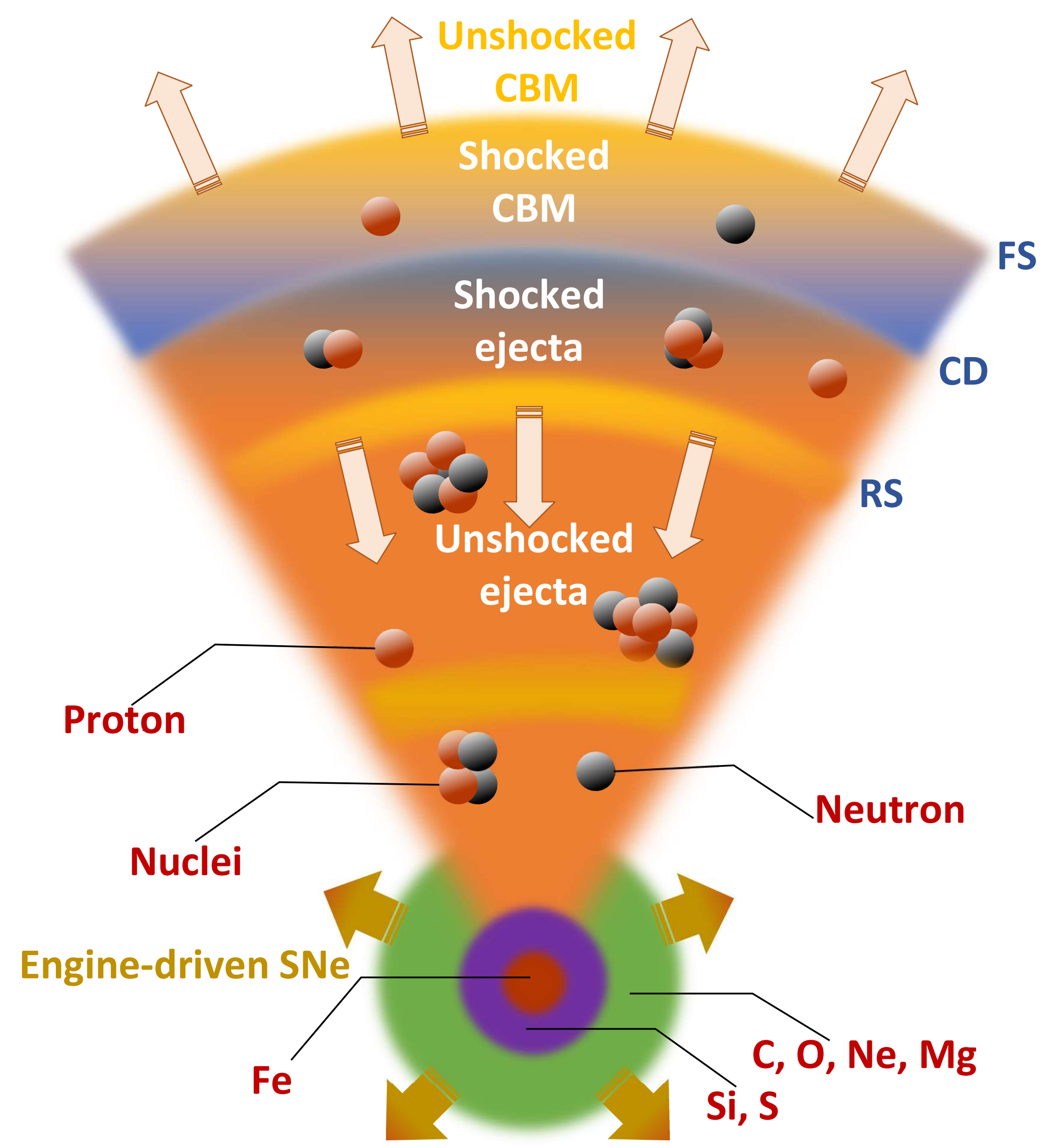

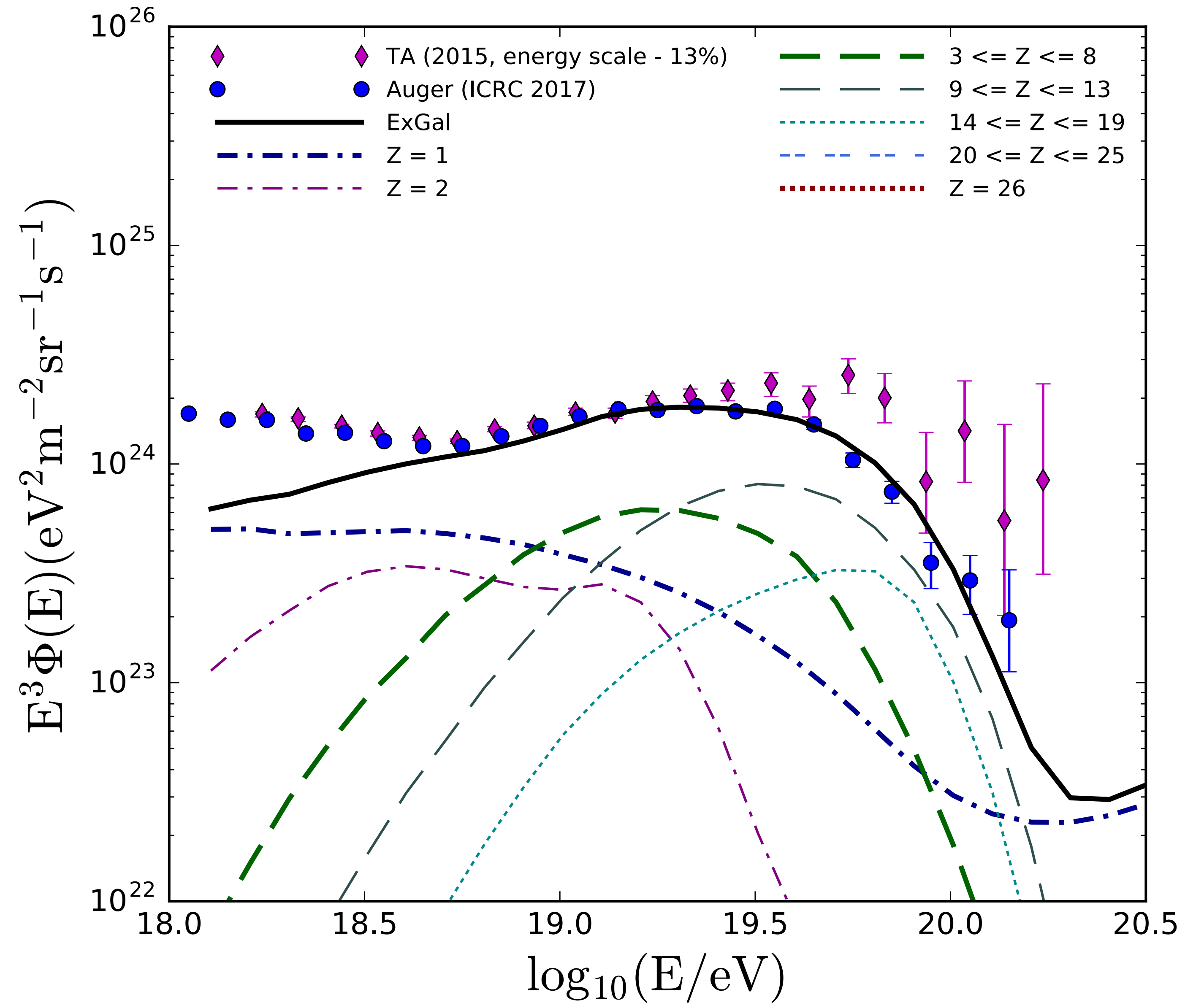

Interplay between
confinement in source
and disintegration of nuclei:
hard energy spectra
(Aloisio et al. 2014, Taylor et al. 2015, Globus et al. 2015, Unger et al. 2015, Fang & Murase 2017)

Reverse shock scenario in
low-luminosity long GRBs
(Zhang, Murase et al 2019+)

Tidal disruption events (TDEs)
of WD or carbon-rich stars
(Farrar, Piran 2009, Pfeffer et al. 2017, Zhang et al 2017)

One-shot acceleration in
rapidly spinning **neutron stars**
(Arons 2003, Olinto, Kotera, Feng, Kirk …)

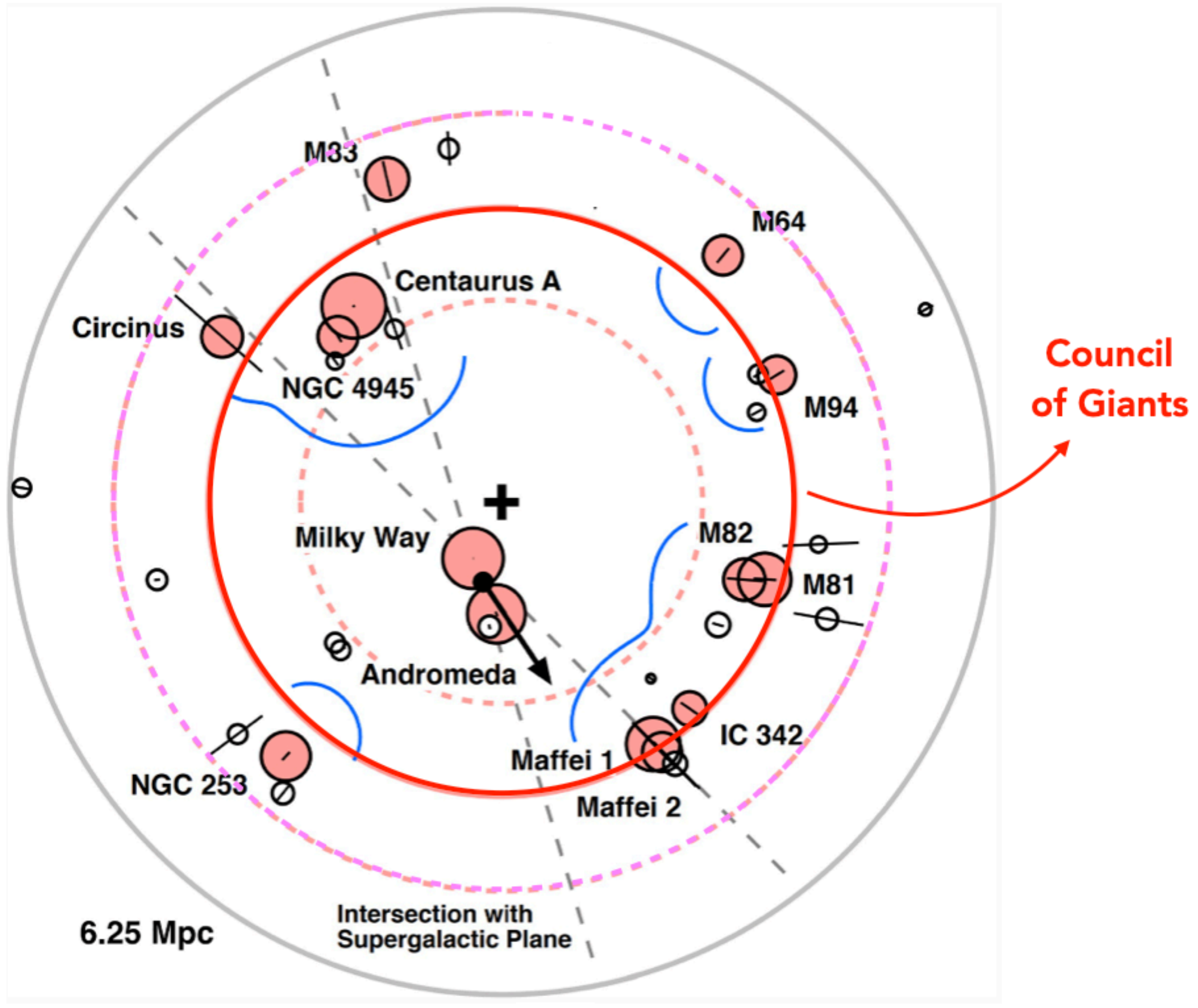

Cen-A bust & **deflection on Council of Giants**, solving isotropy and source diversity problem
(Taylor et al. 2023)

Relativistic reflection of
existing CR population
(Biermann, Caprioli, Wykes, 2012+, Blandford 2023)

Latest addition – binary neutron star mergers

- Universal Maximum Rigidity is natural
  - $M_{BNS} \approx (2.64 \pm 0.14) M_\odot$
  - Gravitationally-driven dynamo
  - strong magnetic fields

Kiuchi+ NatureAstron23

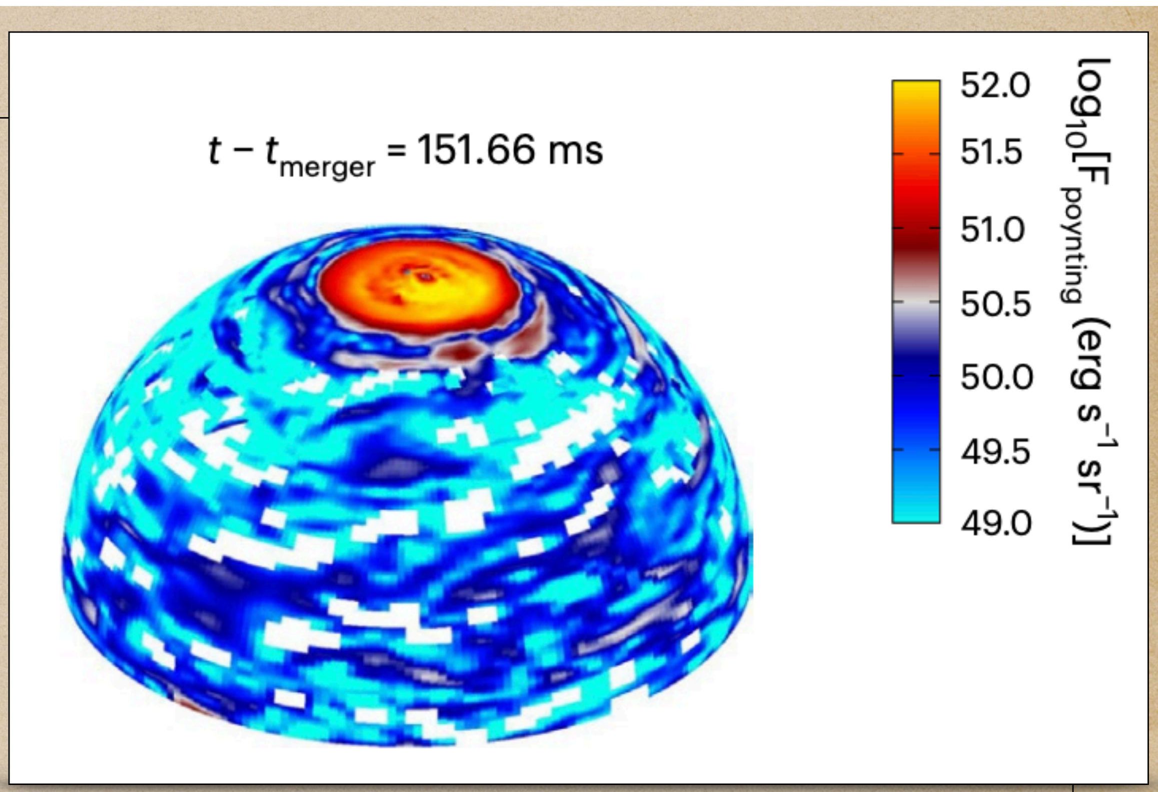

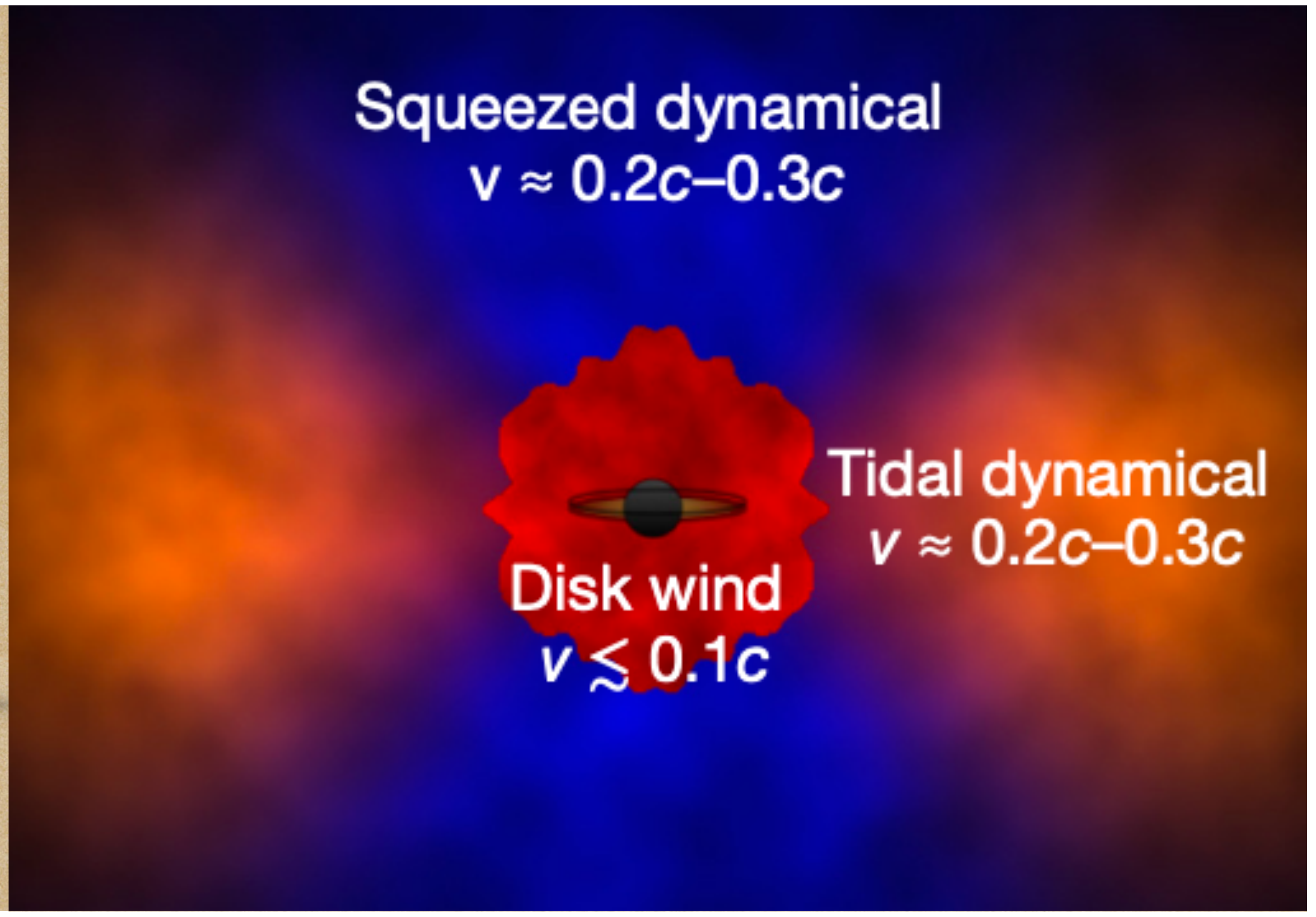

- Energy injection rate: (obs $\approx 6 \times 10^{44}$ erg Mpc^{-3} yr^{-1})
  - BNS rate $\Gamma_{NSmerg} \approx$ 10-1700 Gpc^{-3} yr^{-1} ✔ if $\Gamma_{NSmerg} \gtrsim$ 100 Gpc^{-3} yr^{-1}
  - Energy in jet alone $E_j \approx 10^{51.5}$ erg (Kiuchi+23)
- Effective source density: ✔ as long as magnetic smearing

	Powerful AGN	long GRBs	TDEs	Accretion Shocks	BNS mergers
$n_S \gtrsim 10^{-3.5}$ Mpc^{-3}	[✘]	[✘]	?	?	✔
UHECR energy injection	✔	✘	?	?	[✔]
Ordinary galaxy	✘	✘	✔	[✘]	✔
Universal R_{max}	✘	✘	✘	✘	✔
Highest energy events?	✘	✘	✘	✘	✔

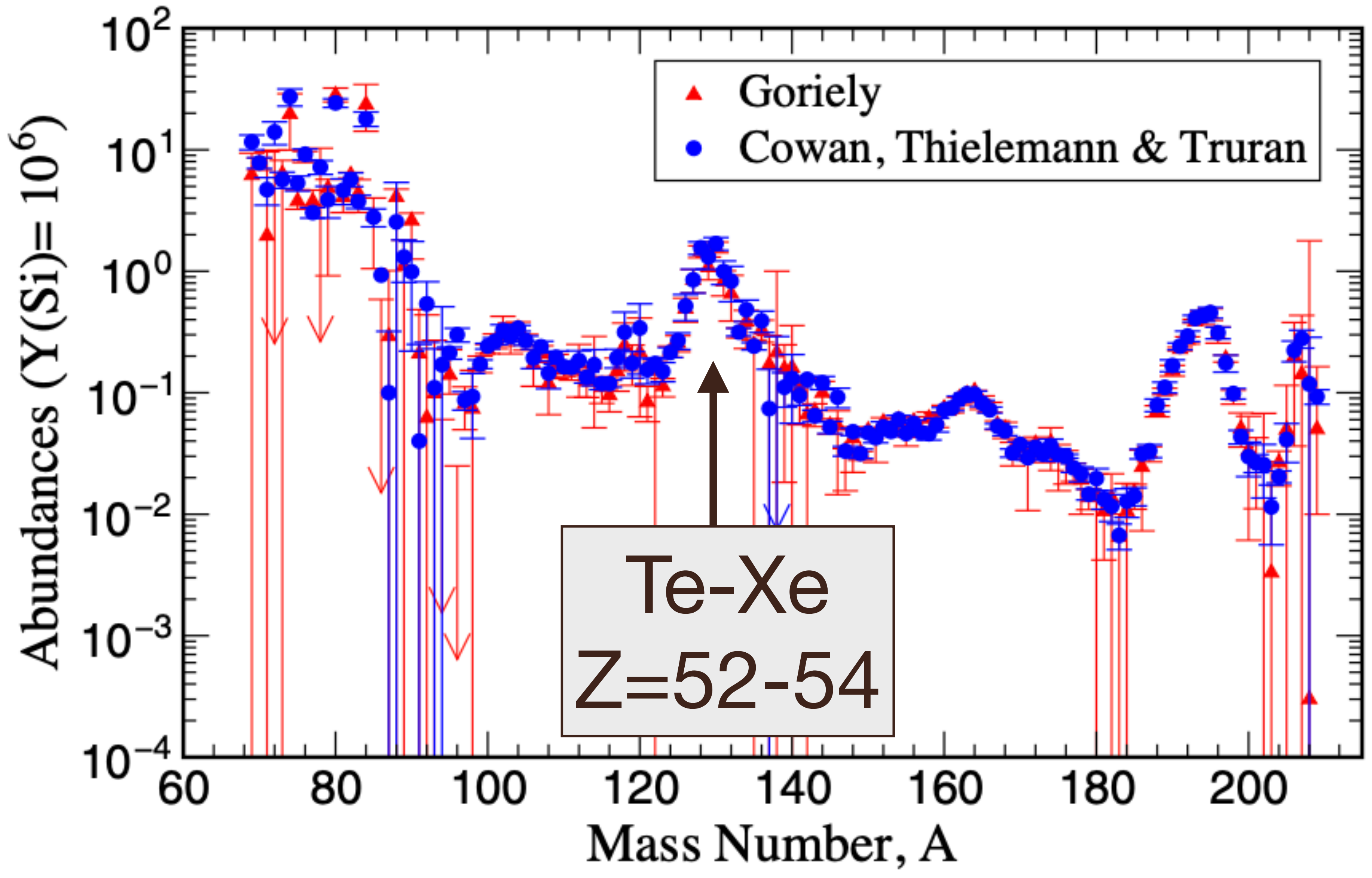

(Farrar Phys. Rev. Lett. 134 (2025) 081003)

Unexpected observations (not looked for)

Auger muon measurement – vertical showers

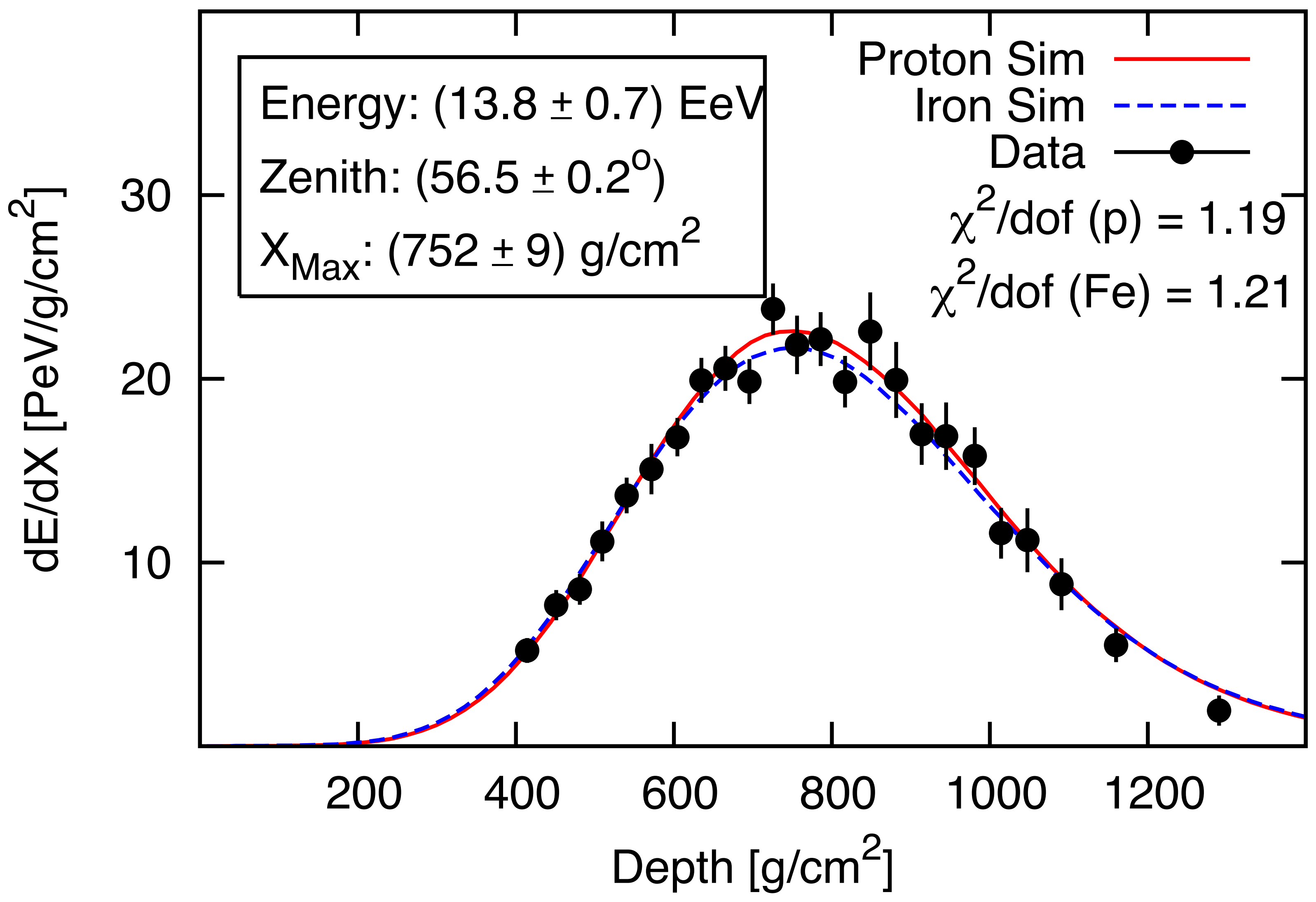

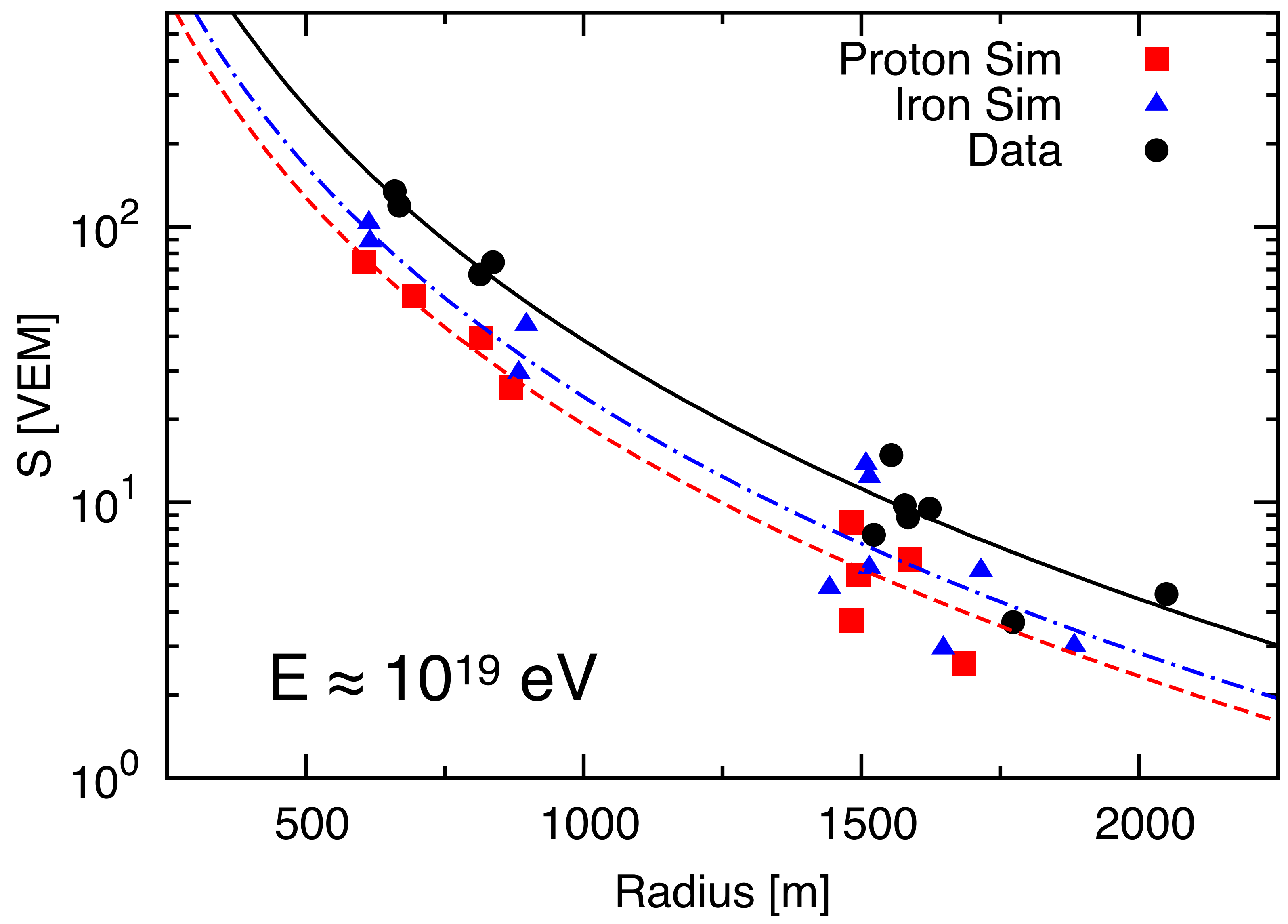

(Auger, PRL 117, 2016)

Energy scaling: em. particles and muons

Muon scaling: hadronically produced muons and muon interaction/decay products

Use showers of different zenith angles

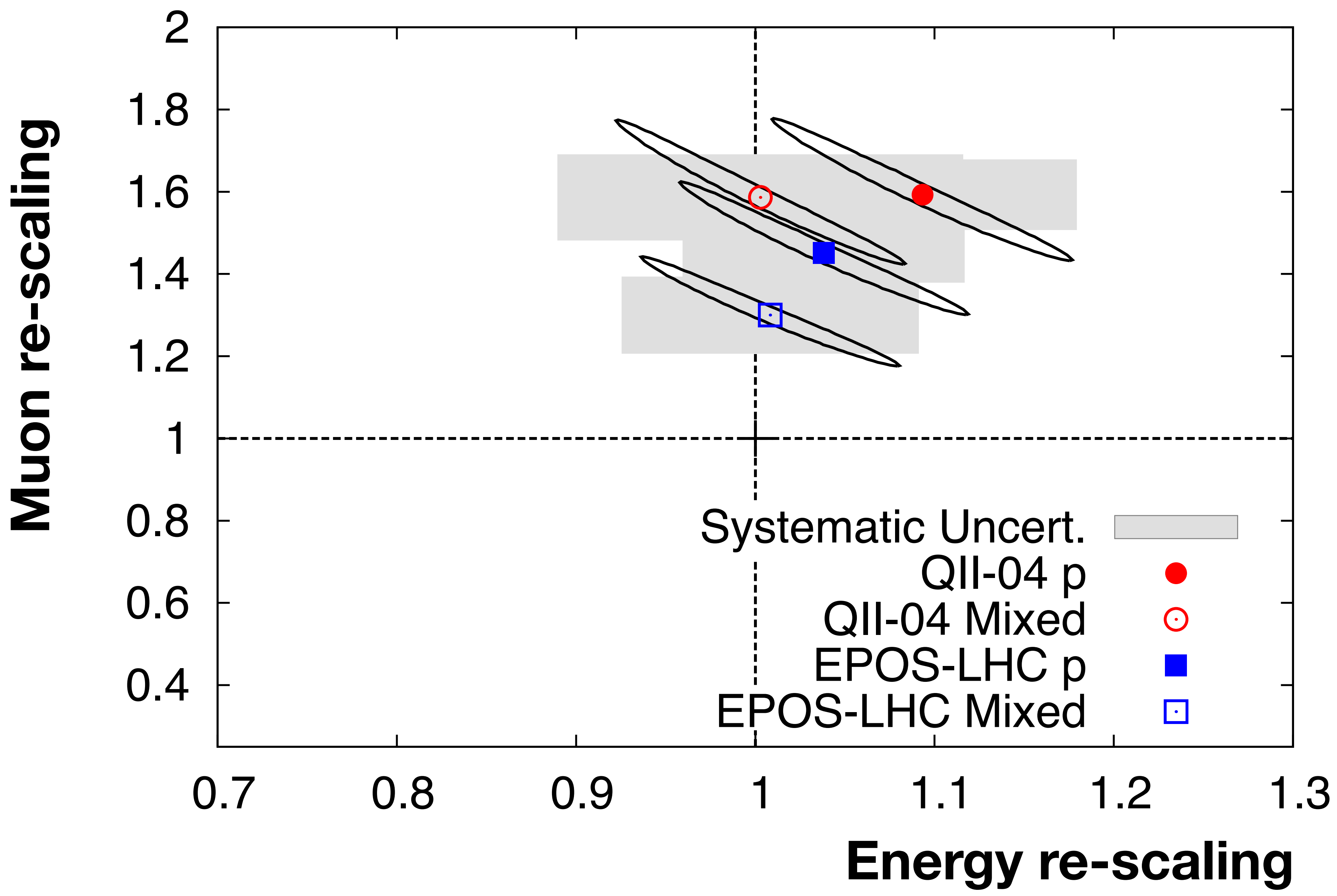

Consistently more muons in data than predicted

Auger muon measurement – inclined showers

Number of muons in showers with θ>65°

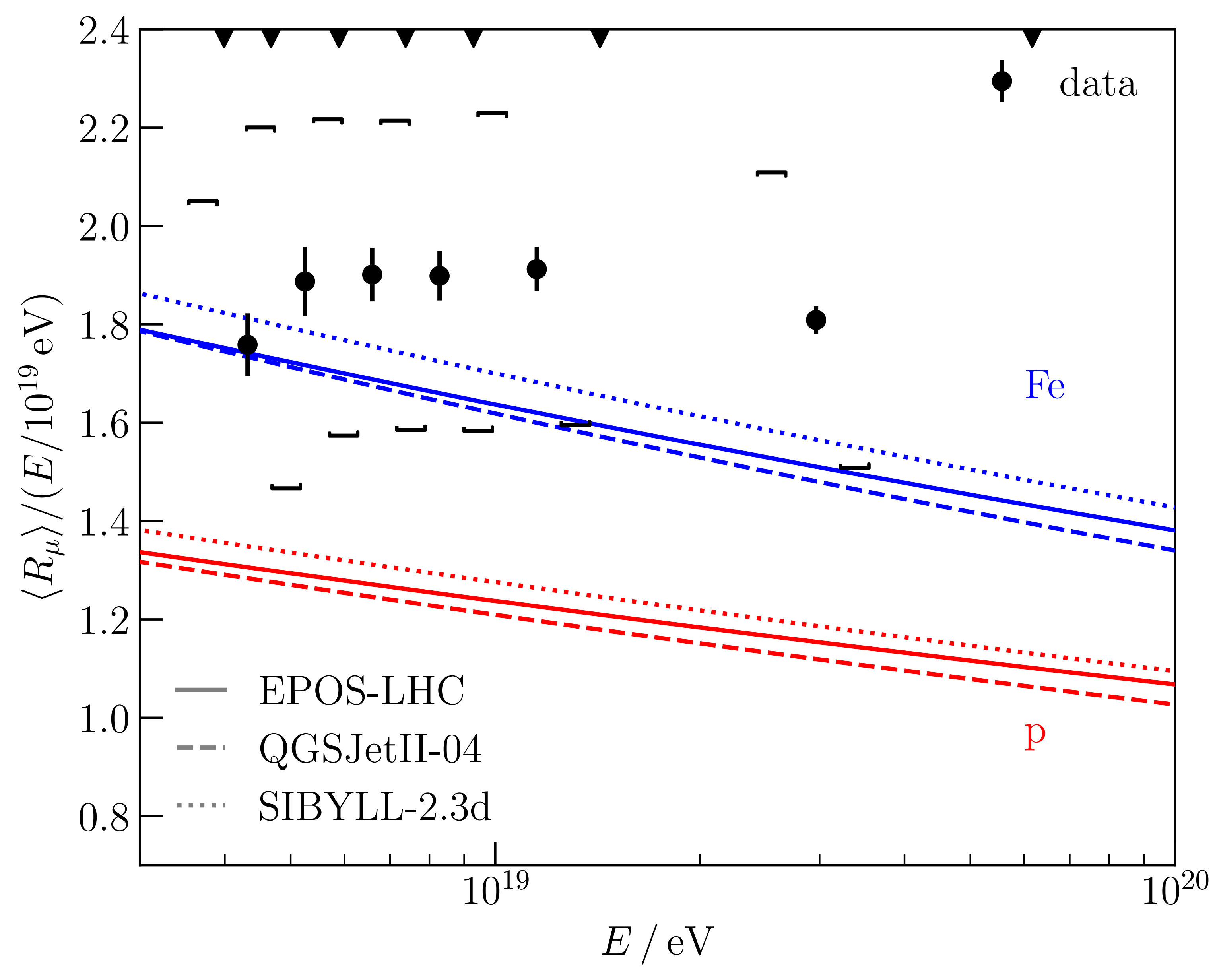

(Auger PRD 2015, PRL 2021)

Shower-to-shower fluctuations

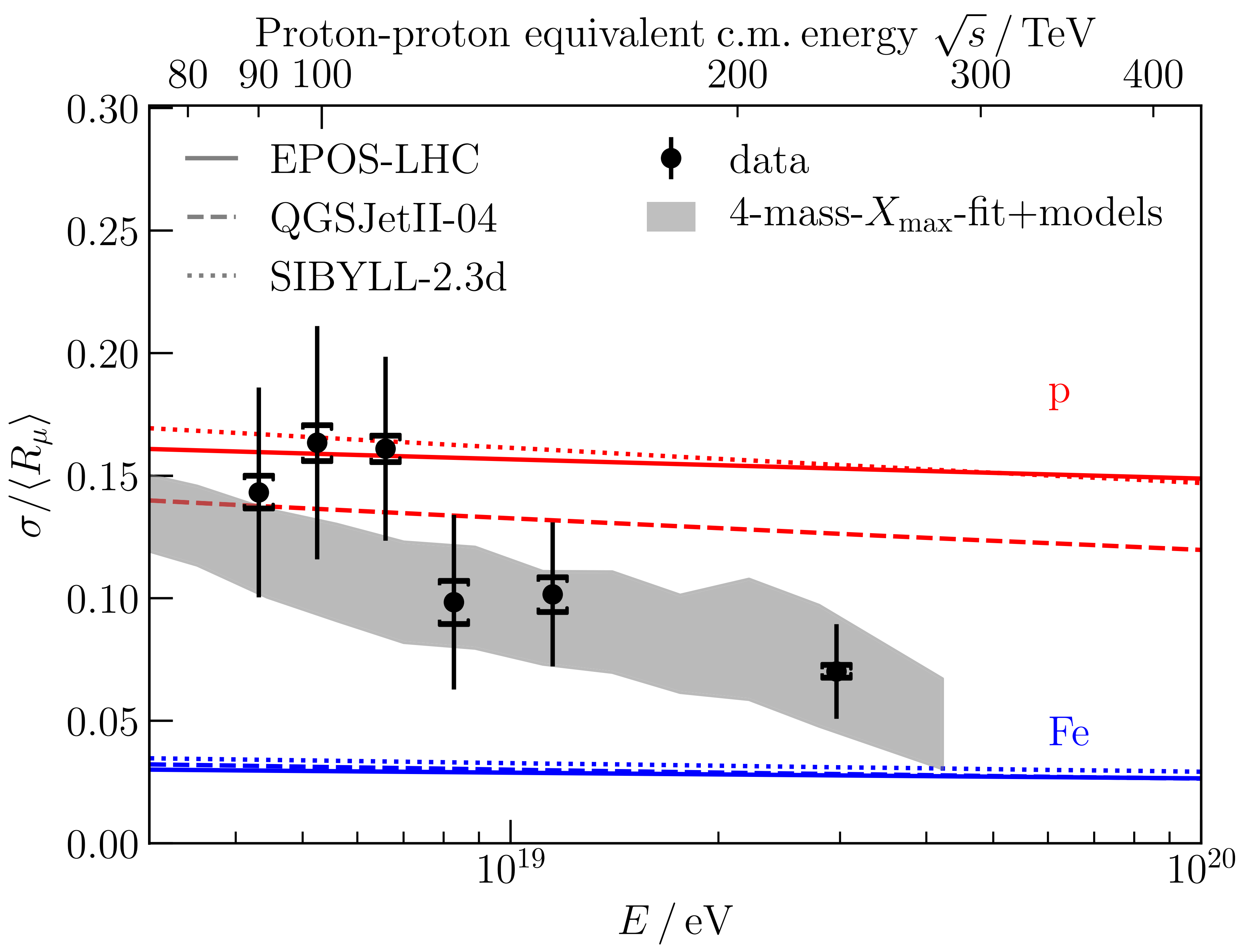

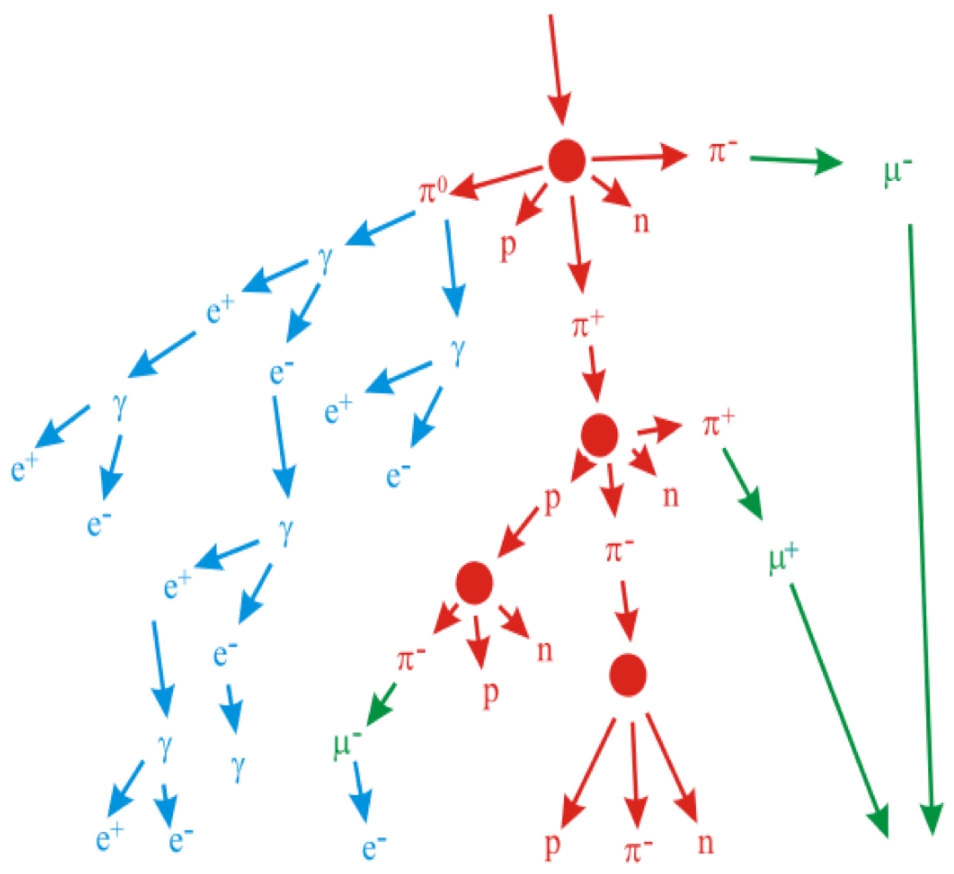

Lorenzo Cazon et al.
Astropart. Phys. 36 (2012) 211
Phys. Lett. B784 (2018) 68
Phys. Rev. D103 (2021) 022001

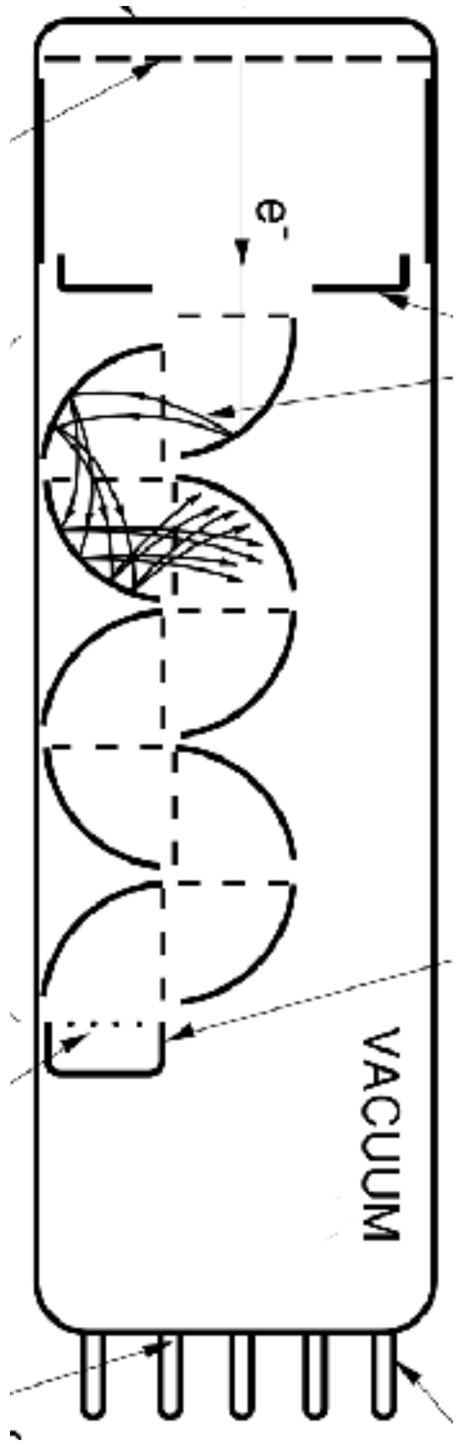

70% of fluctuations from first interaction

Discrepancy of muon number (20–30%), but no in relative shower-to-shower fluctuations

Muon production depends on hadronic energy fraction

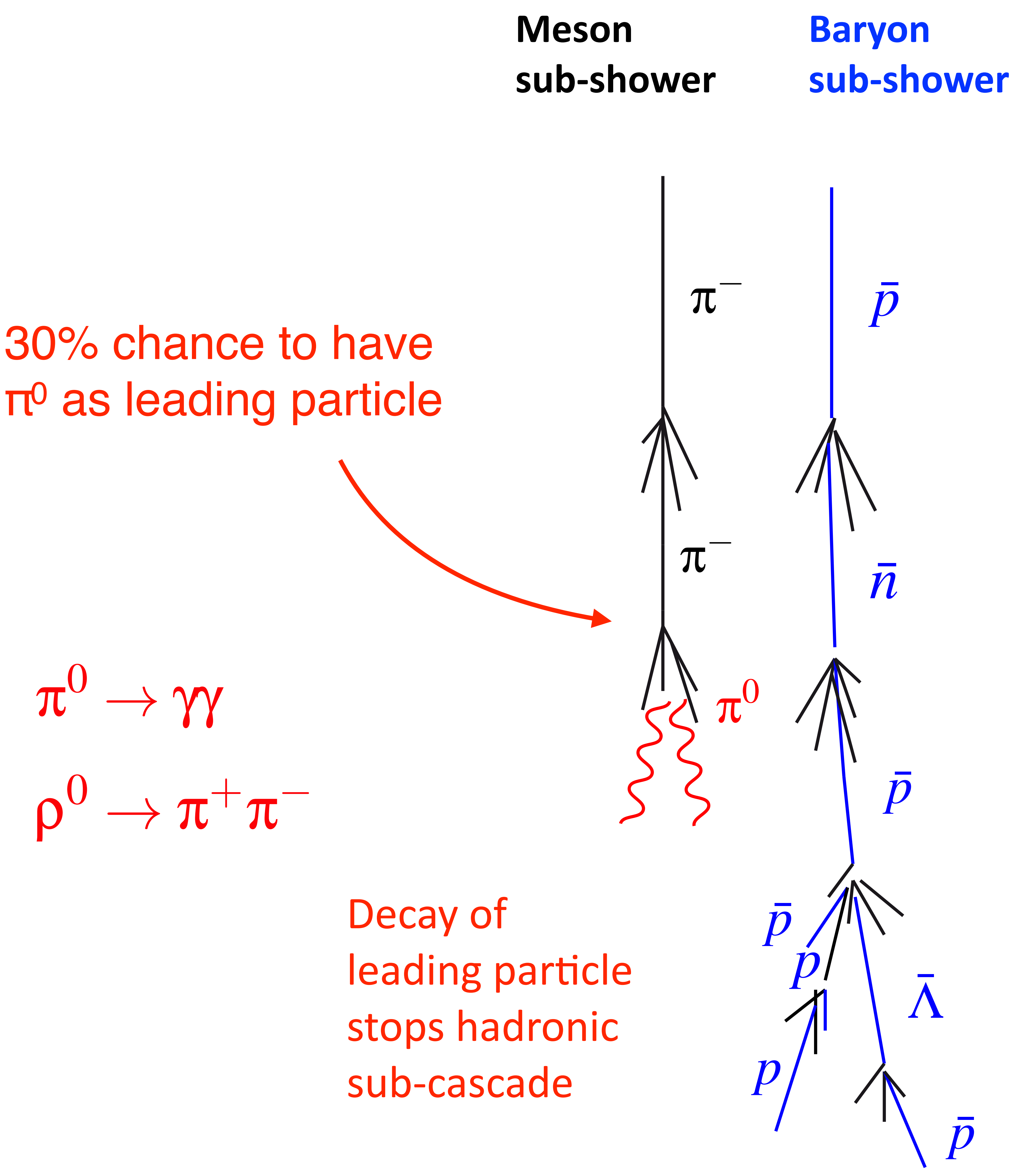

1 Baryon-Antibaryon pair production *(Pierog, Werner 2008)*

- Baryon number conservation
- Low-energy particles: large angle to shower axis
- Transverse momentum of baryons higher
- Enhancement of mainly **low-energy** muons

(Grieder ICRC 1973; Pierog, Werner PRL 101, 2008)

2 Enhanced kaon/strangeness production *(Anchordoqui et al. 2022)*

- Similar effects as baryon pairs
- Decay at higher energy than pions (~600 GeV)

3 Leading particle effect for pions *(Drescher 2007, Ostapchenko 2016)*

- Leading particle for a π could be ρ^0 and not π^0
- Decay of ρ^0 to 100% into two charged pions

4 New hadronic physics at high energy *(Farrar, Allen 2012, Salamida 2009)*

- Inhibition of π^0 decay (Lorentz invariance violation etc.)
- Chiral symmetry restauration

Several of these effects: Core-Corona model (Pierog et al.)

Atmospheric and geo-physics observations

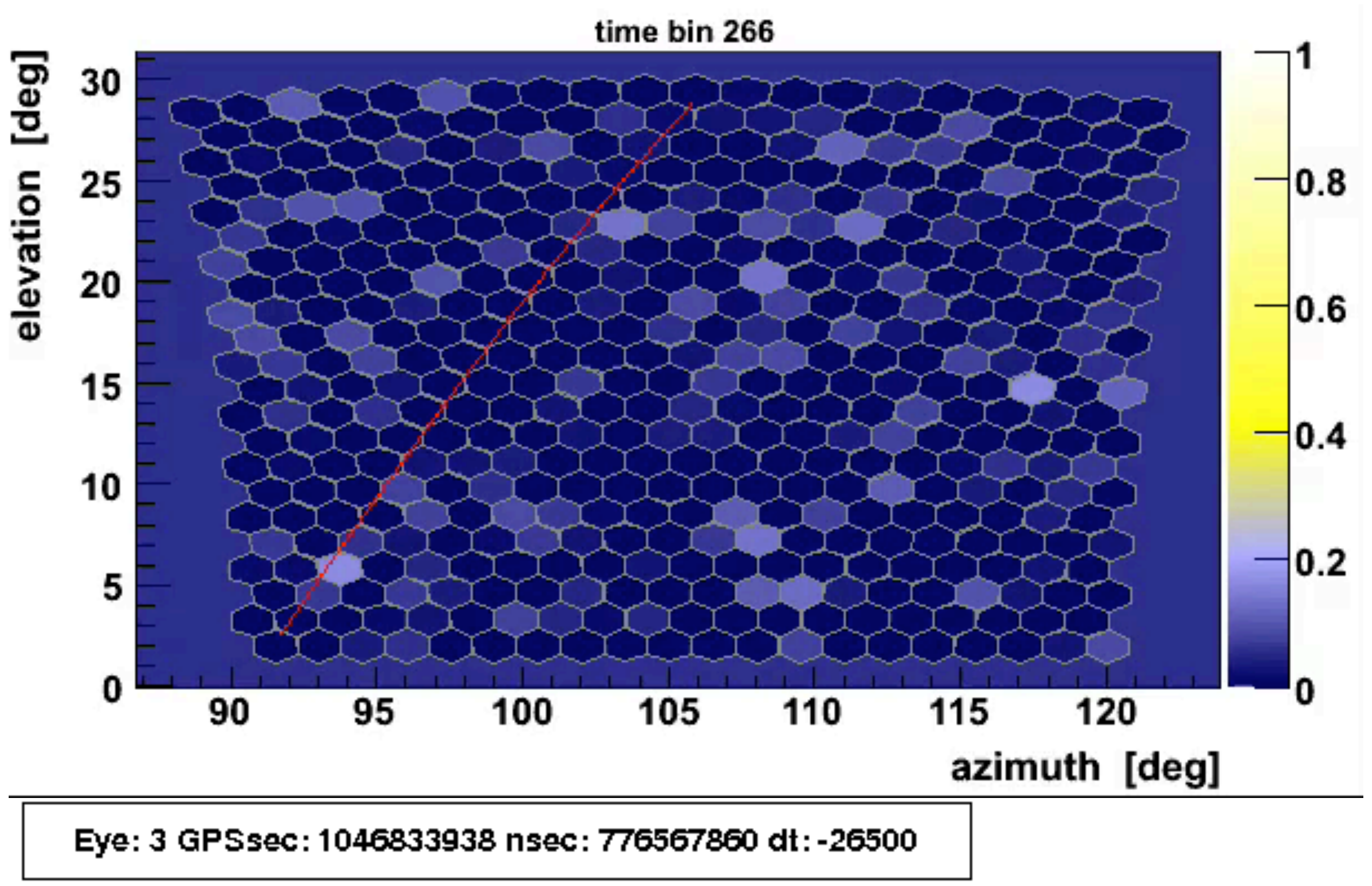

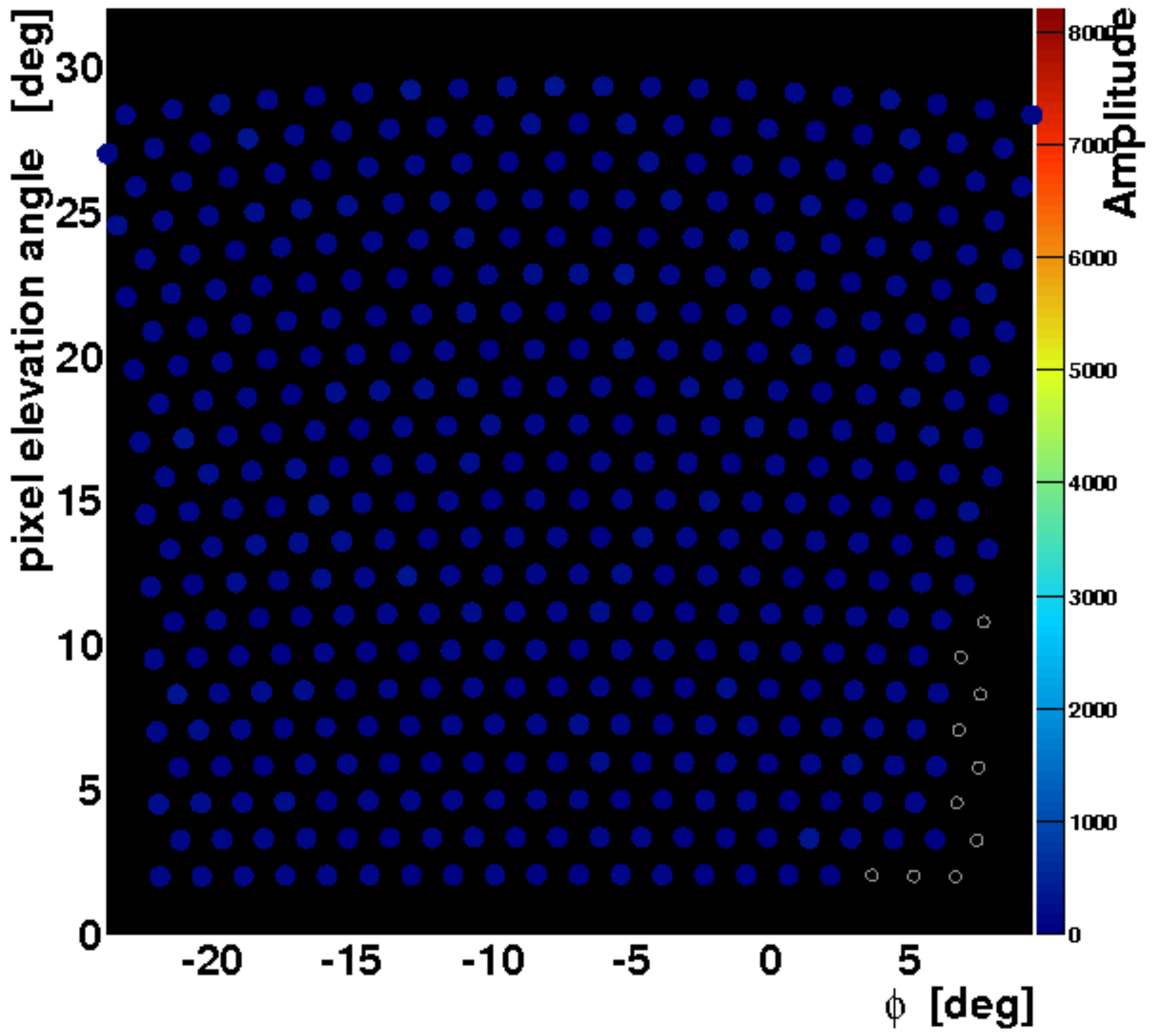

Example: observation of elves with FD telescopes

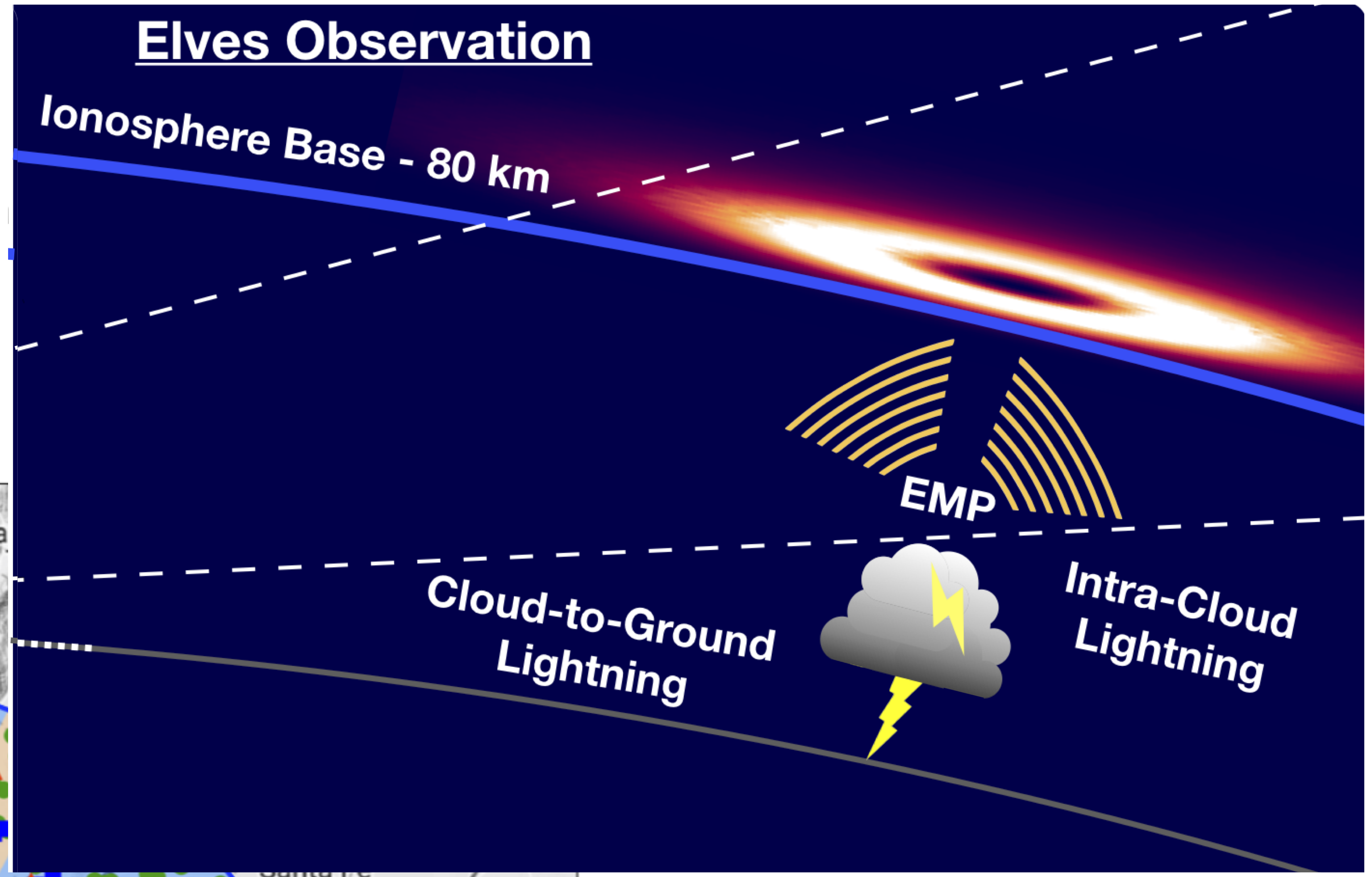

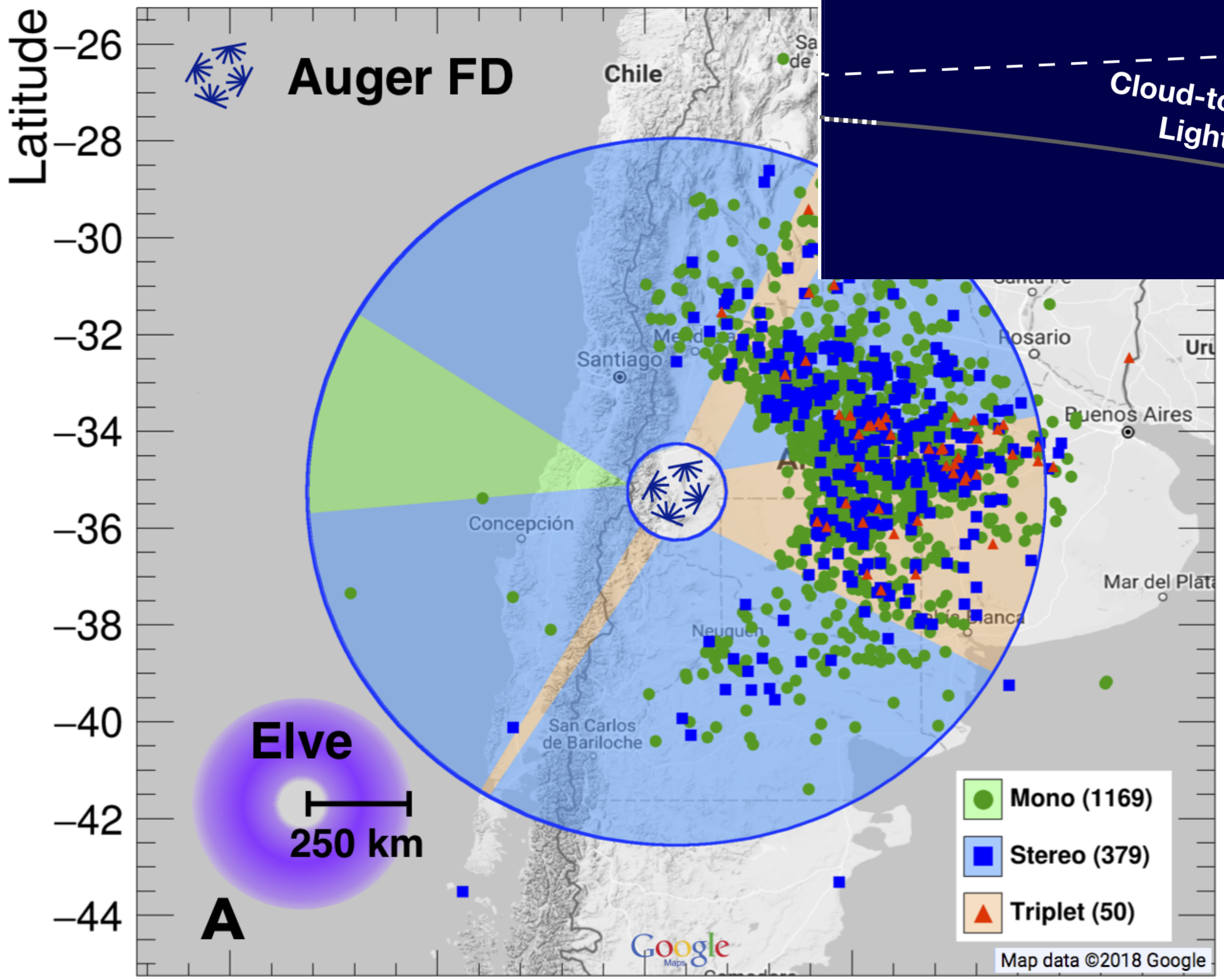

1600 elves

(Auger, Earth and Space Sciences, 2020)

Summary – the global picture by using only data

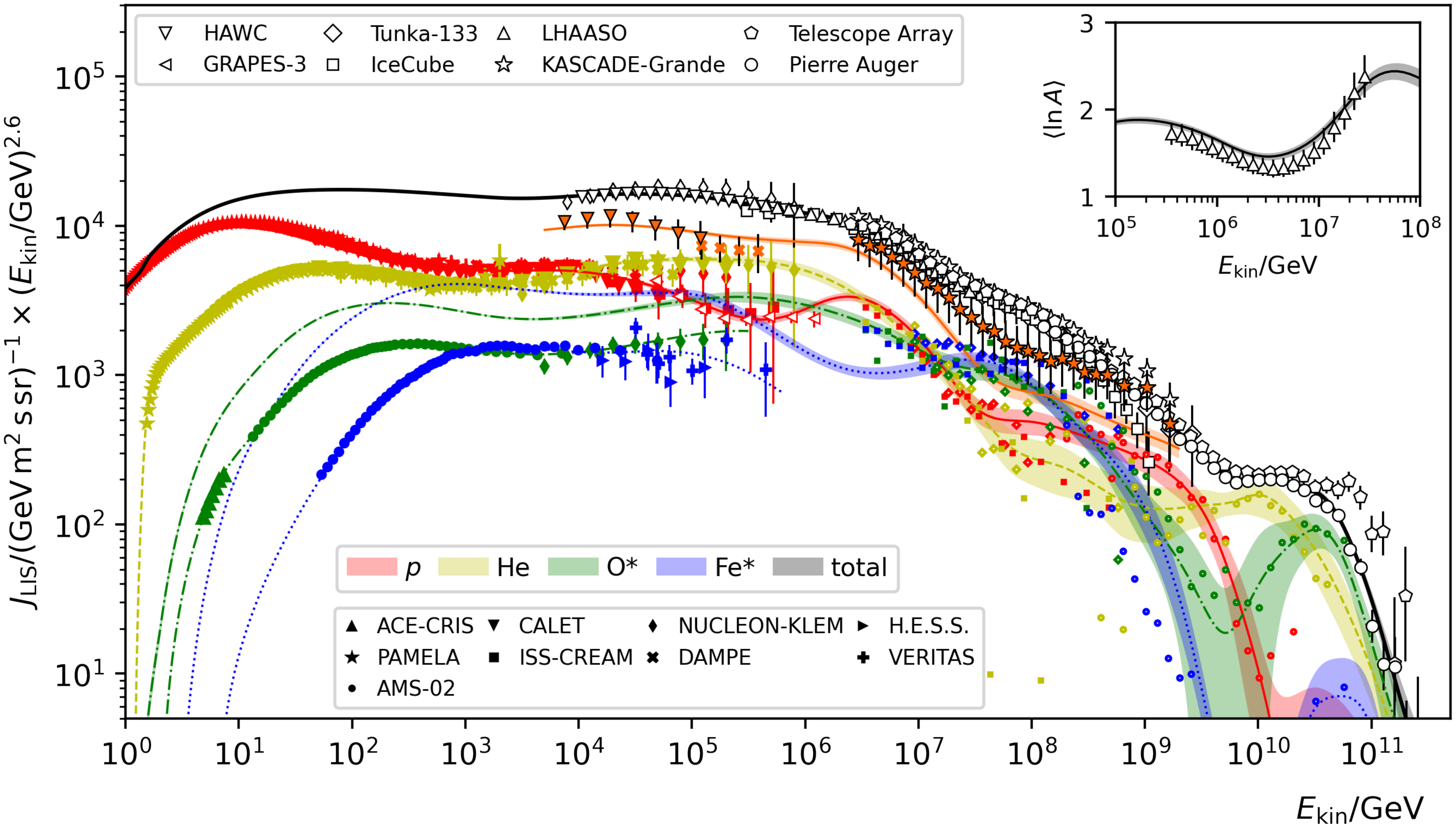

(Global Spline Fit (GSF) 2024, **Kozo Fujisue**, Dembinski, RE, Fedynitch, UHECR 2024)

Summary – constraints on source scenarios

Hillas criterion

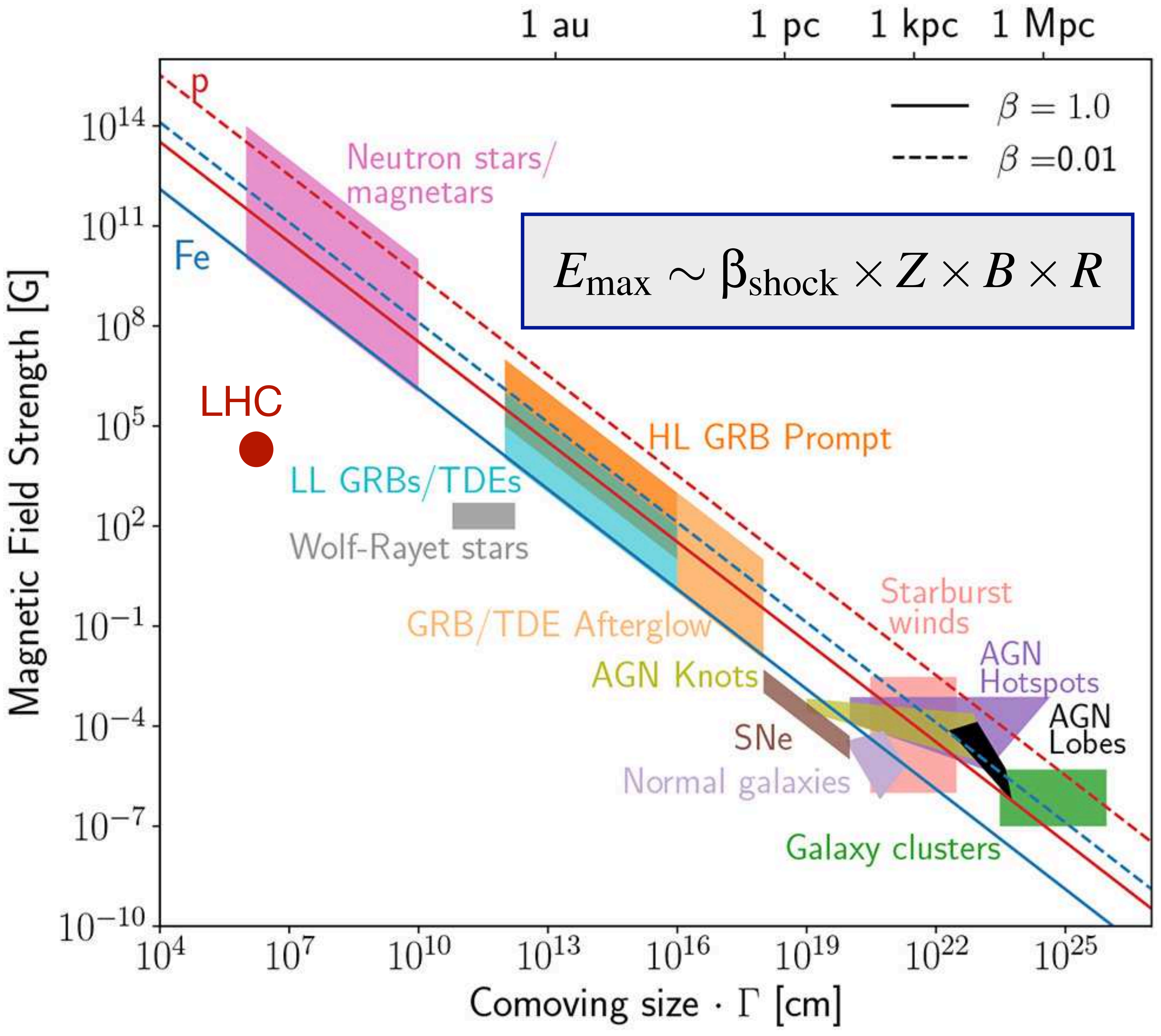

$$E_{\max} \sim \beta_{\text{shock}} \times Z \times B \times R$$

Lovelace energy flux criterion

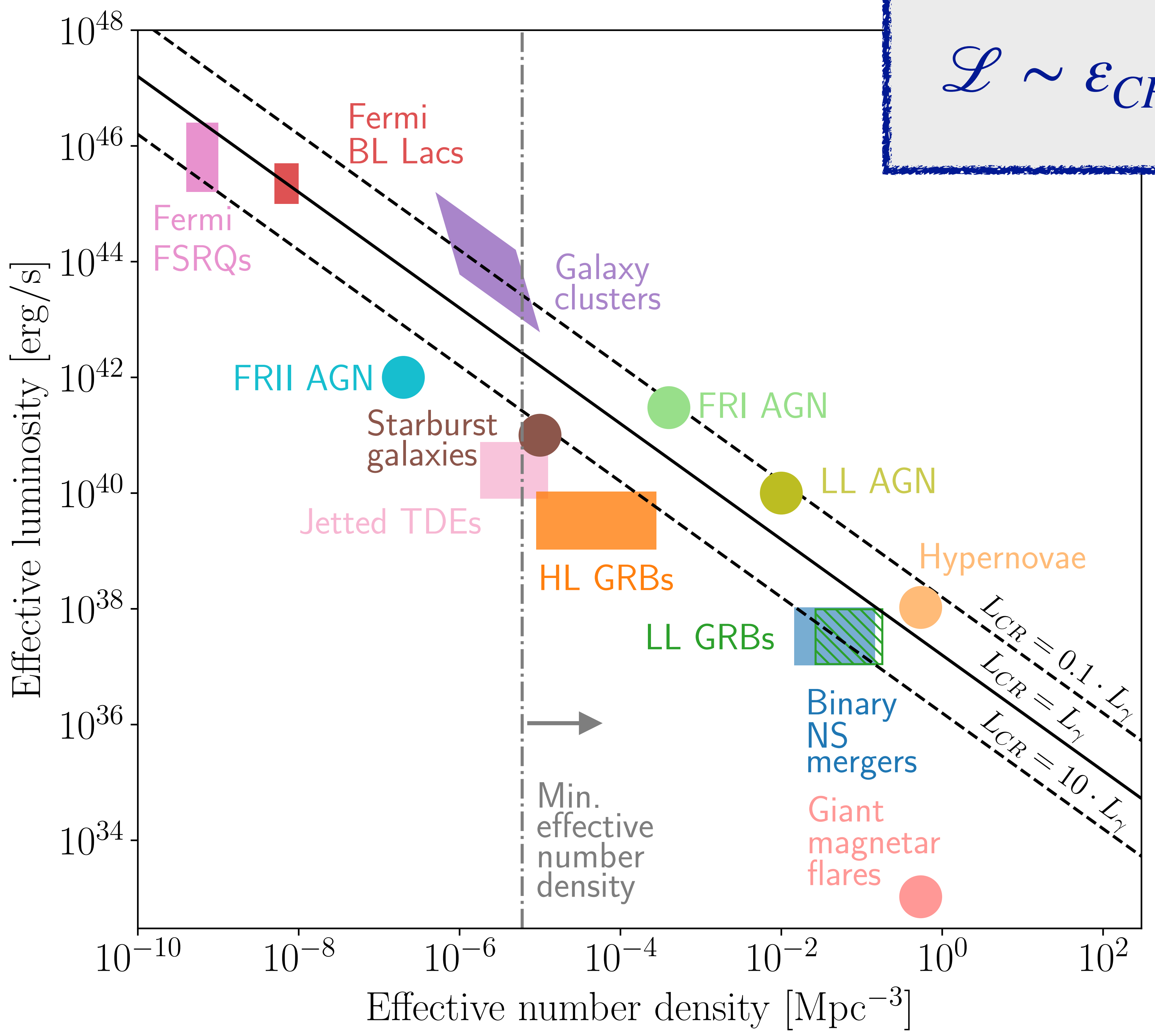

Source injection power

$$\mathscr{L} \sim \varepsilon_{CR}/t_{\text{loss}} = 2 \cdot 10^{44}\,\text{erg Mpc}^{-3}\,\text{yr}^{-1}$$

Detailed calculation:

$$\mathscr{L} \simeq 6 \cdot 10^{44}\,\text{erg Mpc}^{-3}\text{yr}^{-1}$$

Source density

$$\rho_{\text{eff}}(E \sim 10^{18.5}\,\text{eV}) \sim 10^{-4}\,\text{Mpc}^{-3}$$

Heavy mass elements

Hard source spectrum

Source similarity

Large degree of isotropy

Transition to extragalactic sources at low energy

(MIAPP review, Front.Astron.Space Sci. 6 (2019) 23)

Backup slides

The Auger Collaboration in Malargue – November 2022

Stay tuned for new discoveries!

Auger: A 4π MM Observatory
1 Neutrons and charged CRs: $\Theta \leq 80°$
2 UHE Photons: $30° \leq \Theta \leq 60°$
3 Down-Going Neutrinos: $60° \leq \Theta \leq 90°$
4 Earth Skimming Neutrinos: $90° \leq \Theta \leq 95°$
5 HE BSM Particles: $\Theta > 95°$
$UHECR + matter \rightarrow \pi^{\pm} + \pi^{0} + X$
$\hookrightarrow \gamma + \gamma$
$\hookrightarrow \mu + \nu_{\mu} + \nu_{e}$
SHOCK WAVE
p
γ
π^0
$\pi^{\pm}$
e
e
e
μ
ν_μ
ν_e
γ
ν_μ

Multi-messenger observation of sources

AMON
Astrophysical Multimessenger Observatory Network

Analysis of individual events
Stacking analysis of BBH mergers

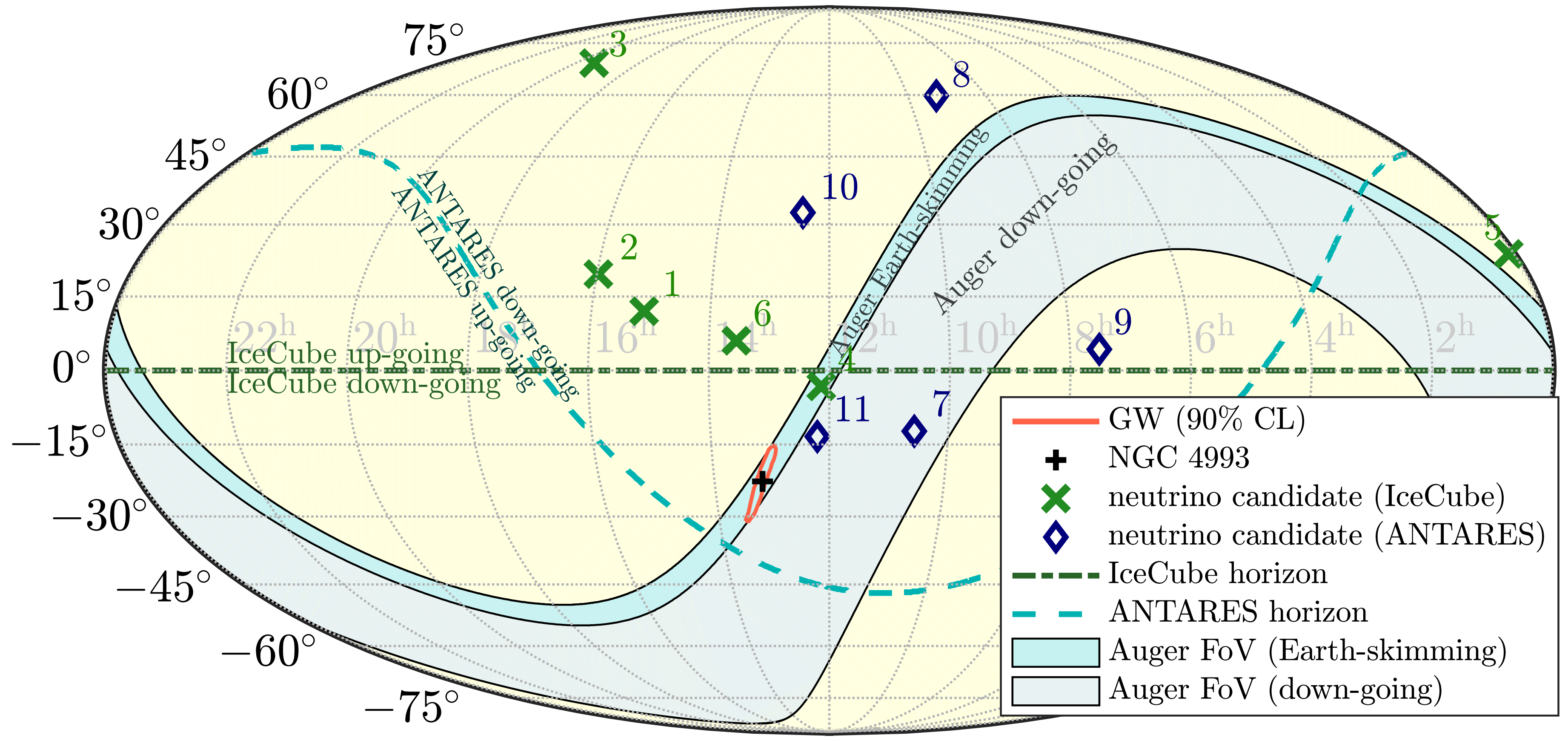

GW170817

ApJL (2017), special issue (70 collaborations)

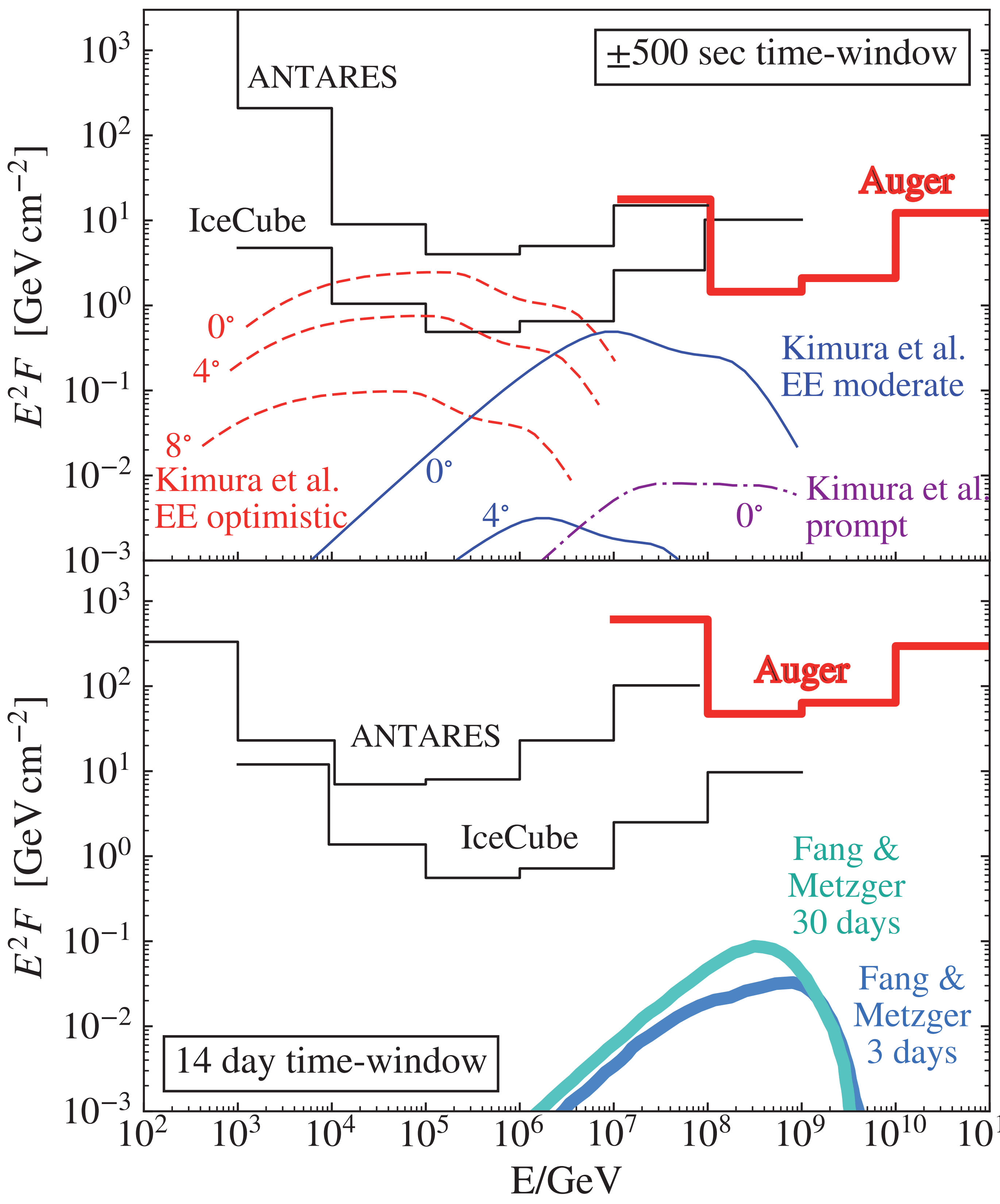

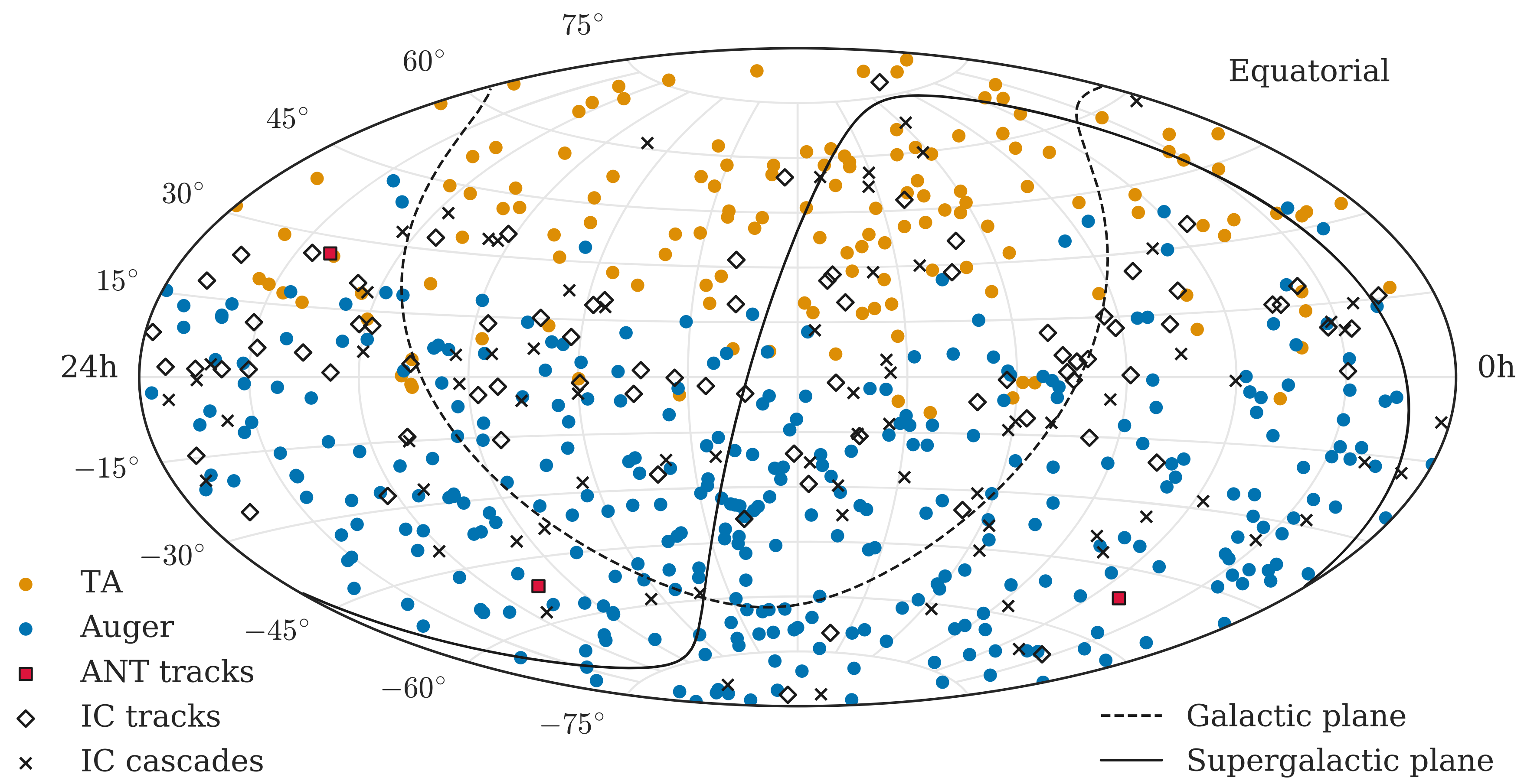

(Auger ICRC 2023)

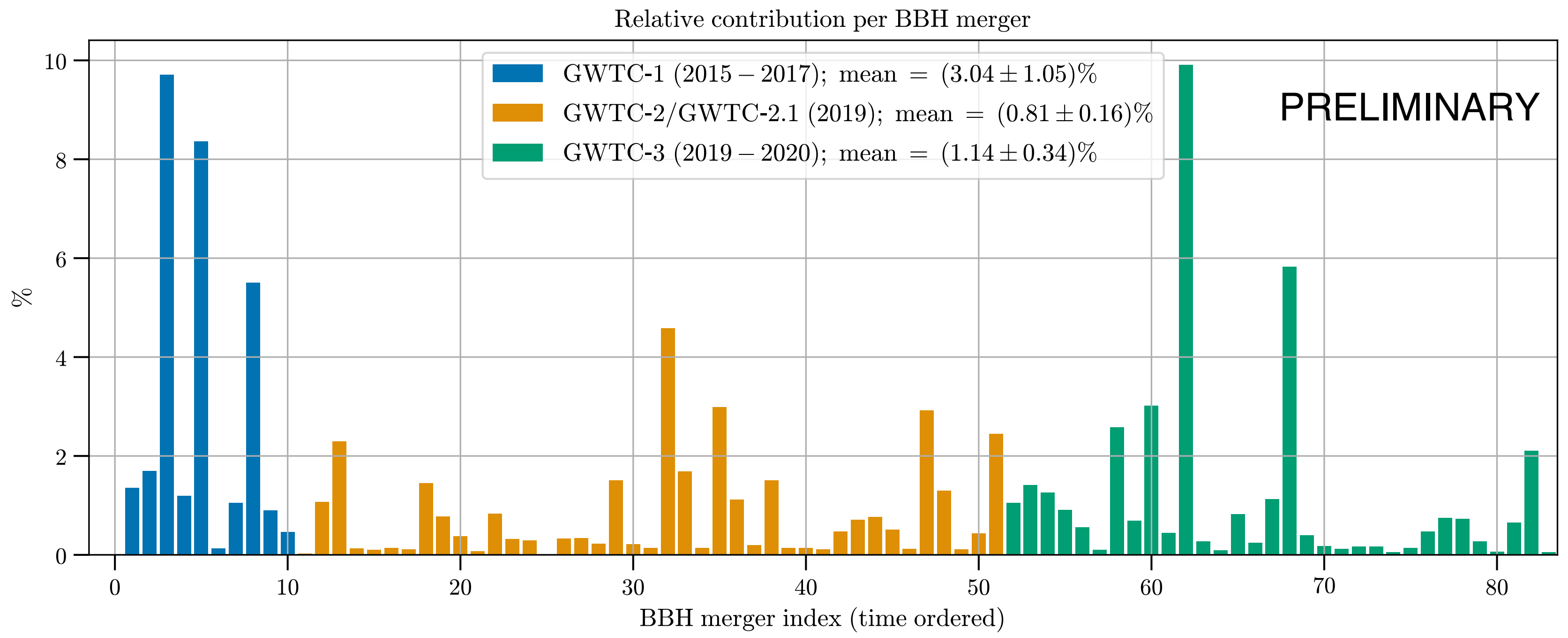

Search for spatial neutrino and UHECR correlations (ApJ 934 (2022) 164)

Instantaneous aperture comparable to IceCube if direction of source is favorable
Multi-messenger: searches for neutrinos and photons in coincidence with GW events

6. Fundamental physics studies

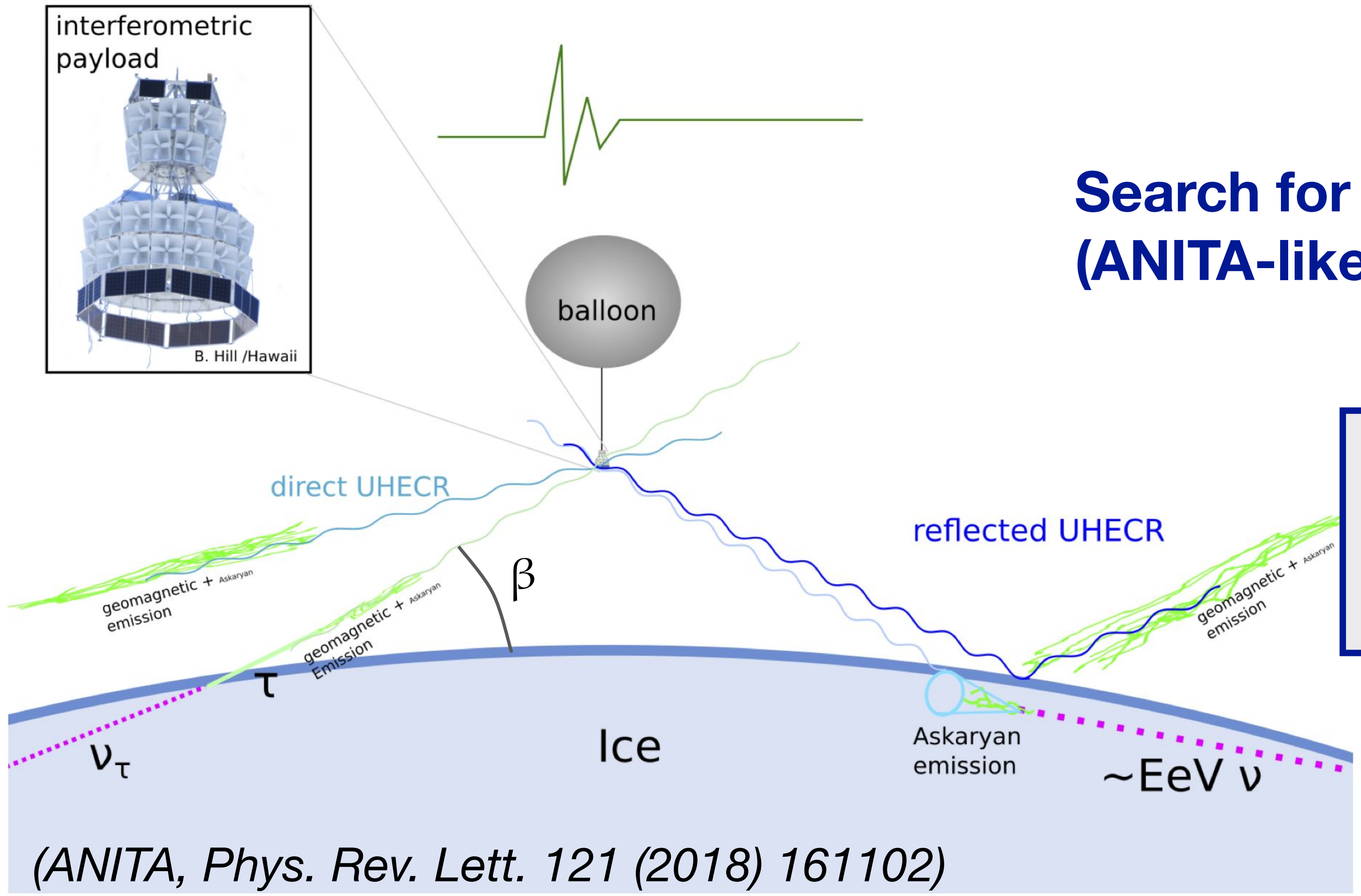

Search for upward going showers (ANITA-like events)

No ANITA-like events seen
~10x exposure of ANITA

Photon and neutrino limits at ultra-high energy

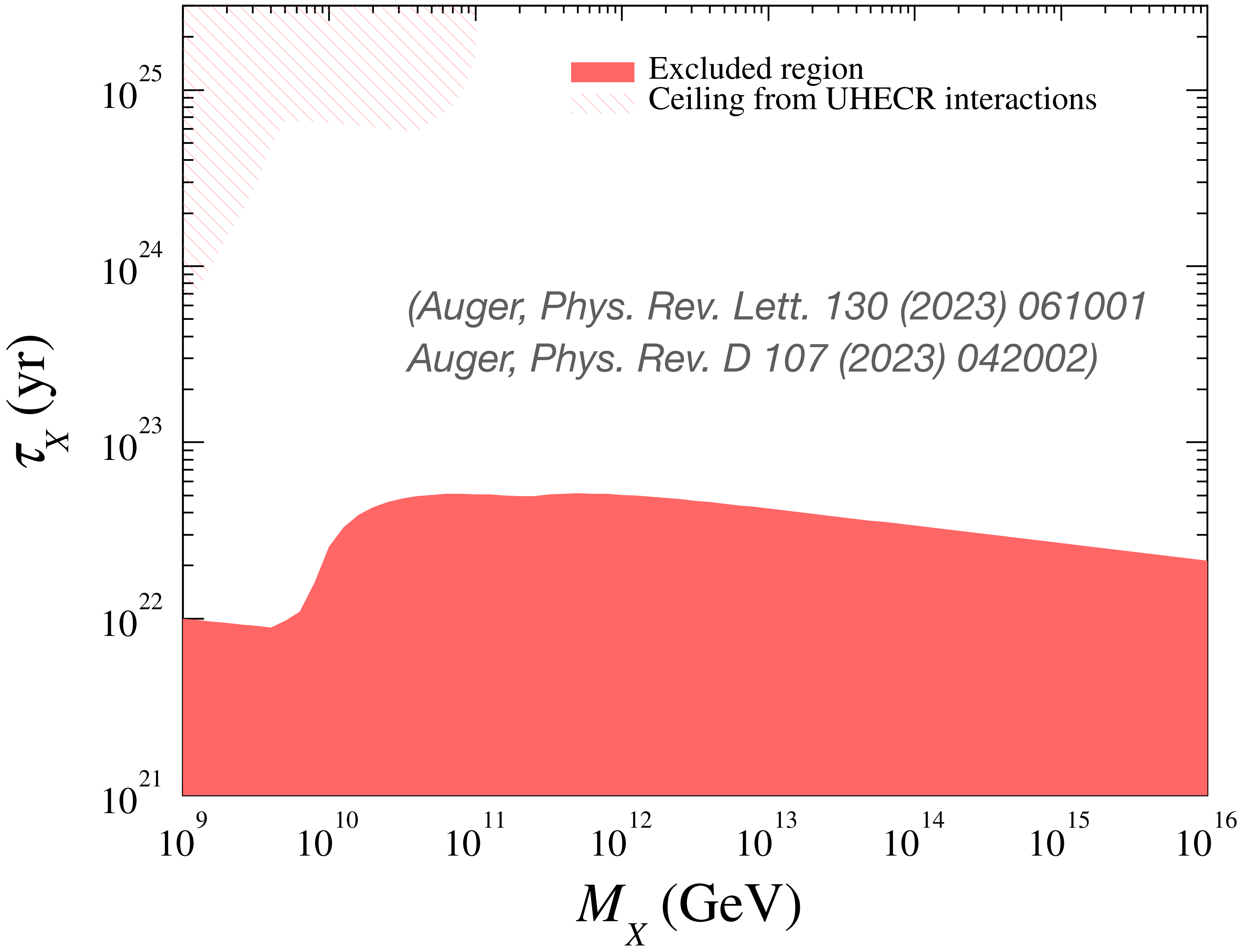

Lorentz-dilated lifetime of neutral pions

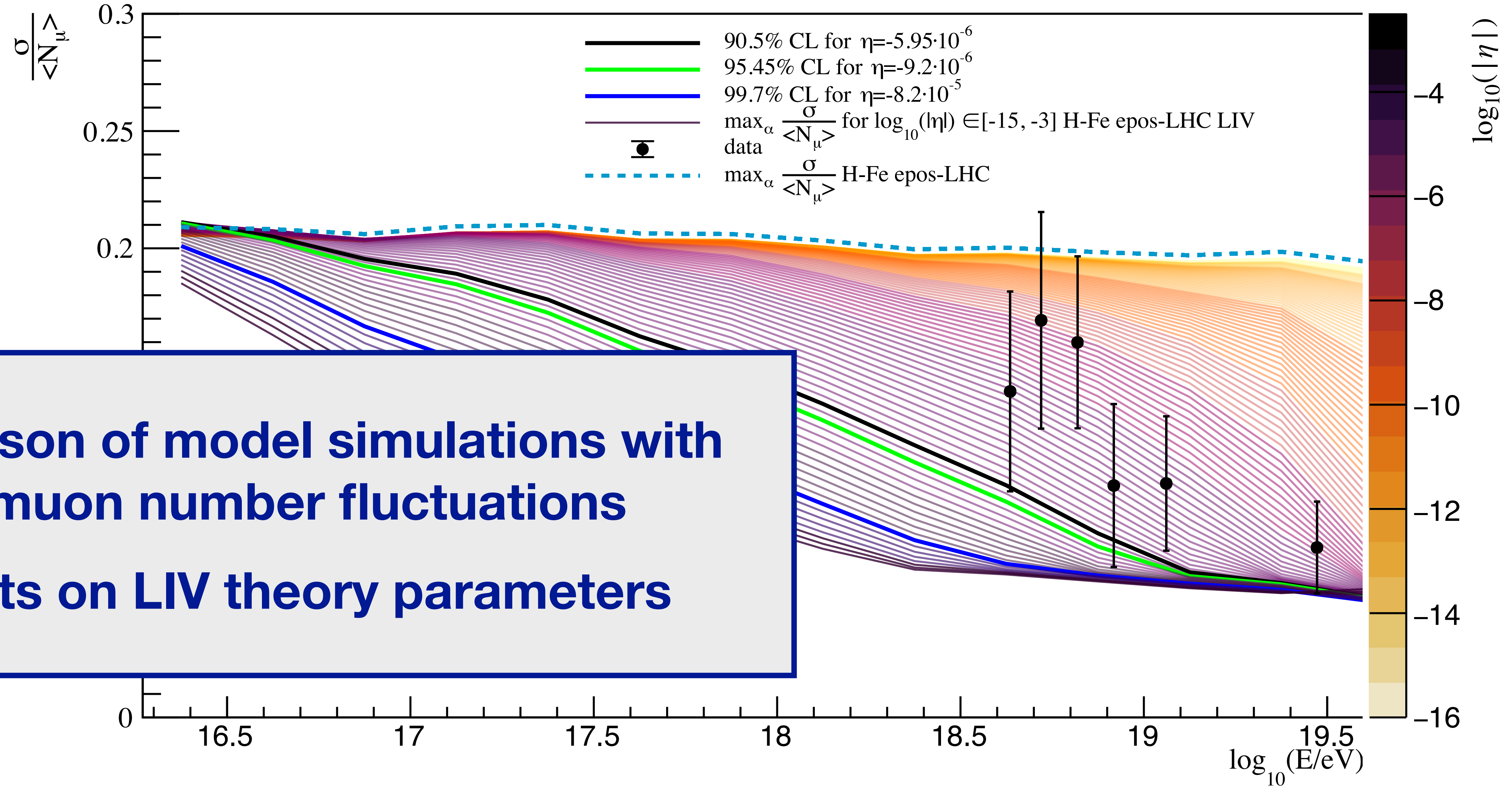

Comparison of model simulations with data on muon number fluctuations

New limits on LIV theory parameters

Limits on parameters of SHDM models (mass, lifetime, decay through instanton processes)

Telescope Array Low-energy Extension – TALE

- Upgrade TA hybrid detector sensitivity down to PeV range → **TALE**

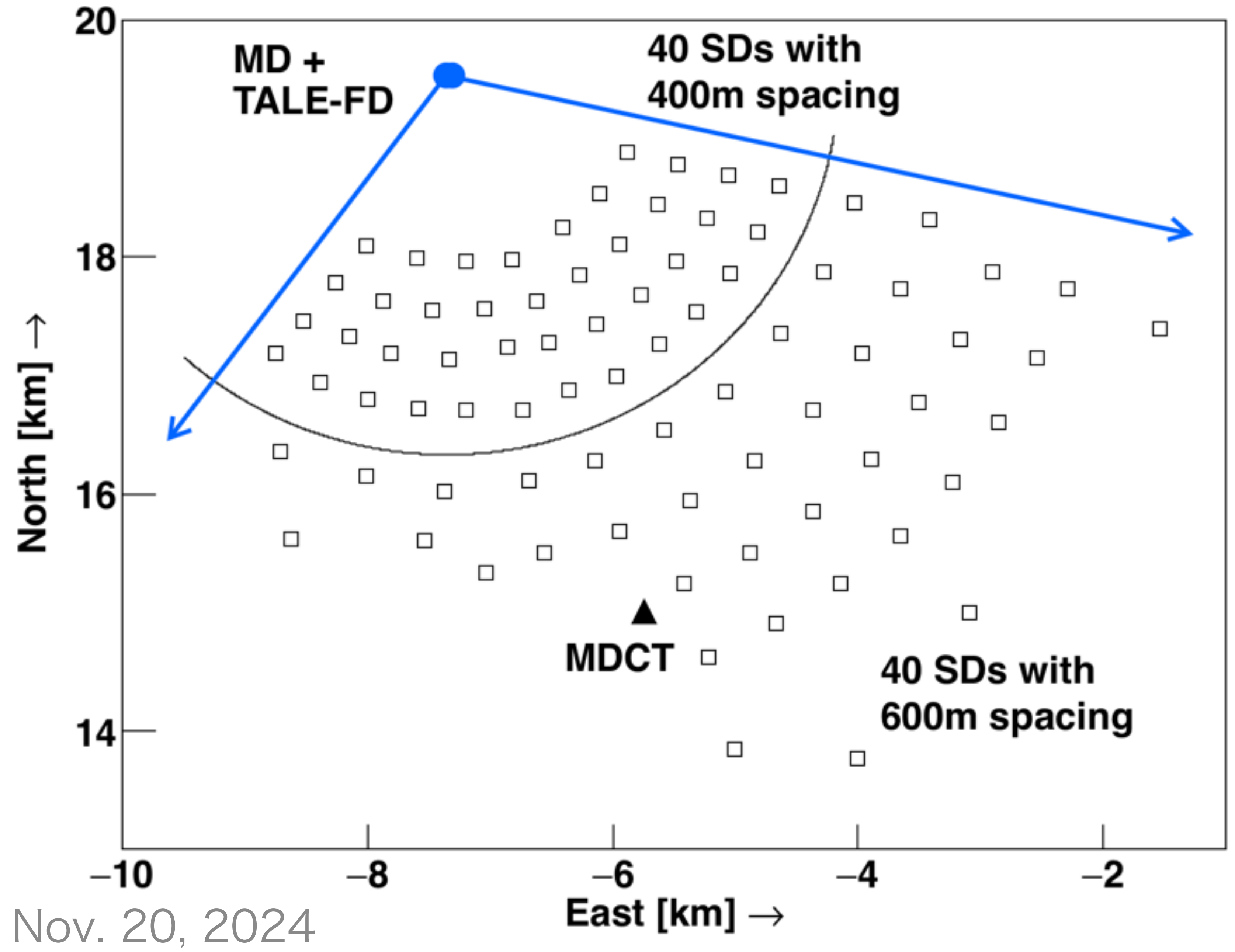

- **10** High-elevation telescopes (31° - 59°)
  - 256pixel, 8bit 10MHz FADC readout
  - Started observation since 2013

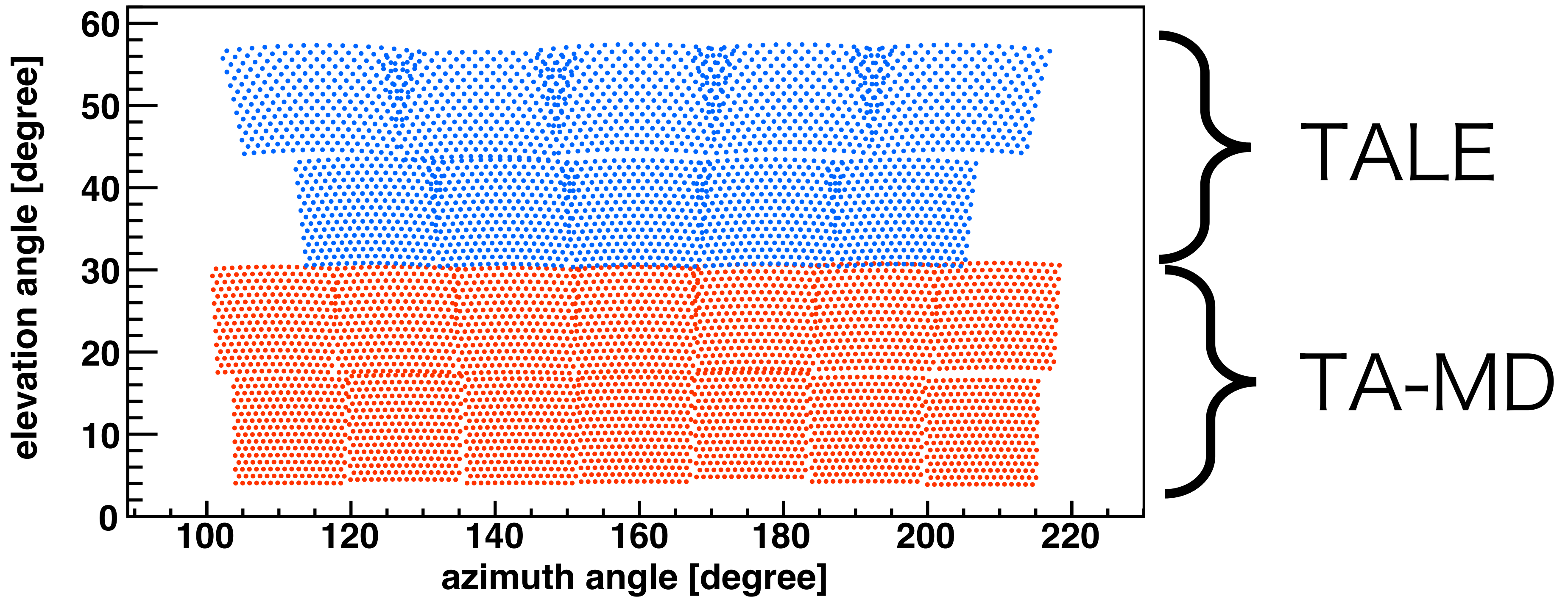

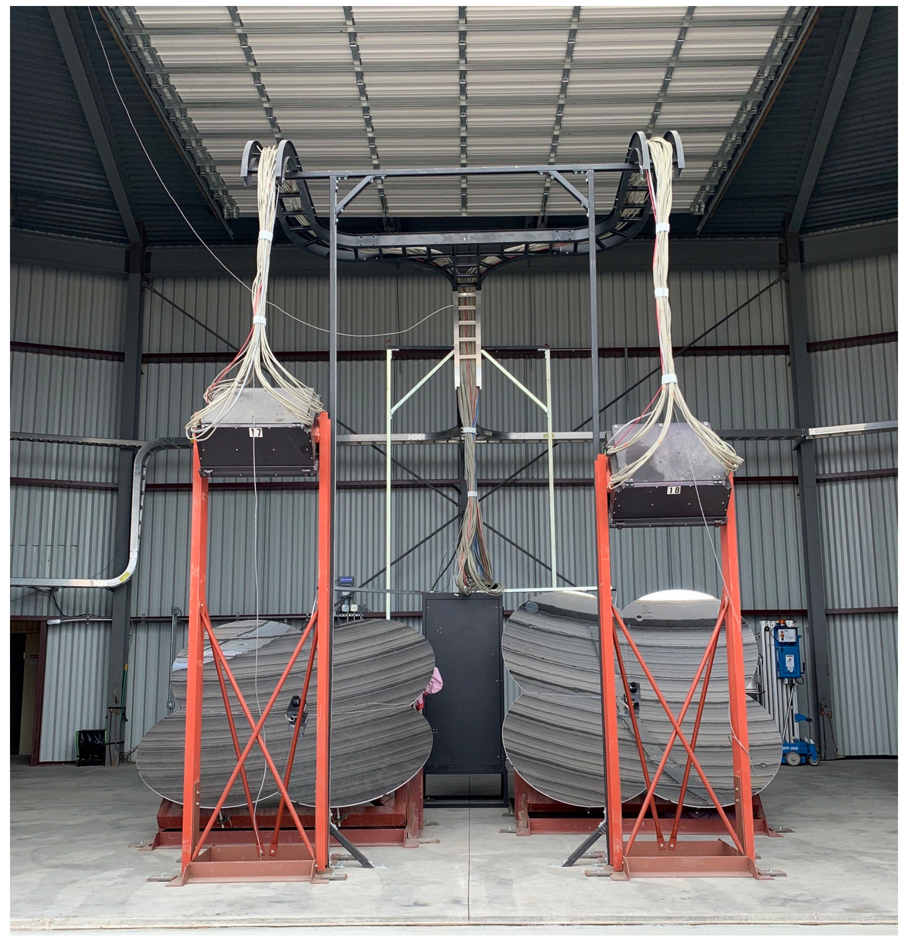

- SD array
  - **40**SDs with **400**m, **40**SDs with **600**m
  - 2 layers Scintillation counter, 3m^2
  - Started observation since 2017

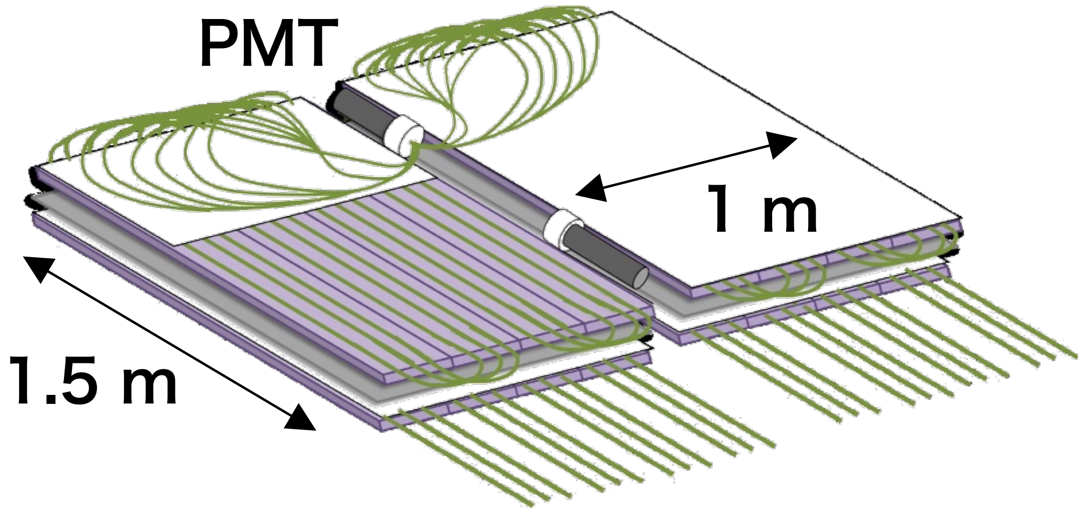

Low-energy composition measurement with TA

- Observed $\langle X_{\rm max} \rangle$ vs. shower energy

TALE FD + new SD array hybrid measurement

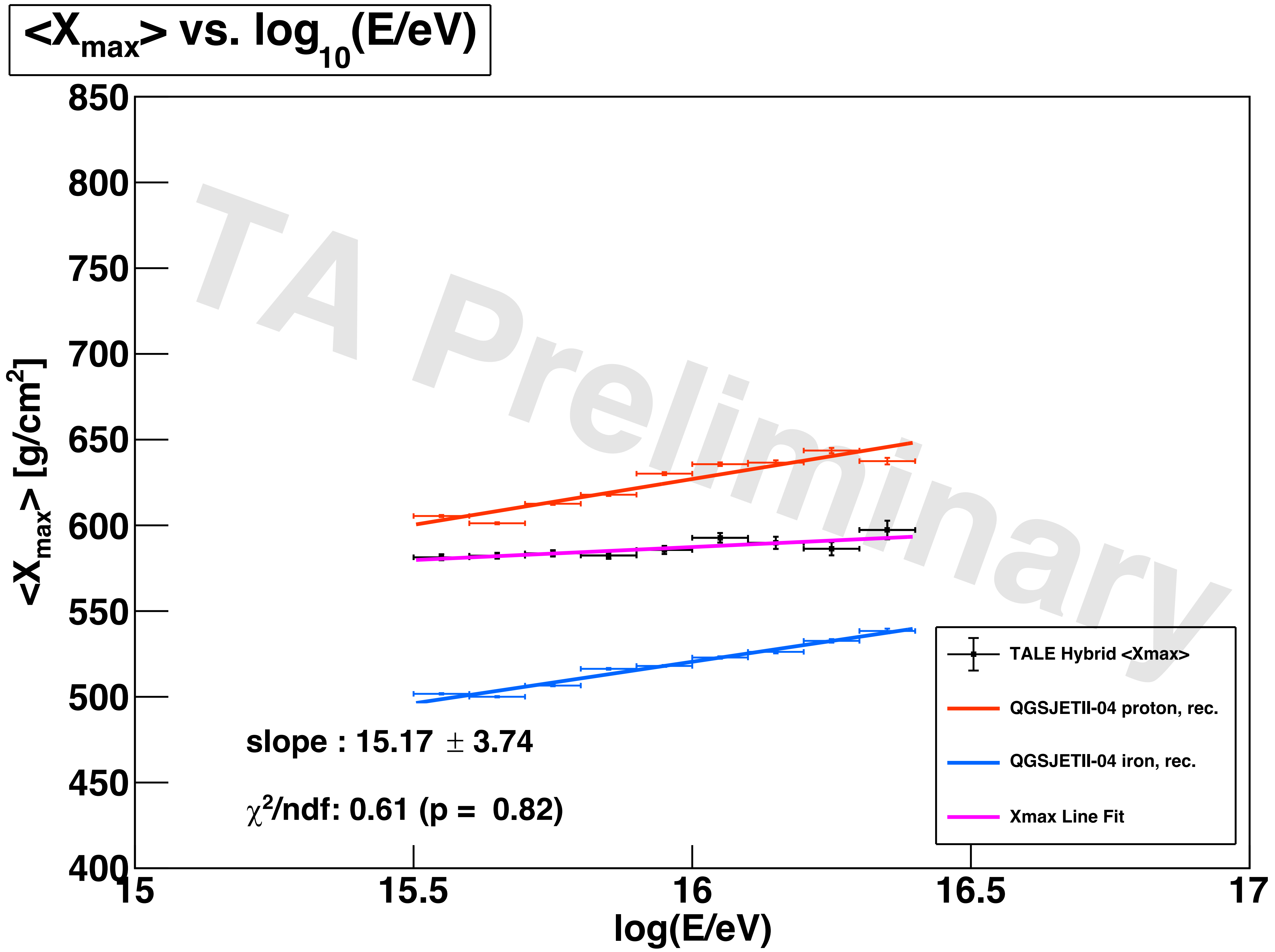

TALE FD + TALE SD array hybrid measurement

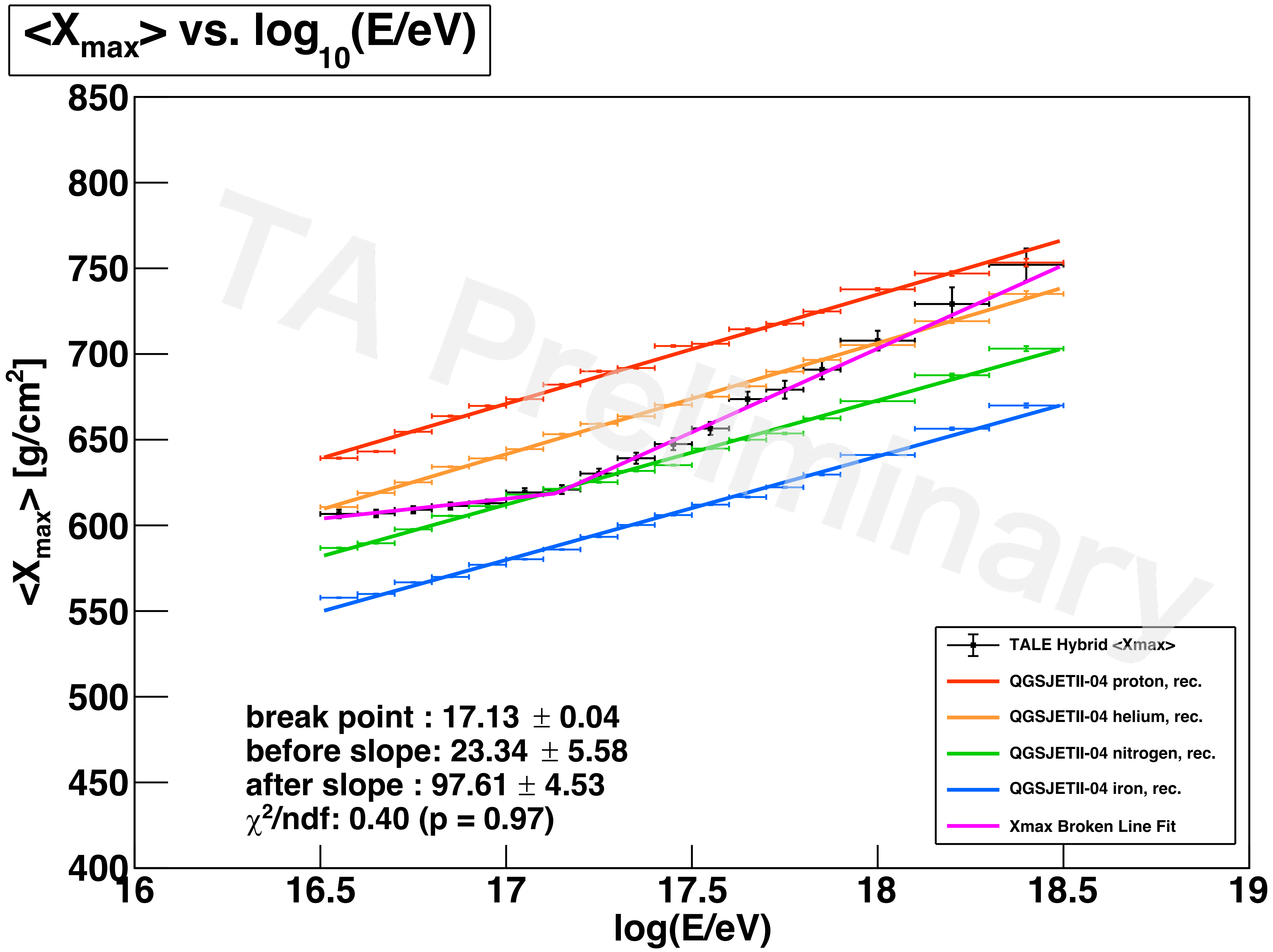

(TA, UHECR 2024)

An invitation: Auger open data

opendata.auger.org

DOI:10.5281/zenodo.4487613

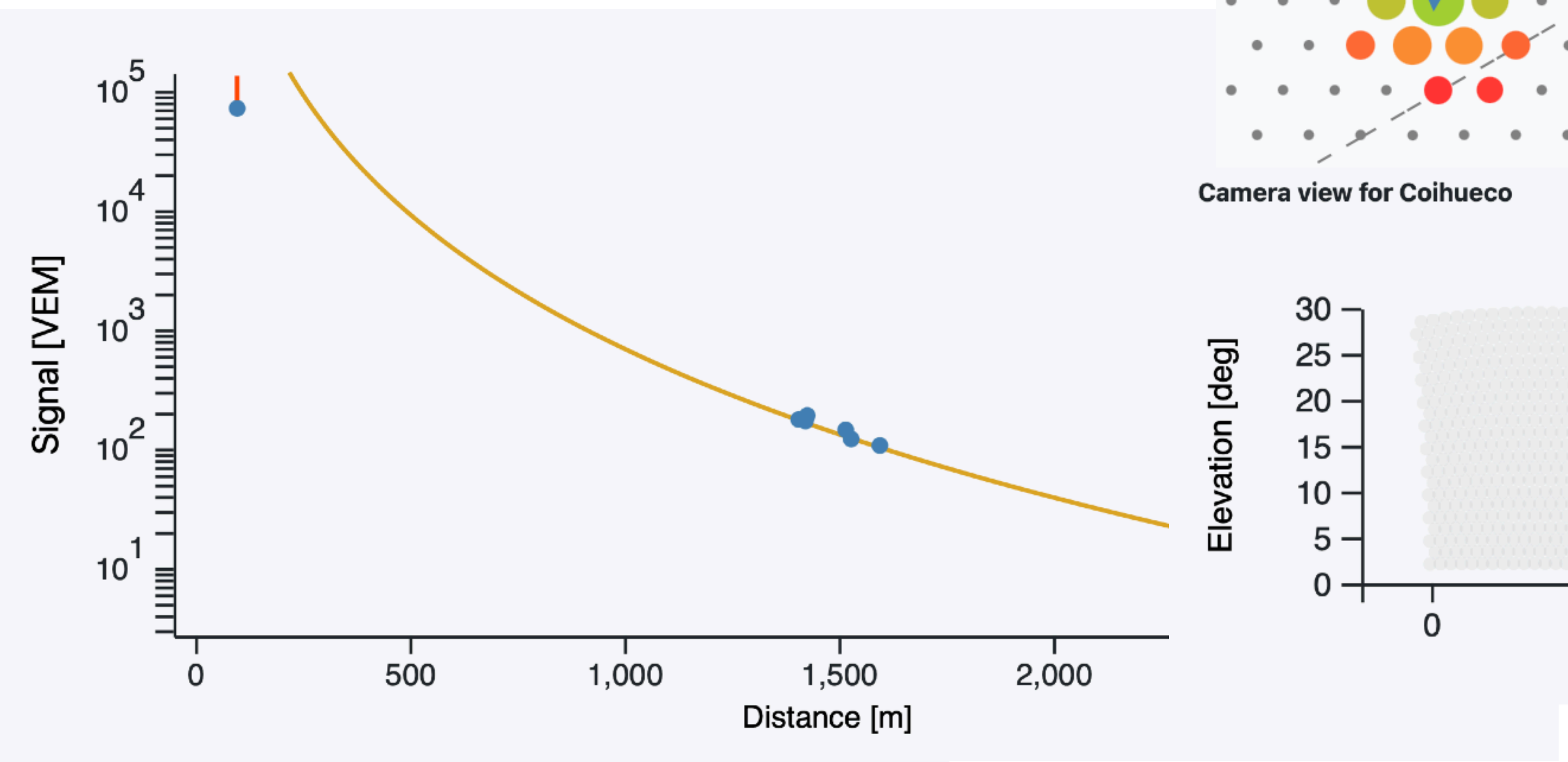

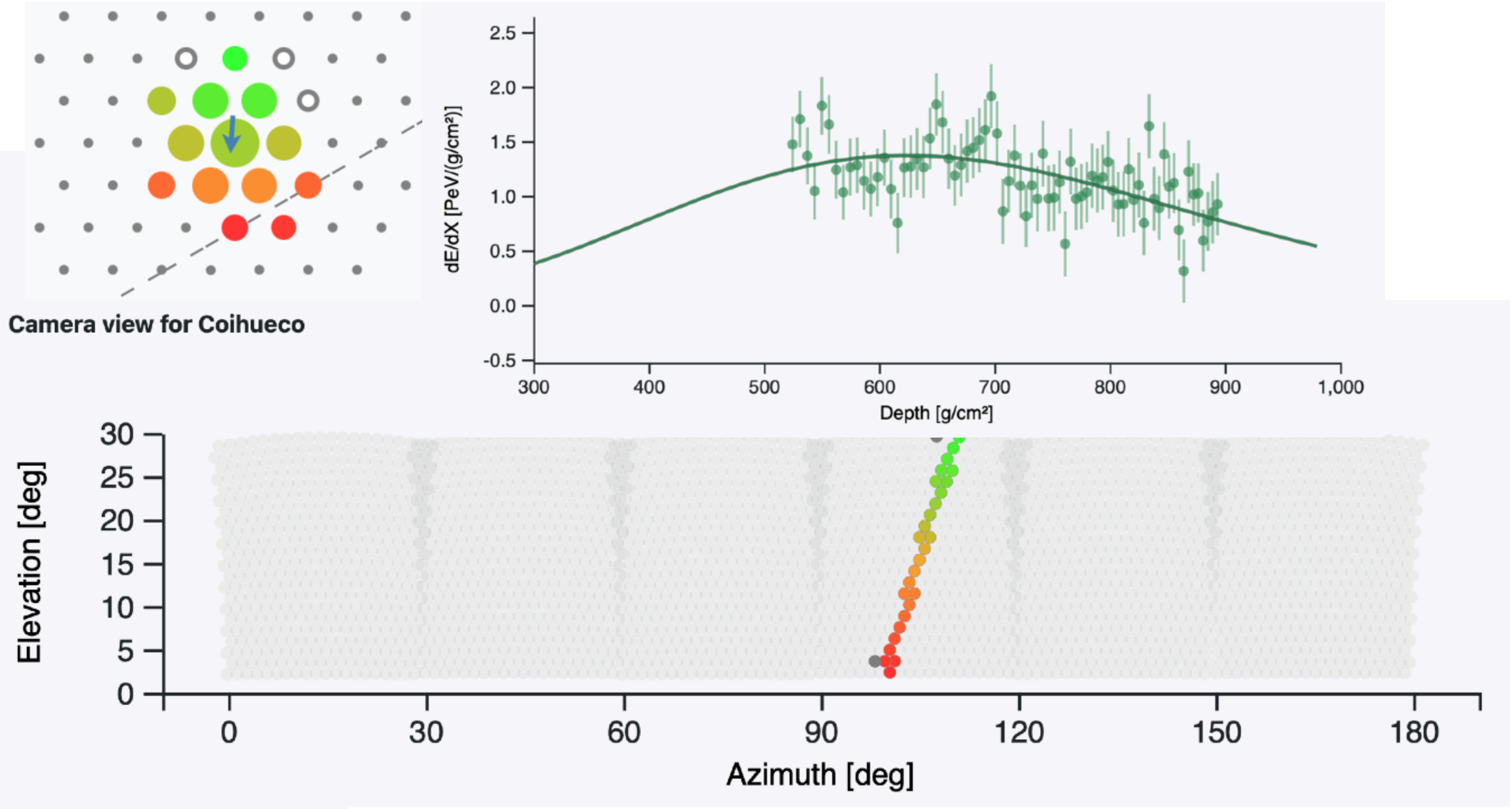

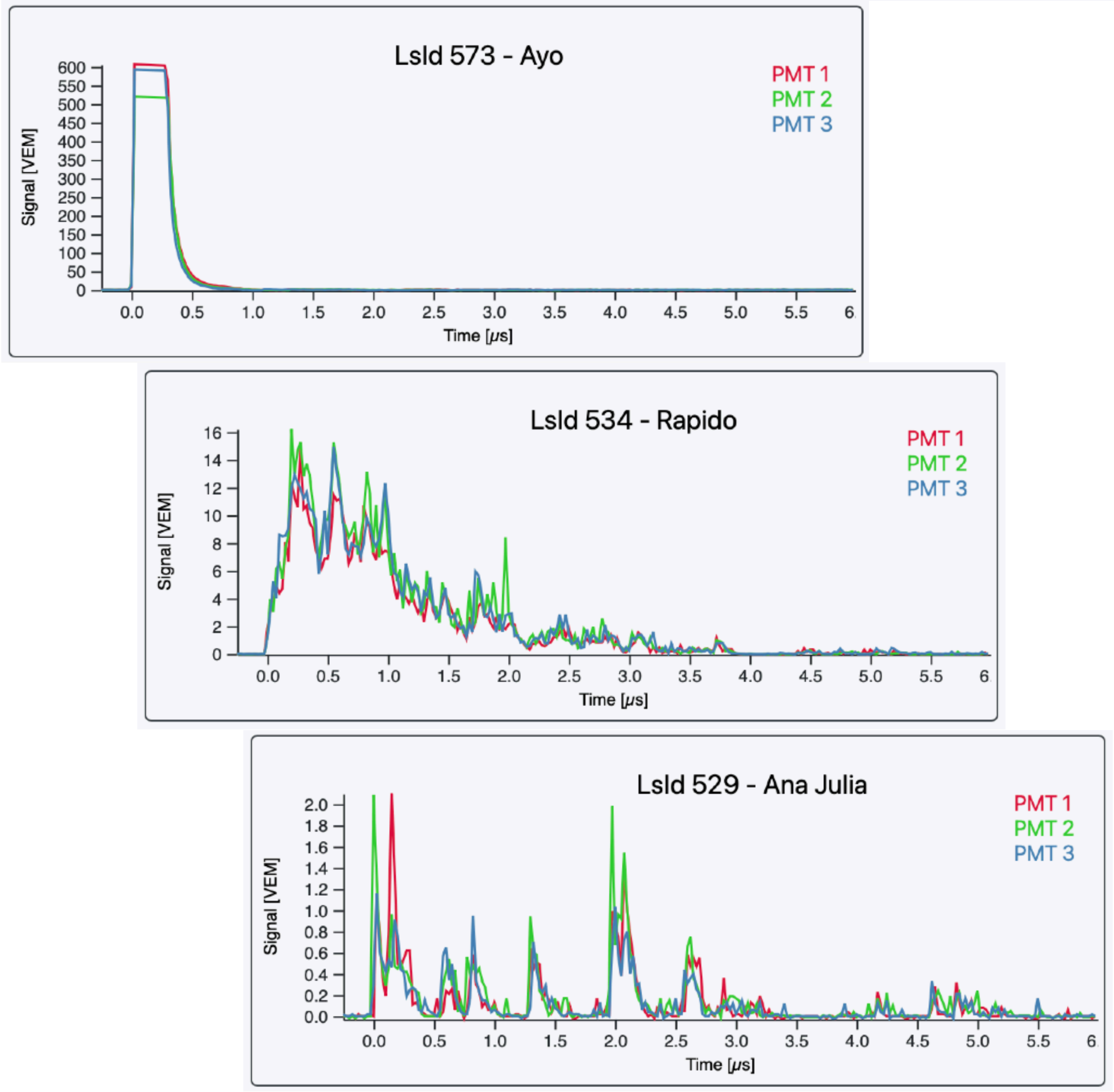


```
In [19]:
Y_0val = FC_CL * 0.9

plt.title("Spectrum with event counts")
plt.errorbar(bin_energy18[cut_nz], flux, [flux_lower, flux_upper], fmt="o")
plt.errorbar(bin_energy18[cut_z], FC_CL, Y_0val, uplims=True, marker="None", color="steelblue",
             markeredgecolor="r", markerfacecolor="r", linewidth=2.0, linestyle="None", capsize
=5)
plt.xscale("log")
plt.yscale("log")
plt.xlabel('E [eV]')
plt.ylabel(r'J$^{Raw}$(E) [km$^{-2}$ sr$^{-1}$ yr$^{-1}$ eV$^{-1}$]')

# expand the range in y to have space for the labels and upper limits
plt.ylim(flux[flux > 0].min()*0.01, flux.max()*7)

# add the counts to the points
for E, J, count in zip(bin_energy18, flux, h):
    if count > 0:
        plt.annotate(count, (E, J), rotation=30, va='bottom')
```

Currently 10% of Auger vertical data
Research-level data in JSON format
Online visualization of events
Data analysis scripts for science plots

You are welcome to use this data

If you have a great idea what to look for we can work with you to apply your analysis also to the full data set

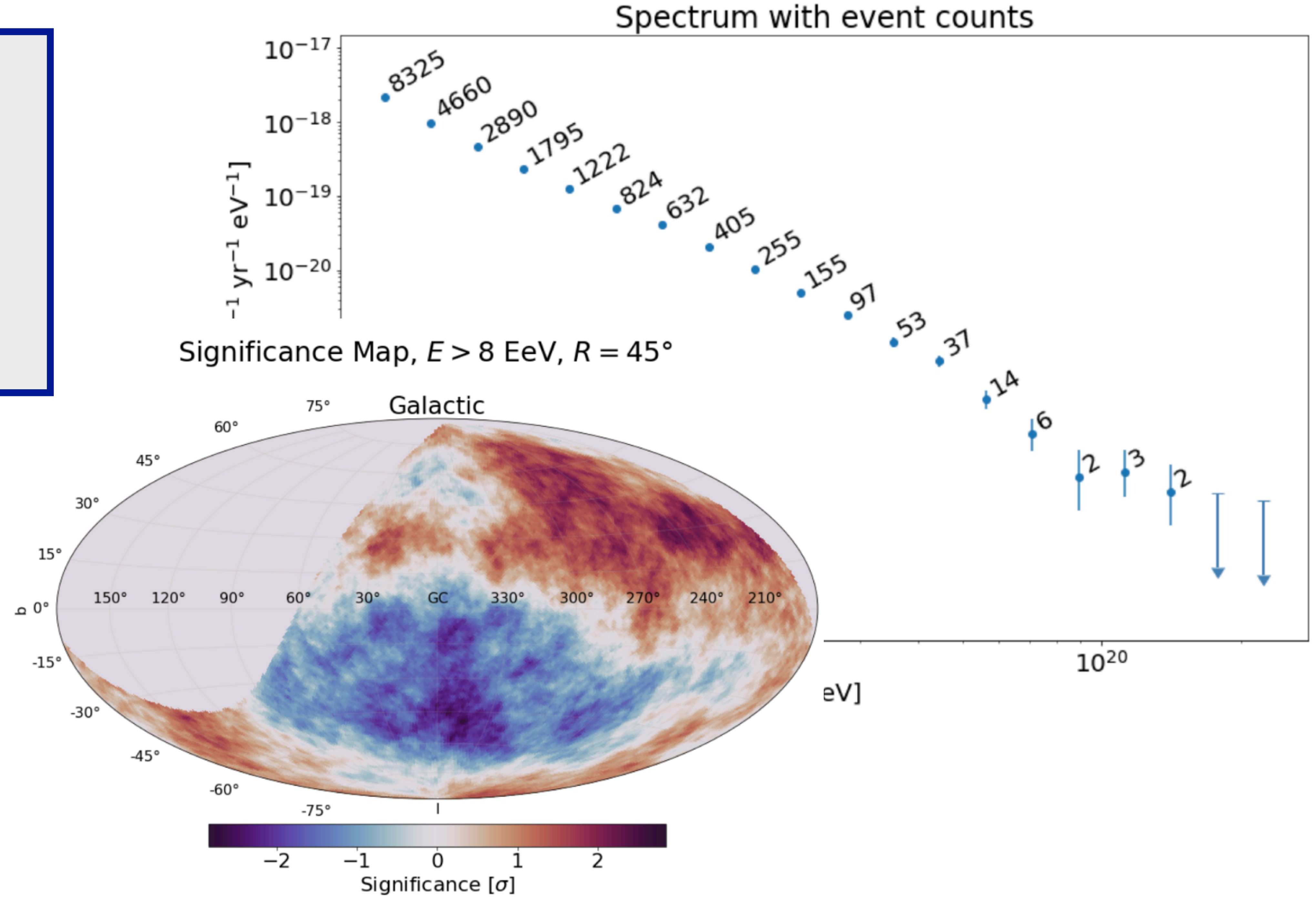

Model calculations for mass composition and flux

(Auger, JCAP 05 (2023) 024 & JCAP 01 (2024) 022)

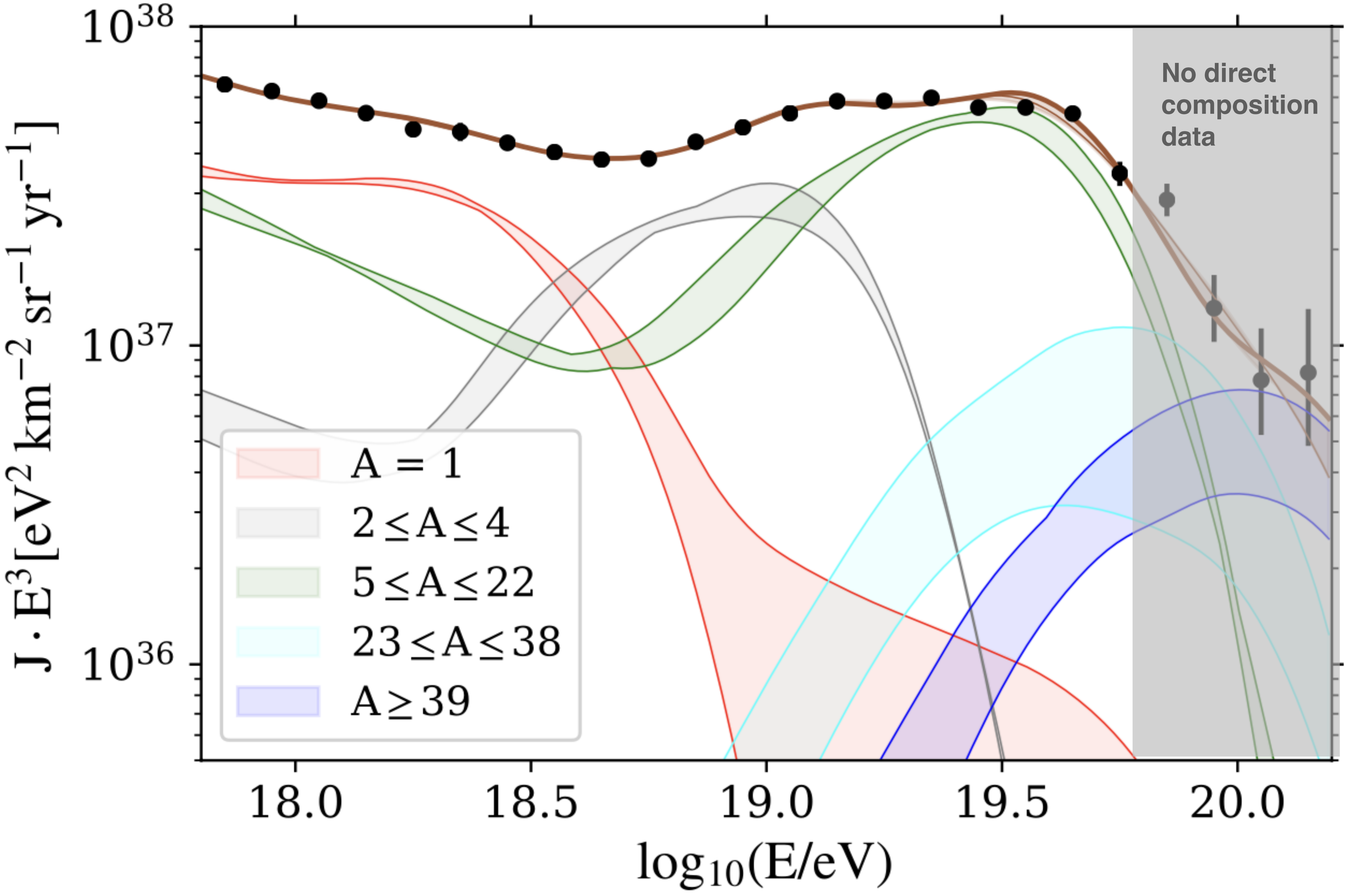

Assumption: source injection spectra universal in rigidity $R = E/Z$ (acceleration, scaling with charge Z)

Transition to heavier nuclei

$$\boxed{E_{p,cut} = 1.4 \ldots 1.6 \times 10^{18}\,\mathrm{eV}}$$

Exceptionally hard injection spectrum

$$\boxed{\frac{dN}{dE} \sim E^{1.5 \ldots 2}}$$

Fermi acceleration

$$E^{-2 \ldots -2.3}$$

Flux suppression due mainly to limit of injection energy of sources

Extragalactic origin of dipole anisotropy

Direction and energy dependence of extragalactic dipole

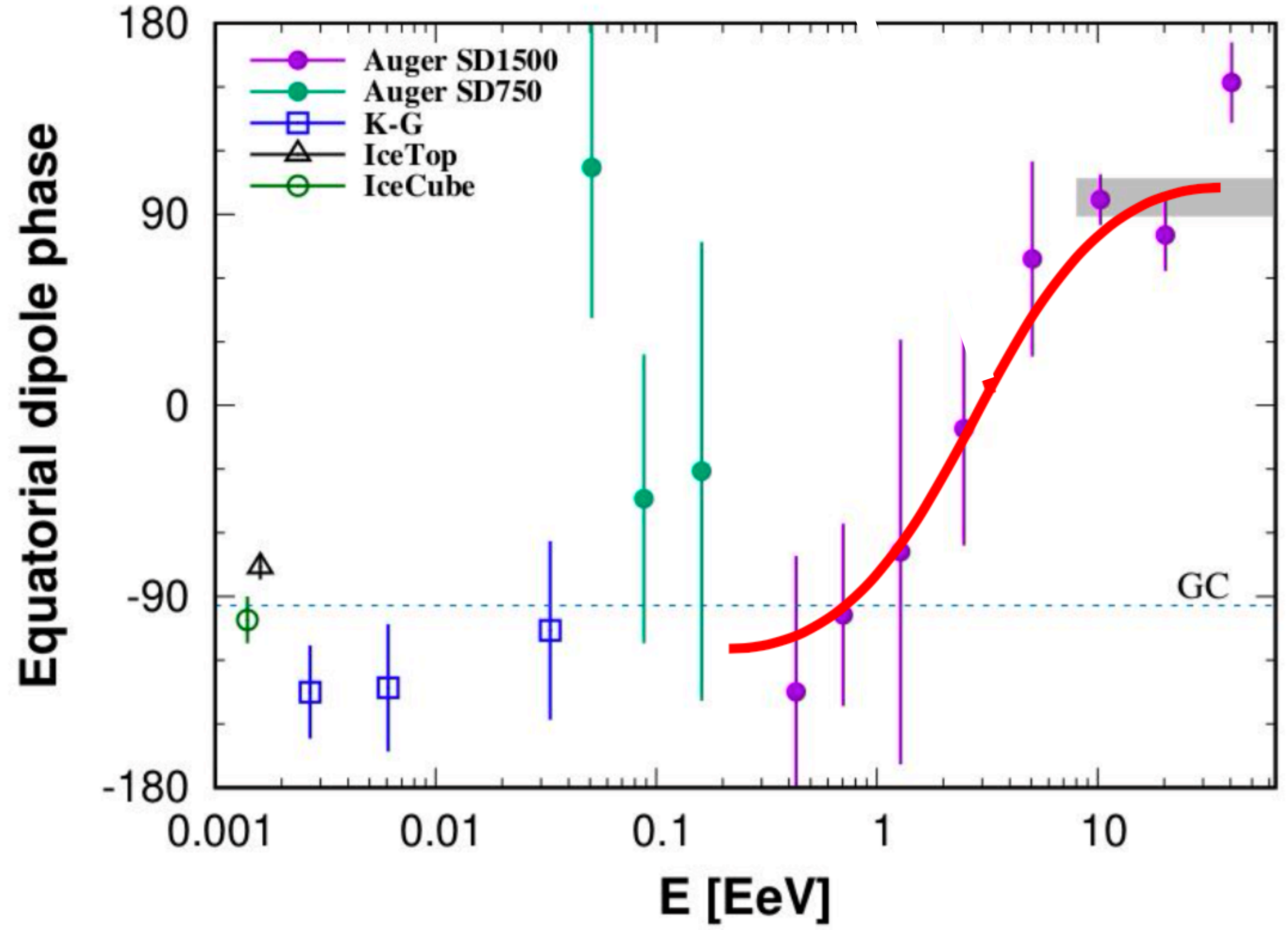

(Auger, ApJ 203, 2012,
Giacinti et al. JCAP 2012, 2015)

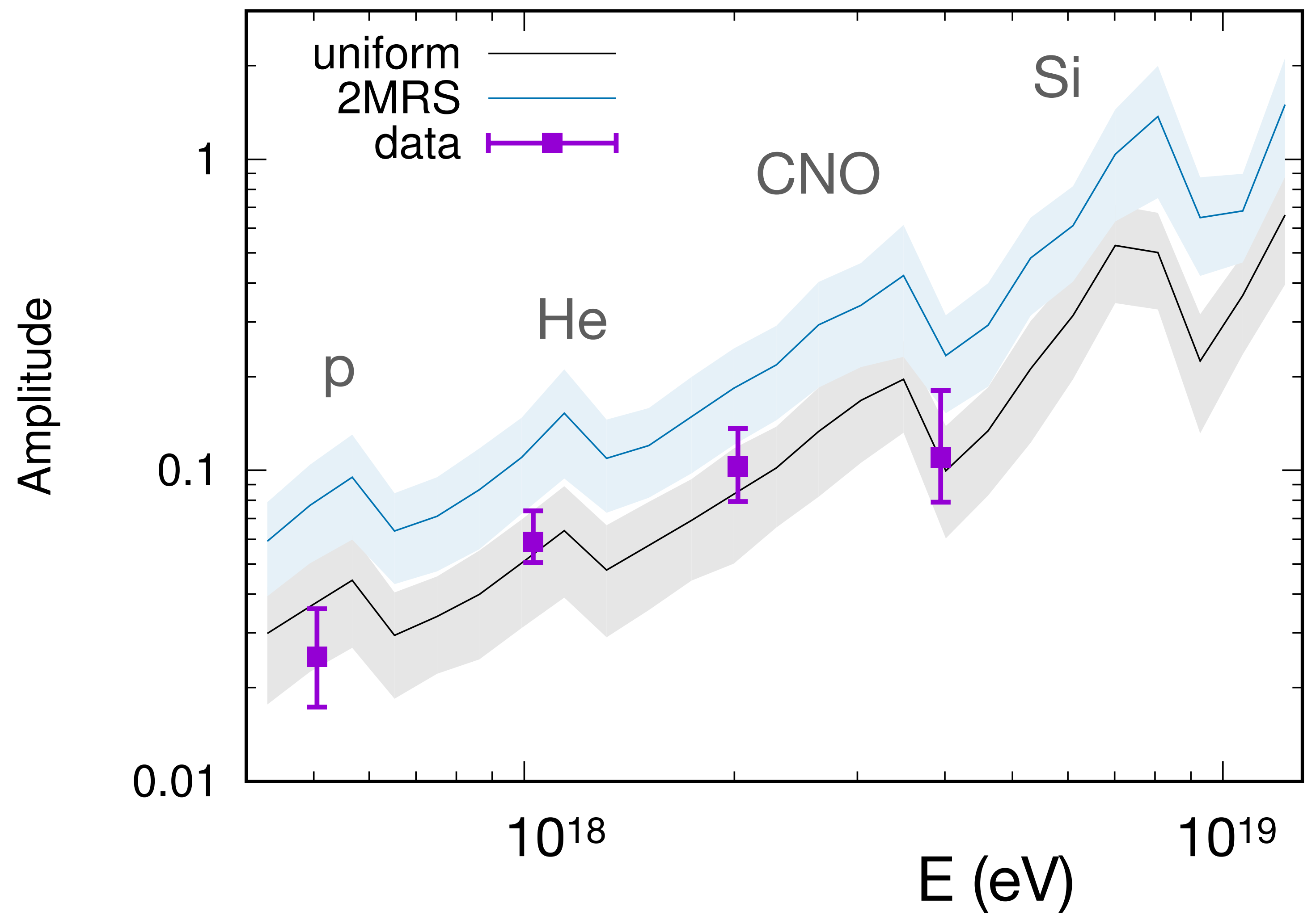

(Auger, ApJ 868 (2018) 1)

(Bister & Farrar, 2312.02645)

(Ding, Globus & Farrar ApJ 913 (2021) L13)

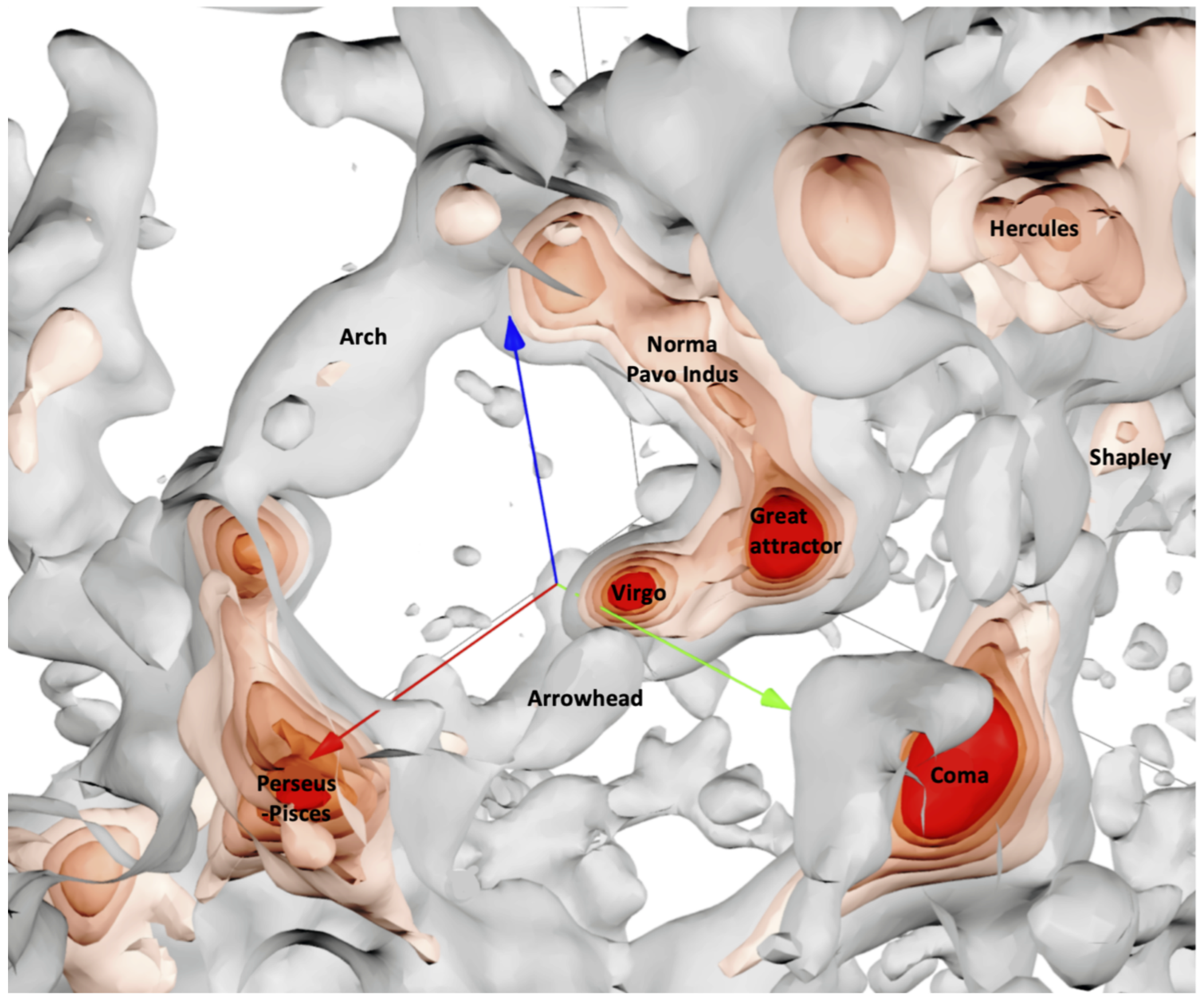

Protons below ankle energy are of extragalactic origin
Dipole anisotropy indicates transition to extragalactic sources
Interplay of source distribution, composition, and mag. horizon

Hadronic interactions – cross section measurement

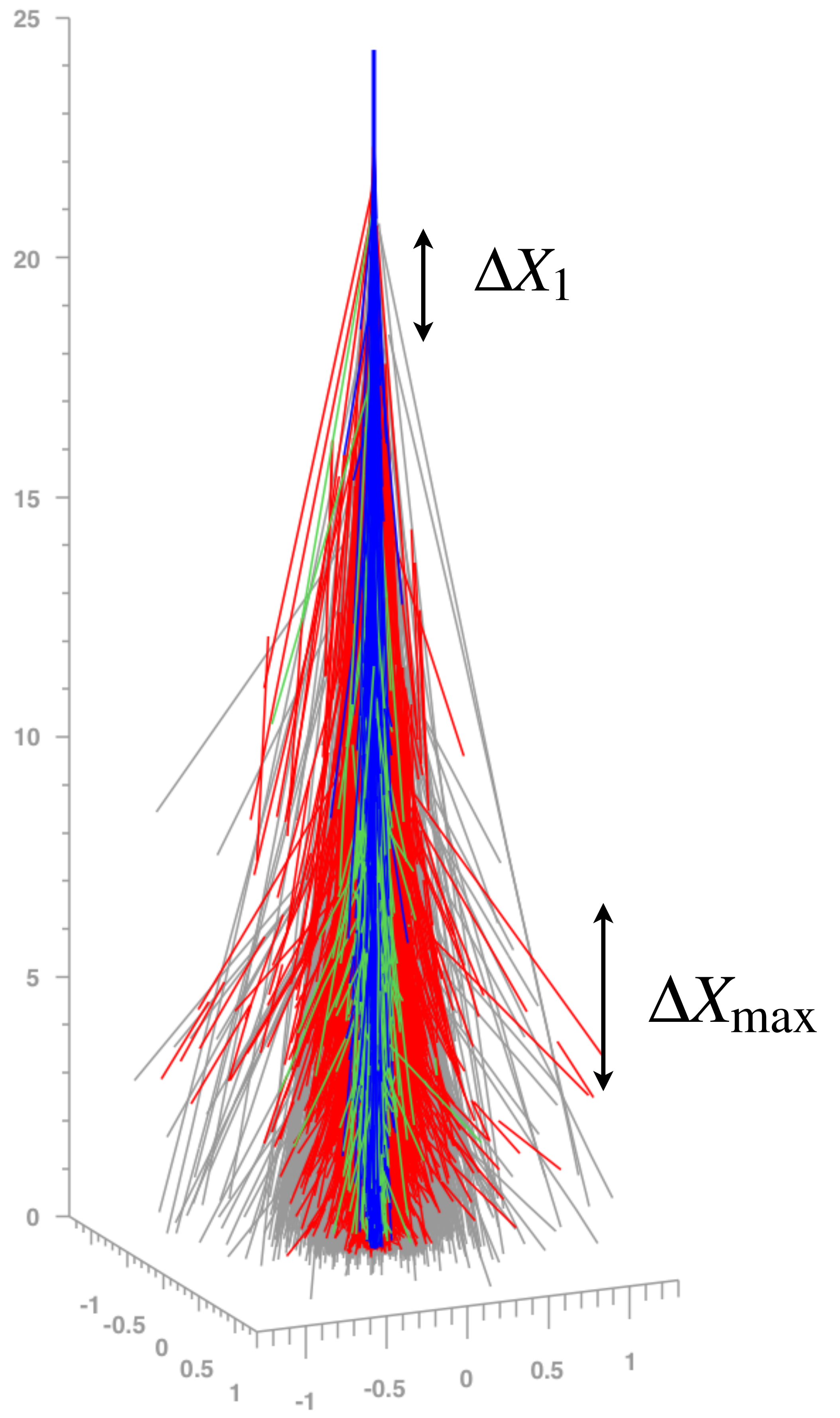

(Auger, PRL 109 (2012) 062002)

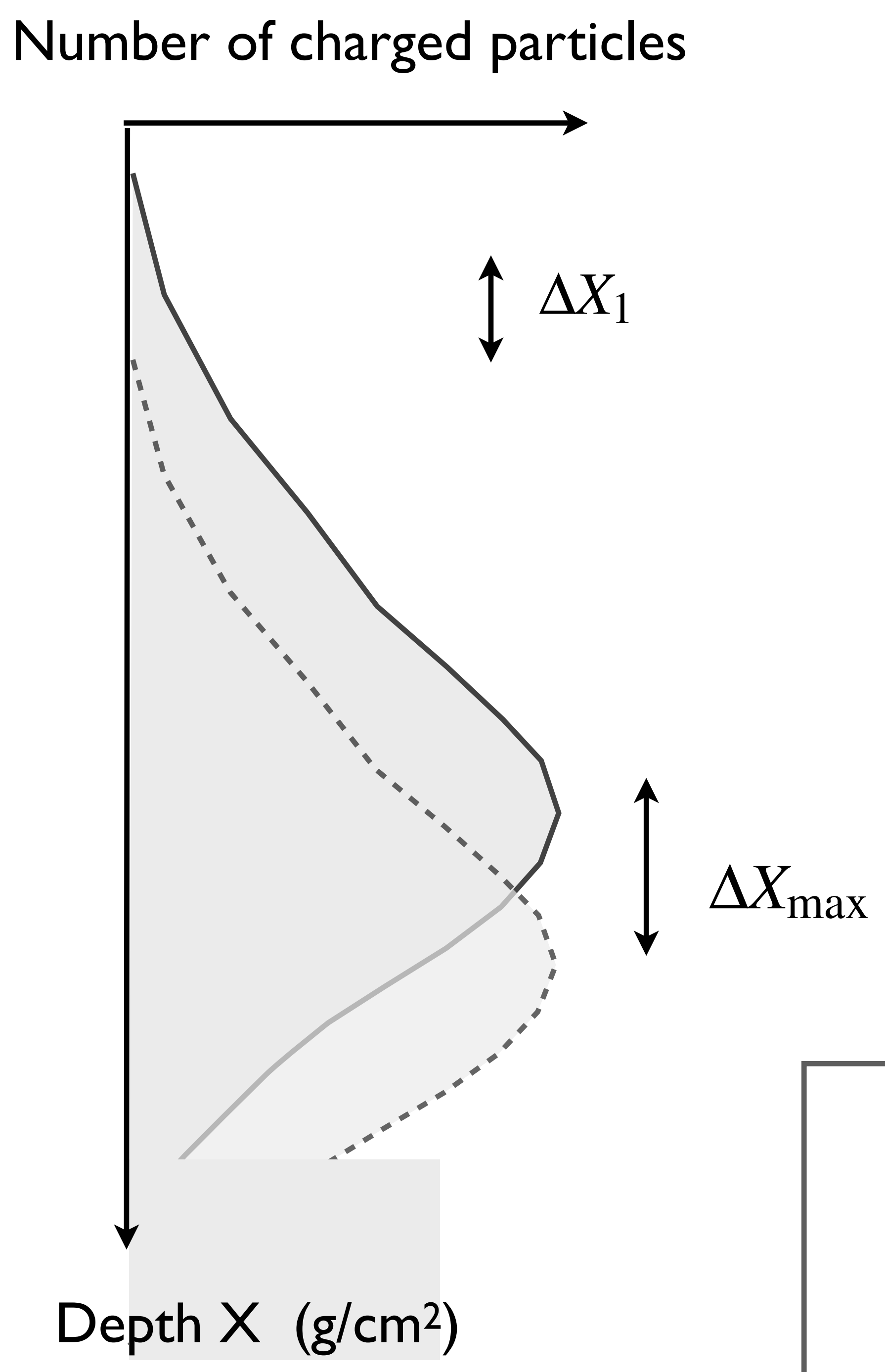

$$\frac{\mathrm{d}P}{\mathrm{d}X_1} = \frac{1}{\lambda_{\mathrm{int}}} e^{-X_1/\lambda_{\mathrm{int}}}$$

$$\sigma_{\mathrm{p-air}} = \frac{\langle m_{\mathrm{air}} \rangle}{\lambda_{\mathrm{int}}}$$

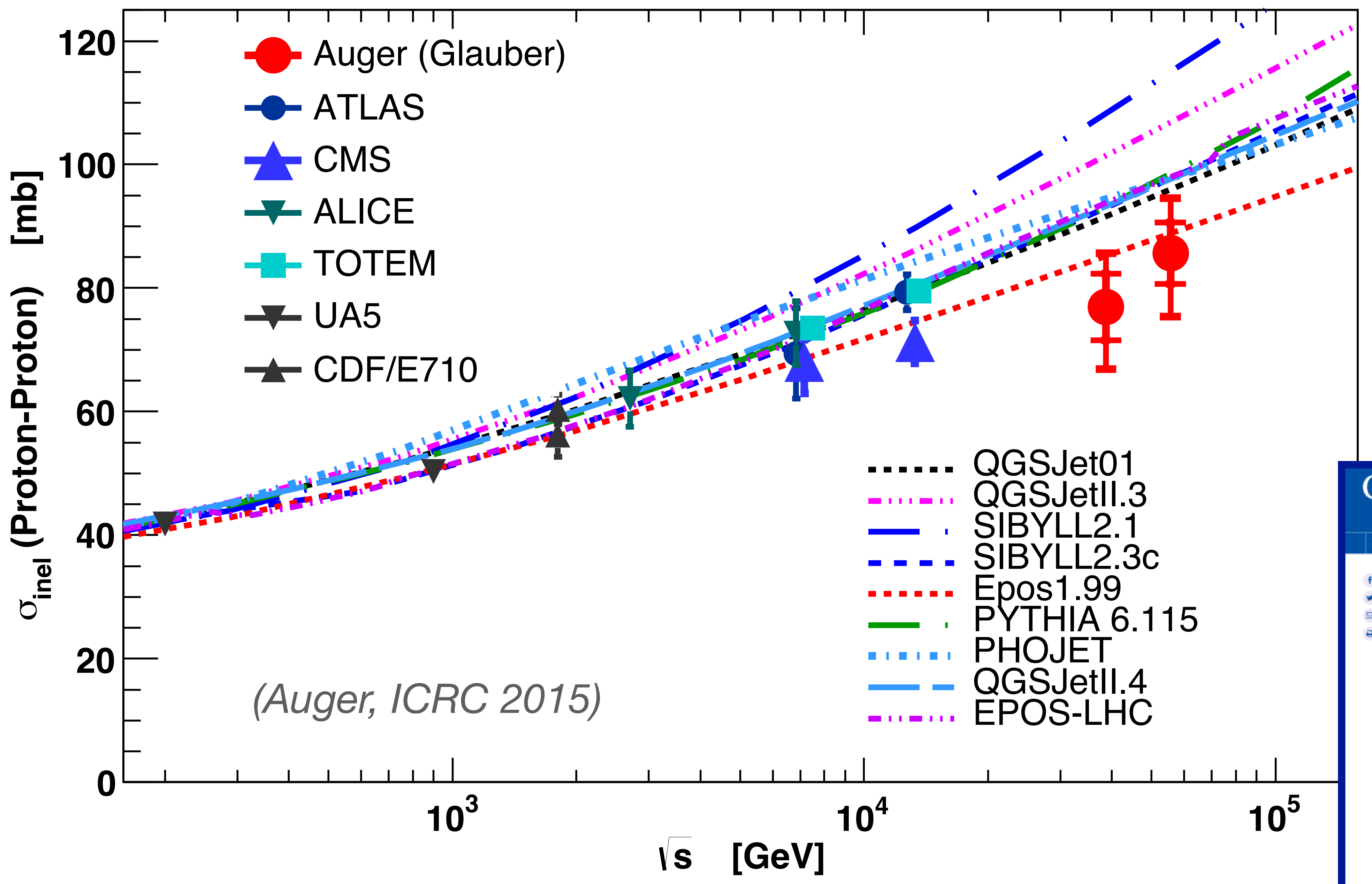

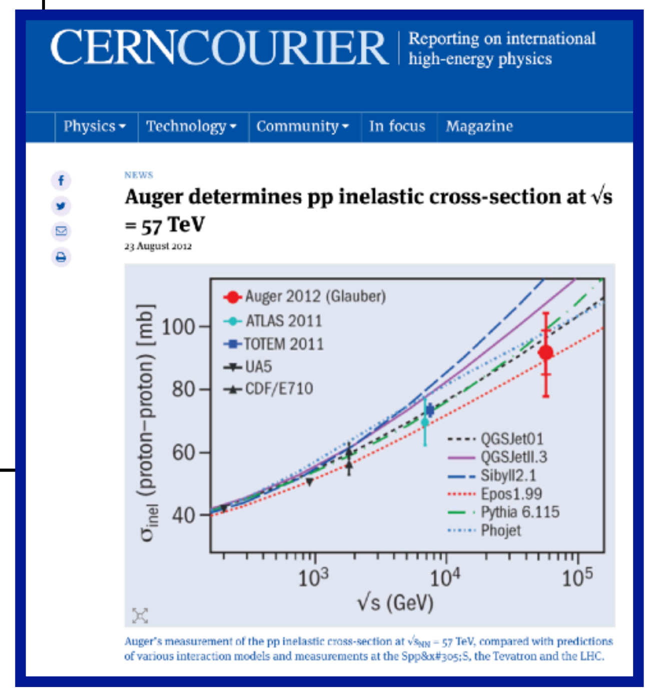

Challenges in analysis

- mass composition
- fluctuations in shower development (model needed for correction)
- conversion from p-air to p-p

Hadronic interactions – cross section measurement

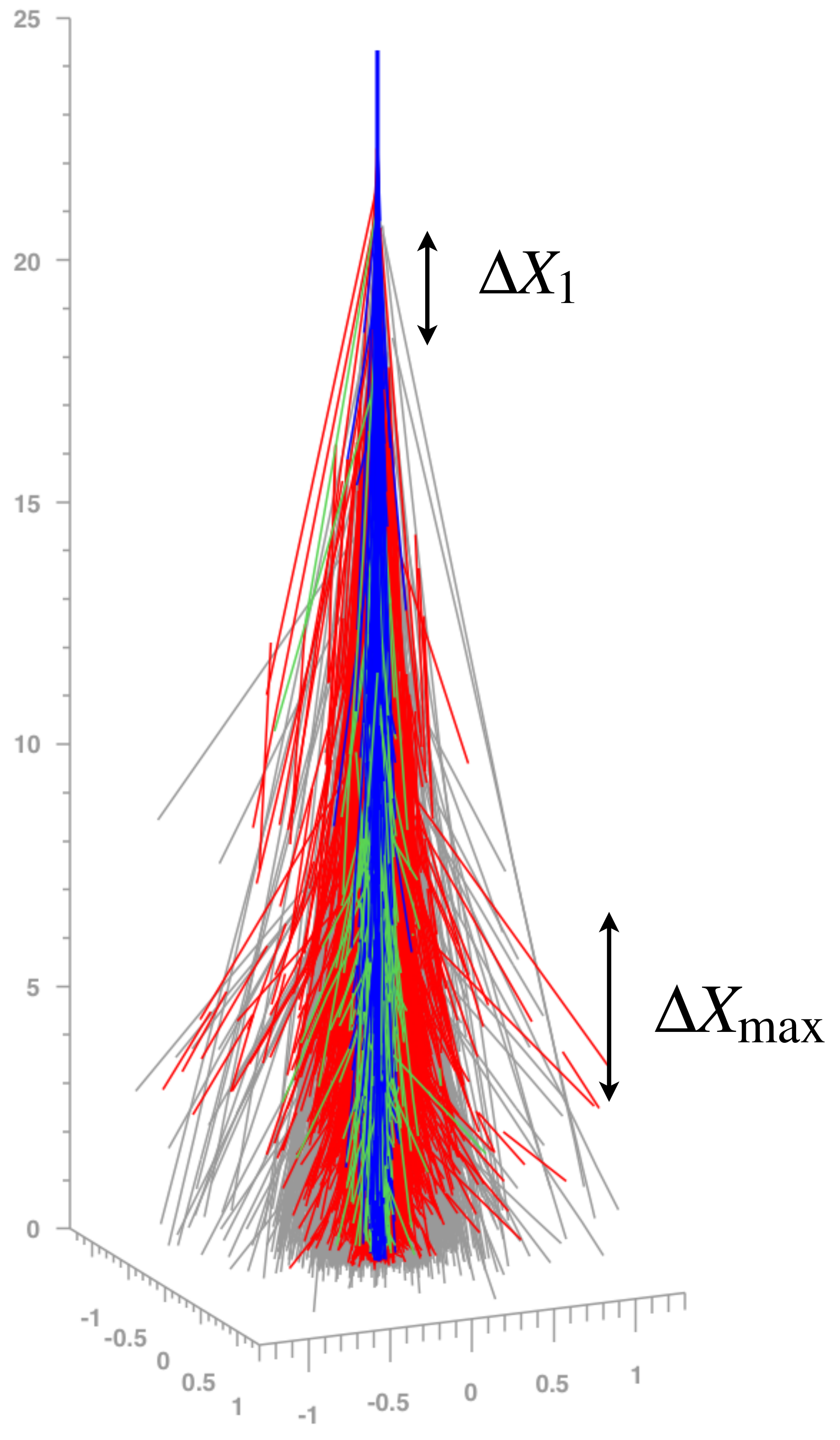

$$\frac{dP}{dX_1} = \frac{1}{\lambda_{int}} e^{-X_1/\lambda_{int}}$$

$$\sigma_{p-air} = \frac{\langle m_{air} \rangle}{\lambda_{int}}$$

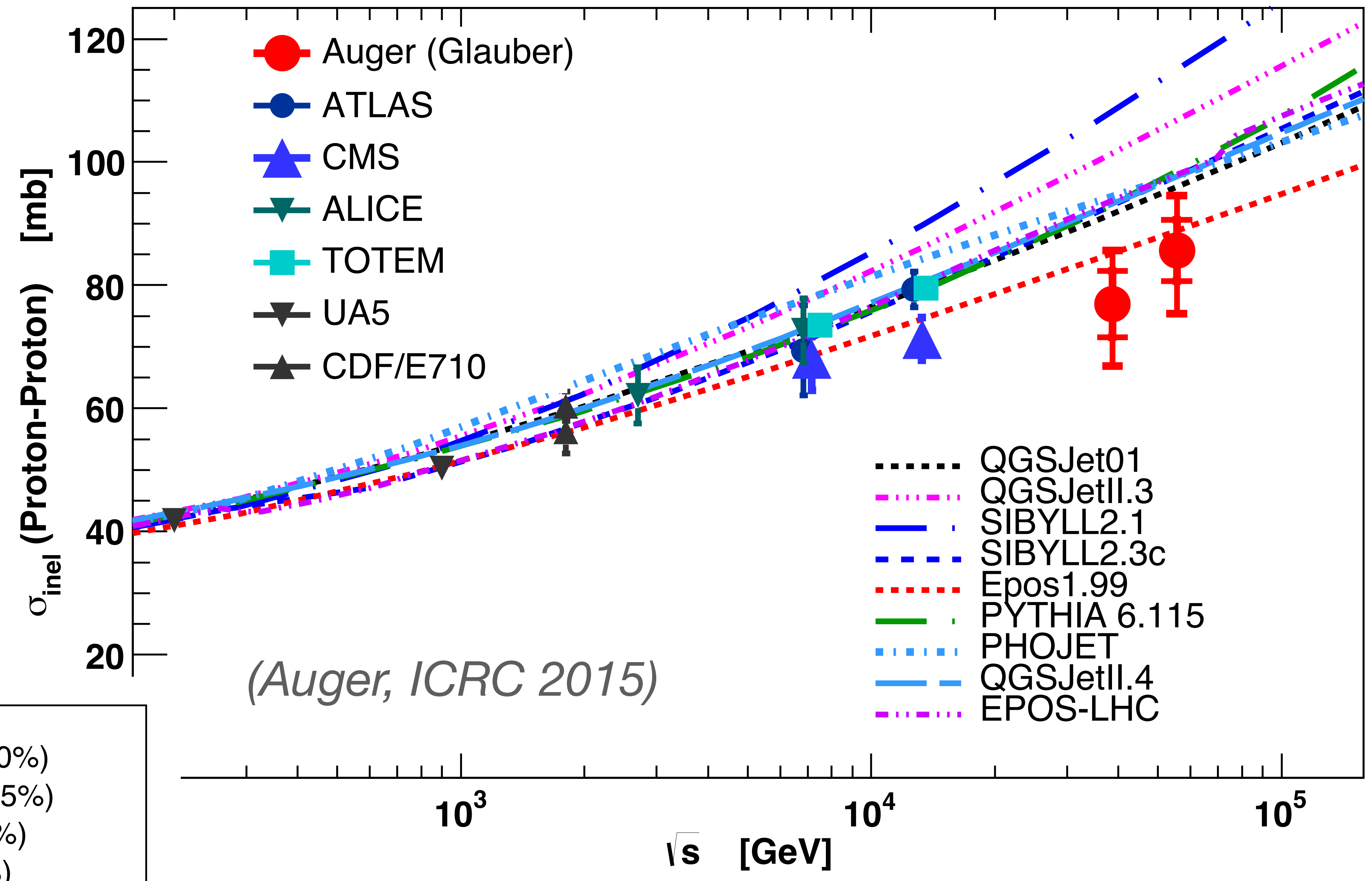

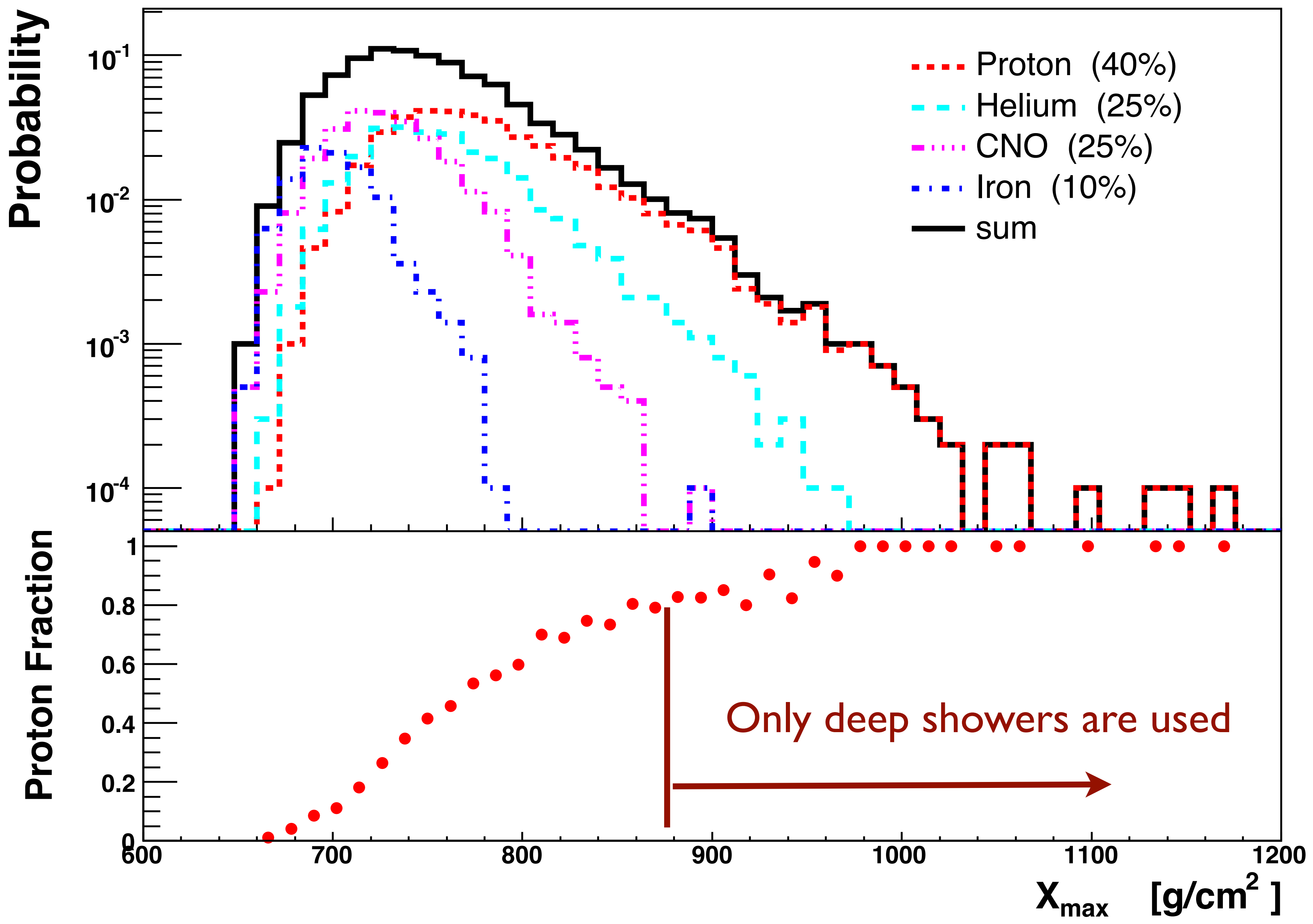

(Auger, PRL 109 (2012) 062002)

Challenges in analysis

- mass composition
- fluctuations in shower development (model needed for correction)

IceCube: discrimination of enhancement scenarios?

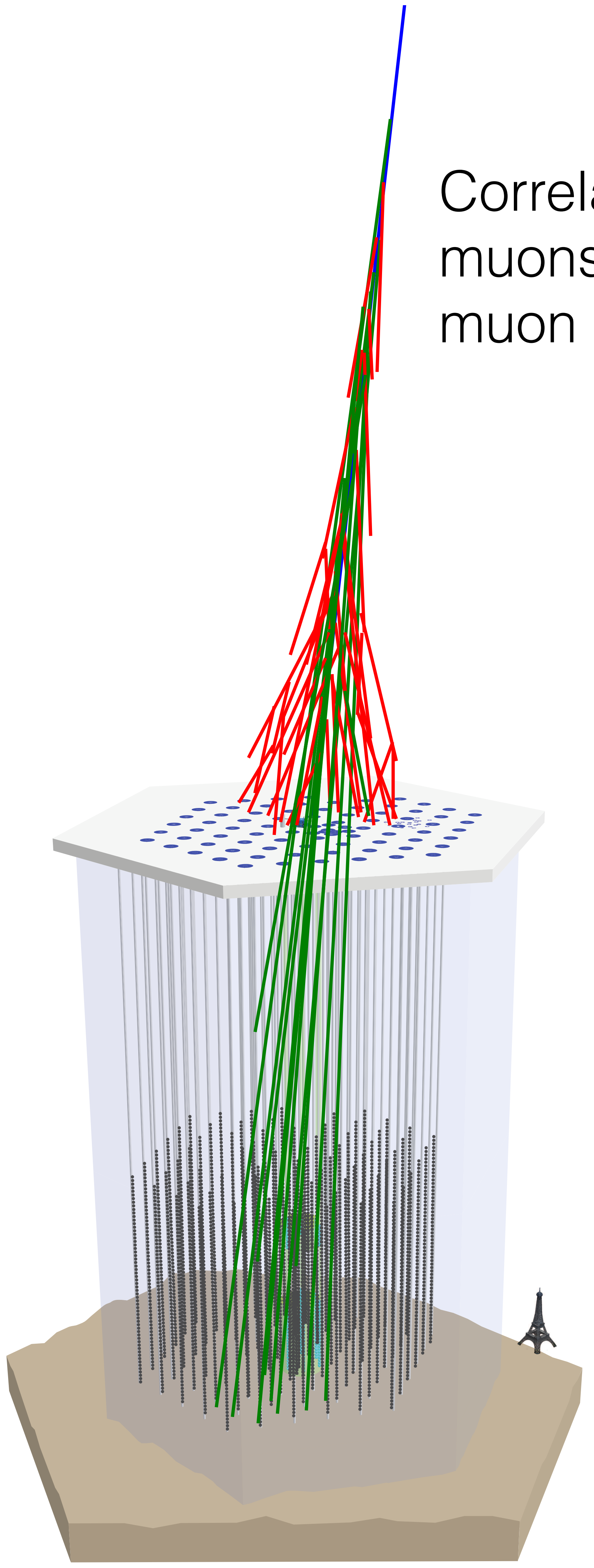

Correlation of low energy muons (surface) and in-ice muon bundles

IceTop: E_μ ~1 GeV

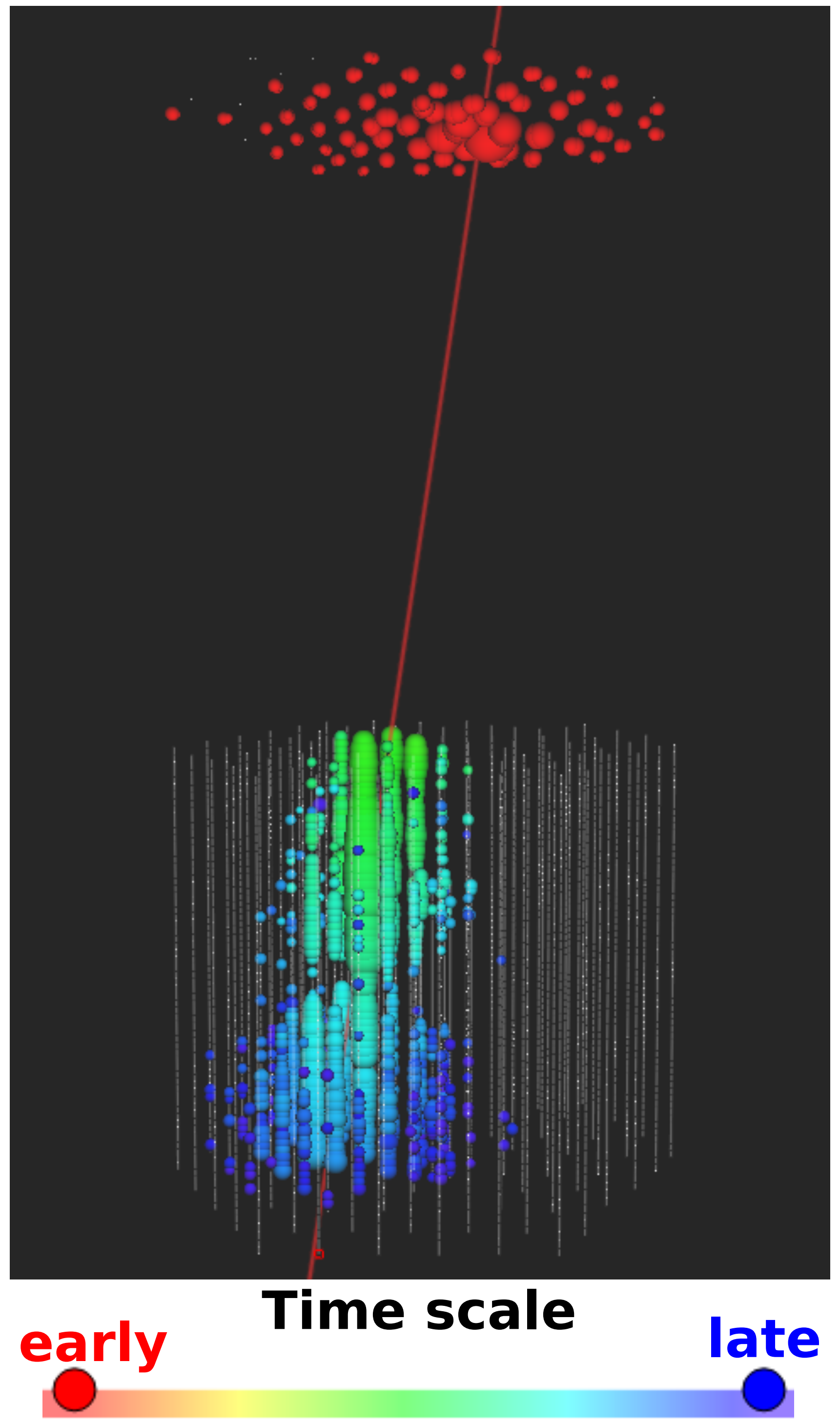

(IceCube, Gonzalez & Dembinski et al. 2016)

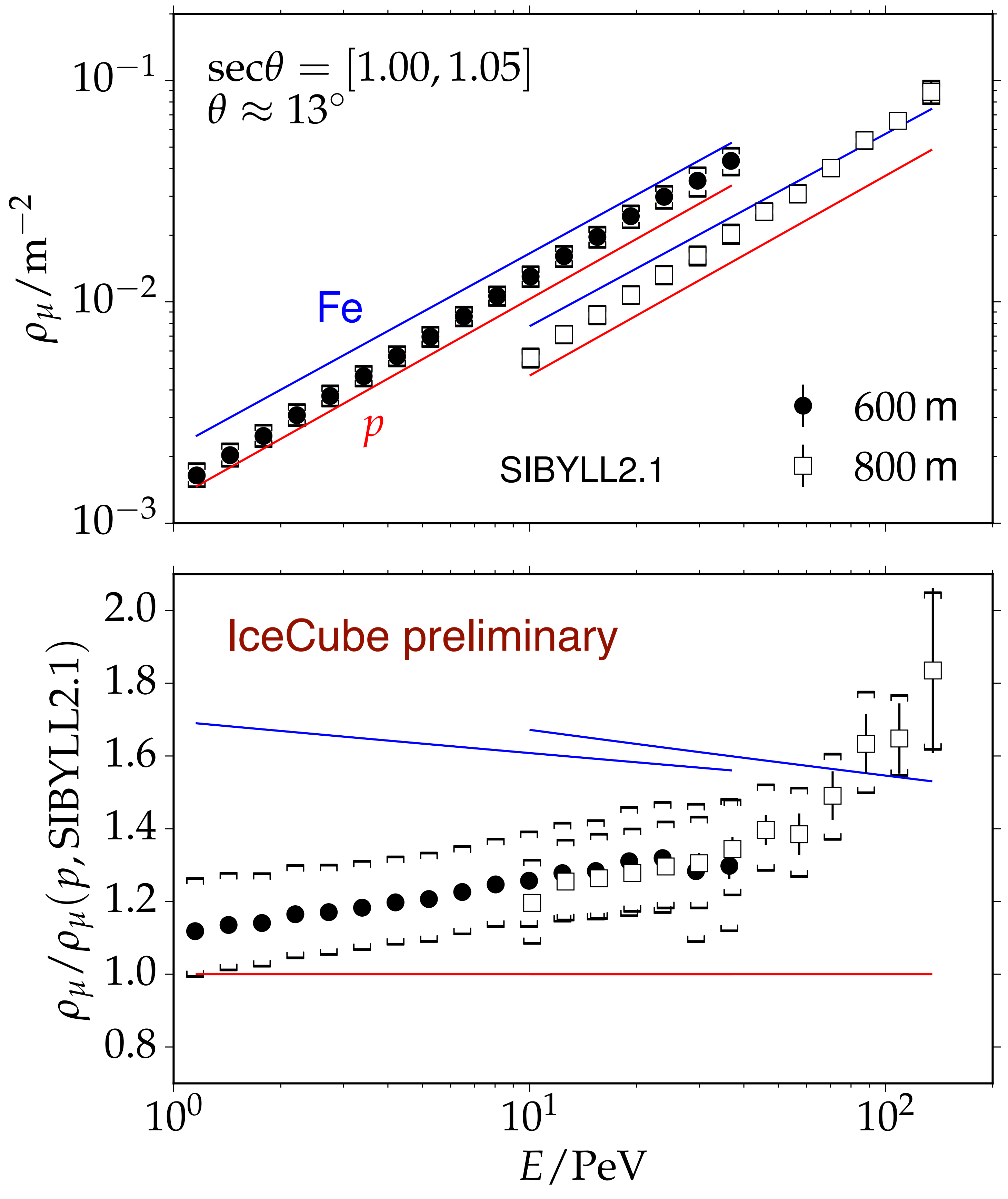

IceCube: E_μ >300 GeV

World data set on depth of shower maximum (X_{max})

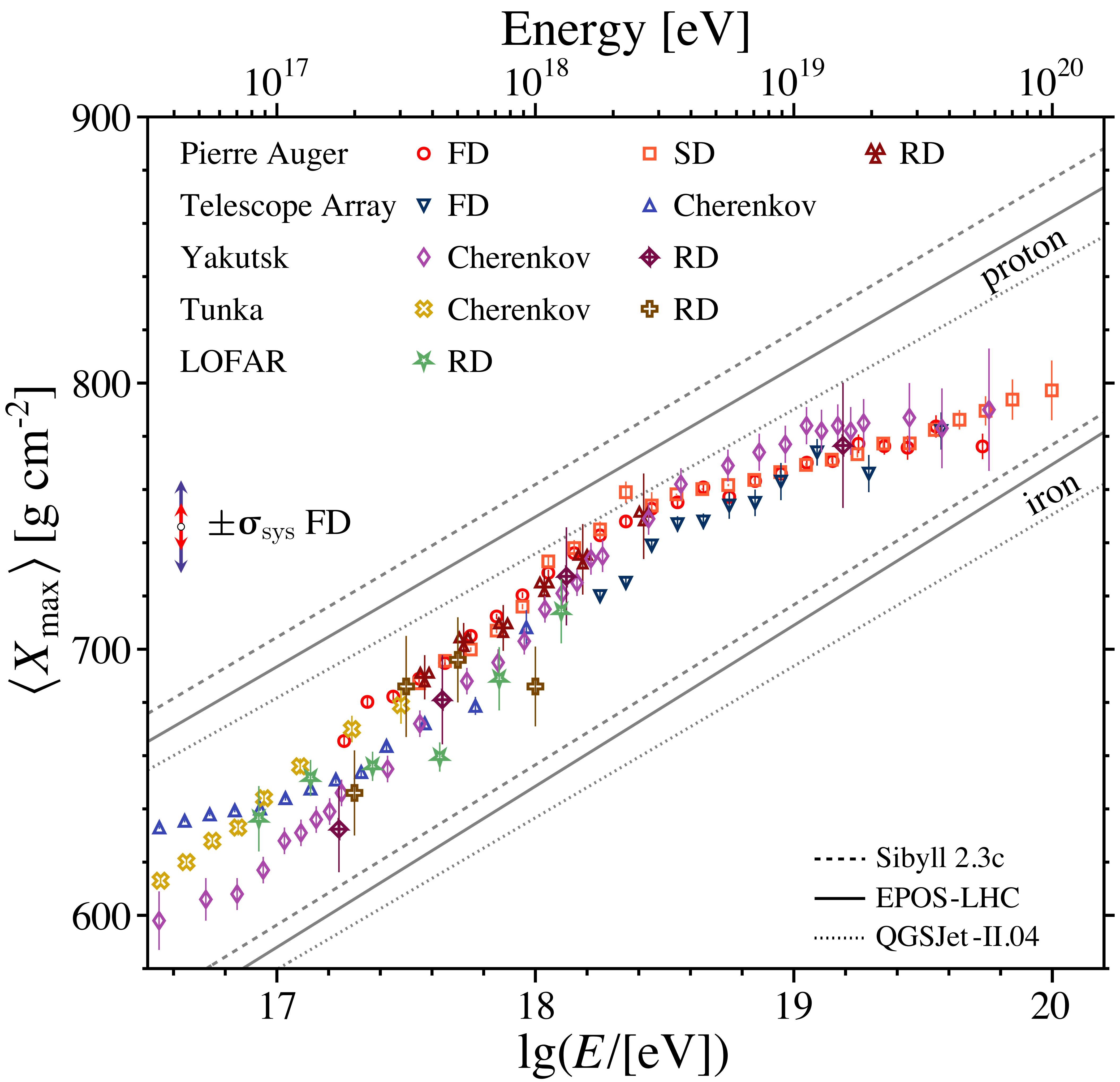

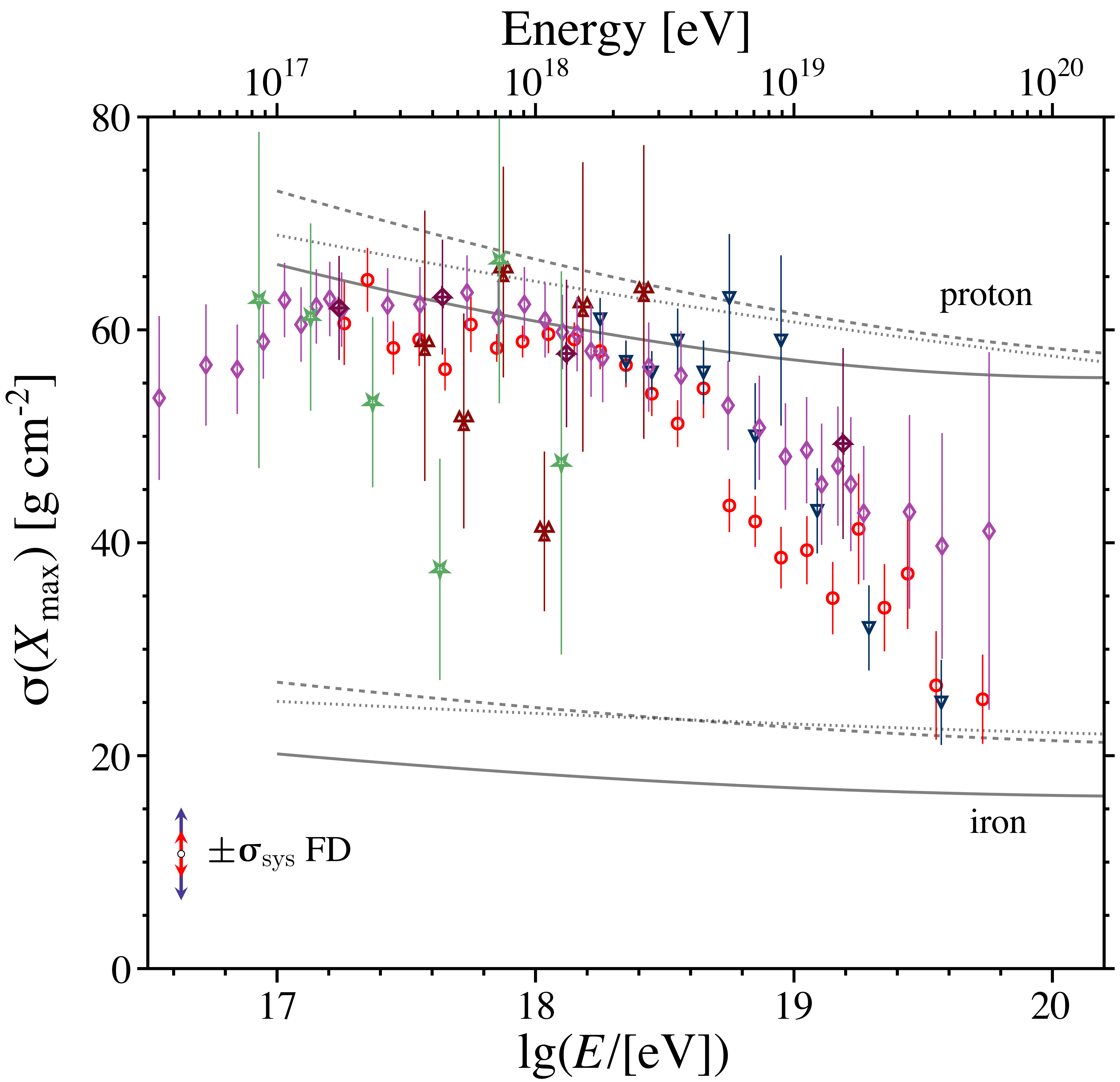

(Coleman et al. Snowmass, Astroparticle Physics 147 (2023) 102794)